THE APPLICATION OF SOLAR DESALINATION FOR WATER PURIFICATION IN CYPRUS

SOTERIS A. KALOGIROU

A thesis submitted in partial fulfilment of the requirements of the University of Glamorgan/Prifysgol Morgannwg for the degree of Doctor of Philosophy

This research programme was carried out in collaboration with the Higher Technical Institute – Nicosia, Cyprus

April 1995

ABSTRACT

This thesis initially reports on the water resources of Cyprus. From this analysis the need for desalination systems to provide fresh water, is established.

A survey of solar desalination systems shows that there are two broad categories of such systems; namely direct and indirect collection systems. The latter type is adopted and a multiple effect process is selected due to its low energy consumption, low equipment cost, simple sea-water treatment requirement and its suitability for variable steam supply conditions.

The design of a parabolic trough collector system is presented based on previous work. Special consideration is given to the radiation intensity distribution on the collector receiver and the mode of tracking selection. The E-W horizontal mode is selected due to its small shadowing effects. Computer programs are developed for all the above analyses and for modelling of the steam generation system. The design of the complete desalination system is also presented.

The collector performance tests show that the test slope and intercept are 0.387 and 0.638 respectively. The preliminary tests indicate the need to reduce start-up energy requirements. A modelling program is developed to optimise the design of the system's flash vessel and this is validated for both steady state and transient conditions. The optimum flash vessel dimensions and capacity reduced the system preheat energy by 30%.

An economic analysis of the collector system is carried out followed by a feasibility study of using the system in a number of applications. It is shown that the system could be viable for the two larger applications (hotel and village) with a water price below 0.89 C£/m^3. It is also shown that it is not cost effective to operate the system solely on solar energy due to a combination of the high system cost and the high percentage of inactive time.

To my wife Rena and my two children Andreas and Anna.

CONTENTS

LIST OF FIGURES V

LIST OF TABLES VII

LIST OF ATTACHED MATERIAL IX

ACKNOWLEDGEMENTS X

NOMENCLATURE XI

CHAPTER 1 INTRODUCTION 1

1.1 HISTORY OF SOLAR DESALINATION 1
1.2 THE WATER PROBLEM 2
1.2.1 Precipitation on Cyprus 2
1.2.2 The Water Demand 4
1.2.3 Comparison of Precipitation and Water Demand 6
1.3 ENVIRONMENTAL PARAMETERS 8
1.4 PROJECT OBJECTIVES 10
1.5 STRUCTURE OF THESIS 10

CHAPTER 2 LITERATURE SURVEY AND SYSTEM SELECTION 12

2.1 DIRECT COLLECTION SYSTEMS 14
2.1.1 Solar Stills 14
2.2 INDIRECT COLLECTION SYSTEMS 16
2.2.1 Multi-stage Flash Process 17
2.2.2 The Multiple Effect Boiling Process 19
2.2.3 The Vapour Compression Process 22
2.2.4 Reverse Osmosis 23
2.2.5 Electrodialysis 24
2.3 PROCESS SELECTION 25

CHAPTER 3 SYSTEM DESIGN 28

3.1 COLLECTOR SYSTEM DESIGN 28
3.1.1 Parabolic Trough Collector Dimensions 28
3.1.2 Collector Intercept Factor Analysis 31
3.1.3 Receiver Design 33
3.1.4 Design of the Tracking Mechanism 36
3.1.4.1 System Description 36
3.1.5 Selection of Mode of Tracking 37
3.1.6 Collector Specifications 43
3.2 DESIGN OF THE STEAM GENERATION SYSTEM 43
3.2.1 Selection of the Steam Generation Method 44
3.2.2 Flash Vessel Design 47
3.2.3 The Complete Steam Generation System 48
3.3 DESIGN OF THE DESALINATION SYSTEM 48
3.3.1 System Circuit Arrangement 48
3.3.2 Description of the MEB Evaporator 48
3.4 SYSTEM MODELLING 53

CHAPTER 4 CONSTRUCTION OF THE SYSTEM 59

4.1 CONSTRUCTION OF THE COLLECTOR 59
4.1.1 Parabola Construction 59
4.1.2 Tracking Mechanism Construction 62
4.1.3 Collector System Construction 62
4.2 CONSTRUCTION OF THE STEAM GENERATION SYSTEM . . . 63
4.2.1 Flash Vessel Construction 63
4.2.2 Framework construction 64
4.2.3 Heat Exchanger Construction 67
4.2.4 Piping 67

CHAPTER 5 COLLECTOR SYSTEM PERFORMANCE 68

5.1 DATA ACQUISITION SYSTEM 68
5.2 COLLECTOR THERMAL PERFORMANCE EVALUATION 71
5.2.1 Collector Thermal Efficiency 71
5.2.2 Collector Time Constant 73
5.2.3 Collector Incidence Angle Modifier 74
5.2.4 Collector Acceptance Angle 78
5.2.5 Dust Accumulation on the Reflector 78
5.3 EVALUATION OF THE SYSTEM PERFORMANCE 80
5.3.1 Pre-heat Energy Evaluation 80
5.3.2 Analysis of the System Performance 82

CHAPTER 6 SYSTEM DEVELOPMENT 86

6.1 SYSTEM REFINEMENT 86
6.1.1 Pre-heat Energy Evaluation of the Modified System 91
6.1.2 Validation of the Optimisation Model 94
6.1.3 Theoretical System Energy Analysis 99
6.2 LARGER SYSTEM PREDICTIONS 99
6.2.1 Small Domestic Application 101
6.2.2 Large Domestic Application 102
6.2.3 Hotel Application 105
6.2.4 Village Application 108
6.2.5 Comparison of the Systems 110
6.3 SYSTEM OPERATION FOR NON-STANDARD CONDITIONS . . 111
6.3.1 System Operation at Higher Collector Temperatures 111
6.3.2 System Operation at Sub-Atmospheric Pressure 112

CHAPTER 7 ECONOMIC ANALYSIS OF THE PROPOSED DESALINATION SYSTEMS 114

7.1 METHOD OF ANALYSIS 115
7.2 COST PARAMETERS 118
7.3 ANALYSIS OF PARTICULAR APPLICATIONS 121
7.3.1 Small Domestic Application 121
7.3.2 Large Domestic Application 123
7.3.3 Hotel Application 124
7.3.3.1 Desalination only system 124
7.3.3.2 Desalination and hot water 125
7.3.4 Village Application 127
7.4 SYSTEM COMPARISONS 128
7.5 SENSITIVITY ANALYSIS/CONCLUSIONS 128

CHAPTER 8 THE FINAL SYSTEM 133

8.1 SPECIFICATIONS 133
8.2 CONCLUSIONS 133
8.3 RECOMMENDATIONS 136

APPENDIX 1 ENVIRONMENTAL CHARACTERISTICS 137

APPENDIX 2 COMPUTER PROGRAM "SKDES" 140

A2.1 PROGRAM DESCRIPTION 140
A2.2 MODE OF TRACKING SELECTION PROGRAM 141
A2.3 FLUX DISTRIBUTION ON A PTC RECEIVER PROGRAM 142
A2.4 INTERCEPT FACTOR CALCULATION PROGRAM 150
A2.5 WEATHER DATA FILE GENERATOR 152
A2.6 SIMULATION PROGRAMS 152
A2.7 SYSTEM OPTIMISATION PROGRAM 158

APPENDIX 3 DATA ACQUISITION SYSTEM PROGRAM 163

APPENDIX 4 SAMPLE ECONOMIC ANALYSIS 166

APPENDIX 5 LIST OF PUBLICATIONS 170

REFERENCES 171

BIBLIOGRAPHY 175

LIST OF FIGURES

Fig. 1.1 Precipitation on Cyprus 3

Fig. 2.1 Solar still 15
Fig. 2.2 Multi-stage flash system - principle of operation 18
Fig. 2.3 Multi-stage flash process plant 19
Fig. 2.4 Multiple effect boiling system - principle of operation 20
Fig. 2.5 Long tube vertical (LTV) multiple effect boiling plant 21
Fig. 2.6 Vapour compression system - principle of operation 23

Fig. 3.1 PTC relations 30
Fig. 3.2 Relations from Jetter [1987] for estimating LCR 34
Fig. 3.3 Distribution of LCR for various incidence angles 35
Fig. 3.4 Tracking mechanism system diagram 37
Fig. 3.5 Collector geometry for various modes of tracking and solar angles diagram 39
Fig. 3.6 Position of E-W tracked surfaces 40
Fig. 3.7 Maximum angle of incidence for day number 90-300 42
Fig. 3.8 Effect of collector axis azimuth on collector performance 42
Fig. 3.9 The steam-flash steam generation concept 46
Fig. 3.10 The direct steam generation concept 46
Fig. 3.11 The unfired-boiler steam generation concept 46
Fig. 3.12 Flash vessel design details 47
Fig. 3.13 The complete steam generation system 49
Fig. 3.14 The complete system circuit diagram 50
Fig. 3.15 The MES evaporator 52
Fig. 3.16 Program "PTCDES1" flow chart 55
Fig. 3.17 Simulation program "PTCDES2" output 56-57

Fig. 4.1 Mould construction detail 61
Fig. 4.2 Fibreglass parabola detail 61
Fig. 4.3 Receiver bracket detail 63
Fig. 4.4 Flash vessel detail 64
Fig. 4.5 Framework detail 65
Fig. 4.6 The complete system 66
Fig. 4.7 Heat exchanger detail 67

Fig. 5.1 Data acquisition system arrangement 69
Fig. 5.2 Data acquisition measurement points 70
Fig. 5.3 Collector performance curve 72
Fig. 5.4 Collector time constant test results "heating" 75
Fig. 5.5 Collector time constant test results "cooling" 76
Fig. 5.6 Incidence angle modifier test results 77
Fig. 5.7 Collector acceptance angle test results 79
Fig. 5.8 Pre-heat cycle graph 81
Fig. 5.9 System steam production against "PTCDES2" program predictions (September 2nd 1993) 83
Fig. 5.10 Comparison between predicted and actual system performance (hot sunny day) 84

Fig. 5.11 Comparison between predicted and actual system performance (cold sunny day) 84

Fig. 6.1 Predicted steam production for various size flash vessels 90
Fig. 6.2 System with flash vessel #1 observed pre-heat cycle 92
Fig. 6.3 System with flash vessel #2 observed pre-heat cycle 93
Fig. 6.4 Comparison of system thermal response for different flash vessels 95
Fig. 6.5 Comparison of actual and predicted heat-up response 96
Fig. 6.6 Comparison of actual and predicted transient response 98
Fig. 6.7 System Sankey diagram 100
Fig. 6.8 Theoretical thermal losses from the system 100
Fig. 6.9 Small domestic application schematic diagram 101
Fig. 6.10 Flash vessel optimisation-small domestic application 102
Fig. 6.11 Large domestic application schematic diagram 104
Fig. 6.12 Hotel application schematic diagram 106
Fig. 6.13 Village application schematic diagram 109
Fig. 6.14 Percentage increase in steam production for various vacuum pressures 113

Fig. 7.1 Water price against operation mode for all applications considered 129
Fig. 7.2 Comparison of water quantity and water price for operation mode #4 130
Fig. 7.3 Water price against pay-back time for operation mode #4 130

Fig. A1.1 Reference year 138
Fig. A1.2 Special reference year 139

Fig. A2.1 SKDES program main menu 140
Fig. A2.2 Input and output of the mode of tracking selection program 143
Fig. A2.3 Flow cart of the mode of tracking selection program 144
Fig. A2.4 Listing of the mode of tracking selection program 145-147
Fig. A2.5 Input and output of the flux distribution on a PTC receiver program 147
Fig. A2.6 Flow chart of the flux distribution on a PTC receiver program 148
Fig. A2.7 Listing of the flux distribution on a PTC receiver program 148-150
Fig. A2.8 Flow chart of the intercept factor calculation program 150
Fig. A2.9 Listing of the intercept factor calculation program 151-152
Fig. A2.10 Listing of the weather data generator program 153
Fig. A2.11 Listing of PTCDES1 program 154-157
Fig. A2.12 Program FLASH flow chart 159
Fig. A2.13 Program FLASH sample output 160
Fig. A2.14 Program FLASH listing 160-162

Fig. A3.1 Listing of program DAS 163-165

LIST OF TABLES

Table 1.1 Distribution of precipitation over the months of the year (years 1951-1980) 4
Table 1.2 The water consumption pattern for 1991 5
Table 1.3 Water consumption and price in various Cyprus towns 6
Table 1.4 Effect of water conservation measures on water consumption 6
Table 1.5 Mean sea-water temperature in Deg.C (Years 1971-1985) 9
Table 1.6 Partial ionic analysis of sea-water and comparison with drinking water standard 9

Table 2.1 Desalination processes 13
Table 2.2 Energy consumption of desalination systems 25
Table 2.3 Comparison of desalination plants 26

Table 3.1 PTC dimensions 31
Table 3.2 Effect of the magnitude of errors in intercept factor estimation 33
Table 3.3 Comparison of energy absorbed for various modes of tracking 38
Table 3.4 Total radiation received for various tracking axis slopes 41
Table 3.5 PTC system specifications 43
Table 3.6 Average day of each month 53
Table 3.7 Predicted monthly energy collection and steam production 58

Table 5.1 Testing instruments specification 69
Table 5.2 Comparison of collector performance efficiency equations 73
Table 5.3 Cumulative summary between actual and predicted system performances 85

Table 6.1 Program "FLASH" input data 89
Table 6.2 Flash vessel dimensions 91
Table 6.3 Comparison between actual and predicted system performance for different flash vessels and capacities 97
Table 6.4 Predicted small domestic application performance 102
Table 6.5 Flash vessel optimisation-large domestic application 103
Table 6.6 Standard vessel dimensions and prices (from manufacturers data) 103
Table 6.7 Predicted large domestic application performance 105
Table 6.8 Flash vessel optimisation - Hotel application 107
Table 6.9 Predicted hotel application performance 107
Table 6.10 Flash vessel optimisation - Village application 108
Table 6.11 Predicted village application performance 110
Table 6.12 Systems comparison 111
Table 6.13 Effect of reduced flow rate on predicted system performance 112
Table 6.14 Comparison of system performance under vacuum and atmospheric conditions 113

Table 7.1 Applications considered in economic analysis 114
Table 7.2 Economic parameters 117
Table 7.3 Cost breakdown of the 3.5m^2 collector model 119
Table 7.4 Parabolic trough collector system costs 119
Table 7.5 Desalination system cost parameters (from manufacturers data) 120

Table 7.6 Types of operation considered in economic analysis 121
Table 7.7 Results of the small domestic application economic analysis 122
Table 7.8 Results of the large domestic application economic analysis (no tax allowances) 123
Table 7.9 Results of the large domestic application economic analysis (with tax allowance) 124
Table 7.10 Results of hotel application economic analysis 125
Table 7.11 Results of hotel application economic analysis (desalination and hot water Winter) 126
Table 7.12 Results of hotel application economic analysis (desalination and hot water Summer) 127
Table 7.13 Results of village application economic analysis 128
Table 7.14 Effect of the desalination and solar cost on water price 131

Table 8.1 System specifications 134

Table A4.1 List of input parameters 167
Table A4.2 Economic analysis sample calculation sheet (hotel case operation mode #4) 168
Table A4.3 Secondary table for calculation of various costs 169

LIST OF ATTACHED MATERIAL

1. Computer Programs

1.1 5 1/4" diskette containing all the computer programs written as part of this project.

2. Papers

2.1 Kalogirou, S., Lloyd, S. and Ward, J. 1992c. A Tracking Mechanism for Medium to High Concentration Ratio Parabolic Trough Collectors, *Proceedings of the second Renewable Energy Congress*, Reading U.K., vol. 2, pp. 1086-1091.

2.2 Kalogirou, S., Eleftheriou, P., Lloyd, S. and Ward, J. 1994a. Design and Performance Characteristics of a Parabolic-Trough Solar-Collector System, *Applied Energy Journal*, vol. 47, pp. 341-354.

ACKNOWLEDGEMENTS

I would like to express my sincere and honest appreciation to my project supervisor Dr. Stephen Lloyd for his great help, enthusiasm and constructive criticism and comments which he has given me throughout the research program.

I would also like to thank the following persons who in various ways have helped me in the execution of this research project:

- Professor John Ward, Head of the Mechanical and Manufacturing Engineering Department of the University of Glamorgan, for his valuable suggestions and stimulating interest.

- Dr. Polyvios Eleftheriou, Lecturer HTI, for his comments, suggestions and constructive criticism.

- Mr. George Iordanou, Head of Mechanical Engineering Department of HTI, for the use of HTI facilities.

Finally I would like to thank my wife Rena and my two children Andreas and Anna, for their ever ending support and patience they have shown during the execution of this project.

NOMENCLATURE

A	Aperture area (m^2)
A_{pump}	Pump surface area (m^2)
A_f	Geometric factor
C	Concentration ratio
c_p	Specific heat capacity (J/kg K)
D	Receiver diameter (m)
d	Market discount rate (%)
DT	Temperature difference (K)
D_i	Internal flash vessel diameter (m)
dr	Receiver mislocation distance (m)
d^*	Universal nonrandom error parameter due to receiver mislocation and reflector profile errors ($d^*=dr/D$)
D_o	External flash vessel diameter including insulation (m)
F_R	Heat removal factor
H	Flash vessel height (m)
H_p	Pump height (m)
I	Beam radiation (W/m^2)
k	Flash vessel thermal conductivity (W/mK)
k_j	Insulation thermal conductivity (W/mK)
$K_{\alpha\tau}$	Incidence angle modifier
m	Mass flow rate (kg/s)
n	Collector thermal efficiency
n_o	Collector optical efficiency
Q_{FS}	Heat loss from flash vessel (W)
Q_{pipes}	Heat loss from pipes (W)
Q_{pump}	Heat loss from pump body (W)
q_u	Rate of useful energy (W)
T	Water temperature (K)
t	Flash vessel wall thickness (m)
T_a	Ambient temperature (K)
T_{fi}	Collector fluid inlet temperature (K)

T_{fo} Collector fluid outlet temperature (K)

T_i Collector inlet temperature (K)

T_o Collector outlet temperature (K)

T_{oi} Collector outlet initial water temperature (K)

T_{ot} Collector outlet water temperature after time t

T_w Flash vessel wall temperature (K)

U_L Heat loss coefficient (W/m^2K)

Greek

β Misalignment angle error, angle according to Fig. 3.2 (degrees)

β^* Universal nonrandom error parameter due to angular errors ($\beta^*=\beta$ C)

γ Intercept factor

ΔT Temperature difference $[T_i-T_a]$ (k)

Θ Angle of incidence (degrees)

Θm Half acceptance angle (degrees)

σ Total reflected energy standard deviation

σ^* Universal random error parameter ($\sigma^*=\sigma$ C)

σ_{mirror} Standard deviation of the variation in diffusivity of the reflective material at normal incidence

σ_{slope} Standard deviation of the distribution of local slope errors at normal incidence

σ_{sun} Standard deviation of the energy distribution of the Sun's rays at normal incidence

ϕ_r Rim angle (degrees)

ABBREVIATIONS

a.c. Alternate current

BS British Standard

CR Concentration Ratio

CdS Cadmium Sulphide

C£ Cyprus Pounds

DAS Data Acquisition System

d.c. Direct current

E Equinox, East

ED Electrodialysis

ER–RO Energy Recovery – Reverse Osmosis

H Height (m)

I/O Input/Output

LCC Life Cycle Cost

LCR Local Concentration Ratio

LCS Life Cycle Savings

LDR Light Dependent Resistor

LTV Long Tube Vertical

MDF Medium Density Fibres

MEB Multiple Effect Boiling

MES Multiple Effect Stack

MSF Multi–Stage Flash

N North, Number of years

P Pressure

ppm Parts per million

PR Performance Ratio

PTC Parabolic Trough Collector

PW Present Worth

PWF Present Worth Factor

RO Reverse Osmosis

RHS Rigid Hollow Section

S South

SS Summer Solstice

T Temperature

TDS Total Dissolve Solids

VC Vapour Compression

W West

WHO World Health Organisation

WS Winter Solstice

Blank page

CHAPTER 1

CHAPTER 1

INTRODUCTION

Water is one of the most abundant resources on earth, covering three-fourths of the planet's surface. Ninety seven percent of the earth's water is salt water in the oceans, and three percent fresh water. This small percentage of the earth's water is in ground-water, lakes and rivers, and this water supplies most of humanity.

One of the most serious problems facing Cyprus today is water shortage. In this chapter, after a historical introduction into solar desalination, an attempt is made to define the problem quantitatively. Some aspects of sea-water quality and temperature are also investigated.

1.1 HISTORY OF SOLAR DESALINATION

Solar distillation has been in practice for a long time. According to Malik *et al.* [1985] the earliest documented work is that of an Arab alchemist in the fifteenth century reported by Mouchot in 1869. Mouchot reported that the Arab alchemist had used polished Damascus mirrors for solar distillation.

The great French chemist Lavoisier (1862) used large glass lenses, mounted on elaborate supporting structures, to concentrate solar energy on the contents of distillation flasks [Malik *et al.*, 1985]. The use of silver or aluminum coated glass reflectors to concentrate solar energy for distillation has also been described by Mouchot.

Solar stills were the first to be used on large scale distilled water production. The first water distillation plant constructed was a system built at Las Salinas, Chile, in 1874 [Malik *et al.*, 1985; Meinel and Meinel, 1976]. The still covered 4700 m^2 and produced up to 23,000 l of fresh water per day, (4.9 l/m^2), in clear Sun. The still was operated for 40 years and was abandoned only after a fresh-water pipe was installed supplying water to the area from the mountains.

The renewal of interest on solar distillation occurred after the first world war at which time several new devices had been developed such as: roof type, tilted wick, inclined tray and inflated stills. A survey of these simple methods of distilled water production, together with some other more complicated ones is presented in chapter 2.

The use of solar concentrators in solar distillation has been reported by Pasteur (1928) [Malik *et al.*, 1985] who used a concentrator to focus solar rays onto a copper boiler containing water. The steam generated from the boiler was piped to a conventional water cooled condenser in which distilled water was accumulated.

1.2 THE WATER PROBLEM

The water problem of Cyprus is analysed by considering two parameters:
- The precipitation; and
- The water demand.

1.2.1 Precipitation on Cyprus

Cyprus, being a relatively small island in the north-eastern part of the Mediterranean Basin, with no permanent rivers and limited ground water resources, relies entirely on the annual precipitation for its survival.

Cyprus has an intense Mediterranean climate with the typical seasonal rhythm strongly marked with respect to temperature, precipitation and weather generally. Rainfall on Cyprus usually occurs as moderate or heavy showers. Long periods of rain are unusual, though moderate or heavy continuous rain may persist for some time. Snowfalls occur every Winter on ground above 1000m [Meteorological Service, 1991].

The Winter in Cyprus is very unstable because the island is near the track of unstable weather systems which cross the Mediterranean sea frequently from West to East. These systems give periods of disturbed weather usually lasting for one to three days and produce most of the annual precipitation. Records of precipitation on Cyprus cover about a hundred years. The annual average precipitation on Cyprus for 70 years (1920-1991)

is shown in Fig. 1.1. The average annual precipitation over the whole island, for the period shown in Fig. 1.1, is 490mm. The period's maximum and minimum precipitation are 757mm (1968) and 182mm (1972) respectively. These values are as high as 154% and as low as 37% of the average for this period. It can be deduced from the data presented in Fig. 1.1 that every 5.4 years there is a drought with precipitation of less than 390mm. This is estimated on the basis of 95% confidence interval and a maximum error of 11.7% [Kalogirou *et al.*, 1993b].

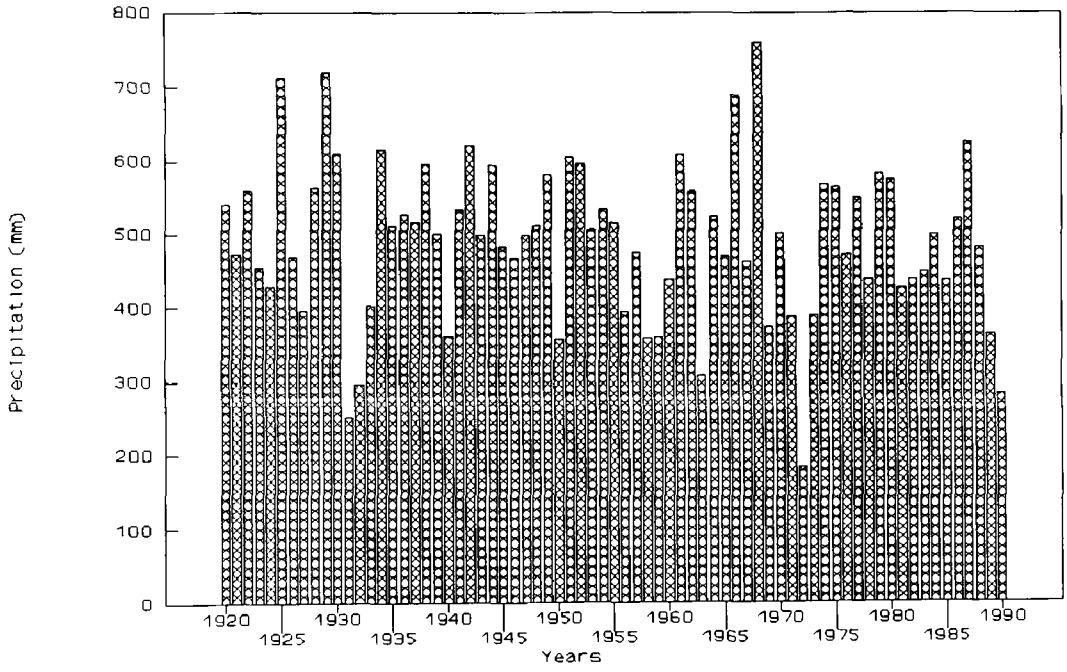

Fig. 1.1 Precipitation on Cyprus

It must be noted that a single value of precipitation for the whole island, as shown in Fig. 1.1, smooths out a much greater variation in particular districts. The greatest amount of precipitation, about 53% of the total, falls on the Troodos mountains (38% of the total island area).

A picture of the precipitation for a typical year for the period 1951–1980 is shown in Table 1.1 [Meteorological Service, 1991]. From this table it can be observed that the most significant rainfall occurs from November to March. The Spring, Summer, and Fall months are very dry.

Month	Amount (mm)	Percent
JAN	99.4	20.9
FEB	69.3	14.5
MAR	56.5	11.9
APR	29.7	6.2
MAY	18.4	3.9
JUN	5.8	1.2
JUL	2.0	0.4
AUG	2.5	0.5
SEP	5.3	1.1
OCT	31.9	6.7
NOV	48.7	10.2
DEC	107.2	22.5

Table 1.1 Distribution of precipitation over the months of the year (years 1951–1980)

1.2.2 The Water Demand

The water demand in 1991 was 250 million m^3. This is apportioned in two main sectors namely irrigation and potable water as shown in Table 1.2 [Lytras, 1991]. For this study the potable water is subdivided into three categories, domestic, tourism and industry. Tourism water consumption is the water used by the hotels, bungalows and tourist villages. From this table it is evident that the greatest percentage of water is used by the agricultural sector (68%).

Cyprus is an agricultural country and the water consumed for irrigation is subsidised by the Government. The Ministry of Agriculture and Natural Resources is currently evaluating the possibility of using new developed varieties of plants which require less water. Recently new ways of watering have been applied to conserve water by directing it to the plants avoiding losses due to evaporation. The Government Authorities are considering a change in the subsidisation scheme in such a way as to make it dependent on production output rather than total water consumption.

Another small but significant amount of water, 6.3% of the total and 19.8% of the potable water, is used by the tourist industry. The number of tourists during 1990 was 1.5 million which is about 260% of the population of the island. Over and above this, the tourists are not as conservation conscious as the locals. From a survey conducted by the author, it is estimated that each tourist utilises approximately 375 litres of water per day, which is about twice the quantity used by the locals. In the coming years the number of tourists expected is even larger which means that the water requirements will increase.

Sector	Quantity (million m^3)	Percent
IRRIGATION	170	68.0
POTABLE WATER	80	32.0
- Domestic	58.1	23.2
- Tourism	15.8	6.3
- Industry	6.1	2.5

Table 1.2 The water consumption pattern for 1991

The total water requirements have been increased by 34.6% over the last ten years for various reasons. The most important ones are the fast economic development which led to a higher standard of living, (swimming pools, dish washers etc.) and the increase in the number of tourists. One economic index which can be used to indicate the magnitude of the economic development is the per capita Gross National Product which, for the same period increased from C£2050 in 1982 to C£4960 at 1991 market prices [Economic Report, 1991]. The problem became more profound after the loss of control of the water resources in the occupied part of Cyprus.

The total consumption of water in the major towns together with the average consumption per consumer and the price per m^3 for the first 40 m^3 is shown in Table 1.3 [Lytras, 1991]. A few important points can be drawn from this table. Firstly the price is not uniform but differs from town to town. This is based on the distance of the town from the location of the dams. Thus for the town of Limassol which is near to the largest dam (of 115 million m^3 capacity) the price is very low whereas for the town of Nicosia the tariffs are higher. Secondly, due to the low price, the consumption in

Limassol is much higher than the other towns. For these reasons a Water Authority will be established in the near future to regulate water consumption and price.

Town	Price (C£/m^3)	Total consumption (million m^3)	Specific consumption (l/day/consumer)[Lytras, 1991]
Nicosia	0.32	12.11	505
Limassol	0.05	11.06	699
Larnaca	0.20	3.86	511
Paphos	0.15	2.21	620
Notes: 1. Data for the year 1991 2. Price is for the first 40 m^3			

Table 1.3 Water consumption and price in various Cyprus towns

Various measures have been applied by the Cyprus Government to conserve water and reduce consumption. These measures applied in the early eighties are focused on conservation campaigns and proved to have some effect as shown in Table 1.4. The mean specific consumption reduction in ten years has been 5.4%. A law came into being in 1991, which imposes fines on people using water irrationally, and specifies the number of days the Water Boards can restrict water supply to consumers according to the water quantities available.

Town	Specific consumption (l/day/consumer)		Percentage reduction
	Year 1991	Year 1982	
Nicosia	505	539	6.3
Limassol	699	723	3.3
Larnaca	511	548	6.8
Paphos	620	650	4.6

Table 1.4 Effect of water conservation measures on water consumption

1.2.3 Comparison of Precipitation and Water Demand

By considering a year with average precipitation of 490mm, the overall precipitation on the island is 4530 million m^3. A large amount of this water, about 44%, is lost by

evapotranspiration, and another large amount, about 28%, is lost by evaporation. The annual surface run-off is estimated at 600 million m^3 (13%) [Meteorological Service, 1991]. It is evident from these figures that only 15% of the annual precipitation (680 million m^3) are available both as surface and ground-water.

The present water management system consists of large dams which are located at the footings of the Troodos mountains, collecting water during the Winter months. A piping network is used throughout the island together with large pumping stations for the distribution of the water to all consumers. In 1991 the total water capacity of the dams reached 275 million m^3 [Lytras, 1991].

It is evident from the above that the water held in the dams (full capacity) is almost equal to the water requirements per year. By adding the water supplied by various boreholes and springs, which for a year with average precipitation provide 370 million m^3 and 30 million m^3 respectively, the total water quantity available is just adequate, with the present rate of consumption, to cover the requirements of a drought year. For such a year the losses due to evaporation and evapotranspiration are much greater than the values indicated for the normal year because the lack of rain is accompanied with high temperatures and high solar radiation.

Whether the policy of building dams, against the erection of desalination systems, was the correct one is a matter of debate. This is because a lot of money is spent in building the dams and no guarantee can be provided that the water shortage problem would be solved as again the dependence on the weather is not alleviated. This is strengthened by the fact that to date the maximum water saved in the reservoirs was 202 million m^3 (1989) which is equal to 74% of the reservoirs capacity.

In addition to the above, the environmental destruction caused by the erection of the dams should not be under estimated. Lately, for the construction of the largest dam, (115 million m^3 capacity) a small village was relocated with all the consequent expenses (borne by the Government) and the resistance from the villagers. The houses of the old village were covered by the waters of the dam.

The Water Development Department believes that the present water management system can supply all the water requirements of Cyprus up to the year 2005. This of course applies provided that the unavoidable drought years of the period, receive precipitation of at least 400mm. Therefore the Cyprus Government is planning to erect a 20,000 m^3/day desalination plant. The selling price of this purified water is estimated to be C£1.00/m^3.

Cyprus enjoys a high level of solar radiation throughout the year, which is probably the greatest natural resource of the island. As early as 1979 the Water Development Department had foreseen the need for a desalination plant on the island. A plant using solar energy was thought to be one of the possibilities. Inspite of the choice for a large scale desalination system, the Department is still trying to establish a pilot desalination plant employing solar energy.

The viability of any desalination system depends on the cost of the water produced. This can be treated in two ways. The fresh water can be added to the available water (from dams, boreholes and wells). In this case a price of C£1.00/m^3 of the produced water is considered feasible for supplying water to towns. Such a price will imply about 30% increase in the current water price for a 20% contribution to the total with desalination water. A second alternative is to use the fresh water in specific sectors of the economy such as the tourist industry. From a survey conducted in eight hotels by the author, it was found that the hotel managers are willing to pay C£1.00/m^3 for water produced by a desalination system. It must be noted that now hotels are buying water, when the need arises, at a price ranging from C£1.30 to C£2.00/m^3 depending on the location of the water source. This is in stark contrast to the farming community who could not justify paying more than present prices of approximately C£0.05 - C£0.10 per m^3.

1.3 ENVIRONMENTAL PARAMETERS

The environmental factors affecting the operation of solar desalination plants are solar radiation, ambient air temperature and the sea-water temperature. Some typical solar radiation and ambient air temperature are shown in Appendix 1 in a tabular form, called the reference year. These were obtained from previous work [Kalogirou, 1991].

The mean sea-water temperature for the three main coastal towns as given by the Department of Fisheries [Surface sea-water temperature, 1988] are shown in Table 1.5. From this table it can be concluded that the sea-water temperature is almost constant throughout the year.

MONTH	Limassol	Larnaca	Paphos
JAN	16.4	16.0	16.2
FEB	15.9	15.5	15.5
MAR	16.4	16.4	16.3
APR	17.3	17.9	17.7
MAY	19.2	20.1	19.6
JUN	21.8	22.8	21.2
JUL	23.3	25.5	23.1
AUG	24.6	26.8	24.5
SEP	24.9	26.5	24.9
OCT	23.8	24.5	23.7
NOV	21.4	21.0	20.9
DEC	18.5	17.8	17.9

Table 1.5 Mean sea-water temperature in Deg.C (Years 1971-1985)

ITEM	Sea-water	Drinking water	Units
PH	7.9	6.5-8.5	-
Chloride (CL)	21,800	250	ppm
Sulphate (SO_4)	2,900	400	ppm
Sodium (Na)	11,800	200	ppm
Total solids	39,000	1000	ppm
Total hardness as $CaCO_3$	7,400	500	ppm

Table 1.6 Partial ionic analysis of sea-water and comparison with drinking water standard

Since the input to any desalination system is sea-water its quality is important. A typical analysis of sea-water performed by the State General Laboratory is shown in Table 1.6 together with the drinking water requirements given by World Health Organisation [WHO, 1984]. The total number of dissolved solids in sea-water is 39,000 ppm (parts per million) which according to the above standard will have to be reduced considerably such that the water is suitable for drinking.

1.4 PROJECT OBJECTIVES

The objectives of this work are:

1. Evaluate the status of the water resources of Cyprus against the water demand.
2. To develop a parabolic trough collector system producing low pressure steam and evaluate its performance.
3. Analyse economically various sizes of desalination systems, powered by low pressure steam, produced by the parabolic trough collector system and examine the viability of the proposed systems.

1.5 STRUCTURE OF THESIS

In chapter 2 a survey of the available desalination systems is presented. Special attention is given to the way solar energy can be utilised. The chapter concludes with a selection of a system which best matches with parabolic trough collectors and this is employed in the subsequent analysis.

Chapter 3 deals with the design of the system. This include the design of the collector, of the steam generation system, and of the complete desalination circuit. Special consideration is given to the intercept factor evaluation, the distribution of energy on the collector receiver pipe, and on the mode of tracking selection. For all these items special computer programs are written and used as tools for the design. Lastly, modelling of the steam generation system is presented.

In chapter 4 the construction details of the experimental system are presented. The system consists of the parabolic trough collector and the steam generation system.

In chapter 5 the results of the various experiments are presented. These include the results obtained from the testing of the collector and of the complete system. The system pre-heat energy is then evaluated. The steam production rate is measured and compared with the results of the simulation program.

Chapter 6 deals with the refinement of the system in order to reduce the start-up energy requirement. The optimisation is carried out by the use of a computer program written for the purpose. The program is validated both under steady state and transient conditions. Performance predictions for the four types of application considered namely, two domestic, a hotel and a village, are presented.

Chapter 7 deals with the economic analysis of the system. After the system construction cost is established, a model is developed for the calculation of its cost. The viability of the system for the four types of application considered, is investigated.

The last chapter outlines the conclusions gleaned from this research project together with suggestions for further work.

Blank page

CHAPTER 2

CHAPTER 2

LITERATURE SURVEY AND SYSTEM SELECTION

Water is essential to life. The importance of supplying hygienic potable water can hardly be overstressed. Man has been dependent on rivers, lakes and underground water reservoirs for fresh water requirements in domestic life, agriculture and industry. However, the rapid industrial growth and population explosion all over the world has resulted in a large escalation of demand for fresh water. Added to this is the problem of pollution of the rivers and lakes by industrial waste and the large amount of sewage discharged. On a global scale man-made pollution of natural sources of water is becoming the single largest cause for the fresh water shortage [Malik *et al.*, 1985].

The only inexhaustible sources of water are the oceans. Their main drawback, however, is the high salinity of such water. It would be attractive to tackle the water shortage problem with the desalination of such water; this water may be mixed with brackish water to increase the amount of fresh water and bring the concentration of salts to around 500 ppm [Malik *et al.*, 1985].

Desalination can be achieved by a number of techniques. These can be classified into the following categories:

- Phase change or thermal processes.
- Membrane or single phase processes.

In Table 2.1 the most important technologies in use are listed. In the phase change or thermal processes the distillation of sea-water can be achieved by utilising a thermal energy source. Such thermal energy can be obtained from a conventional fossil fuel source, nuclear energy or from a non conventional solar energy source. In the membrane processes electricity is used either for driving high pressure pumps or for ionisation of the salts contained in the sea-water.

The desalination processes require significant quantities of energy to achieve the separation. This is highly significant as it is a recurrent cost which few of the water-short areas of the world can afford. The Middle East is unique in that, because of the

oil income it has enough money to invest and run desalination equipment. Many other areas of the world have neither the cash nor the oil resource to allow them to develop in a similar manner. According to Marinos *et al.* [1991] and Morris and Hanbury [1991] the installed capacity of desalinated water systems in 1990 reached 13 million m^3/day which by the year 2000 is expected to double. The dramatic increase in desalinated water supply will create a series of problems, the most significant of which are those related to energy consumption. It has been estimated that a production of 13 million m^3/day requires 130 million tons of oil per year. So there is a further problem. Even if oil was much more widely available could we afford to burn it at a scale to provide everyone with fresh water? Given the current understanding of the greenhouse effect and the importance of carbon dioxide levels it is debatable. Thus, apart from satisfying the additional energy demand, environmental pollution would be a major concern.

DESALINATION PROCESSES	
PHASE CHANGE PROCESSES	MEMBRANE PROCESSES
1. Multi-stage flash (MSF) 2. Multiple effect boiling (MEB) 3. Vapour compression (VC) 4. Freezing 5. Solar stills - conventional stills - special stills - wick type stills - multiple wick type stills	1. Reverse osmosis (RO) - RO without energy recovery - RO with energy recovery (ER-RO) 2. Electrodialysis (ED)

Table 2.1 Desalination processes

If desalination is accomplished by conventional technology then it will require the burning of substantial quantities of fossil fuels. Given that conventional sources of energy are polluting, sources of energy that are not polluting will have to be developed. Fortunately there are many parts of the world that are short of water but have exploitable renewable sources of energy that could be used to drive desalination processes. Cyprus is such a place where the potential water shortage problem fortunately coincides with an abundance of solar radiation.

Solar desalination is used by nature to produce rain which is the main source of fresh

water supply. Solar radiation falling on the surface of the sea is absorbed as heat and causes evaporation of the water. The vapour rises above the surface and is moved by the winds. When this vapour cools down to its dew point, condensation occurs and fresh water precipitates as rain. All available manmade distillation systems are a duplication, on a small scale, of this natural process.

Solar energy can be used for sea-water desalination either by producing the thermal energy required to drive the phase change processes or by producing electricity required to drive the membrane processes. The solar desalination systems are thus classified into two categories i.e. direct and indirect collection systems. As their name implies the direct collection systems use the solar energy to produce distillate directly in the same equipment whereas in the indirect collection systems two sub-systems are employed one for solar energy collection and one for desalination. The conventional desalination systems are similar to the solar ones as the same equipment applies. Their prime difference is that in the former either a conventional boiler is used to provide the heat required or mains electricity is used to provide the electric power required, whereas, in the latter solar energy is applied.

2.1 DIRECT COLLECTION SYSTEMS

2.1.1 Solar Stills

A representative example of direct collection systems is the conventional solar still which uses the greenhouse effect to evaporate salty water. It consists of a basin, in which a constant amount of sea-water is maintained, enclosed in a vee-shaped glass envelope (see Fig. 2.1). The Sun's rays pass though the glass roof and are absorbed by the blackened bottom of the basin. As the water is heated its vapour pressure is increased. The resultant water vapour is condensed on the underside of the roof and runs down into the troughs which conduct the distilled water to the reservoir. The still acts as a heat trap, because the roof is transparent to the incoming sunlight, but it is opaque to the infrared radiation emitted by the hot water (i.e. the greenhouse effect). The roof encloses all the vapour and prevents losses and at the same time keeps the wind from reaching the salty-water and cooling it. The stills require frequent flushing which is

usually done during the night. Flushing is performed to prevent salt precipitation [Mustachi and Cena, 1981]. The design problems encountered with this type of still are [Eibling *et al.*, 1971; Mustachi and Cena, 1981] the brine depth, the vapour tightness of the enclosure, the distillate leakage, methods of thermal insulation, and the cover slope, shape and material. A typical still efficiency, defined as the ratio of the energy utilised in vaporising the water in the still to the solar energy incident on the glass cover, is 35% (maximum) and their daily production is about 3–4 l/m^2 [Daniels, 1974].

Several attempts have been made to use simple and more economic materials such as plastics. These have advantages over glass stills in that they are cheaper, less breakable, lighter in weight for transportation, and easier to set up and mount. Their main disadvantage is their shorter life [Daniels, 1974].

A lot of variations of the basic shape shown in Fig. 2.1 were developed by various researchers to increase the production rate of solar stills [Eibling *et al.*, 1971; Kreider and Kreith, 1981; Tleimat, 1978]. Some others have used different techniques to increase the production of stills.

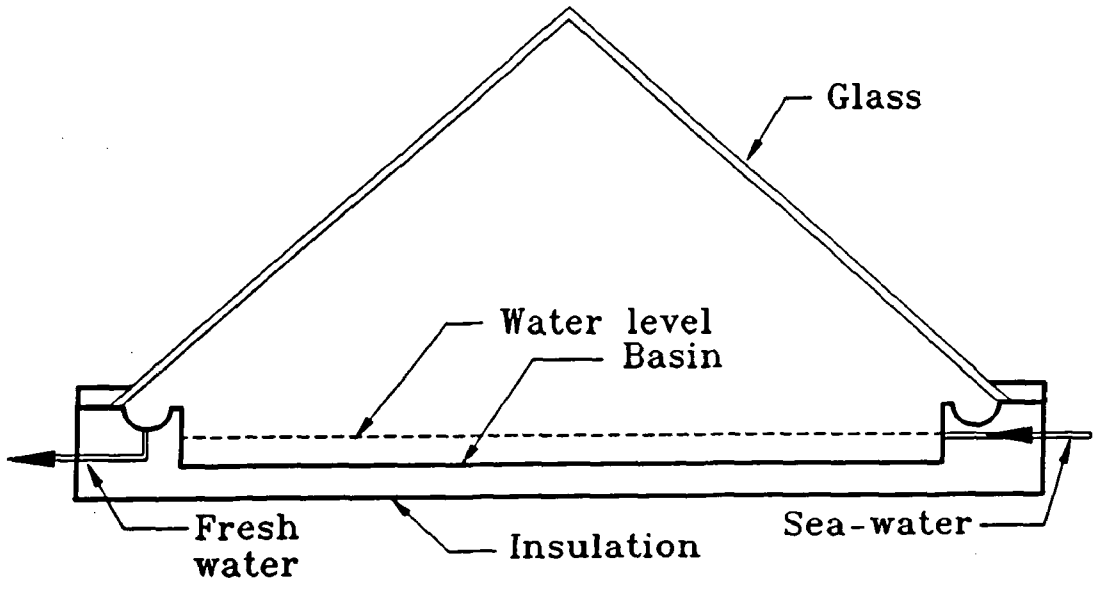

Fig. 2.1 Solar still

Rajvanshi [1981] used various dyes to enhance the performance of the solar still. These dyes darkened the water colour and therefore allow it to absorb solar radiation more readily. He concluded that with the use of black napthalamine at a concentration of

172.5 ppm, the still output could be increased by as much as 29%. The use of these dyes is perfectly safe because the evaporation in the still was performed at 60°C whereas the boiling point of the dye is in the order of 180°C. Thus, only the water evaporates.

Akinsete and Duru [1979] were successful in increasing the production of a still by lining its bed with charcoal. In particular, the presence of charcoal leads to a marked reduction in the start-up time by reducing the thermal inertia of the system. They claimed that this is due to the capillary action exhibited by the charcoal whenever is partially immersed in a liquid, its reasonably black colour and its surface roughness.

Lobo and Araujo [1978] developed a simple multi-effect basin type solar still. This still provides 40–55% increase in the fresh water produced as compared to the standard one depending on the solar radiation. The idea was to use two stills one on top of the other, the top one being made completely from glass or plastic and separated into small partitions.

A different category of still is the wick type in which a black cloth is used (usually inclined), which by capillary action draws salty water from a sink and this is then evaporated on the cloth surface. Sodha *et al.* [1981] developed a simple multiple wick type solar still in which blackened wet jute cloth forms the liquid surface. A series of jute cloth pieces of increasing length were used, separated by thin black polyethylene sheets, resting on a foam insulation. Their upper edges are dipped in a saline water tank where suction by capillary action of the cloth fibre provides a thin sheet of liquid on the cloth which is evaporated by solar energy. The results showed a 4% increase in the efficiency of the still as compared with the conventional stills.

2.2 INDIRECT COLLECTION SYSTEMS

The general principle of these systems is the implementation of two separate sub-systems, one for the collection of solar energy (i.e. the collector), and one for transforming the collected energy into fresh water (i.e. the plant). The collector sub-system will not be discussed here. The plant sub-system can be based on one of the following operating principles:

1. Phase change processes:
   - Multi-stage Flash (MSF)
   - Multiple Effect Boiling (MEB)
   - Vapour Compression (VC)
2. Membrane processes
   - Reverse Osmosis (RO)
   - Electrodialysis (ED)

The operating principle of the phase change processes is orientated towards re-using the latent heat of evaporation to pre-heat the feed whilst at the same time condensing the steam to produce fresh water. The energy requirements of these systems is normally defined in terms of units of distillate produced per unit of steam or per 2326 kJ (1000 Btu) heat input which corresponds to the latent heat of vaporisation at 73°C. This is known as the performance ratio (PR) [Spiegler and Laird, 1980a]. The operating principle of the membrane processes is orientated towards producing the electricity directly from solar energy which is used to drive the plant. For these processes the energy consumption is usually expressed in kWh/m^3.

2.2.1 Multi-stage Flash Process

The multi-stage flash (MSF) process is composed of a series of elements, called stages. In each stage condensing steam is used to pre-heat the sea-water feed. By fractionating the overall temperature differential between warm source and sea-water into a large number of such stages the system approaches the ideal total latent heat recovery. The operation of this system requires pressure (vacuum) gradients in the plant. The principle of operation of this process is shown in Fig. 2.2. Current commercial installations are designed with 10-30 stages (2°C temperature drop per stage). The typical daily output of these systems are 60-100 l/m^2 depending on the number of stages [Mustachi and Cena, 1978].

A practical cycle representing the MSF process is shown in Fig. 2.3. The system is divided into two main sections the heat recovery and the heat rejection. The sea-water feed is taken into the plant and fed through the heat rejection section, the function of which is to reject thermal energy from the plant and to allow the product and brine to

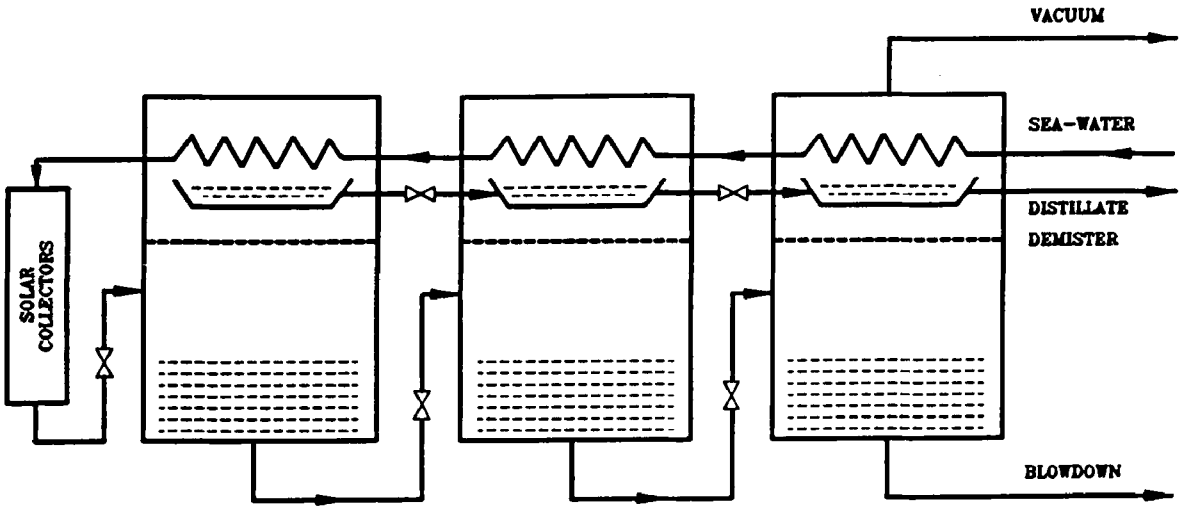

Fig. 2.2 Multi-stage flash system - principle of operation

leave the plant at the lowest possible temperature. The feed is then mixed with a large mass of water which is recirculated round the plant, known as the brine recirculation flow. This water now passes through a series of heat exchangers, its temperature being raised as it does so. After passing through the last of these, the water enters the solar collector array or a conventional brine heater having its temperature raised until it is approximately equal to the saturation temperature at the maximum system pressure. The water then enters the first stage through an orifice and in so doing has its pressure reduced. As the water was already at the saturation temperature for a higher pressure, it becomes superheated and has to give off vapour to become saturated again (flashing). The vapour produced passes through a wire mesh (demister) to remove any entrained brine droplets and thence into the heat exchanger. In this, the vapour is condensed and drips into a distillate tray. This process is then repeated all the way down the plant as both brine and distillate streams flash as they enter subsequent stages which are at successively lower pressures. In MSF the number of stages is not tied rigidly to the performance ratio required from the plant. In practice, the minimum must just be greater than the performance ratio, while the maximum is imposed by the boiling point elevation. The minimum interstage temperature drop must exceed the boiling point elevation for flashing to occur at a finite rate. This is advantageous because as we increase the number of stages, the terminal temperature difference over the heat exchangers increases and hence less heat transfer area is required with obvious savings in plant capital cost [Morris and Hanbury, 1991].

MSF is the most widely used desalination process, in terms of capacity. This is in part due to the simplicity of the process, the performance characteristics and the scale control.

A disadvantage of this process is that exact levels of pressures are required in the different stages and therefore some transient time is required to establish the normal running operation of the plant. This makes the MSF relatively unsuitable for solar energy applications unless a storage tank is used for thermal buffering [Tata, 1980].

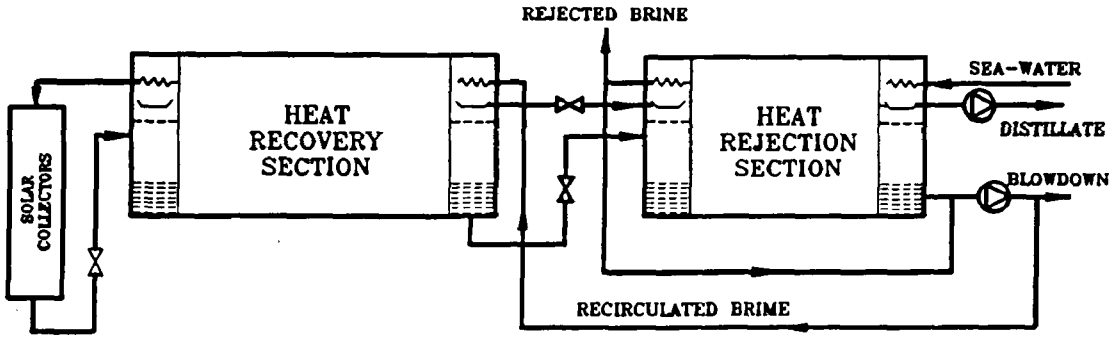

Fig. 2.3 Multi-stage flash process plant

Moustafa *et al.* [1985] reports on the performance of a 10m^3/day solar MSF desalination system tested in Kuwait. The system consisted of a 220m^2 parabolic trough collectors, 7,000 litre thermal storage and 12-stage MSF desalination system. The thermal storage system was used to level off the thermal energy supply and allow the production of fresh water to continue during periods of low radiation and night-time. The output of the system is reported to be over ten times the output of solar stills for the same solar collection area.

2.2.2 The Multiple Effect Boiling Process

The multiple effect boiling (MEB) process, shown in Fig. 2.4, is again composed of a number of elements, which, in this case are called effects. The steam from one effect is used as a heating fluid in another effect which, while condensing causes evaporation of a part of the salty solution. The produced steam goes through the following effect, where, while condensing, makes some of the other solution evaporate and so on. For this to be possible the heated effect must be kept at a pressure lower than that of the effect

from which the heating steam originates. The solutions condensed by all effects, are used to pre-heat the feed [Mustachi and Cena, 1981].

In this process vapour is produced by two means, by flashing and by boiling, but the majority of the distillate is produced by boiling. Unlike MSF plant the MEB process usually operates on a once through system having no large mass of brine recirculated round the plant. This reduces the pumping requirements and also reduces scaling tendencies.

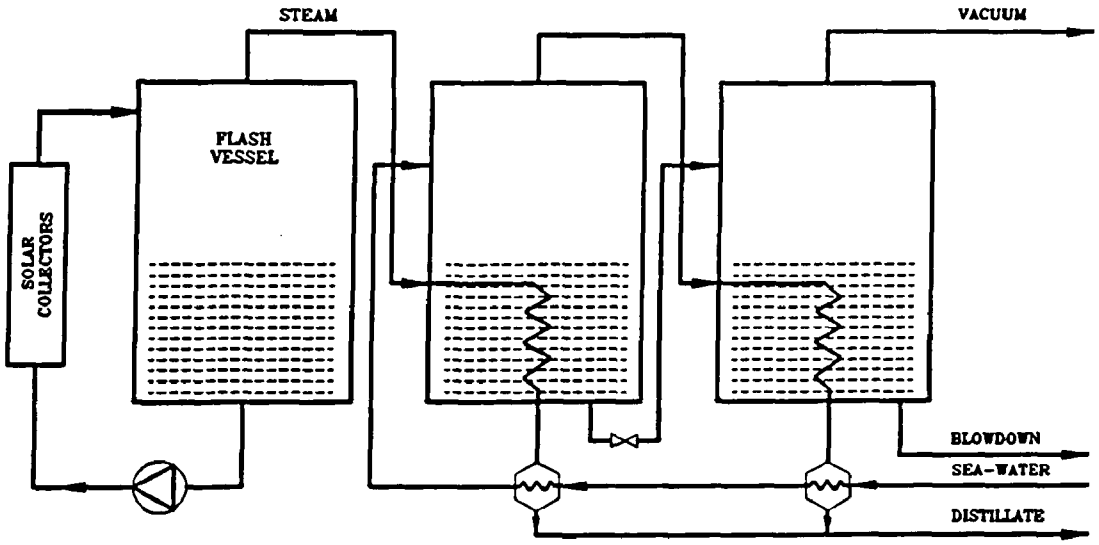

Fig. 2.4 Multiple effect boiling system - principle of operation

There are many possible variations of MEB plants, depending on the combinations of heat transfer configurations and flowsheet arrangements used. Early plants were of the submerged tube design, and used only two to three effects. Modern systems have got round the problem of low evaporation rate by making use of the thin film designs with the feed liquid distributed on the heating surface in the form of a thin film instead of a deep pool of water. Such plants may have vertical or horizontal tubes. The vertical tube designs are of two types, the climbing film natural and forced circulation type, and the long tube vertical straight falling film. In the long tube vertical (LTV) plants, shown in Fig. 2.5, the brine boils inside the tubes and the steam condenses outside. In the horizontal tube falling film design the steam condenses inside the tube with the brine evaporating on the outside.

As with the MSF plant, the incoming brine passes thought a series of heaters but after passing through the last of these, instead of entering the brine heater, the feed enters the top effect where the heating steam raises its temperature to the saturation temperature for the effect pressure. Further amounts of steam, either from a solar collector system or from a conventional boiler, are used to produce evaporation in this effect. The vapour then goes, in part, to heat the incoming feed and in part to provide the heat supply for the second effect which is at a lower pressure and receives its feed from the brine of the first effect. This process is repeated all the way down the plant. The distillate also passes down the plant. Both the brine and distillate flash as they travel down the plant due to the progressive reduction in pressure.

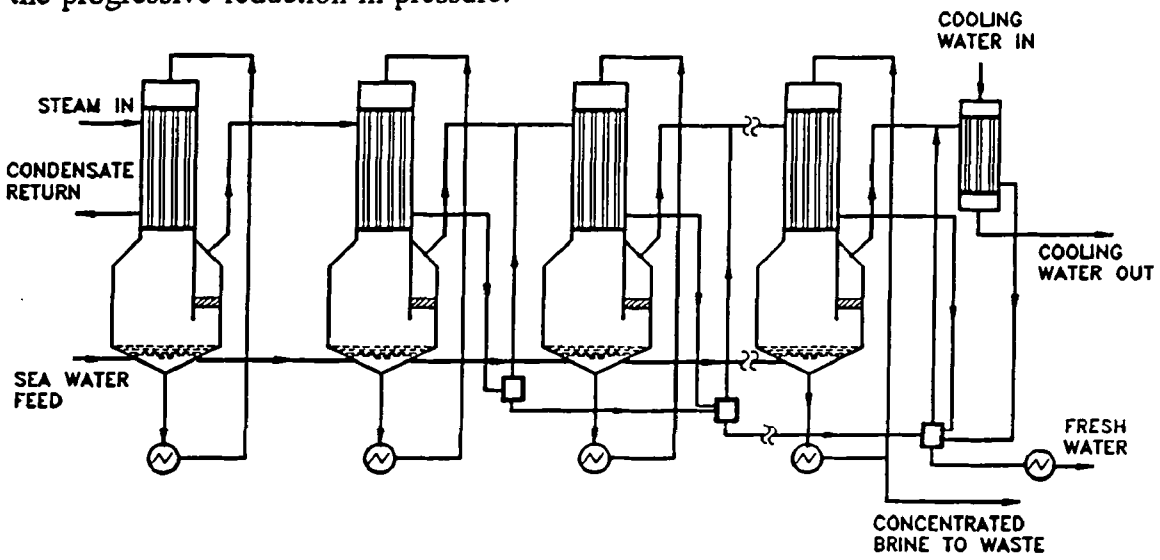

Fig. 2.5 Long tube vertical (LTV) multiple effect boiling plant

Unlike MSF, the performance ratio for an MEB plant is more rigidly linked to, and cannot exceed, a limit set by the number of effects in the plant. For instance, a plant with 13 effects might typically have a PR of 10. However, an MSF plant with a PR of 10 could have 13 to 35 stages depending on the design. MSF plants have a maximum PR of 13 approximately. Normally the figure is between 6 and 10. MEB plants commonly have performance ratios as high as 12 to 14 [Morris and Hanbury, 1991].

The main difference between this process and the MSF is that the steam of each effect just travels to the following effect where it is immediately used for pre-heating the feed. This process requires more complicated circuit equipment in comparison with MSF; on the other hand, it has the advantage that is suitable for solar energy utilisation because

the level of operating temperature and pressure equilibrium is less critical [Tata, 1980].

A 14 effect MEB plant with nominal output of $3m^3/hr$ coupled with $2,672m^2$ parabolic trough collectors (PTC) is presented by Zarza *et al.* [1991a and 1991b]. The system is installed at the plataforma solar de Almeria in Southern Spain. It also incorporates a $155m^3$ thermocline thermal storage tank. The circulated fluid through the solar collectors is a synthetic oil heat transfer fluid (3M santotherm 55). The performance ratio obtained by the system varies from 9.3 to 10.7 depending on the condition of the evaporator tube bundle surfaces. The authors estimated that the efficiency of the system can be increased considerably by recovering the energy wasted when part of the cooling water in the final condenser is rejected. The recovery will be performed with a double effect absorption heat pump.

2.2.3 The Vapour Compression Process

In a vapour compression (VC) plant the heat recovery is based on raising the pressure of the steam from a stage by means of a compressor, see Fig. 2.6. Condensation temperature is thus increased and the steam can be used to provide energy to the same stage it came from, or to other stages [Mustachi and Cena, 1978 and 1981].

As in a conventional MEB system, the vapour produced in the first effect is used as the heat input to the second effect which is at a lower pressure. The vapour produced in the last effect is then passed to the vapour compressor where it is compressed, its saturation temperature being raised in the process, before being returned to the first effect. The compressor represents the major energy input to the system and as the latent heat is effectively recycled around the plant, the process has the potential for delivering high performance ratios [Morris and Hanbury, 1991].

Parametric cost estimates and process designs have been carried out and show that this type of plant is not particularly convenient, unless it is combined with an MEB system. Further, it appears that the mechanical energy requirements have to be provided with a primary drive such as a diesel engine, and cooling the radiator of such an engine provides more than enough heat for the thermal requirements of the process, making the

solar collector system redundant [Eggers, 1979]. Therefore the vapour compression system can be used in conjunction with MEB system and operated at periods of low solar radiation or overnight.

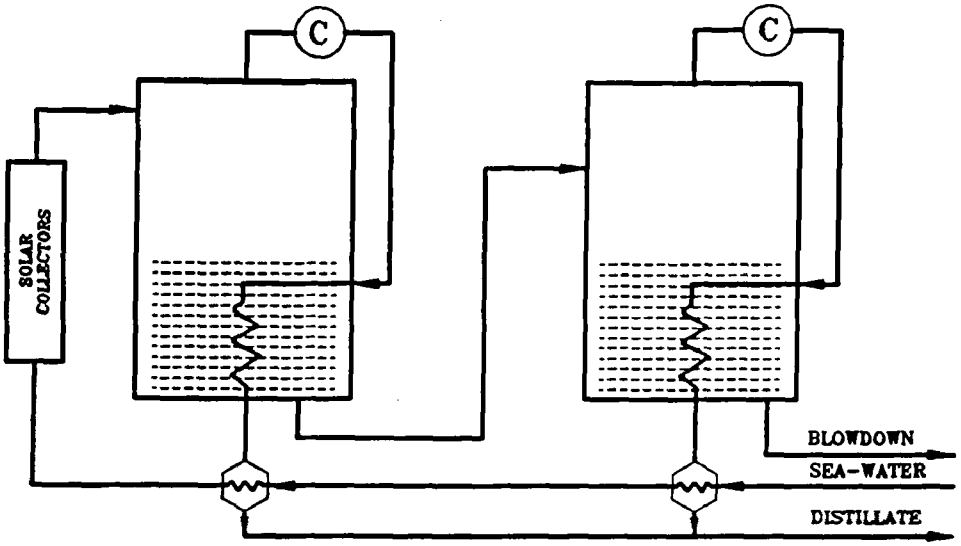

Fig. 2.6 Vapour compression system - principle of operation

The main problems associated with VC process are [Morris and Hanbury, 1991]:

1. Vapour carry over of brine into the compressor which results in corrosion of the compressor blades.
2. Limitations in the size of the plant due to compressor capacities.

2.2.4 Reverse Osmosis

This system depends on the properties of certain semi-permeable membranes which, when used to separate water from a salt solution, allow fresh water to pass into the brine compartment under the influence of osmotic pressure. If a pressure in excess of this value is applied to the salty solution, fresh water will pass from the brine into the water compartment. Theoretically, the only energy requirement is to pump the feed water at a pressure above the osmotic one. In practice higher pressures must be used in order to have a sufficient amount of water passing through a unit area of membrane [Spiegler and Laird, 1980b]. Solar energy can be used with RO (reverse osmosis) systems as a prime mover source driving the pumps [Luft, 1982] or with the direct production of electricity with photovoltaic panels [Grutcher, 1983]. The output of RO systems is about 500-1000 litres per day per square metre of membrane, depending on the amount of

salts in the raw water and the condition of the membrane.

The membranes, being in effect very fine filters, are very sensitive to fouling, both biological and non-biological. To avoid fouling careful pre-treatment of the feed is necessary before it is allowed to come into contact with the membrane surface. In larger plants and in plants powered from photovoltaic solar panels the reject brine pressure is recovered in a brine turbine. Such systems are called energy recovery reverse osmosis (ER-RO).

Tabor [1990] analyzed a system using a RO desalination unit driven by solar photovoltaic panels or from a solar-thermal plant. He concluded that the cost of the fresh water is about the same when compared with RO system operated from mains power supply. This is due to the high cost of the solar equipment.

2.2.5 Electrodialysis

This system works by reducing salinity by transferring ions from the feed water compartment, through membranes, under the influence of an electrical potential difference. Saline feedwater contains dissolved salts separated into positively charged sodium and negatively charged chlorine ions (see Table 1.6). These ions will move towards an oppositively charged electrode immersed in the solution, i.e. positive ions (cations) will go to the negative electrode (cathode) and negative ions (anions) to the positive electrode (anode). If special membranes, alternatively cation-permeable and anion- permeable, separate the electrodes, the centre gap between these membranes will be depleted of salts [Spiegler and Laird, 1980a]. As the energy requirements of the system are proportional to the water's salinity, electrodialysis (ED) is more economic when the salinity of the feedwater is not more than about 6,000 ppm of dissolved solids. Similarly, due to the low conductivity which increases the energy requirements of very pure water, the process is not suitable for water of less than about 400 ppm of dissolved solids.

Solar energy can by used with electrodialysis by directly producing the voltage difference required with photovoltaic panels.

2.3 PROCESS SELECTION

After the description of different types of desalination processes the one that best couples with parabolic trough collectors can be selected. The selection is based on the following factors:

1. Suitability of the process for PTC application.
2. The effectiveness of the process with respect to energy consumption.
3. The capital cost of the equipment.
4. The sea-water treatment requirements.

As PTC's provide thermal energy a phase change indirect collection process would appear to be most appropriate in this application. However recently, reverse osmosis is gaining ground, therefore the various processes described in section 2.2 will be compared with respect to their energy and sea-water treatment requirements and their capital cost.

From a survey of manufacturers data, the energy required for various desalination processes is obtained as shown in Table 2.2.

Process	Heat input (KJ/kg of product)	Mechanical power input (kWh/m^3 of product)	Prime energy consumption (kJ/kg of product)
MSF	294	3.7	338.4
MEB	123	2.2	149.4
VC	-	16	192
RO	-	12	144
ER-RO	-	7.9	94.8
ED	-	12	144
Note: Assumed conversion efficiency of electricity generation of 30%			

Table 2.2 Energy consumption of desalination systems

It can be seen from this table that the process with the smallest energy requirement is RO with energy recovery. But this is only viable for very large systems due to the high

cost of the energy recovery turbine. The next lowest is the RO without energy recovery and the MEB. A comparison of the desalination equipment cost and the sea-water treatment requirement as obtained from a survey of manufacturers data is shown in Table 2.3. The MEB is the cheapest of all the plants listed and also requires the simplest sea-water treatment. RO although requiring a smaller amount of energy is expensive and requires a complex sea-water treatment.

The main scope of this project is to utilise a renewable energy source for desalination. Therefore one alternative is to use a RO system powered with photovoltaic cells. According to Zarza *et al.* [1991b] who compared the RO powered with photovoltaic generated electricity with MEB plant coupled to PTC's:

1. The total cost of fresh water produced by an MEB plant coupled to parabolic trough collectors is less than that of the RO plant with photovoltaic cells due to the high cost of the photovoltaic generated electricity.
2. The highly reliable MEB plant operation makes its installation possible in those countries with high insolation levels but with a lack of personnel with expertise. As any serious mistake during operation of a RO plant can ruin its membranes, these plants must be operated by skilled manpower.

Distillation processes are also preferred for desalination because water is boiled, which ensures that the distilled water does not contain any micro-organisms.

ITEM	MSF	MEB	VC	RO
Scale of application	Medium-large	Small-medium	Small	Small-large
Sea-water treatment	Scale inhibiter Anti foam chemical	Scale inhibiter	Scale inhibiter	Sterilizer Coagulant Acid Deoxidiser
Equipment price (C£/m^3) (1993 prices)	1200-2000	1250-1900	1800-2900	2000-2550 Membrane replacement every 3-4 years

Table 2.3 Comparison of desalination plants

As can be seen from section 2.2 PTC's has been used in various applications coupled with both MSF and MEB desalination systems. According to Tables 2.2 and 2.3 the MEB process requires less specific energy, is cheaper and requires only a very simple sea-water treatment when compared with MSF. In addition the MEB process exhibits various advantages when compared to other distillation processes. According to Porteous [1975] these are as follows:

1. Energy economy as the brine is not heated to above its boiling point as in MSF process. This leads to inherently less irreversibilities in the MEB process as the vapour is used at the temperature at which it is generated.
2. The feed is at its lowest concentration at the highest plant temperature so that scale formation risks are minimised.
3. The feed flows through the plant in series and as the maximum concentration only occurs in the last effect the worst boiling point elevation is confined to this effect.
4. The other processes have a high electrical demand because of the recirculation pump in the MSF or the vapour compressor in the VC systems.
5. MSF is prone to equilibrium problems which reflect themselves in a reduction in performance ratio. In MEB plants the vapour generated in one effect is used in the next and performance ratio is not subject to equilibrium problems.
6. Plant simplicity is promoted by the MEB process as less effects are required to give a certain PR.

Therefore the MEB process appears to be the most suitable to be used with parabolic trough collectors. Parabolic trough collectors can be used for producing the input power to MEB system in the form of low pressure steam. The temperature required for the heating medium is 70-100°C. The design of the proposed PTC, of the steam generation system and of the desalination system circuit now follows in chapter 3.

Blank page

CHAPTER 3

CHAPTER 3

SYSTEM DESIGN

This chapter deals with the design of the parabolic trough collector (PTC), of the steam generation system, and of the desalination system circuit.

First of all the design of the collector is presented. Special consideration is given to the analysis of the intercept factor and to the design of the receiver. This is followed by the tracking mechanism design which includes the mode of tracking selection.

Lastly, the desalination system is designed including the design of the steam generation system and the desalination system circuit arrangement.

In addition to the modelling and simulation program a number of computer programs were written and used as tools for the design of the system. All the programs are written in modular form so that they can be run independently. A controlling program called "SKDES" was written for menu driven operation of the different modules. Detailed instructions on how to run the programs along with their listing are shown in Appendix 2.

3.1 COLLECTOR SYSTEM DESIGN

3.1.1 Parabolic Trough Collector Dimensions

Parabolic trough collectors are employed for a variety of applications including industrial steam production [Murphy and Keneth, 1982] and hot water production [Kalogirou and Lloyd, 1992b]. Parabolic trough collectors are preferred for solar steam generation because high temperatures can be obtained without any serious degradation in the collector efficiency. In this project the PTCs are used for purified water production by producing the steam for a MEB evaporator.

One measure of performance of a PTC is the instantaneous efficiency. This can be

obtained by an energy balance on the receiver of the collector. The instantaneous efficiency is defined as the rate at which useful energy (q_u) is delivered to the working fluid per unit of aperture area divided by the beam solar flux (I) at the collector aperture plane. Another important performance parameter is the optical efficiency which is defined as the ratio of the energy absorbed by the receiver to the energy incident on the concentrator's aperture. The optical efficiency depends on the optical properties of the various materials involved, the geometry of the collector, and the various imperfections arising from the construction of the collector. The geometry of the collector dictates the geometric factor (A_f) which is a measure of the effective reduction of the aperture area due to abnormal incidence effects. Relations for the instantaneous efficiency, the optical efficiency, the parabolic shape, and the geometric factor are shown in Fig. 3.1.

It is evident from the relations presented in Fig. 3.1 that the collector performance depends on the collector dimensions which are interrelated. For example, an increase in receiver diameter increases the intercept factor (defined as the ratio of the energy intercepted to the energy reflected by the parabola) and therefore the optical efficiency, but at the same time decreases the concentration ratio (CR) and consequently the thermal efficiency.

The design of the collector employed in this system is based on previous work [Kalogirou, 1991] in which the optimisation and design of a PTC were carried out. The collector previously constructed had an aperture area of 1 m^2. For the purpose of this project a bigger aperture area of 3.5 m^2 was constructed. This area leads to a size of aperture which with the optimum concentration ratio of 21.2 gives a receiver diameter of 22mm (standard pipe size).

The specifications of the previously constructed collector model are detailed in [Kalogirou and Lloyd, 1992a] and [Kalogirou and Lloyd, 1992b]. Using the same design procedures which are described in Kalogirou *et al.* [1994a, appended], the new collector dimensions can be obtained as shown in Table 3.1.

The design of the collector receiver and tracking mechanism, including the analysis of intercept factor and mode of tracking selection, now follows.

PTC GENERAL RELATIONS

Concentration ratio: $C = \frac{W_a}{\pi D}$

Parabola aperture: $W_a = 2\, r_r \sin(\phi_r) = 4\, f \tan(\frac{\phi_r}{2})$

Geometric factor: $A_f = \frac{\frac{2}{3} W_a h_p + f W_a \left(1 + \frac{W_a^2}{48 f^2} \right)}{A_a}$

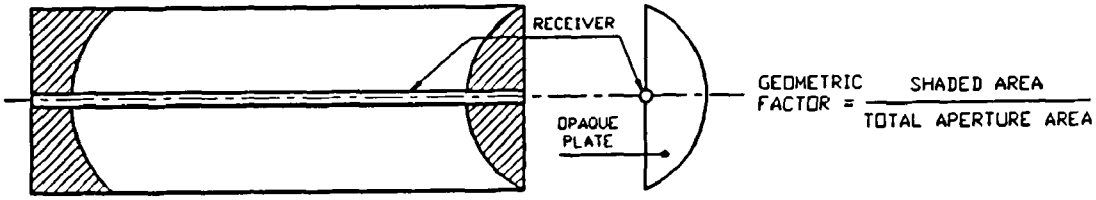

PTC EFFICIENCY RELATIONS

Optical efficiency: $n_o = \rho_m\, \tau_c\, \alpha_a\, \gamma\, [(1 - A_f \tan(\theta))\cos(\theta)]$

Rate of useful energy: $q_u = n_o\, I\, A_a - U_L(T_r - T_a) A_r$

Thermal efficiency: $n = \frac{q_u}{I A_a} = n_o - \frac{U_L(T_r - T_a)}{I C}$

$$= F_R \left[n_o - \frac{U_L (T_i - T_a)}{I C} \right]$$

SYMBOLS:

D	=	Receiver diameter (m)
r_r	=	Rim radius (m)
f	=	Focal distance (m)
ϕ	=	Parabolic angle (deg)
ϕ_r	=	Rim angle (deg)
h_p	=	Parabola height (m)
ρ_m	=	Mirror reflectivity
τ_c	=	Transmittance of cover material
α_a	=	Receiver absorptivity
γ	=	Intercept factor
Θ	=	Angle of incidence (deg)
A_a	=	Collector aperture area (m^2)
A_r	=	Receiver area (m^2)
T_r	=	Mean receiver temperature (K)
T_a	=	Ambient air temperature (K)
T_i	=	Receiver inlet temperature (K)
I	=	Direct solar radiation (W/m^2)
F_R	=	Heat removal factor
U_L	=	Heal loss coefficient (W/m^2K)

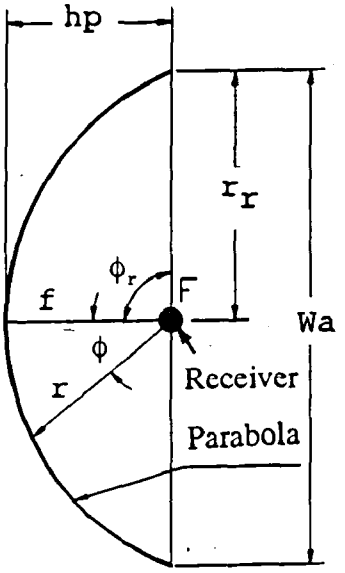

Fig. 3.1 PTC relations

ITEM	VALUE
Collector aperture area	$3.5m^2$
Collector aperture	1.46m
Aperture-to-length ratio	0.64
Rim angle	90°
Glass-to-receiver diameter ratio	2.17
Receiver diameter	22mm
Concentration ratio	21.2

Table 3.1 PTC dimensions

3.1.2 Collector Intercept Factor Analysis

The most complex parameter involved in the determination of optical efficiency of a PTC is the intercept factor (γ). This is defined as the ratio of the energy intercepted by the receiver to the energy reflected by the focusing device [Duffie and Beckman, 1980; Sodha *et al.*, 1984]. Its value depends on the size of the receiver, the surface angle errors of the parabolic mirror, and solar beam spread. According to Guven and Bannerot [1986] these errors, or imperfections, are of two types namely random and nonrandom.

Random errors are defined as those errors which are truly random in nature and, therefore, can be represented by normal probability distributions. They are treated statistically and give rise to spreading of the reflected energy distribution [Guven and Bannerot, 1986]. These errors are identified as apparent changes in the Sun's width, scattering effects associated with the reflective surface and scattering effects caused by random slope errors (i.e. distortion of the parabola due to wind loading). Nonrandom errors arise in manufacture/assembly and/or in operation of the collector. These can be identified as reflector profile imperfections, misalignment errors and receiver location errors [Guven and Bannerot, 1986]. Random errors are modeled statistically, by determining the standard deviation of the total reflected energy distribution at normal incidence [Guven and Bannerot, 1986] as shown in equation 3.1.

$$\sigma = \sqrt{\sigma_{sun}^2 + 4\ \sigma_{slope}^2 + \sigma_{mirror}^2} \qquad (3.1)$$

where: σ_{sun} standard deviation of the energy distribution of the Sun's rays at normal incidence

σ_{slope} standard deviation of the distribution of local slope errors at normal incidence

σ_{mirror} standard deviation of the variation in diffusivity of the reflective material at normal incidence

Nonrandom errors are determined from a knowledge of the misalignment angle error β (i.e. the angle between the reflected ray from the centre of Sun and the normal to the reflector's aperture plane) and the displacement of the receiver from the focus of the parabola (dr). As reflector profile errors and receiver mislocation along the Y axis essentially have the same effect a single parameter is used to account for both. According to Guven and Bannerot [1986] random and nonrandom errors can be combined with the collector geometric parameters, concentration ratio (C) and receiver diameter (D) to yield error parameters universal to all collector geometries. These are called "universal error parameters" and an asterisk is used to distinguish them from the already defined parameters. Using the universal error parameters the formulation of the intercept factor γ is possible [Guven and Bannerot, 1985]:

$$\gamma = \frac{1+\cos\phi_r}{2\sin\phi_r}\int_0^{\phi_r} Erf\left(\frac{\sin\phi_r\,(1+\cos\phi)\,(1-2d^*\sin\phi) - \pi\beta^*(1+\cos\phi_r)}{\sqrt{2}\pi\sigma^*\,(1+\cos\phi_r)}\right)$$

$$-Erf\left(-\frac{\sin\phi_r(1+\cos\phi)\,(1+2d^*\sin\phi) + \pi\beta^*(1+\cos\phi_r)}{\sqrt{2}\pi\sigma^*\,(1+\cos\phi_r)}\right)\frac{d\phi}{(1+\cos\phi)} \qquad (3.2)$$

where:

ϕ_r Rim angle

σ^* Universal random error parameter ($\sigma^*=\sigma\ C$)

β^* Universal nonrandom error parameter due to angular errors ($\beta^*=\beta\ C$)

d^* Universal nonrandom error parameter due to receiver mislocation and reflector profile errors ($d^*=dr/D$)

For the evaluation of the intercept factor a computer program was written. The program operates as part of a main program called "SKDES". The principle of operation of the program is that the two error functions within the integral are estimated for one degree steps of angle ϕ and then the integral is numerically evaluated using the Simpson integration method.

For a carefully fabricated collector [Guven and Bannerot, 1986]:
σ_{mirror} = 0.002 rad and σ_{slope} = 0.004 rad and for clear-sky conditions σ_{sun} = 0.004 rad [Rabl and Bednt, 1982]. Therefore:

$$\sigma = \sqrt{(0.004)^2 + 4\ (0.004)^2 + (0.002)^2} = 0.00916 rad$$

β = 0.2°= 0.0035 rad (maximum tracking error, see section 3.1.4.1)

dr = 3mm (approximately)

By using these values the program results in γ = 0.94
The significance of the above parameters in the calculation of the intercept factor is shown in Table 3.2.

σ_{mirror} (rad)	σ_{slope} (rad)	dr (mm)	Intercept factor
0.002	0.004	0	0.98
0.004	0.004	3	0.93
0.002	0.006	3	0.88
0.002	0.008	3	0.81

Table 3.2 Effect of the magnitude of errors in intercept factor estimation

As it can be seen from the data presented in Table 3.2 the standard deviation of the distribution of local slope errors are the most important. This is because the σ_{slope} term in Eq. 3.1 is multiplied by a factor of 4. It is therefore concluded that extra care should be used for the construction of the parabolic surface.

3.1.3 Receiver Design

This is the heart of the parabolic trough collector system. The receiver of the model consists of a copper pipe surrounded by a glass envelope. The solar radiation falling on the collector aperture is reflected and concentrated onto the receiver. As shown by Jetter [1987] this radiation is not evenly distributed. Relations were derived by Jetter [1987]

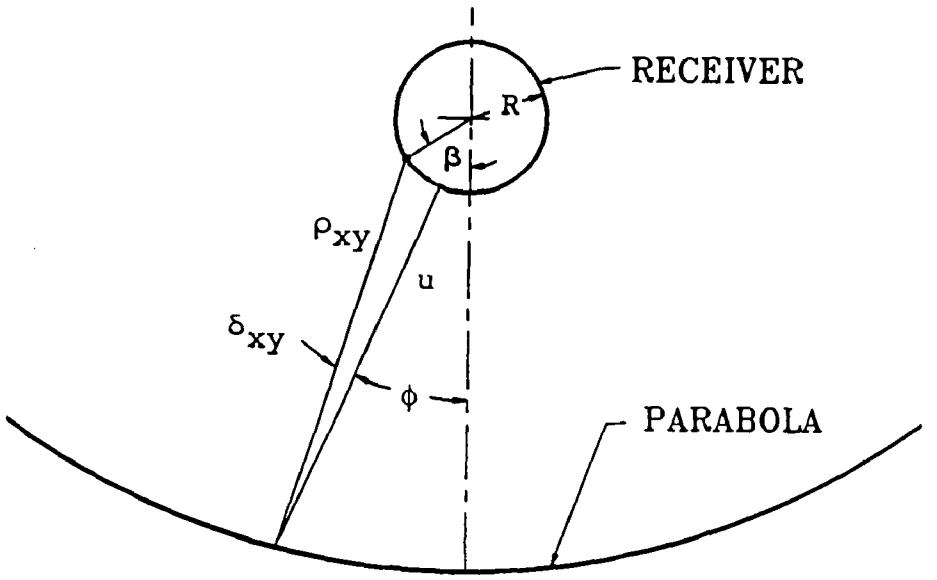

$$u = \frac{f}{\cos^2(\frac{\phi}{2})} \qquad \rho_{xy} = \sqrt{R^2 + u^2 - 2\,u\,R\cos(\beta-\phi)}$$

$$\delta_{xy} = \sin^{-1}\left[\frac{R\sin(\beta-\phi)}{\rho_{xy}}\right] \qquad \delta_o = \sin^{-1}\left[\cos(\theta)\sin(\delta_{xy})\right]$$

$$\phi_o = \tan^{-1}\left[\frac{\tan(\theta)}{\cos(\delta_{xy})}\right] \qquad F_{(\phi)} = F_{1(\phi)}\cos^2(\phi_o)$$

$$F_{1(\phi)} = \frac{u\cos\left(\frac{\phi}{2} - \delta_{xy}\right)}{\rho_{xy}\cos(\frac{\phi}{2})\cos(\phi_o)} \qquad \cos(\varepsilon) = \frac{\cos(s)}{\cos(\delta_o)}$$

$$\cos(\theta_o) = \cos(\phi_o)\left[\sin(\delta_{xy})\cos(\beta-\phi) - \sin(\delta_{xy})\sin(\beta-\phi)\right]$$

$$LCR = \frac{\rho_m}{\sigma\sqrt{2\,\pi}}\int_{-\phi_r}^{\phi_r} F_{(\phi)}\,Exp\left[\frac{-\delta_o^2}{2\,\sigma^2}\right] erf\left[\frac{\epsilon}{\sigma\sqrt{2}}\right] d\phi\,\cos(\theta_o)$$

SYMBOLS:

f	=	Focal distance (m)
R	=	Receiver radius (m)
s	=	Angular radius of sun (deg)
ϕ_r	=	Rim angle (deg)
Θ	=	Angle of incidence (deg)
σ	=	Standard deviation of errors (rad)

Fig. 3.2 Relations from Jetter [1987] for estimating LCR

for estimating this distribution (see Fig. 3.2) which is expressed as the local concentration ratio (LCR) i.e. the ratio of the concentrated to the incoming radiation. The LCR depends on the angle β, shown in Fig. 3.2, the incidence angle Θ, the total standard deviation of the errors, and the collector geometric parameters.

Using the expressions shown in Fig. 3.2, a computer program was written as a separate module of the program "SKDES" (see Appendix 2). The results of the program are shown graphically in Fig. 3.3. The value of σ used in this case is 0.00918 rad which is obtained by using Eq.3.1 and including the square of the tracking error standard deviation (0.606 mrad) under the radical. As the distribution is symmetrical about a vertical axis, only half of the graph is shown. Similar results, with respect to the shape of the distribution, were obtained by Thomas *et al.* [1986] by using a CdS photoresistor mounted on the periphery of a cylindrical ebonite tube, at full moon.

From the foregoing analysis the flux distribution on the receiver can be calculated and this was then used in the computer modelling program. The local CR exhibits significant variations.

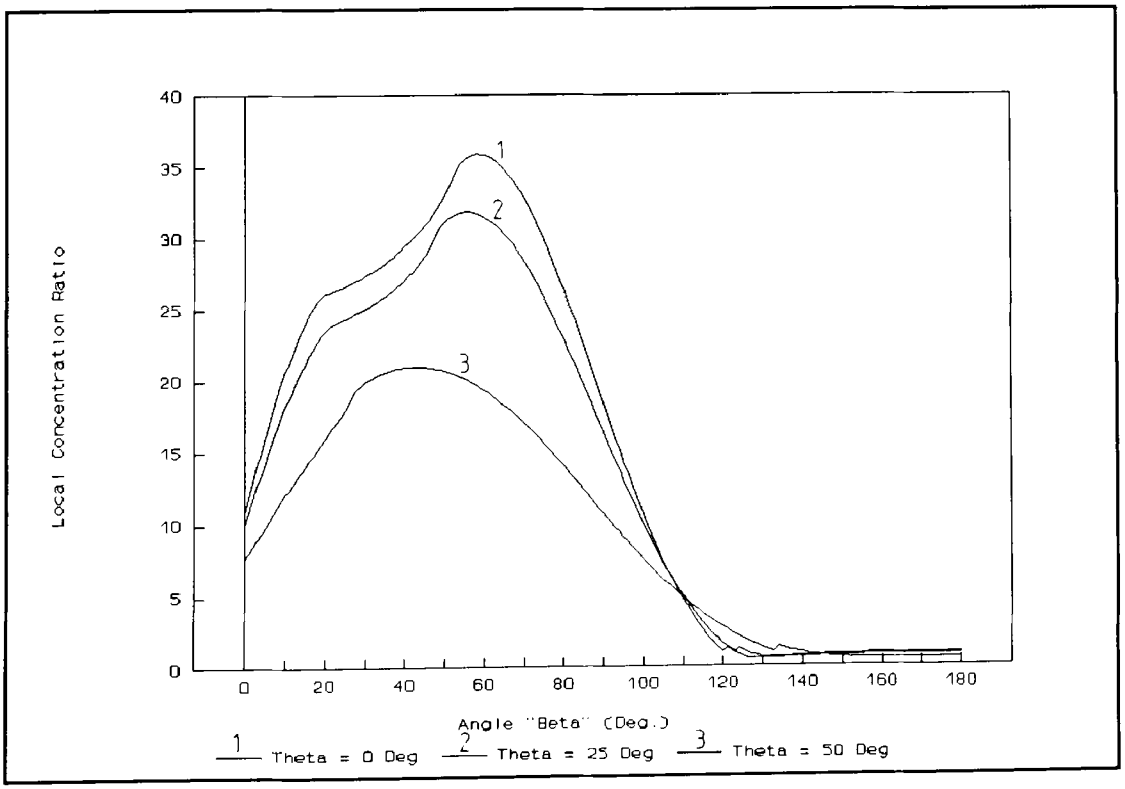

Fig. 3.3 Distribution of LCR for various incidence angles

3.1.4 Design of the Tracking Mechanism

A tracking mechanism must be able to follow the Sun with a specified degree of accuracy, and return the collector to its original position at the end of the day or at the beginning of the next day and also overcome the problem of intermittent cloud cover.

3.1.4.1 System Description

The system which was designed to operate with the required high tracking accuracy consists of a small motor which rotates the collector via a speed reduction gearbox. A control system is used to detect the Sun's position and operate the motor [Kalogirou, 1991; Kalogirou *et al.*, 1992c, appended].

The system employs three sensors of which one is installed on the East side of the collector shaded by the frame, whereas the other two are installed on the collector frame, see Fig.3.4. The first sensor acts as the "focus" sensor i.e. it will only receive direct sunlight when the collector is focused. The second sensor is the "cloud" sensor and cloud cover is assumed when illumination falls below a certain level. The third sensor is the "daylight" sensor. The function of the control system is to make sure that at all times the three sensors receive sunlight (i.e. the collector is continuously focused). The present sensors are light dependent resistors (LDRs) type ORP 12 supplied by RS components Ltd.

A more detailed, description together with information on the construction of the mechanism can be found in [Kalogirou, 1991] and [Kalogirou *et al.*, 1992c, appended] where the performance of the mechanism is also reported. The tracking mechanism proved to be reliable, effective, and accurate. The accuracy of the system depends on the intensity of the Sun's illumination. In the worst case, with radiation of the order of 100 W/m^2, the accuracy of the mechanism was 0.2°. This variation was reduced to 0.05° with radiation levels of about 600 W/m^2.

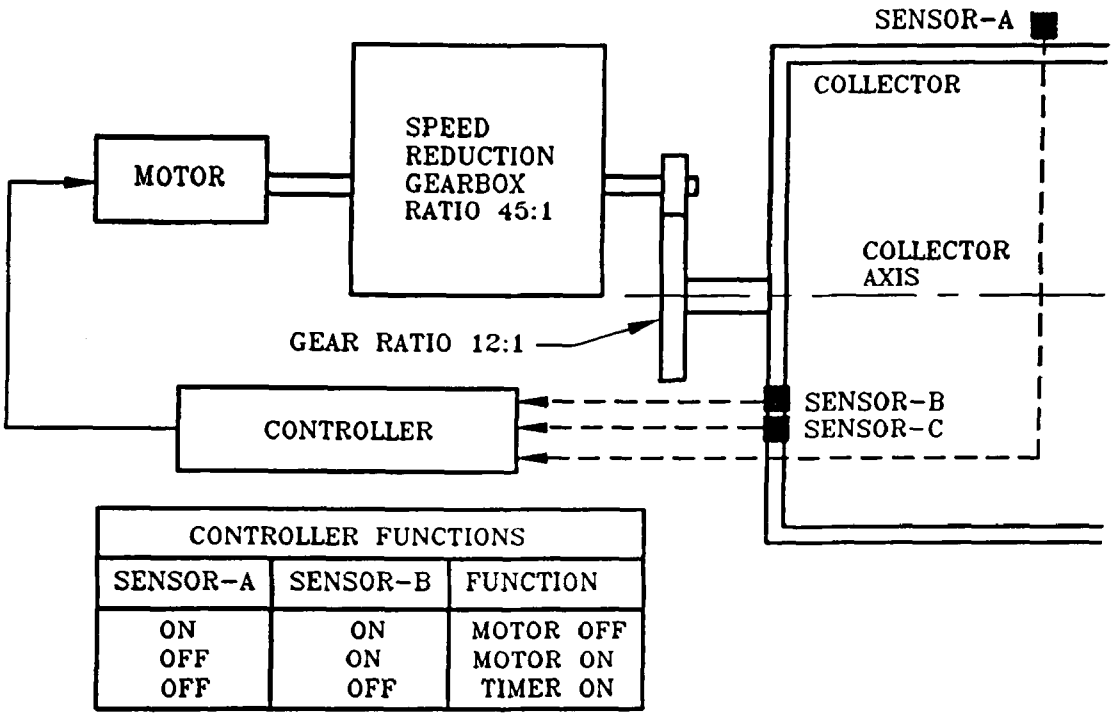

CONTROLLER FUNCTIONS		
SENSOR-A	SENSOR-B	FUNCTION
ON	ON	MOTOR OFF
OFF	ON	MOTOR ON
OFF	OFF	TIMER ON

Fig. 3.4 Tracking mechanism system diagram

3.1.5 Selection of Mode of Tracking

The mode of tracking affects the amount of incident radiation falling on the collector surface in proportion to the cosine of the incidence angle. The amount of energy falling on a surface of $1m^2$ for four modes of tracking (see Fig. 3.5) for the Summer and Winter solstices and the equinoxes is shown in Table 3.3 [Kalogirou, 1991]. The amount of energy shown in Table 3.3 is obtained by applying a radiation model [Meinel and Meinel, 1976]. This is affected by the incidence angle which is different for each mode.

The performance of the various modes of tracking can be compared to the full tracking mode which collects the maximum amount of solar radiation, shown as 100% in Table 3.3. Such a system is usually avoided because of its high cost, as approximately double the equipment is required to move the collector in two directions. From Table 3.3 it is obvious that the polar and the E-W horizontal modes are the most suitable for one axis tracking as their performance is very close to full tracking. Therefore these two modes will be analysed further to select the one which collects the maximum energy. This analysis will not be limited to the horizontal and polar axes but, a range of angles in between (0-35°) will be considered.

Tracking mode	Solar energy (kWh/m^2)			Percent to full tracking		
	E	SS	WS	E	SS	WS
Full tracking	8.43	10.60	5.70	100.0	100.0	100.0
E-W Polar	8.43	9.73	5.23	100.0	91.7	91.7
N-S Horizontal	6.22	7.85	4.91	73.8	74.0	86.2
E-W Horizontal	7.51	10.36	4.47	89.1	97.7	60.9
Note: E - Equinoxes, SS - Summer Solstice, WS - Winter Solstice						

Table 3.3 Comparison of energy absorbed for various modes of tracking

For this purpose another module running with "SKDES" was written (see Appendix 2). The program considers every day of the year, for all the sunshine hours of each day, and outputs the total energy delivered by the collector. The program takes into account only optical losses i.e. the optical efficiency and the loss of the optical efficiency due to the geometric factor which is influenced by the angle of incidence. The incidence angle is calculated by considering the surface slope and surface azimuth angles of the tracking surface [Braun and Mitchell, 1983]. The relations used by the program are shown in Fig. 3.6 where definitions of the various angles employed are also included. The various angle definitions can be seen in Fig. 3.5 from the diagram of the solar angles.

The results from the program are shown in Table 3.4 for two cases, the whole year and the period between days 90-300. This period is between April and October where a solar system is more useful. It can be seen that the optimum collector axis slope is 30° for the whole year and 20° for the shorter period. The percentage losses in efficiency are also shown in this table and for the shorter estimation period are of approximately 6.1% for the E-W horizontal mode and 4.7% for the polar mode. However, the horizontal mode exhibits one advantage which makes this mode of tracking very popular-namely very small shadowing effects are encountered in multi-collector installations, which enhances land utilisation. The only shadowing present with the E-W horizontal mode is during the first and last hours of the day where the collectors are tilted fully East and fully West respectively. Therefore this mode of tracking seems more suitable.

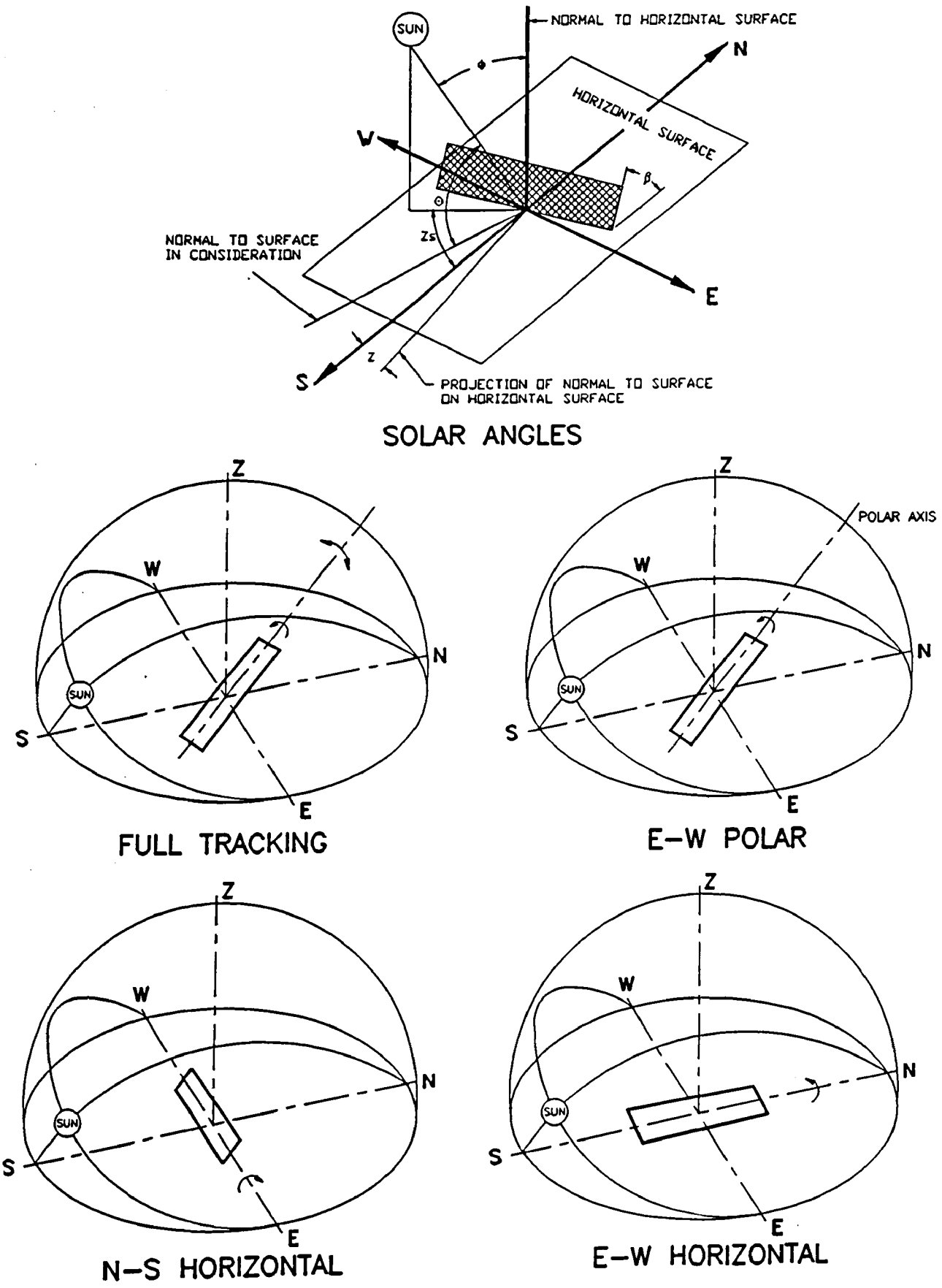

Fig. 3.5 Collector geometry for various modes of tracking and solar angles diagram

POSITION OF THE SUN

Incidence angle $\cos(\theta)=\cos(\phi)\cos(\beta)+\sin(\phi)\sin(\beta)\cos(z_s-z)$

Zenith angle $\cos(\phi) = \sin(\delta)\sin(L) + \cos(\delta)\cos(L)\cos(H)$

Declination angle $\delta = 23.45 \sin\left(\frac{360\ (\ 284+N\ )}{365}\right)$

Solar azimuth angle : $z_s = k1\ k2\ z_{so} + \left(\frac{1 - k1\ k2}{2}\right) k3\ 180°$

where:

$\sin(z_{so}) = \frac{\sin(H)\cos(\delta)}{\sin(\phi)}$ $\qquad$ $\cos(Hew) = \cot(L)\tan(\delta)$

$$k1 = \begin{cases} +1 \text{ if } |H| < Hew \\ -1 \text{ otherwise} \end{cases} \qquad k2 = \begin{cases} +1 \text{ if } L(L-\delta) \geq 0 \\ -1 \text{ otherwise} \end{cases} \qquad k3 = \begin{cases} +1 \text{ if } H \geq 0 \\ -1 \text{ otherwise} \end{cases}$$

TRACKING SURFACES

Type	Surface azimuth	Surface slope
Horizontal axis E-W Tracking	$z = z^1 + 90°$ if $z_s - z^1 \geq 0$ $z = z^1 - 90°$ if $z_s - z^1 < 0$	$\beta = \beta_o + k4\ 180°$ where: $\tan(\beta_o)=\tan(\phi)\cos(z-z_s)$ $k4 = \begin{cases} 0 \text{ if } \beta_o \geq 0 \\ 1 \text{ otherwise} \end{cases}$
Sloped axis E-W Tracking	$z=z_o + k5\ k6\ 180°$ where: $z_o=z^1+\tan^{-1}(X)$ $X=\frac{\sin(\phi)\sin(z_s-z^1)}{\cos(\theta^1)\sin(\beta^1)}$ $k5 = \begin{cases} 0 \text{ if } (z_o-z^1)(z_s-z^1)\geq 0 \\ 1 \text{ otherwise} \end{cases}$ $k6 = \begin{cases} +1 \text{ if } (z_s-z^1)\geq 0 \\ -1 \text{ otherwise} \end{cases}$	$\beta = \beta_o^1 + k7\ 180°$ where: $\tan(\beta_o^1) = \frac{\tan(\beta^1)}{\cos(z-z^1)}$ $k7 = \begin{cases} 0 \text{ if } \beta_o^1 \geq 0 \\ 1 \text{ otherwise} \end{cases}$

DEFINITIONS:

- β Surface slope: angle between the surface normal and the vertical.
- β^1 Slope of tracking axis: angle between the axis line and the projection of the axis line into the horizontal plane.
- z Surface azimuth: angle between the projection of the normal to the surface into the horizontal plane and the local meridian. West from south positive and east negative.
- z^1 Azimuth of the tracking axis; angle between the project of the axis line onto the horizontal plane and local meridian. Same sign convention as surface azimuth.
- Θ^1 Angle of incidence for a surface with a slope and azimuth equal to those of the tracking axis.

SYMBOLS:

N = Day of year (1-365) L = Latitude H = Hour angle

Fig. 3.6 Position of E-W tracked surfaces

The maximum angle of incidence for the E–W horizontal mode of tracking, for each day of the period between days 90–300, is shown in Fig. 3.7. It can be seen that the maximum angle of incidence of 48.8° appears at day number 300 (end of October), whereas for the days between 115 to 230 the maximum angle of incidence is not greater than 20°.

Tracking axis slope (deg.)	Case 1: Days 1–365		Case 2: Days 90–300	
	Total radiation received (kWh/m^2)	Percentage difference from maximum in total radiation collected	Total radiation received (kWh/m^2)	Percentage difference from maximum in total radiation collected
0	1616.2	13.7	1222.9	6.1
5	1690.0	9.8	1259.4	3.2
10	1755.1	6.3	1287.3	1.1
15	1805.5	3.6	1301.4	0.2
20	1840.8	1.7	**1301.7**	0.0
25	1863.3	0.5	1290.9	0.8
30	**1873.5**	0.0	1270.2	2.1
35	1871.7	0.1	1240.8	4.7

Table 3.4 Total radiation received for various tracking axis slopes

Another effect which can be investigated with this program is that of the tracking axis azimuth angle. This is shown in Fig. 3.8 where the percentage loss in performance for different tracking axis azimuth angles for the two cases investigated is plotted. It can be seen from Fig. 3.8, that the maximum performance is obtained by having the collector axis parallel with the N–S axis and that the same loss of performance is present, by using the same angle, either in the positive or negative directions. It can be concluded from Fig. 3.8 that the horizontal mode is less sensitive to misalignment which adds some merit to the already mentioned advantages of this mode of tracking.

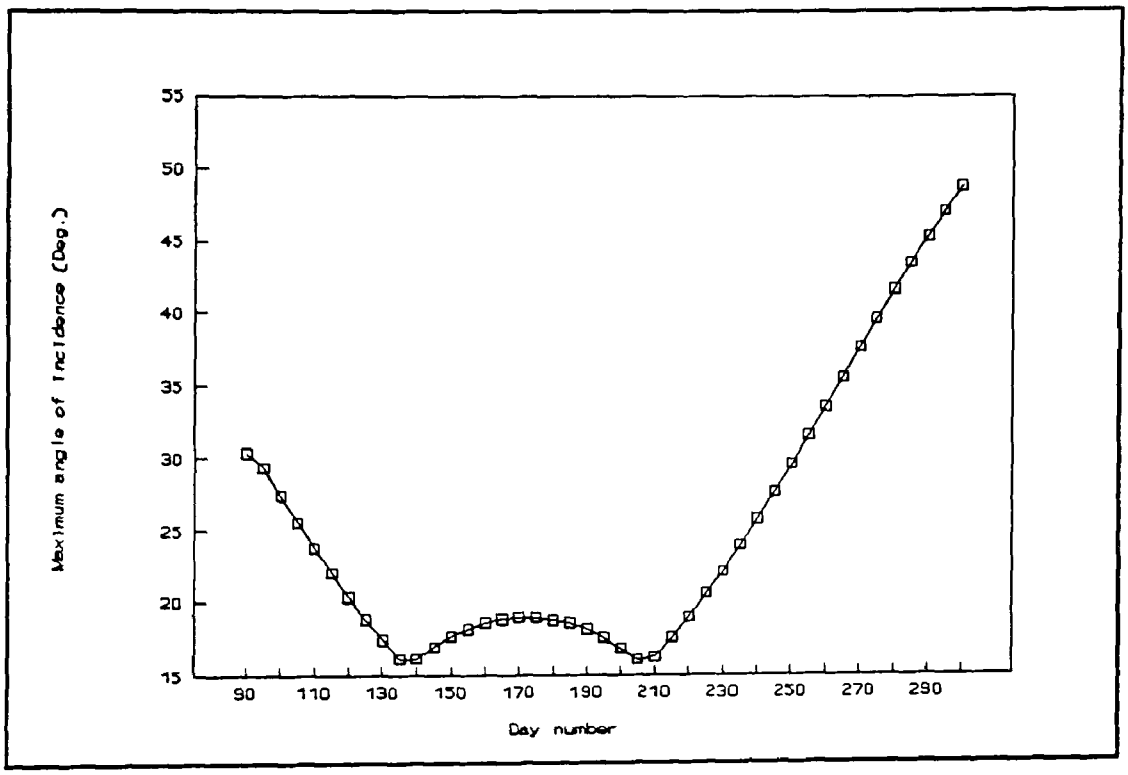

Fig. 3.7 Maximum angle of incidence for day number 90-300

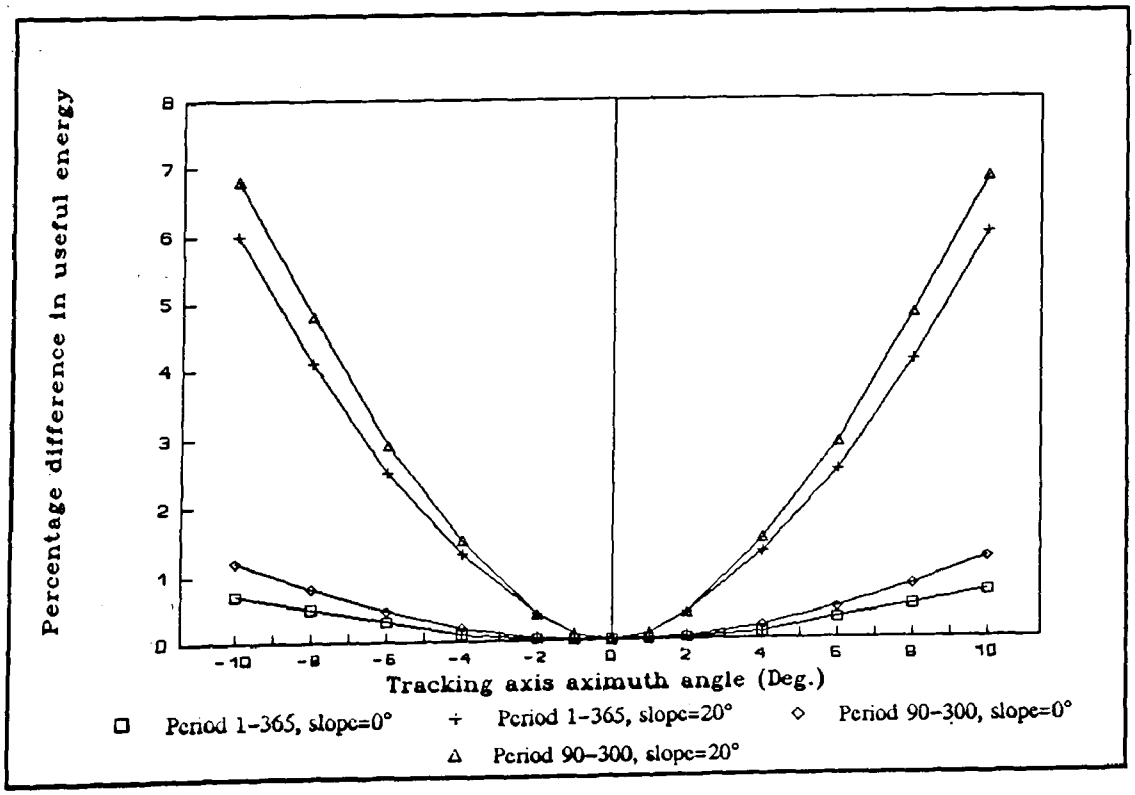

Fig. 3.8 Effect of collector axis azimuth on collector performance

3.1.6 Collector Specifications

Table 3.5 below gives a summary of all the elements of the collector as derived from the above design process.

ITEM	VALUE/TYPE
Collector aperture area	$3.5m^2$
Collector aperture	1.46m
Aperture-to-length ratio	0.64
Rim angle	90°
Glass-to-receiver ratio	2.17
Receiver diameter	22mm
Concentration ratio	21.2
Collector intercept factor	0.9506
Maximum optical efficiency	0.654
Tracking mechanism type	Electronic
Mode of tracking	E-W horizontal

Table 3.5 PTC system specifications

3.2 DESIGN OF THE STEAM GENERATION SYSTEM

Three methods have been employed to generate steam using parabolic trough collectors:

- The steam-flash concept, in which pressurised water is heated in the collector and then flashed to steam in a separate vessel.
- The direct or in-situ concept, in which two phase flow is allowed in the collector receiver so that steam is generated directly.
- The unfired-boiler concept, in which a heat-transfer fluid is circulated through the collector and steam is generated via heat-exchange in an unfired boiler.

All these systems have certain advantages and disadvantages and these will be analysed here to select the best system. This will be followed by the flash vessel design.

3.2.1 Selection of the Steam Generation Method

A diagram of a steam–flash system is shown in Fig. 3.9. Water, pressurised to prevent boiling, is circulated through the collector and then flashed across a throttling valve into a flash vessel. Treated feedwater input maintains the level in the flash vessel and the subcooled liquid is recirculated through the collector. The in–situ boiling concept, shown in Fig. 3.10, uses a similar system configuration without a flash valve. Subcooled water is heated to boiling and steam forms directly in the receiver tube. Capital costs associated with a direct–steam and a flash–steam system would be approximately the same [Hurtado and Kast, 1984].

Although the steam–flash system uses water, a superior heat transport fluid, the in–situ boiling system is more advantageous. The flash system uses a sensible heat change in the working fluid, which makes the temperature differential across the collector relatively high. The rapid increase in water vapour pressure with temperature requires corresponding increase in system operating pressure to prevent boiling. Increased operating temperatures reduce the thermal efficiency of the solar collector. Increased pressures within the system require a more robust design of collector components, such as receivers and piping. The differential pressure over the delivered steam pressure required to prevent boiling is supplied by the circulation pump and is irreversibly dissipated across the flash valve. When boiling occurs in the collectors, as in an in–situ boiler, the system pressure drop and consequently, electrical power consumption is greatly reduced. In addition, the latent heat–transfer process minimises the temperature rise across the solar collector. Disadvantages of in–situ boiling are the possibility of a number of stability problems [Peterson and Keneth, 1982] and the fact that even with a very good feedwater treatment system, scaling in the receiver is unavoidable. In multiple row collector arrays, the occurrence of flow instabilities could result in loss of flow in the affected row. This in turn could result in tube dryout with consequent damage of the receiver selective coating. No significant instabilities were reported by Hurtado and Kast [1984] when experimentally testing a single row 120 ft system.

A diagram of an unfired boiler system is shown in Fig. 3.11. In this system, the heat–transfer fluid should be nonfreezing and noncorrosive, system pressures are low and

control is straightforward. These factors largely overcome the disadvantages of water systems, and are the main reasons for the predominant use of heat-transfer oil systems in current industrial steam-generating solar systems.

The major disadvantage of the system result from the characteristics of the heat-transfer fluid. These fluids are hard to contain, and most heat-transfer fluids are flammable. Decomposition, when the fluids are exposed to air, can greatly reduce ignition-point temperatures, and leaks into certain types of insulation can cause combustion at temperatures that are considerably lower than measured self-ignition temperatures. Heat-transfer fluids are also relatively expensive and present a potential pollution problem that makes them unsuitable for food industry applications [Murphy and Keneth, 1982]. Heat-transfer fluids have much poorer heat-transfer characteristics than water. They are more viscous at ambient temperatures, are less dense, and have lower specific heats and thermal conductivities than water. These characteristics mean that higher flow rates, higher collector differential temperatures, and greater pumping power are required to obtain the equivalent quantity of energy transport when compared to a system using water. In addition, heat-transfer coefficients are lower, so there is a larger temperature differential between the receiver tube and the collector fluid. Higher temperatures are also necessary to achieve cost effective heat exchange. These effects result in reduced collector efficiency.

From the above discussion it is obvious that the water-based systems are more simple and safer for desalination. With proper selection of flow rate and desalination system steam supply pressure, the pump power can be kept to a minimum. This reduces the main disadvantage of the steam-flash system against the in-situ system and as their costs are similar the steam-flash system is selected. For the 3.5m^2 collector area and by considering a maximum value of solar radiation of 1000 W/m^2, the outlet temperature of the water, for a 100°C inlet temperature (pressure in the separator equal to atmospheric and flow rate equal to 0.042 kg/s) would be 120°C. This is considered a reasonable value, not causing the collector to work at excessively high temperatures, and only requires a pressure of 2 bar to avoid boiling. The pump selected can operate up to 6 bar-a pressure far above that required.

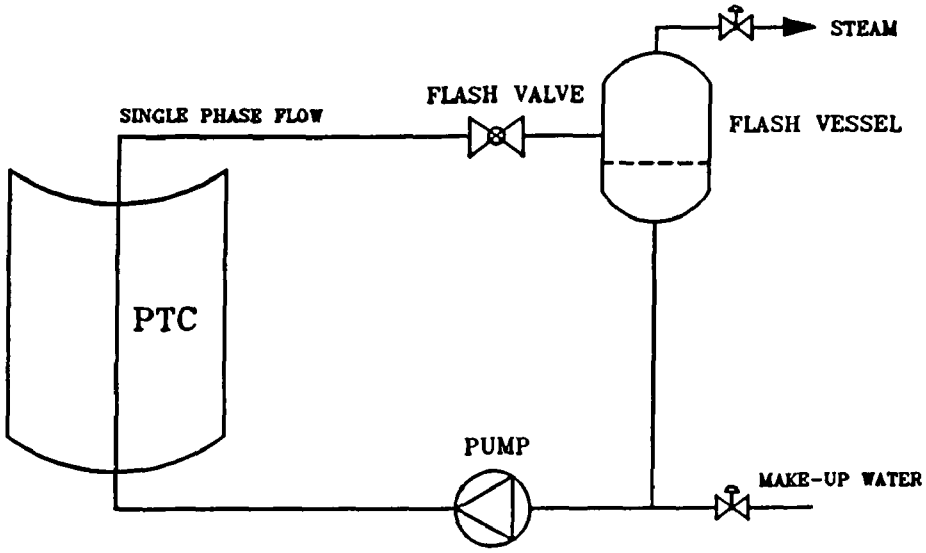

Fig. 3.9 The steam-flash steam generation concept

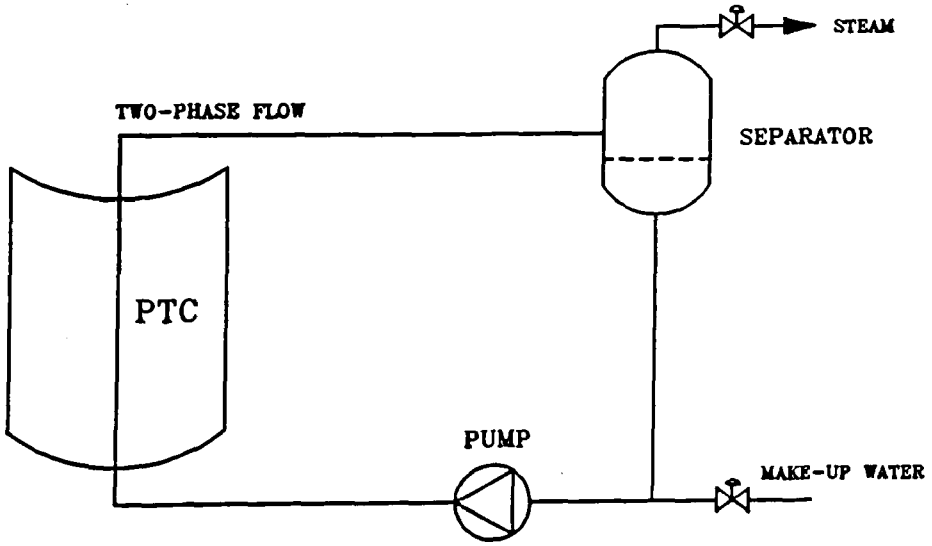

Fig. 3.10 The direct steam generation concept

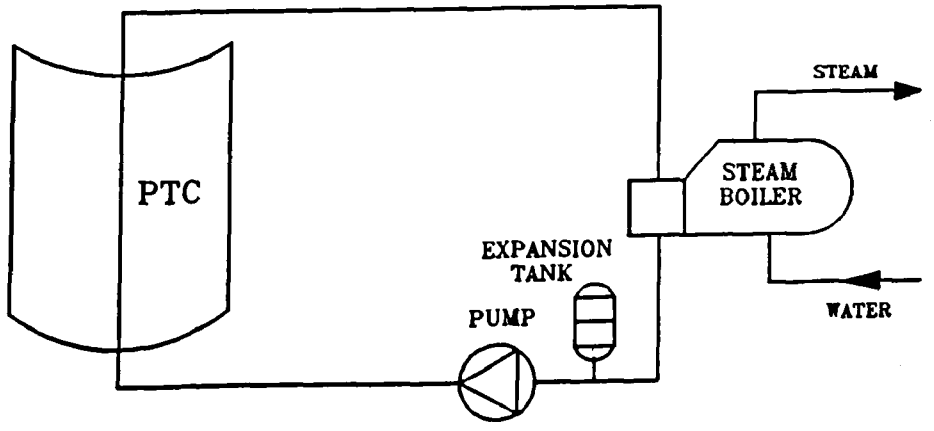

Fig. 3.11 The unfired-boiler steam generation concept

3.2.2 Flash Vessel Design

In order to separate steam at lower pressure, a flash vessel is used. This is a vertical vessel as shown in Fig. 3.12, with the inlet for the water located about one third of the way up its side. The standard design of flash vessels require that the diameter of the vessel is chosen so that the steam flows towards the top outlet connection at no more than about 3 m/s. This should ensure that any water droplets can fall through the steam in contra-flow, to the bottom of the vessel. Adequate height above the inlet is necessary to ensure separation. The separation is also facilitated by having the inlet projecting downwards into the vessel. The water outlet connection is sized to minimise the pressure drop from the vessel to the pump inlet to avoid cavitation. The flash valve connected to the vessel inlet is spring loaded for adjustment purposes.

The flash vessel design parameters are shown in Fig. 3.12. By using a similar approach as above, the maximum amount of steam that the collector can produce at peak solar radiation flashing off to atmospheric pressure is 0.0016 kg/s or 0.00268 m^3/s. A velocity of 3 m/s gives a diameter of 33.7mm. A diameter of 75mm is selected which gives a velocity of 0.61 m/s.

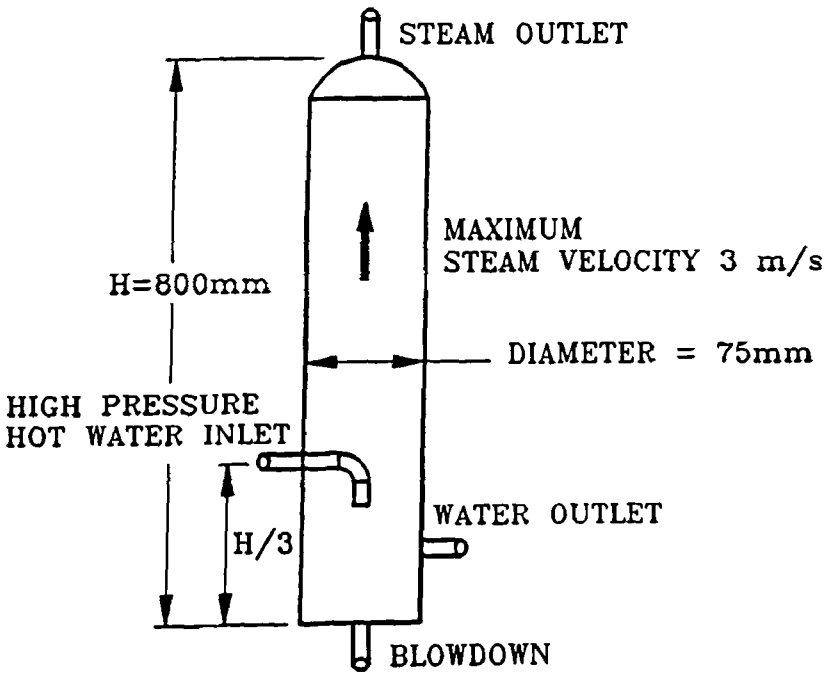

Fig. 3.12 Flash vessel design details

3.2.3 The Complete Steam Generation System

A diagram of the complete steam generation system with pipe sizes is shown in Fig. 3.13. A flow meter is included for the measurement of water flow rate. Other instruments employed are pressure gauges, designated P, at the pump outlet and at the flash vessel, thermocouples, designated by T, for temperature measurements and a pyranometer for solar radiation measurement. Thermocouples and the pyranometer are used in conjunction with a data acquisition system (see section 5.1) for the collector performance evaluation. A heat exchanger is also included to condense the steam produced by the system. In this way the system production rate can be measured.

3.3 DESIGN OF THE DESALINATION SYSTEM

3.3.1 System Circuit Arrangement

The circuit must be able to carry the sea-water from the sea to the MEB evaporator and return the rejected brine back to the sea. These two streams must be remote from each other to avoid potential mixing problems. The circuit diagram shown in Fig. 3.14 shows details of only the intake stream. Whenever possible intake from a well next to the coast line is preferred because as the water passes through the sand it is filtered. The water after passing through a filter is directed to the MEB evaporator last effect to cool the steam produced in the previous effect. Part of this water is then returned to the sea as warm brine and part as feedwater directed to the evaporator top effect after a scale inhibitor is ejected (see Fig. 3.15). In Fig. 3.14 the solar collectors and the steam generation system piping layout is also shown. A back-up boiler is also shown in Fig. 3.14. This is necessary in an actual system for the operation of the evaporator during days of low insolation and/or during the night.

3.3.2 Description of the MEB Evaporator

Of the various types of MEB evaporators the Multiple Effect Stack (MES) type is

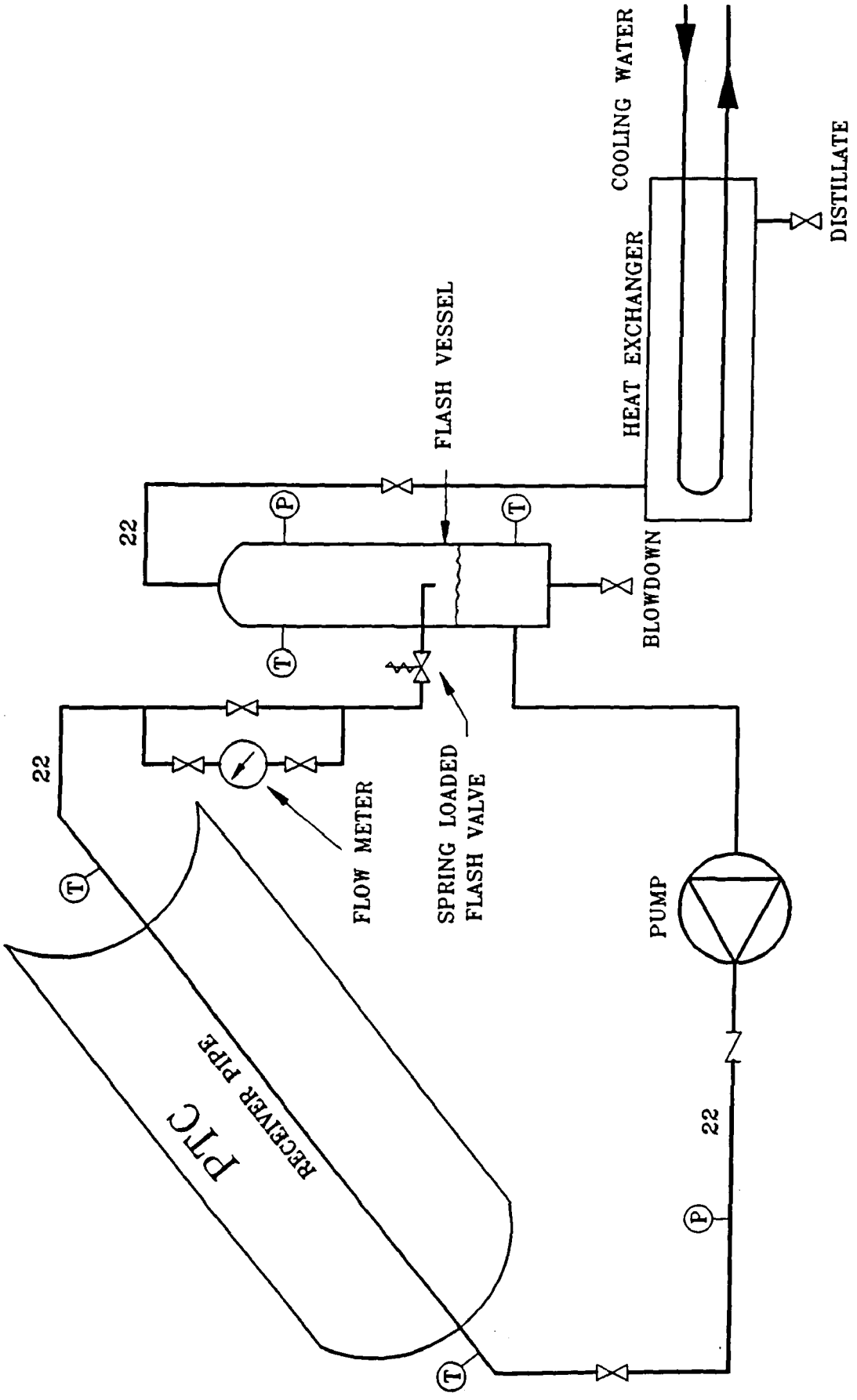

Fig. 3.13 The complete steam generation system

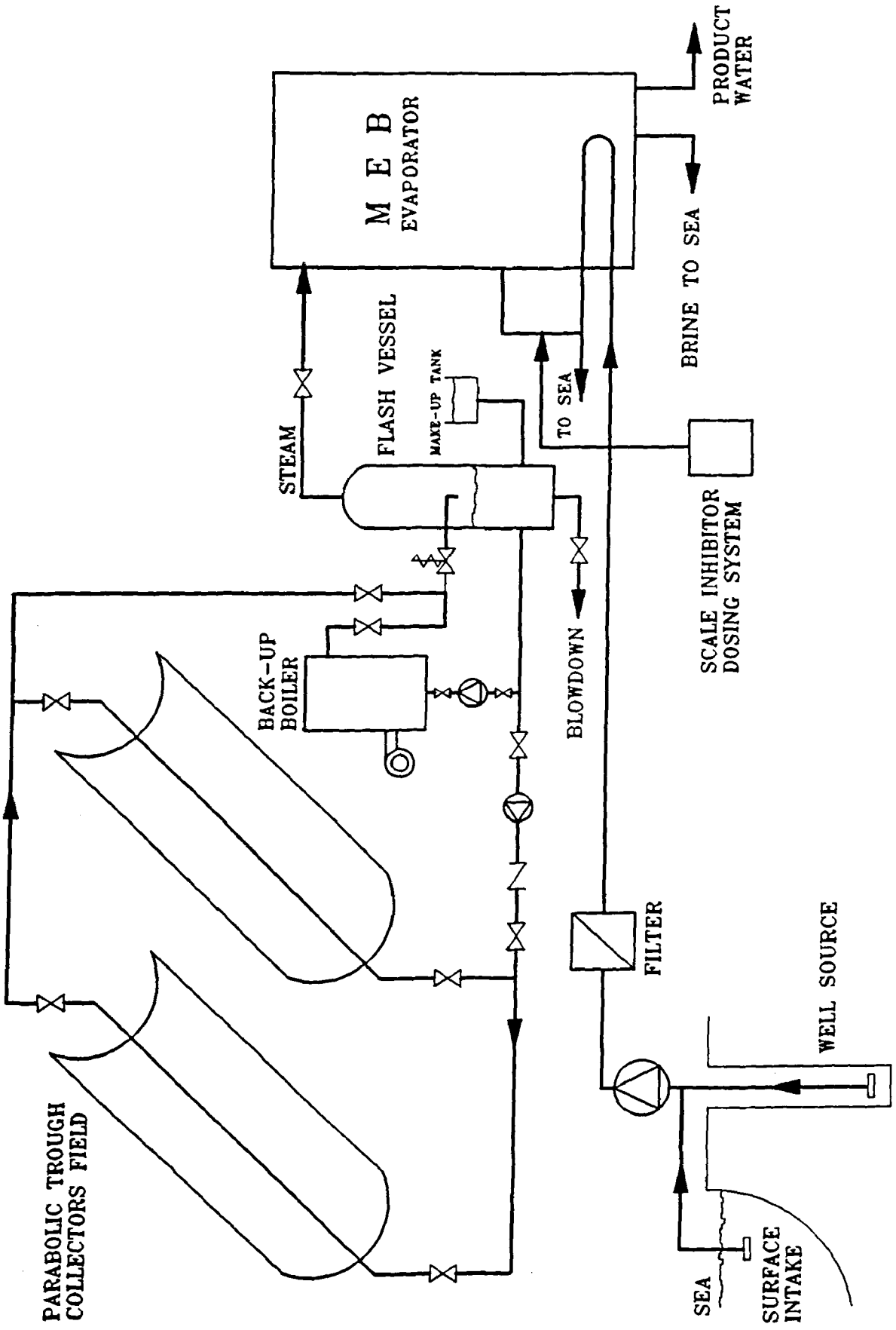

Fig. 3.14 The complete system circuit diagram

selected. This features a number of advantages the most important of which is its stable operation between virtually zero and 100% output even when sudden changes are made, and its ability to follow a varying steam supply without upset.

In Fig. 3.15 a four effect MES evaporator is shown. Sea-water is sprayed into the top of the evaporator and descends as a thin film over the horizontally arranged tube bundle in each effect. In the top (hottest) effect, steam from the solar collector system condenses inside the tubes. Because of the low pressure created in the plant by the vent ejector system, the thin sea-water film simultaneously boils on the outside of the tubes, creating new vapour at a lower temperature than the condensing steam.

The sea-water falling to the floor of the first effect is cooled by flashing through nozzles into the second effect which is at a lower pressure. The vapour made in the first effect is ducted into the inside of the tubes in the second effect, where it condenses to form part of the product. Again, the condensing warm vapour causes the cooler external sea-water film to boil at the reduced pressure.

The evaporation-condensation process is repeated from effect to effect down the plant, creating an almost equal amount of product inside the tubes of each effect. The vapour made in the last effect is condensed on the outside of a tube bundle cooled by raw sea-water. Most of the warmer sea-water is then returned to the sea, but a small part is used as feedwater to the plant. After being treated with acid to destroy scale-forming compounds, the feedwater passes up the stack through a series of pre-heaters that use a little of the vapour from each effect to gradually raise its temperature, before it is sprayed into the top of the plant.

The product water from each effect is flashed in cascade down the plant so that it can be withdrawn in a cool condition at the bottom of the stack. The concentrated brine is also withdrawn at the bottom of the stack.

The MES process is completely stable in operation and automatically adjusts to changing steam conditions even if they are suddenly applied, so is suitable for load following applications. It is a once-through process that minimises the risk of scale formation

without incurring a large chemical scale dosing cost. The typical product purity is less than 5 ppm TDS and does not deteriorate as the plant ages. Therefore the product water can be used as a make-up to the flash vessel.

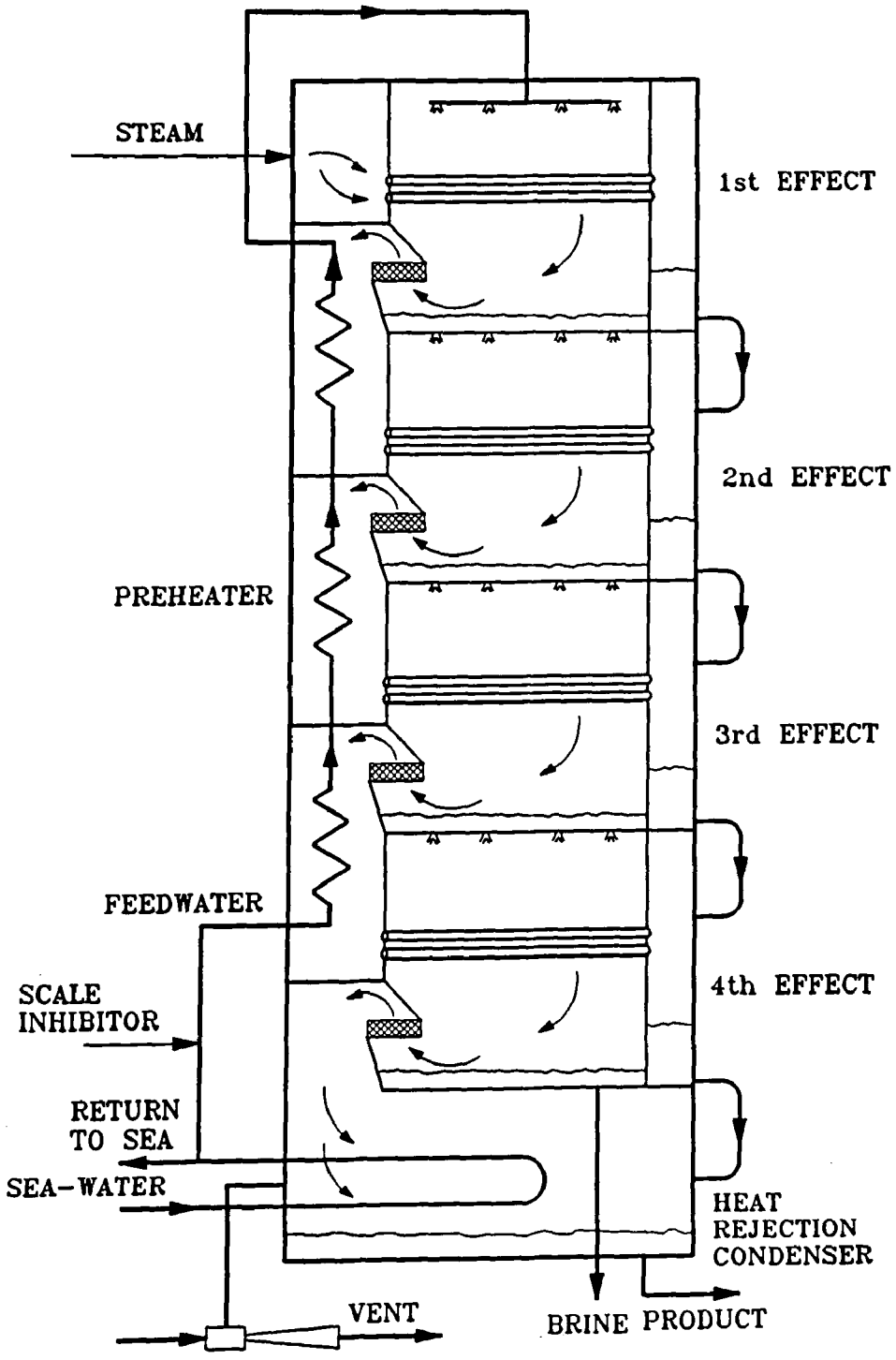

Fig. 3.15 The MES evaporator

3.4 SYSTEM MODELLING

The modelling programs written as part of this research project are separate modules running with "SKDES" and are used to determine the quantity of the steam produced by the steam generation system i.e. the collector and the flash vessel. Two versions of the program were written one called "PTCDES1" and the other "PTCDES2". The difference between the two versions is that in the former the receiver is considered as a unit whereas in the latter a more detailed analysis of the receiver is employed. For this analysis the local concentration ratios around the receiver are considered (see section 3.1.3).

Details on the operation of the programs, together with the input requirements are given in Appendix 2. The principle of operation of the programs is that they employ the values of the solar radiation and ambient air temperature for the special reference year shown in Appendix 1. The values of the solar radiation are not used as they appear in Appendix 1 because these values are for beam radiation on a horizontal surface. Therefore the beam radiation values are corrected hourly for the collector inclination.

In the analysis a representative day for each month is taken as shown in Table 3.6. These are chosen because the value of extraterrestrial solar radiation is closest to the month's average at that day [Duffie and Beckman, 1980].

MONTH	DAY	MONTH	DAY	MONTH	DAY	MONTH	DAY
January	17	April	15	July	17	October	15
February	16	May	15	August	16	November	14
March	16	June	11	September	15	December	10

Table 3.6 Average day of each month

In both programs the actual measured collector performance parameters of test slope and intercept are required. The programs take into account, in addition to the sensible heat and the thermal capacity of all the system components, all the heat losses from the system i.e. the flash vessel body, pipes and pump body. Relations describing these losses are given in chapter 6. After all these losses are estimated the flash vessel inlet water

temperature is determined. From the difference in enthalpy of this hot water to the water contained in the flash vessel the steam production is calculated. The program "PTCDES1" flow chart is shown in Fig. 3.16. The accuracy of the simulation depends to a great extent on the validity of the reference year. This was investigated when modelling performance for hot water production from PTC's [Kalogirou *et al.*, 1993a]. Although the variation reported was 7% this can not be generalised as an expected variation.

A typical output of the program "PTCDES2" for the 3.5 m^2 collector model is shown in Fig. 3.17. The monthly total useful energy and the mean daily steam production from both programs are shown in Table 3.7. The maximum percentage difference in total useful energy between the two is 10.1% with the greatest differences occurring in the cold months. This is due to the fact that the thermal losses which are ambient temperature dependent are higher and consequently the ratio of the losses to the total useful energy is greater, so that the cosine losses are also higher and these in combination with the small collector effective aperture area in these months are responsible for the greater differences. For larger effective aperture areas the difference is much smaller. These differences do not markedly affect the annual results as they are concentrated during the Winter months where the system production is small. This is demonstrated by the fact that the difference in yearly production is only 1.2%.

By comparing the results shown in Table 3.7 with the values of precipitation distribution shown in Table 1.1 the main advantage of solar desalination can be revealed. The system is in phase with the weather i.e. during periods of dry weather the system production is at its greatest.

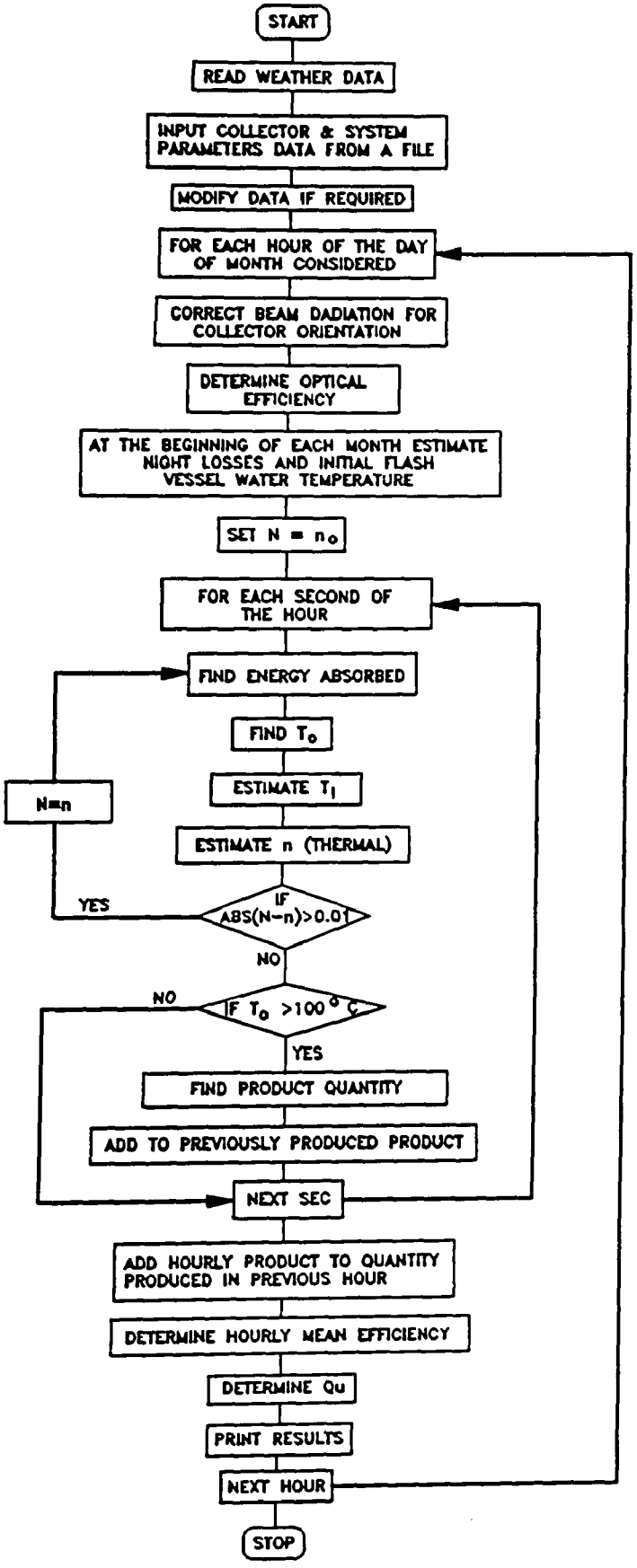

Fig. 3.16 Program "PTCDES1" flow chart

MONTH = JANUARY

TIME	COLLECTOR EFFICIENCY	HOURLY PRODUCTION[1]	CUMULATIVE PRODUCTION[1]	USEFUL ENERGY[2]	ENERGY LOSS[2]
8.00	0.37	0.00	0.00	31.04	8.63
9.00	0.32	0.00	0.00	141.27	33.00
10.00	0.22	0.00	0.00	105.02	68.98
11.00	0.16	0.00	0.00	40.52	90.11
12.00	0.15	0.00	0.00	26.95	100.75
13.00	0.17	0.00	0.00	46.06	113.20
14.00	0.21	0.00	0.00	87.03	137.38
15.00	0.26	0.18	0.18	126.03	155.00
16.00	0.32	0.23	0.40	155.01	156.21
17.00	0.07	0.00	0.40	0.00	133.13

Month average production = 0.116 kg/m^2-day
Month Total USEFUL ENERGY = 758.9 Wh

MONTH = FEBRUARY

TIME	COLLECTOR EFFICIENCY	HOURLY PRODUCTION[1]	CUMULATIVE PRODUCTION[1]	USEFUL ENERGY[2]	ENERGY LOSS[2]
8.00	0.44	0.00	0.00	80.33	16.59
9.00	0.37	0.00	0.00	172.80	54.25
10.00	0.27	0.00	0.00	121.10	100.05
11.00	0.22	0.00	0.00	80.86	132.93
12.00	0.21	0.10	0.10	87.45	151.99
13.00	0.22	0.15	0.25	101.36	152.32
14.00	0.26	0.21	0.46	139.84	151.91
15.00	0.31	0.26	0.72	176.25	152.85
16.00	0.39	0.39	1.12	265.55	153.76
17.00	0.26	0.00	1.12	0.00	134.52

Month average production = 0.320 kg/m^2-day
Month Total USEFUL ENERGY = 1225.5 Wh

MONTH = MARCH

TIME	COLLECTOR EFFICIENCY	HOURLY PRODUCTION[1]	CUMULATIVE PRODUCTION[1]	USEFUL ENERGY[2]	ENERGY LOSS[2]
7.00	0.52	0.00	0.00	58.28	12.87
8.00	0.48	0.00	0.00	219.51	56.78
9.00	0.41	0.14	0.14	286.48	134.76
10.00	0.37	0.49	0.63	324.76	151.38
11.00	0.34	0.50	1.13	329.54	149.06
12.00	0.34	0.53	1.66	344.13	147.31
13.00	0.35	0.56	2.23	360.00	146.16
14.00	0.39	0.69	2.91	436.41	145.00
15.00	0.44	0.89	3.80	568.22	145.91
16.00	0.50	1.02	4.82	656.24	147.57
17.00	0.53	0.92	5.74	603.72	149.29
18.00	0.22	0.00	5.74	0.00	128.34

Month average production = 1.640 kg/m^2-day
Month Total USEFUL ENERGY = 4187.3 Wh

MONTH = APRIL

TIME	COLLECTOR EFFICIENCY	HOURLY PRODUCTION[1]	CUMULATIVE PRODUCTION[1]	USEFUL ENERGY[2]	ENERGY LOSS[2]
7.00	0.56	0.00	0.00	181.97	33.79
8.00	0.51	0.15	0.15	361.37	118.65
9.00	0.50	0.88	1.03	557.40	144.78
10.00	0.48	1.05	2.08	655.73	142.09
11.00	0.46	1.12	3.20	702.02	140.13
12.00	0.45	1.03	4.23	644.49	138.76
13.00	0.47	1.06	5.29	664.65	138.56
14.00	0.49	1.14	6.43	710.02	138.16
15.00	0.52	1.18	7.61	735.90	139.73
16.00	0.54	1.00	8.61	625.97	141.71
17.00	0.54	0.68	9.29	430.38	144.04
18.00	0.26	0.00	9.29	0.00	126.04

Month average production = 2.654 kg/m^2-day
Month Total USEFUL ENERGY = 6269.9 Wh

MONTH = MAY

TIME	COLLECTOR EFFICIENCY	HOURLY PRODUCTION[1]	CUMULATIVE PRODUCTION[1]	USEFUL ENERGY[2]	ENERGY LOSS[2]
6.00	0.52	0.00	0.00	72.65	14.90
7.00	0.54	0.00	0.00	277.75	70.55
8.00	0.55	0.68	0.68	502.59	136.52
9.00	0.55	1.18	1.85	735.08	134.65
10.00	0.54	1.43	3.28	895.52	131.50
11.00	0.53	1.48	4.76	922.33	128.97
12.00	0.53	1.44	6.20	899.17	127.62
13.00	0.53	1.29	7.49	807.25	127.62
14.00	0.55	1.27	8.76	795.91	127.43
15.00	0.56	1.27	10.03	793.18	129.56
16.00	0.57	1.10	11.13	686.00	131.13
17.00	0.53	0.92	12.05	576.00	133.87
18.00	0.49	0.78	12.83	486.59	137.41
19.00	0.09	0.00	12.83	0.00	118.62

Month average production = 3.665 kg/m^2-day
Month Total USEFUL ENERGY = 8450.0 Wh

MONTH = JUNE

TIME	COLLECTOR EFFICIENCY	HOURLY PRODUCTION[1]	CUMULATIVE PRODUCTION[1]	USEFUL ENERGY[2]	ENERGY LOSS[2]
6.00	0.51	0.00	0.00	197.58	36.29
7.00	0.53	0.37	0.37	441.06	118.80
8.00	0.57	1.30	1.67	811.07	130.34
9.00	0.58	1.74	3.41	1087.48	126.43
10.00	0.57	1.94	5.34	1210.94	123.31
11.00	0.56	2.00	7.34	1249.54	120.99
12.00	0.56	2.04	9.38	1272.68	119.44
13.00	0.57	2.02	11.40	1265.00	119.25
14.00	0.58	1.99	13.39	1244.00	118.48
15.00	0.59	1.88	15.28	1178.27	121.00
16.00	0.58	1.69	16.97	1058.05	122.37
17.00	0.54	1.32	18.29	826.02	124.12
18.00	0.49	1.21	19.50	755.52	128.59
19.00	0.22	0.00	19.50	0.00	114.46

Month average production = 5.572 kg/m^2-day
Month Total USEFUL ENERGY = 12597.2 Wh

Fig. 3.17 Simulation program "PTCDES2" output

MONTH = JULY

TIME	COLLECTOR EFFICIENCY	HOURLY PRODUCTION[1]	CUMULATIVE PRODUCTION[1]	USEFUL ENERGY[2]	ENERGY LOSS[2]
6.00	0.51	0.00	0.00	137.21	25.56
7.00	0.54	0.36	0.36	485.02	108.81
8.00	0.58	1.46	1.82	910.33	125.87
9.00	0.58	1.88	3.69	1173.76	122.16
10.00	0.57	2.05	5.75	1282.06	118.87
11.00	0.56	2.15	7.90	1343.00	116.16
12.00	0.56	2.20	10.10	1374.49	114.04
13.00	0.56	2.23	12.32	1392.46	113.28
14.00	0.58	2.30	14.62	1435.45	112.70
15.00	0.59	2.17	16.79	1357.79	114.62
16.00	0.59	1.84	18.64	1150.75	116.56
17.00	0.55	1.38	20.02	864.08	119.48
18.00	0.50	1.07	21.09	666.40	123.16
19.00	0.17	0.00	21.09	0.00	108.29

Month average production = 6.024 kg/m^2-day
Month Total USEFUL ENERGY = 13572.8 Wh

MONTH = AUGUST

TIME	COLLECTOR EFFICIENCY	HOURLY PRODUCTION[1]	CUMULATIVE PRODUCTION[1]	USEFUL ENERGY[2]	ENERGY LOSS[2]
7.00	0.57	0.00	0.00	372.65	68.56
8.00	0.56	1.13	1.13	721.24	128.00
9.00	0.55	1.52	2.65	950.49	124.12
10.00	0.53	1.71	4.36	1066.24	120.23
11.00	0.51	1.77	6.12	1103.25	117.34
12.00	0.51	1.83	7.95	1140.50	115.02
13.00	0.52	1.86	9.80	1159.06	114.25
14.00	0.54	1.93	11.73	1203.24	113.68
15.00	0.56	1.90	13.63	1189.18	115.98
16.00	0.59	1.85	15.48	1156.74	118.10
17.00	0.58	1.52	17.00	948.31	121.21
18.00	0.54	1.23	18.23	770.25	125.29

Month average production = 5.209 kg/m^2-day
Month Total USEFUL ENERGY = 11781.1 Wh

MONTH = SEPTEMBER

TIME	COLLECTOR EFFICIENCY	HOURLY PRODUCTION[1]	CUMULATIVE PRODUCTION[1]	USEFUL ENERGY[2]	ENERGY LOSS[2]
7.00	0.54	0.00	0.00	234.14	42.85
8.00	0.50	0.60	0.60	549.31	124.64
9.00	0.47	1.18	1.78	736.92	128.79
10.00	0.44	1.23	3.02	770.77	125.09
11.00	0.42	1.26	4.28	788.09	122.38
12.00	0.42	1.31	5.59	819.57	120.25
13.00	0.44	1.40	6.99	875.48	119.47
14.00	0.47	1.47	8.46	916.67	119.28
15.00	0.51	1.55	10.01	968.75	121.59
16.00	0.55	1.71	11.72	1070.32	124.10
17.00	0.58	1.84	13.56	1149.06	126.42
18.00	0.26	0.00	13.56	0.00	112.33

Month average production = 3.873 kg/m^2-day
Month Total USEFUL ENERGY = 8879.1 Wh

Fig. 3.17 Simulation program "PTCDES2" output (cont.)

MONTH = OCTOBER

TIME	COLLECTOR EFFICIENCY	HOURLY PRODUCTION[1]	CUMULATIVE PRODUCTION[1]	USEFUL ENERGY[2]	ENERGY LOSS[2]
7.00	0.48	0.00	0.00	75.74	15.44
8.00	0.43	0.00	0.00	274.48	70.52
9.00	0.36	0.39	0.39	323.06	133.36
10.00	0.31	0.52	0.91	323.01	133.12
11.00	0.28	0.51	1.42	318.99	130.78
12.00	0.29	0.58	1.99	359.05	129.02
13.00	0.32	0.74	2.73	461.12	128.43
14.00	0.38	1.03	3.76	643.86	128.02
15.00	0.44	1.33	5.10	833.92	130.34
16.00	0.50	1.47	6.57	918.31	133.06
17.00	0.33	0.00	6.57	0.00	122.09

Month average production = 1.876 kg/m^2-day
Month Total USEFUL ENERGY = 4531.5 Wh

MONTH = NOVEMBER

TIME	COLLECTOR EFFICIENCY	HOURLY PRODUCTION[1]	CUMULATIVE PRODUCTION[1]	USEFUL ENERGY[2]	ENERGY LOSS[2]
8.00	0.37	0.00	0.00	87.43	17.68
9.00	0.29	0.00	0.00	143.96	49.58
10.00	0.21	0.00	0.00	113.76	88.83
11.00	0.17	0.00	0.00	71.00	118.00
12.00	0.17	0.02	0.02	53.81	137.70
13.00	0.20	0.18	0.20	112.41	142.13
14.00	0.26	0.36	0.57	226.87	141.94
15.00	0.35	0.67	1.24	422.34	143.47
16.00	0.43	0.97	2.21	619.00	145.32
17.00	0.11	0.00	2.21	0.00	124.77

Month average production = 0.632 kg/m^2-day
Month Total USEFUL ENERGY = 1850.6 Wh

MONTH = DECEMBER

TIME	COLLECTOR EFFICIENCY	HOURLY PRODUCTION[1]	CUMULATIVE PRODUCTION[1]	USEFUL ENERGY[2]	ENERGY LOSS[2]
8.00	0.35	0.00	0.00	48.75	11.41
9.00	0.28	0.00	0.00	162.71	42.54
10.00	0.19	0.00	0.00	105.39	82.57
11.00	0.15	0.00	0.00	49.35	106.22
12.00	0.14	0.00	0.00	28.06	118.55
13.00	0.16	0.00	0.00	57.55	133.80
14.00	0.21	0.16	0.16	124.71	150.44
15.00	0.30	0.46	0.61	303.37	152.18
16.00	0.25	0.00	0.61	0.00	137.70
17.00	0.11	0.00	0.61	0.00	106.54

Month average production = 0.175 kg/m^2-day
Month Total USEFUL ENERGY = 879.9 Wh

Notes:
1. Steam production in kg
2. Useful energy and energy loss in Wh

Month	PTCDES1 Results		PTCDES2 Results		Percentage difference in useful energy
	Useful energy (Wh)	Mean steam production (kg/m^2 day)	Useful energy (Wh)	Mean steam production (kg/m^2 day)	
January	831.6	0.146	758.9	0.116	+8.7
February	1365.5	0.379	1225.5	0.320	+10.2
March	4296.3	1.688	4187.3	1.640	+2.5
April	6296.2	2.666	6269.9	2.654	+0.4
May	8420.4	3.652	8450.0	3.665	-0.3
June	12578.6	5.563	12597.2	5.572	-0.1
July	13555.6	6.017	13572.8	6.024	-0.1
August	11828.2	5.431	11781.1	5.209	+0.4
September	8945.4	3.903	8879.1	3.873	+0.7
October	4716.3	1.960	4531.5	1.876	+3.9
November	2045.3	0.721	1850.6	0.632	+9.5
December	975.1	0.216	879.9	0.175	+9.8
Annual	2275.6 kWh	970.3 kg/m^2	2249.5 kWh	952.7 kg/m^2	1.2

Table 3.7 Predicted monthly energy collection and steam production

Blank page

CHAPTER 4

CHAPTER 4

CONSTRUCTION OF THE SYSTEM

The system constructed as part of this project includes the collector and the steam generation system. In this chapter detailed drawings and photographs are presented and the construction is described.

4.1 CONSTRUCTION OF THE COLLECTOR

4.1.1 Parabola Construction

It is desirable that the parabola of the PTC must be produced in such a way so as to be low priced and accurate and the construction method must be amenable to a low-labour cost and/or a mass production manufacturing process.

In order to achieve cost effectiveness in mass production the collector structure must feature a high stiffness-to-weight ratio so as to keep the material content to a minimum. Such a structure can be obtained by fibreglass which is a material of proven rigidity under severe weather conditions.

The importance of the accuracy of the parabola has already been stressed. The parabola is constructed with fibreglass which is an exact copy of a mould. Therefore great care must be applied in the construction of the mould. For this a synthetic wood with medium Density Fibres (MDF) of 18mm thickness was used. This material has good dimensional stability, is able to withstand fine cuts, and exhibits very good resistance to humidity.

A mould support of MDF was constructed as a "master" using hand tools. The outline of the required parabola drawn on a piece of tracing paper on a high accuracy plotter was glued onto a sheet of MDF and the wood was crafted as close to the drawing line as possible. This piece of MDF was used as a master for the production of the other supports on a Vertical Spindle Moulder machine using the master as a guide [Kalogirou

et al., 1994b].

The parabolic forms constructed in this way were mounted perpendicularly, on a cross support constructed from a sheet of MDF wood as shown in Fig. 4.1. Care was taken to fix the parabolic forms in line with each other. The accuracy of the structure was checked with a long aluminium straight edged bar. The structure was laid on the floor to increase the dimensional stability of the final mould. A 4mm smooth surface melamine sheet was fixed on top of these parabolic forms with small nails. Stucco was used for the elimination of any marks left by the nails and this was sandpapered after setting. The mould was now ready to be used in the casting of the collector trough.

A wax parting compound was first applied to the surface of the mould. This is used to allow easy separation of the casting from the mould. A gel-coat polyester resin was then brushed onto the surface and allowed to cure. This forms the inside surface of the parabola, i.e. the face where the reflective material will be subsequently fixed. After this coating has set, a layer of polyester resin and woven fibreglass cloth was built up on top of the coat, rolled and allowed to set. This gave to the casting a 2mm thickness. After the fibreglass has set, plastic conduits were fixed on the surface, in the longitudinal and transverse direction as shown in Fig. 4.2, with paper tape. These conduits were then covered with a further layer of polyester resin and woven fibreglass cloth which were laid, rolled and allowed to set. The reinforcement produced by the shape of the plastic conduits increase the rigidity of the casting. As an alternative a plastic water hose could have been used as the strength of the material does not contribute significantly in the reinforcement. The total thickness of the casting is typically 4mm (mean value).

After allowing sufficient time for curing, the casting was pulled from the mould. The time between the various steps depends on the ambient temperature and varies between 1-24 hours. It is important, however, to ensure complete curing of the resin [Kalogirou *et al.*, 1994b]. The final step was to fix the reflective material. For this purpose a self adhesive material (i.e. Scotchcal 5400) with a reflectance of 0.85 was used.

Virtually all the above operations involved in the fabrication of the casting can be performed by a semi-skilled worker. Clearly the method of parabola construction

described above can be used for mass production of parabolas, either as individual castings using the same mould, or in batch production using a number of identical moulds.

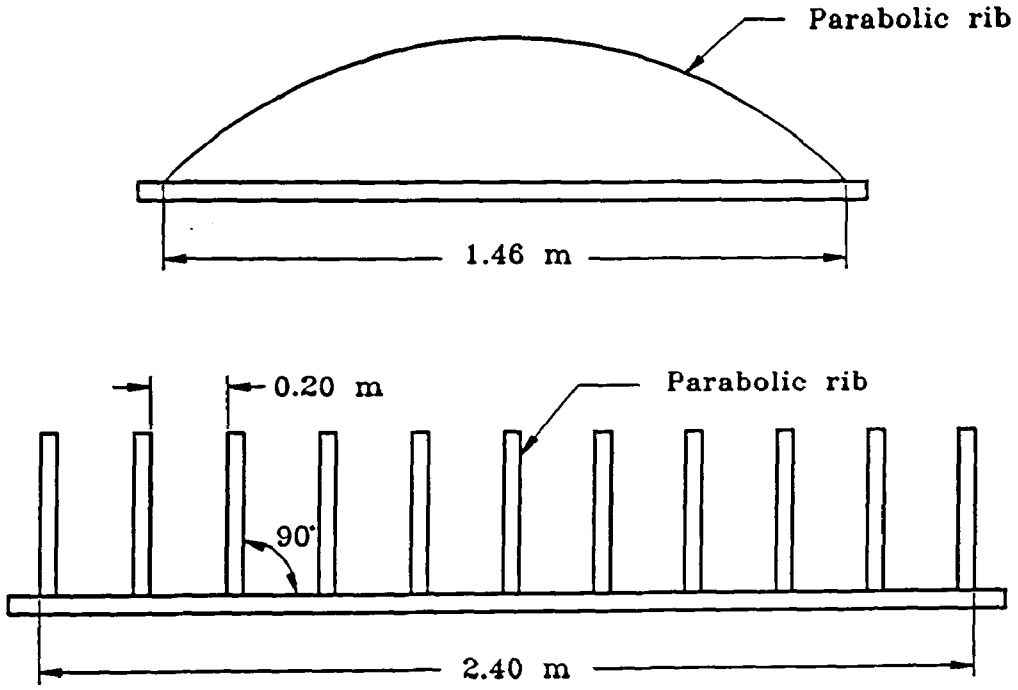

Fig. 4.1 Mould construction detail

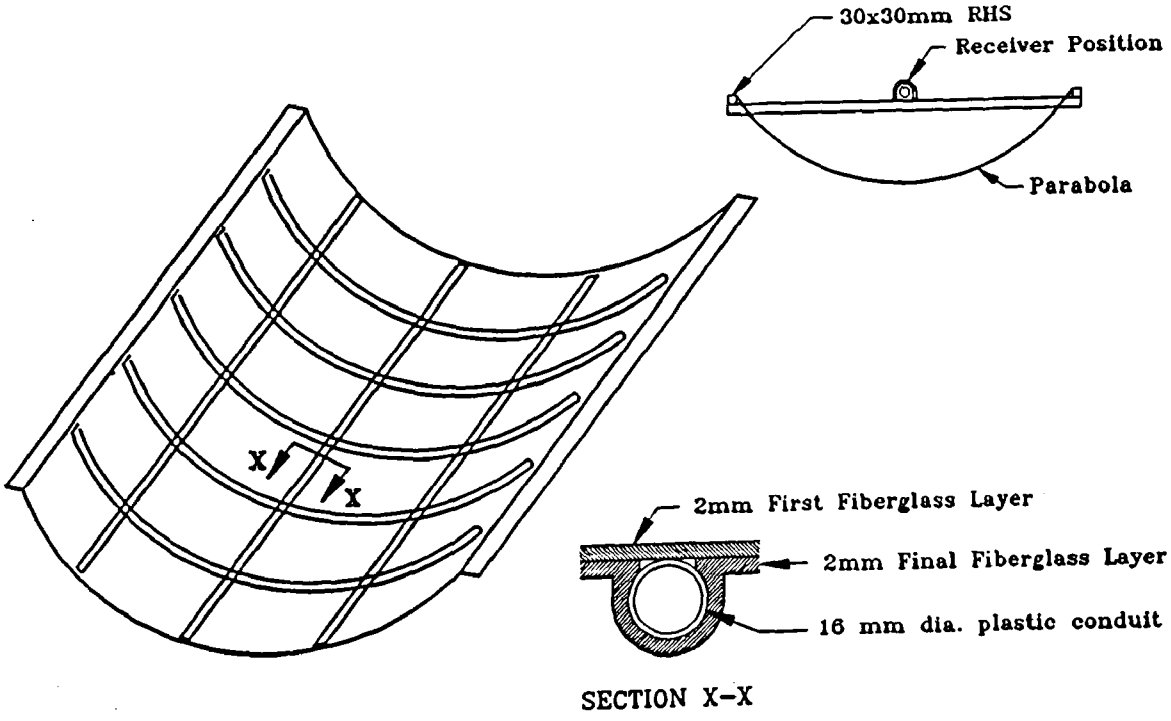

Fig. 4.2 Fibreglass parabola detail

The cost of the parabola is estimated to be C£ 15 per m^2 of aperture area for a 90° rim angle. The parabola was tested under a dead load corresponding to the force applied by a wind blowing at 40 m/s. The resultant deflection at the centre of the parabola as measured with a dial gauge was 1.2mm which is considered adequate as it results in only a 2.1% reduction in intercept factor.

4.1.2 Tracking Mechanism Construction

Details of the tracking mechanism construction are given in [Kalogirou, 1991]. The gear motor employed by the system is suitable for a 24V a.c. supply. The 12V d.c. signal produced by the control system, as described in [Kalogirou, 1991 and Kalogirou *et al.*, 1992c, appended], operates a relay which connects power to a transformer which reduces the mains supply to a value suitable for the gear motor.

The gear motor rotates at 8 rpm. The reduction gearbox has a ratio of 45:1 so that the output speed from the gearbox is 0.18 rpm. This output is fed to a small gear (25mm in pitch diameter) which drives a large gear (300mm in pitch diameter) installed on the collector (see Fig. 3.4). Thus the final rotational speed of the collector is 0.015 rpm i.e. about 50 minutes are required to re-position the collector from full East to full West.

4.1.3 Collector System Construction

The fibreglass parabola was fixed on a rigid hollow section (RHS) frame supported on two bearings via a bracket the detail of which is shown in Fig. 4.3. The bearings were supported on the frame of the system. The receiver pipe passed through the bearings and in this way flexible connections on the inlet and outlet of the collector were avoided. Plastic rings were inserted between the receiver pipe and the bearing walls for insulation purposes. A receiver bracket is used as a support at the middle of the collector to avoid sagging of the receiver pipe. The bracket is fixed by two steel wires on the RHS frame and it thus keeps the receiver in focus even at extreme collector inclinations. The glass from two fluorescent tubes was used for glazing of the receiver. The fluorescent coating was cleaned from these tubes by water. The fixing of the two glass tubes around the receiver pipe was achieved by means of spacers consisting of plastic rings for insulation

purposes.

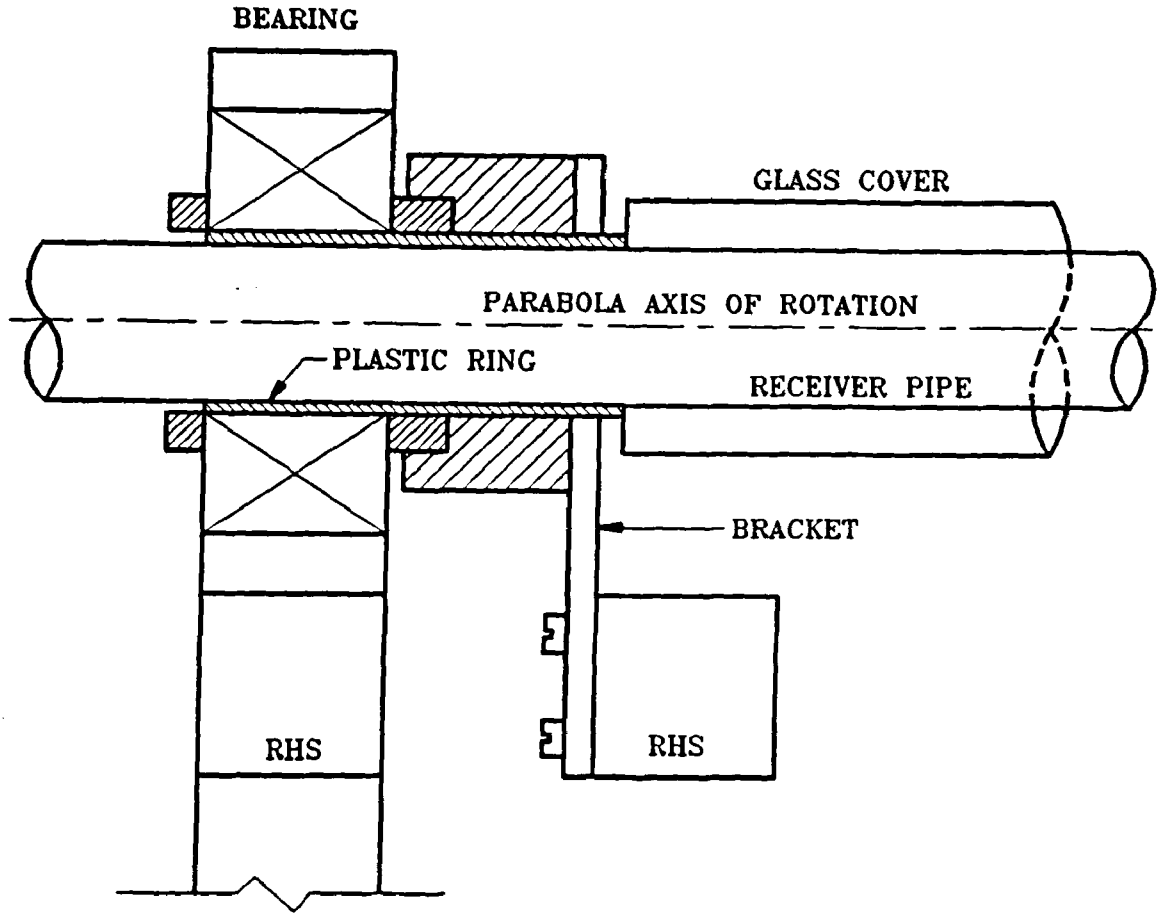

Fig. 4.3 Receiver bracket detail

4.2 CONSTRUCTION OF THE STEAM GENERATION SYSTEM

4.2.1 Flash Vessel Construction

The vessel was constructed from a 75mm diameter copper pipe with dimensions as shown in Fig. 4.4. The vessel is made in two parts for easy maintenance. The joining of the two parts is accomplished with two copper flanges sealed with a gasket inserted in between. Two steel flanges are used for the tightening of the two parts. The vessel is completed by a drain valve and a pressure gauge.

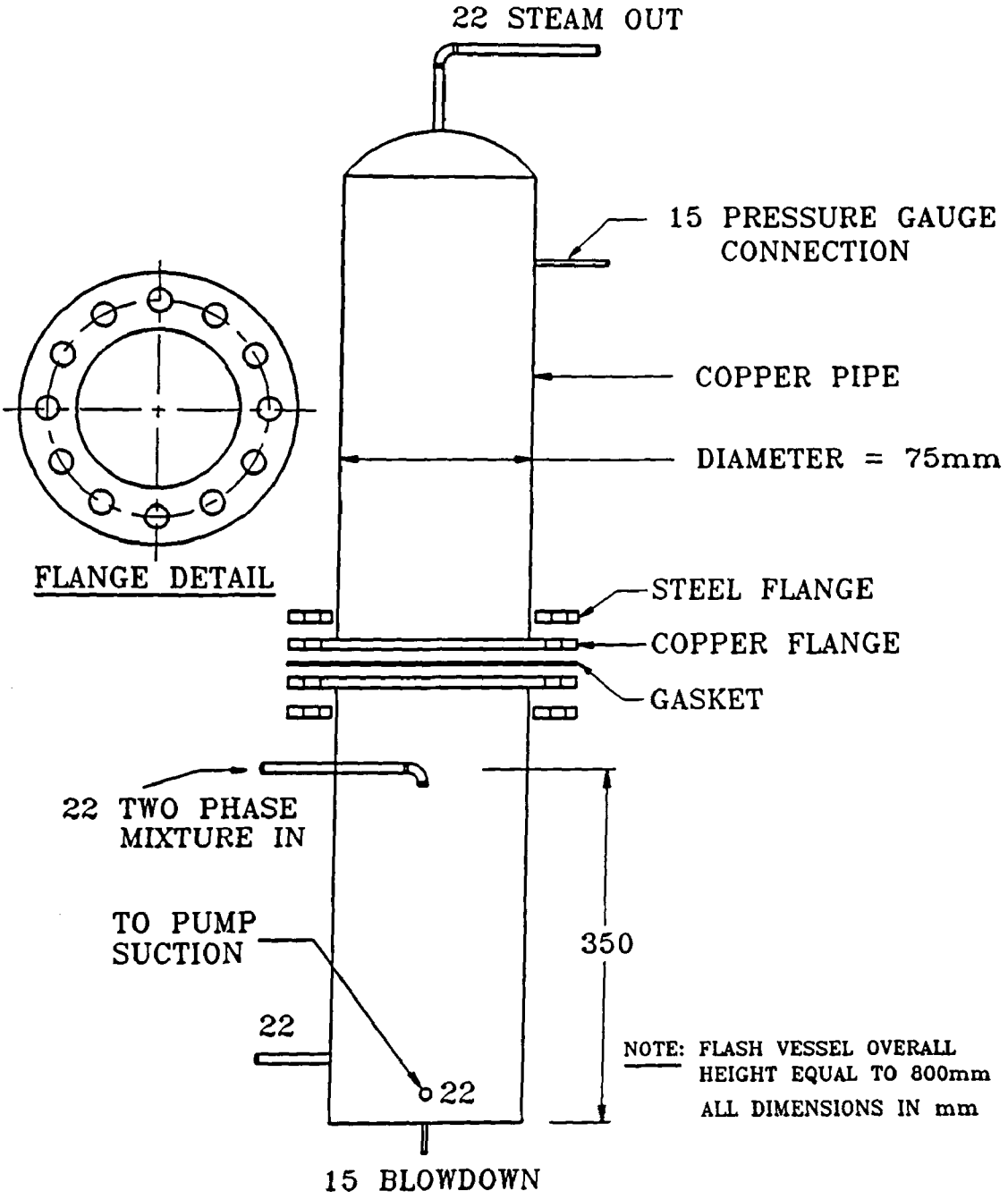

Fig. 4.4 Flash vessel detail

4.2.2 Framework construction

The frame of the system must be able to:

1. Allow accurate positioning and mounting of the collector,
2. Offer adequate rigidity and

3. Provide space for the installation of ancillary parts such as the high pressure pump and the flash vessel, and withstand their weight.

All these were achieved with the construction shown in Fig. 4.5. The whole setup was mounted on wheels to allow easy transportation of the system. A photograph of the finished system is shown in Fig. 4.6. Details of the collector parts mentioned earlier are also shown in this figure.

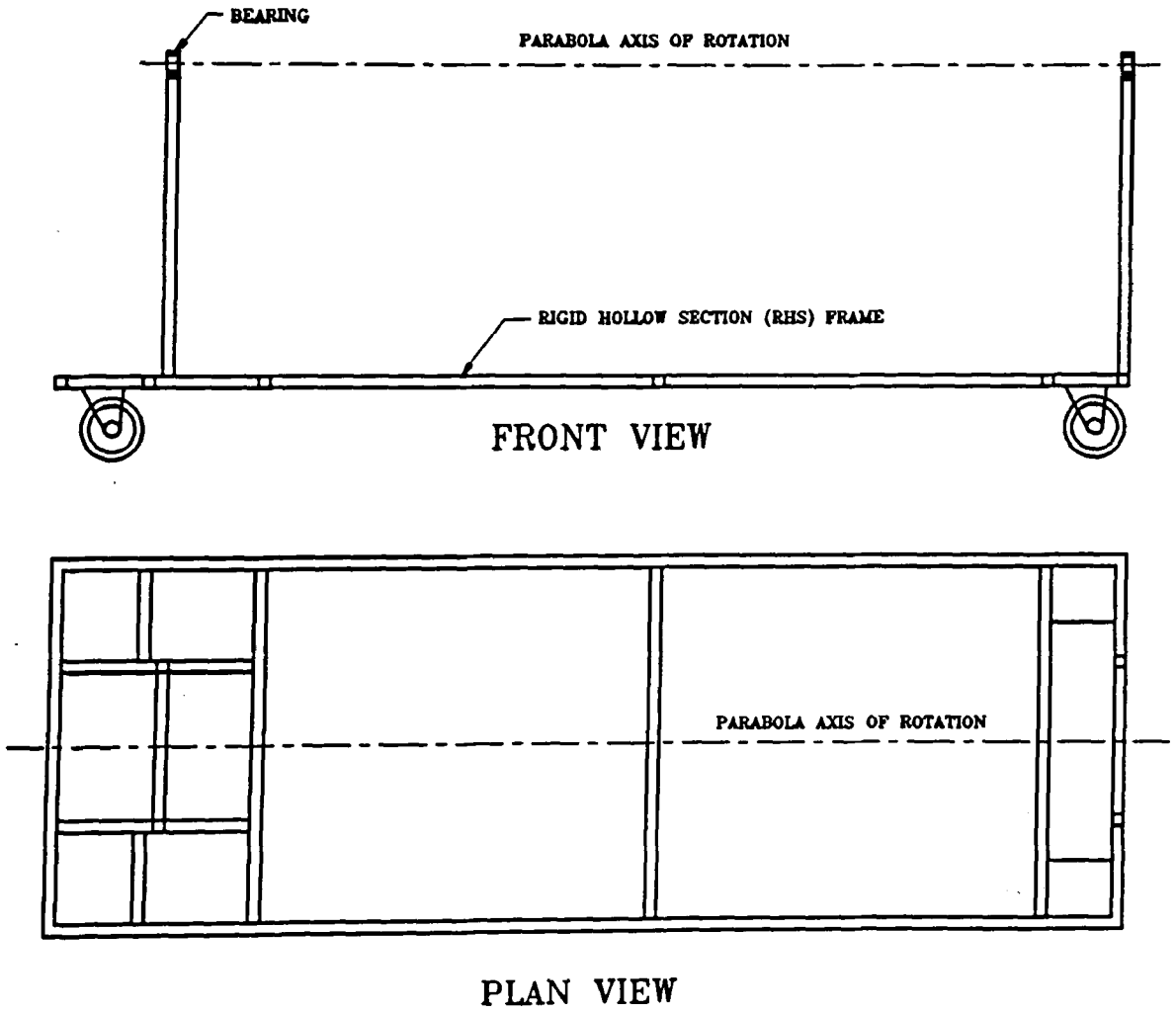

Fig. 4.5 Framework detail

Fig. 4.6 The complete system

4.2.3 Heat Exchanger Construction

The details of the heat exchanger constructed are shown in Fig. 4.7. The heat exchanger consists of a copper pipe envelope 75mm in diameter and a Wednesbury Micraversion heat exchanger of 0.23m^2 total surface area.

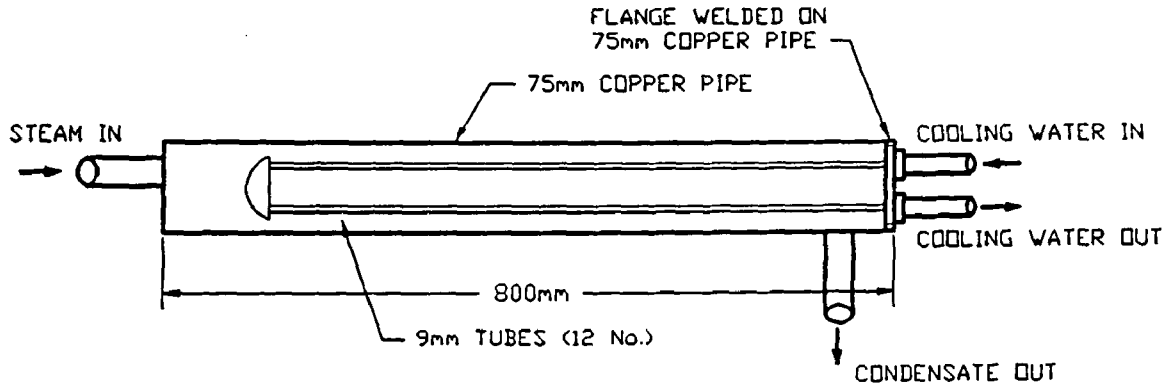

Fig. 4.7 Heat exchanger detail

4.2.4 Piping

The pump and flash vessel installation showing the pipe layout is also shown in Fig. 4.6. A pressure gauge is installed at the pump outlet after the one way valve to show the pump delivery pressure. All the pipes are made from copper to BS 2781-x. The fittings were either welded or compression type and the latter allows easy dismantling of the piping.

Blank page

CHAPTER 5

CHAPTER 5

COLLECTOR SYSTEM PERFORMANCE

In this chapter the results of the various tests carried out with the collector will be presented. The data acquisition system is first described followed by the performance tests on the collector. Finally, the system as a whole was tested on a daily basis, to evaluate the steam production capacity of the system. This will be compared to the predicted performance given by the computer simulation (see section 3.4).

5.1 DATA ACQUISITION SYSTEM

The testing of the system, and of the collector, was carried out using a data acquisition system. This is a micro processor based system consisting of a DAS-8 computer board, an EXP-16 multiplexer, and a computer program written in BASIC.

Data acquisition systems (DAS) are I/O expansion boards that convert digital computers into fast high precision data acquisition and signal analysis instruments. The board is of multilayer construction with integral ground plane to minimise noise and crosstalk at high frequencies. DAS usually receive data from the environment via transducers. DAS are characterised by high sampling rates, (up to 100kHz) which allow fast processing of the signals. In this case a rate of 50 readings per second was used.

DAS-8 had 8 analog I/O channels. The input voltage, the DAS-8 can accept, ranges from tenths of a volt up to 10 volts, with an accuracy of 12 bits (2.44 mV/bit).

In this project the DAS-8 was connected to an EXP-16 sub-multiplexer as shown in Fig. 5.1. The EXP-16 is a 16 channel multiplexer which allows multiplexing of 16 different signals (6 are used in this case) to a single DAS-8 analog input channel. A cold junction sensor is provided allowing temperature compensation of thermocouples connected to the EXP-16.

The program used in conjunction with DAS-8 and multiplexer allowed averaging of the

data, and provided the choice of writing the data to a file for further processing. The listing of the program is shown in Appendix 3.

The data acquisition system was able to measure temperature and solar radiation as shown in Fig. 5.2. The water flow rate was measured manually with an Omega high precision turbine flowmeter. This was adequate as the flowrate was kept constant throughout the tests. The specifications of the various instruments used are shown in Table 5.1.

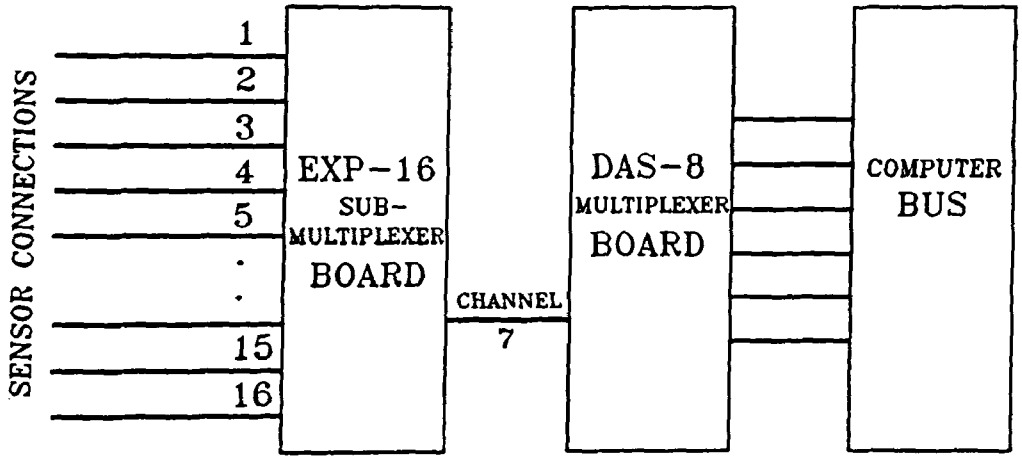

Fig. 5.1 Data acquisition system arrangement

Parameter	Instrument	Manufacturer	Specification
Temperature	Thermocouples	/	Type - K
Solar radiation	Eppley Radiometer	Eppley Laboratories Inc.	Model 8-48
Flowrate	Turbine flowmeter	Omega	FTB-4105 P

Table 5.1 Testing instruments specification

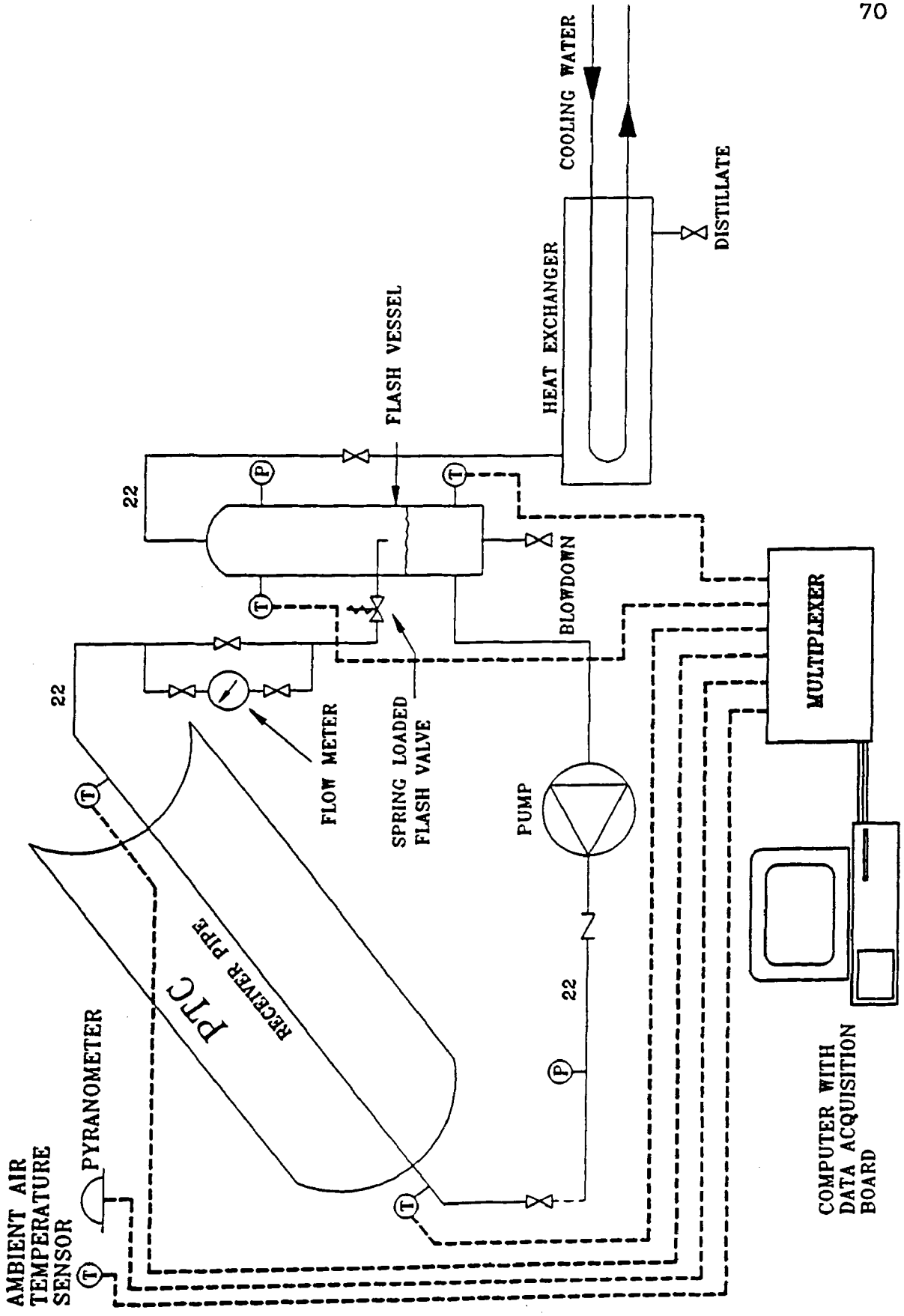

Fig. 5.2 Data acquisition measurement points

5.2 COLLECTOR THERMAL PERFORMANCE EVALUATION

The thermal performance of the solar collector is determined in part by obtaining values of instantaneous efficiency for different combinations of incident radiation, ambient temperature, and inlet fluid temperature. This requires experimental measurement of the rate of incident solar radiation onto the solar collector as well as the rate of energy addition to the transfer fluid as it passes through the collector, all under steady state or quasi-steady state conditions. In addition, tests were performed to determine the time response characteristics of the collector. The variation of steady-state thermal efficiency with incident angles between the direct beam and the normal to collector aperture area at various Sun and collector positions was also determined [ASHRAE Standard 93, 1986].

5.2.1 Collector Thermal Efficiency

According to ASHRAE standard 93 [1986] the performance of a concentrating collector operating under steady state conditions can be successfully described by the following relationship:

$$q_u = F_R\, A \left[I\, n_o - \frac{U_L}{C} \left(T_{fi} - T_a\right) \right] = m\, c_p \left(T_{fo} - T_{fi}\right) \qquad (5.1)$$

The thermal efficiency of the collector is given by:

$$n = F_R \left[n_o - \frac{U_L}{I\, C} \left(T_{fi} - T_a\right) \right] = \frac{m\, c_p \left(T_{fo} - T_{fi}\right)}{A\, I} \qquad (5.2)$$

Equation 5.2 indicates that if the efficiency, n, for a concentrating collector, is plotted against $(T_{fi}-T_a)/I$ a straight line will result. The slope is equal to $F_R\, U_L/C$ and the Y intercept is equal to $F_R\, n_o$.

The performance curve of the prototype model as derived from a total of three series of tests is shown in Fig. 5.3. By using the ordinary least squares method, the line that best fits the data points can be obtained with a slope equal to 0.387 and an intercept of 0.638.

Intercept = $F_R\, n_o = 0.638$

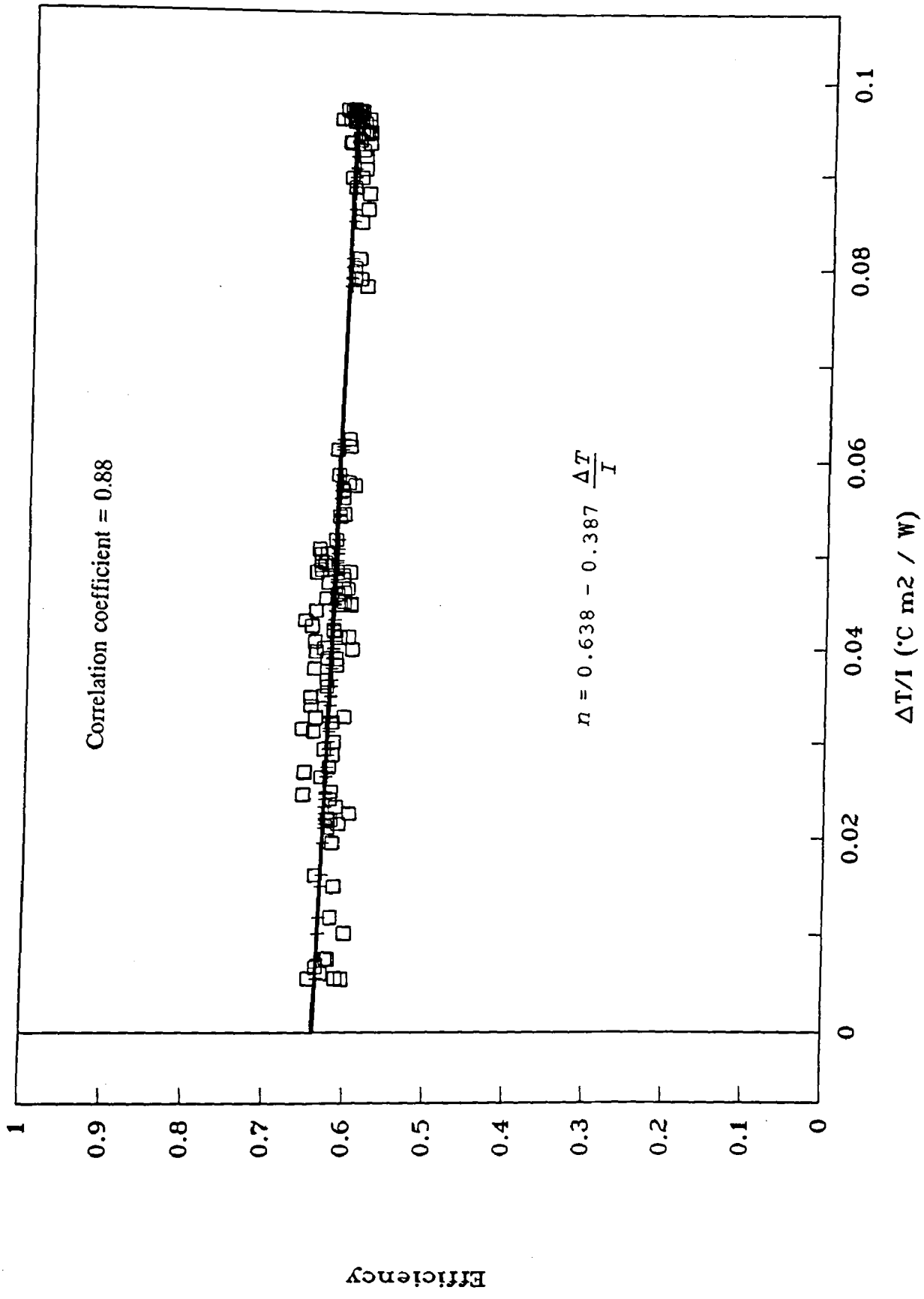

Fig. 5.3 Collector performance curve

Slope = $F_R\ U_L/C$ = 0.387 W/m^{2}K

Therefore the collector equation can be written as:

$$n = 0.638 - 0.387\ (\frac{\Delta T}{I}) \qquad (5.3)$$

By using a calculated value of F_R = 0.994 and a concentration ratio, C = 21.1:

Optical efficiency, n_o = 0.642

Heat loss coefficient, U_L = 8.2 W/m^{2}K

The former indicates a good optical behaviour whereas the latter shows a low energy loss coefficient. The efficiency equation compares well with other reported collectors as shown in Table 5.2.

Efficiency equation	Reference
$n = 0.66 - 0.233\ \frac{\Delta T}{I}$	Murthy and Keneth, 1982
$n = 0.65 - 0.382\ \frac{\Delta T}{I}$	Hurtado and Kast, 1984
$n = 0.642 - 0.441\ \frac{\Delta T}{I}$	Kalogirou, 1991
$n = 0.638 - 0.387\ \frac{\Delta T}{I}$	Present

Table 5.2 Comparison of collector performance efficiency equations

5.2.2 Collector Time Constant

It is necessary to determine the time response of the solar collector in order to be able to evaluate the transient behaviour of the collector, and to select the correct time intervals for the quasi-steady state or steady state efficiency tests.

Whenever transient conditions exist, Equations 5.1 and 5.2 do not govern the thermal performance of the collector since part of the absorbed solar energy is used for heating up the collector and its components.

The time constant of a collector is the time required for the fluid leaving the collector to reach 63% of its ultimate steady value after a step change in incident radiation. The collector time constant is a measure of the time required for the following relationship to apply [ASHRAE standard 93, 1986]:

$$\frac{T_{ot} - T_i}{T_{oi} - T_i} = \frac{1}{e} = 0.368 \qquad (5.4)$$

where T_i = collector entering water temperature [°C]

T_{oi} = collector outlet initial water temperature [°C]

T_{ot} = collector outlet water temperature after time t [°C]

Prapas *el al.* [1988] recommend that both "heating"and "cooling" time constants have to be reported. These are shown graphically in Figures 5.4 and 5.5. From the graphs it can be shown that the "heating" and "cooling" time constants for the collector constructed, operating at the design flowrate of 0.012 l/s m^2, are 52 sec and 48 sec respectively. Both indicate that the collector has a fast response compared to flat plate collectors which is about 3 minutes.

5.2.3 Collector Incidence Angle Modifier

The incidence angle modifier determines the drop of optical efficiency with change of incidence angle. This is shown in Fig. 5.6. The test results obtained are denoted by the small squares. By using a curve fitting method (second order polynomial fit), the curve that best fits the points can be obtained:

For Θ in degrees:

$$K_{\alpha\tau} = 1 - 5.05x10^{-3}\,\Theta - 1.71x10^{-4}\,\Theta^2 + 7.21x10^{-7}\,\Theta^3 \qquad (5.4)$$

For Θ in radians:

$$K_{\alpha\tau} = 1 - 0.289\,\Theta - 0.561\,\Theta^2 + 0.136\,\Theta^3 \qquad (5.5)$$

where $K_{\alpha\tau}$ = incidence angle modifier

Θ = incidence angle.

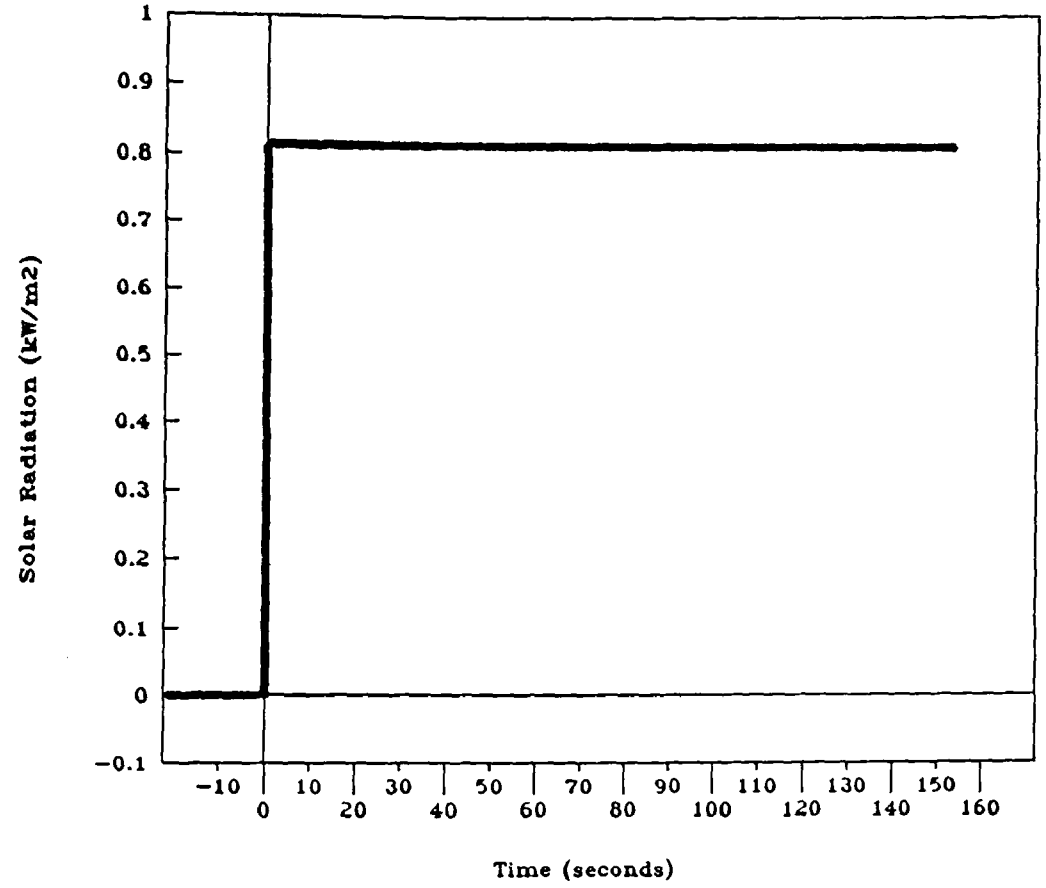

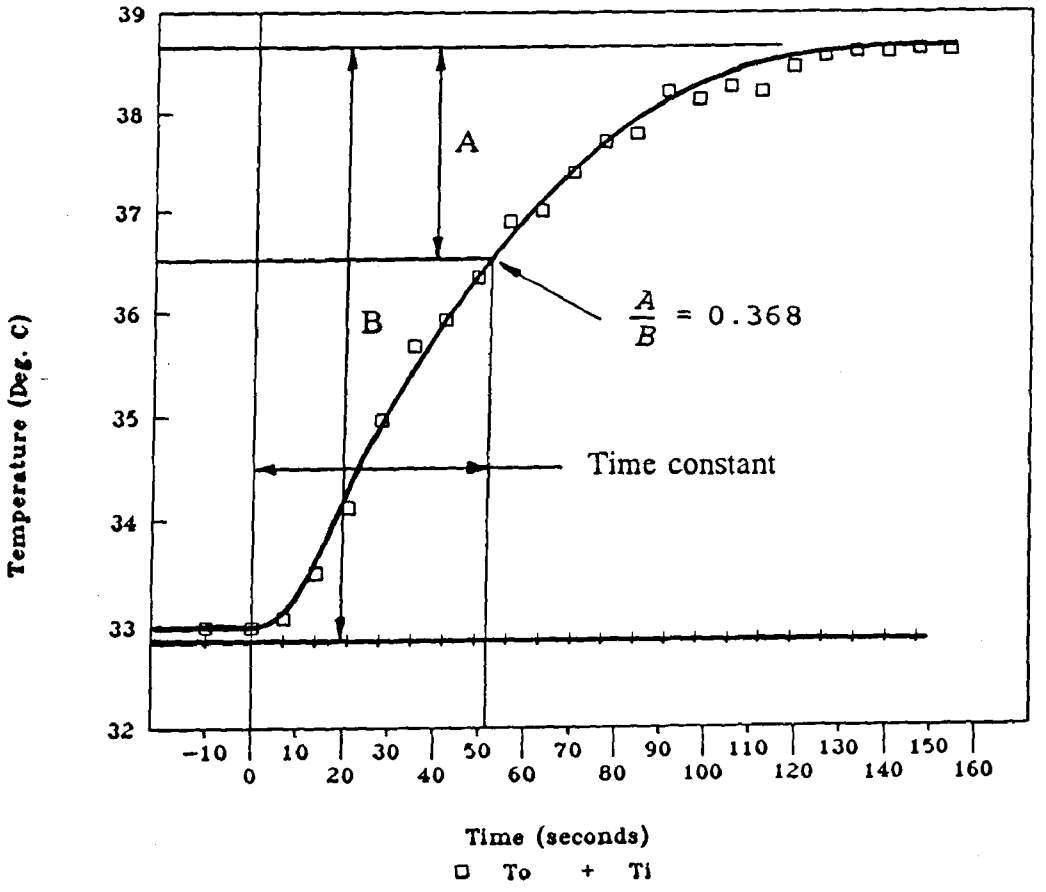

Fig. 5.4 Collector time constant test results "heating"

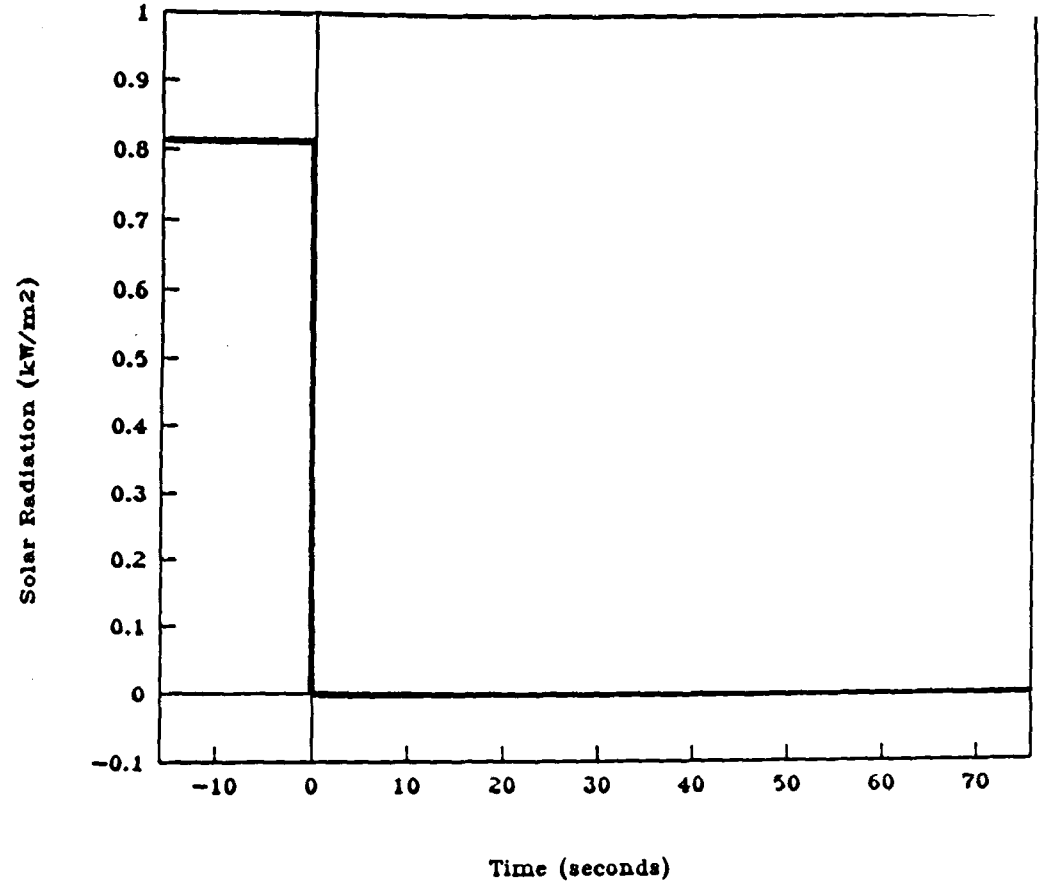

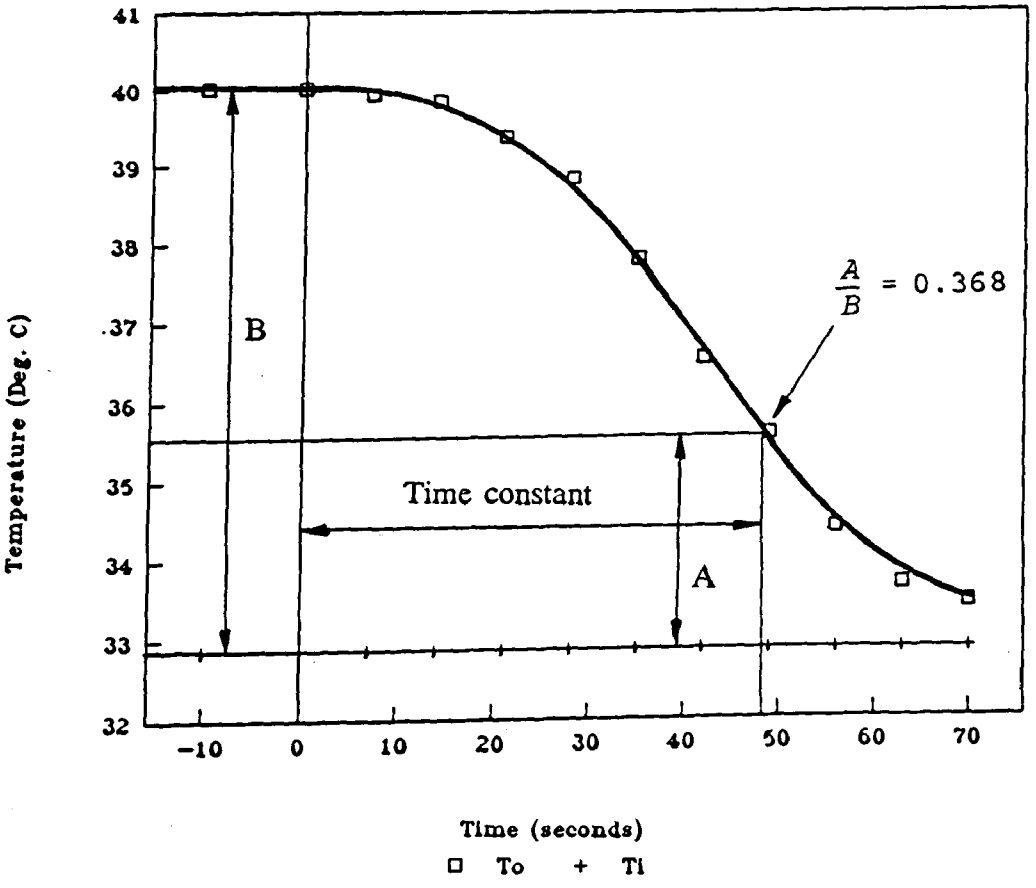

Fig. 5.5 Collector time constant test results "cooling"

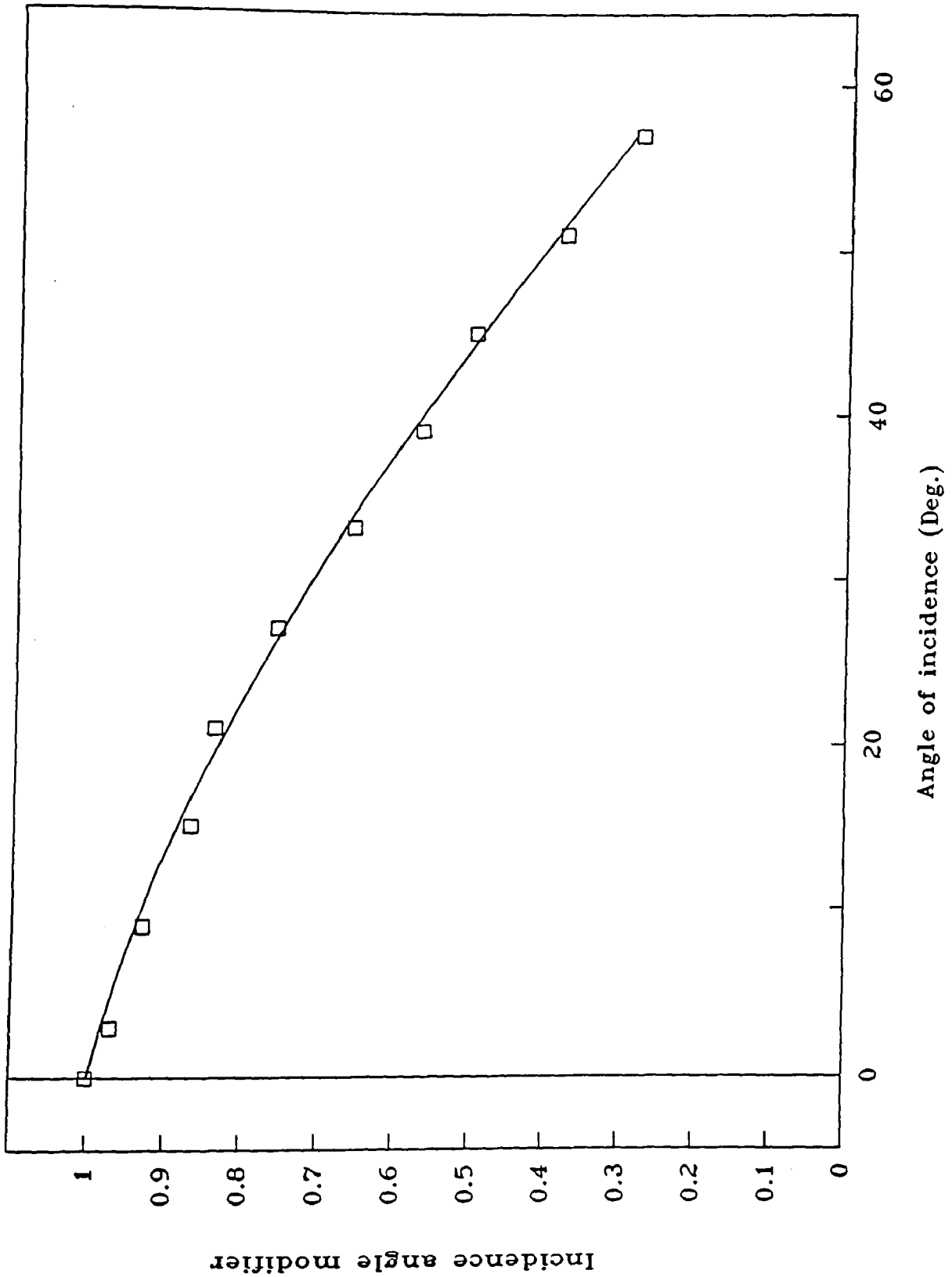

Fig. 5.6 Incidence angle modifier test results

5.2.4 Collector Acceptance Angle

Another test performed with the model was the determination of the collector acceptance angle, which characterises the effect of errors in the tracking mechanism angular orientation. This was found with the tracking mechanism disengaged and the efficiency was measured at various out of focus angles as the Sun is travelling over the collector plane. The results are shown in Fig. 5.7 where the angle of incidence measured from the normal to the tracking axis (i.e. out of focus angle) is plotted against the efficiency factor i.e. the ratio of the maximum efficiency at normal incidence to the efficiency at a particular out of focus angle.

A definition of the collector acceptance angle is the range of incidence angles (as measured from the normal to the tracking axis) in which the efficiency factor varies by no more than 2% from the value of normal incidence [ASHRAE standard, 1986]. Therefore from Fig. 5.7 the collector half acceptance angle, Θm, is 0.5°. As the tracking mechanism is accurate to 0.2° [Kalogirou *et al.*, 1992c, appended], the collector will always operated at maximum efficiency.

5.2.5 Dust Accumulation on the Reflector

The effect of dirty reflective surfaces on efficiency has been previously reported [Kalogirou, 1991] and Deffenbaugh *et al.* [1986]. For typical urban environments the loss in efficiency is a maximum of 0.6% per day with a typical value of 0.2% per day. The latter investigators suggested an optimum wash frequency of 45 days with an annual loss of energy collection of 8.5%. A more frequent practical wash cycle is 30 days (i.e. monthly) with a reduction of 5.5%. These results are local climate dependent but the environment of San Antonio in Texas, USA (30° latitude), where the testing was performed, according to Deffenbaugh *et al.* [1986], is very similar to Nicosia–Cyprus (35° latitude). The yearly mean radiation differs by 1% whereas mean annual air temperatures differ by 9%. For this reason the above results are considered as reasonably applicable for Nicosia–Cyprus.

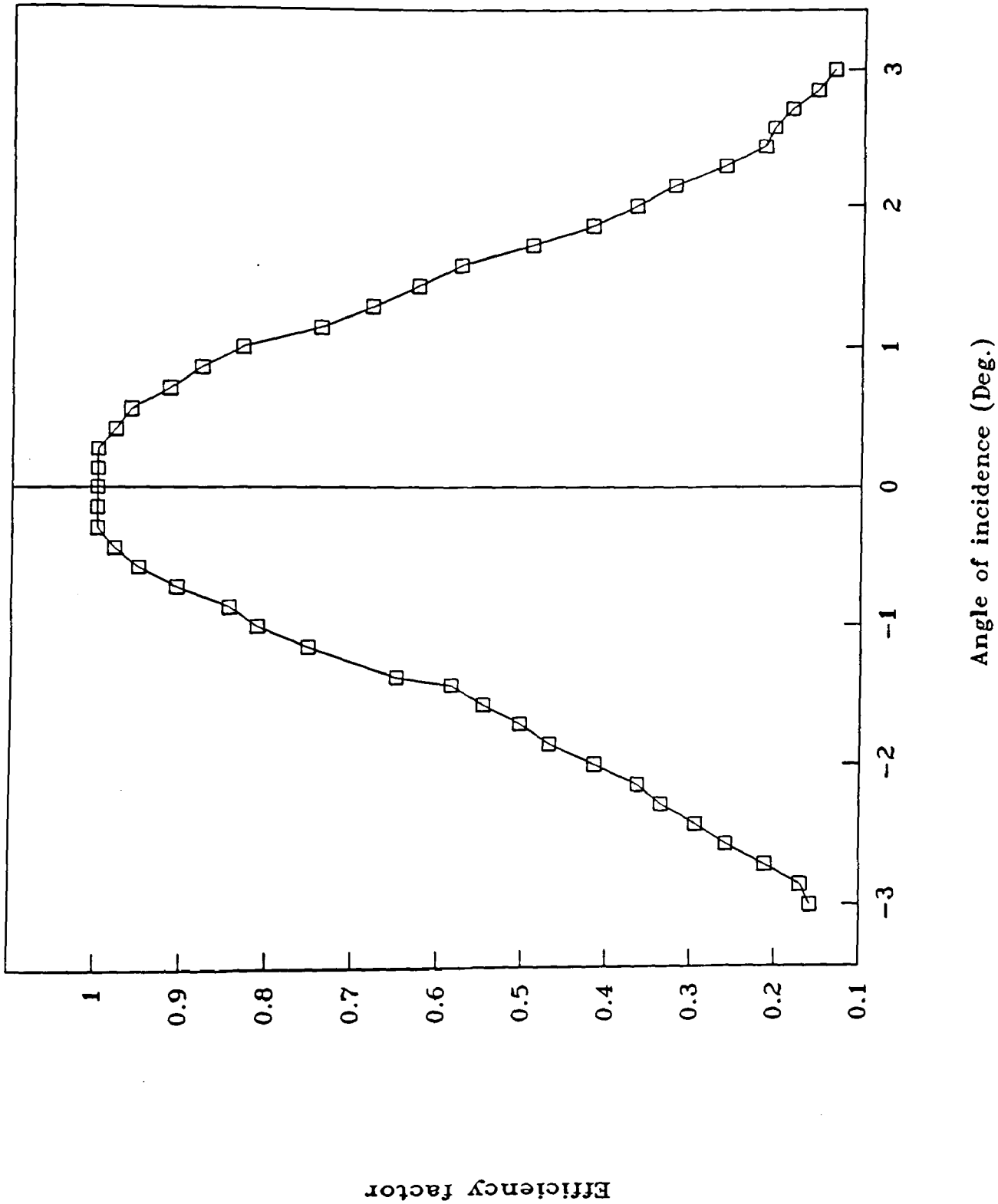

Fig. 5.7 Collector acceptance angle test results

5.3 EVALUATION OF THE SYSTEM PERFORMANCE

First the transient system performance was evaluated to investigate the energy required to pre-heat the system followed by the evaluation of the daily steam production. Finally a comparison of the experimental results with the predicted results is presented.

5.3.1 Pre-heat Energy Evaluation

For a cold start the amount of energy required to pre-heat the system depends on the thermal capacity of the various system components, on the total water quantity and on the thermal losses.

The pre-heat energy can be measured by recording the temperatures at various points in the system together with the solar radiation falling on the collector aperture area. For this purpose a computer data acquisition system was set up utilising K-type thermocouples for temperature measurement and an Eppley radiometer for recording the solar radiation. The measurement position of each thermocouple is shown in Fig. 5.8.

The measured temperatures during a cold start of the system, together with the corresponding solar radiation are shown in Fig. 5.8. The system is at the end of the pre-heat cycle when the temperature at T4 (flash vessel top) reaches the temperature T3 (flash vessel bottom). This indicates that steam is now being produced at a steady rate and that the flash vessel has approximately reached the steady state temperature. From the data shown in Fig. 5.8 this is achieved after approximately 46 minutes. During this time period the insolation was approximately 655 W/m^2 which represents the total energy available to the collector of 6.1 MJ. It can be seen from Fig. 5.8 that the temperature at the top of the flash vessel (T4), slowly increases by conduction from the bottom of the vessel until the collector outlet temperature reaches 100°C. When this happens the temperature increases more rapidly but more energy is still needed, (about 1.3 MJ) to pre-heat this part of the vessel. The steam produced during this period is condensed on the relatively cold vessel walls until their temperature reaches the value of (T3) at which point the pre-heat cycle is completed and the system starts producing useful steam. The temperature difference between T3 and T2 is attributed mainly to heat

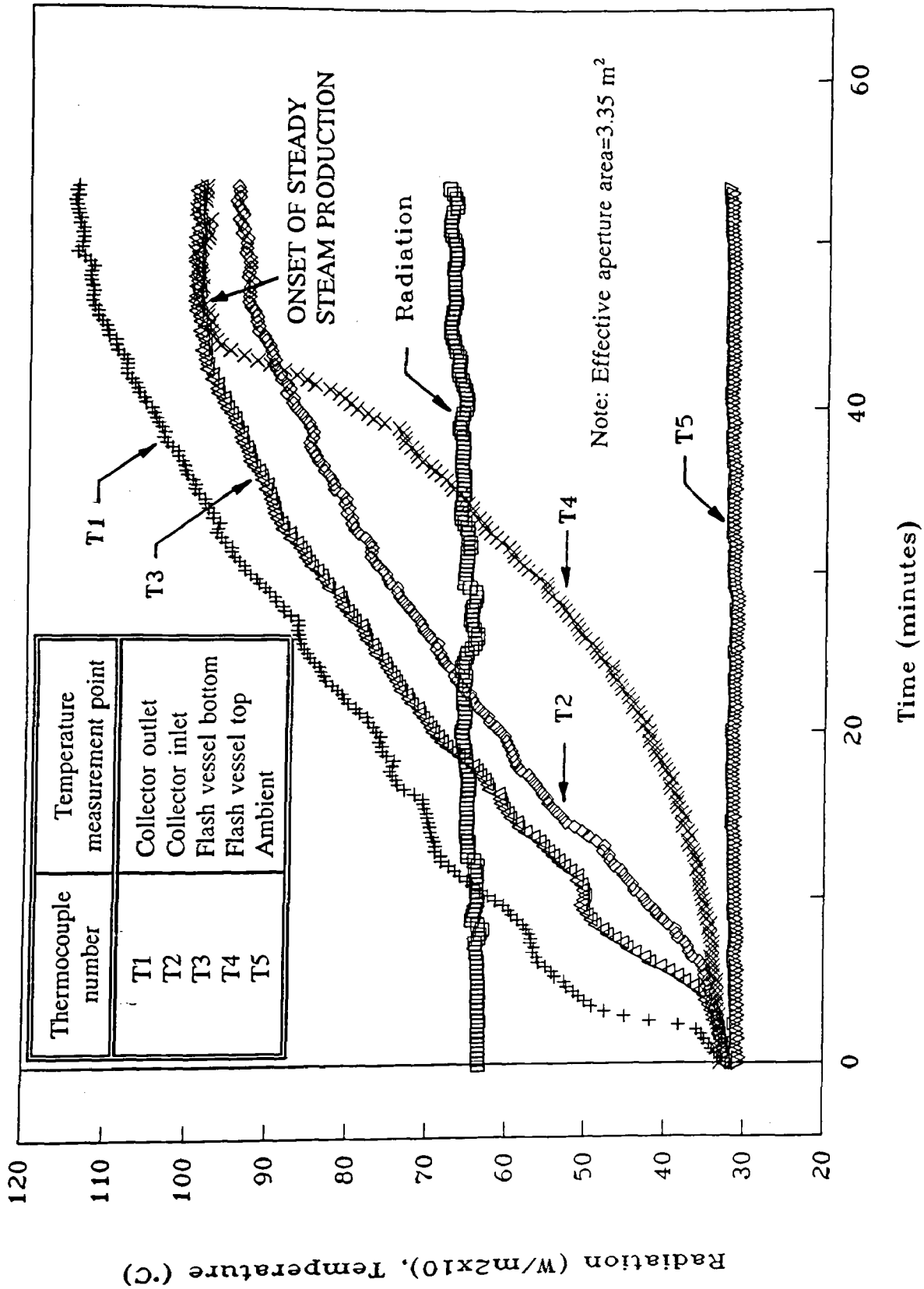

Fig. 5.8 Pre-heat cycle graph

losses from the pump body and piping. A flash vessel of 75mm diameter, 800mm height of 1.5 litres water content was used for this experiment.

5.3.2 Analysis of the System Performance

The predicted system steam production is compared with the actual steam production for a test on September the 2nd in Fig. 5.9. The predictions of program "PTCDES2" are used here and that will be shown later to be more accurate than "PTCDES1". The steam production rate was obtained by measuring hourly the make-up water required to keep the level of the water in the flash vessel constant. The production for that particular day was 12 litres as compared to 13.2 litres predicted by the simulation program. The percentage difference between the two is 9.1 % which is partially attributed to differences between the weather conditions considered by the program and the actual situation. Therefore a different approach was necessary for the evaluation of the simulation accuracy. This is investigated by performing all day experiments during which both the steam production and the weather conditions were recorded. The measured weather data were then used in the simulation programs "PTCDES1" and "PTCDES2" the outputs of which are compared with the actual performance data. The experiments were performed for two days, one with high ambient temperature (hot) and one with a low value (cold). For these experiments a flash vessel (#1, in chapter 6) of 54mm diameter, 600mm height with a 0.6 litre water content was used.

The programs were modified slightly by deleting the statements converting the horizontal beam radiation into radiation falling on the collector surface as the latter was measured during the experiment directly.

Comparisons between the predicted and actual performance are shown in Fig. 5.10 and Fig. 5.11 where the cumulative steam production is plotted for both cases. It can be seen from the figures that both programs are accurate for the hot sunny day whereas the difference is greater for the cold one and this is attributed mainly to the cosine losses. The total system production together with the percentage differences between the actual and the predicted system performance are shown in Table 5.3. The small percentage difference shown in the last column of Table 5.3 clearly indicates that the models give

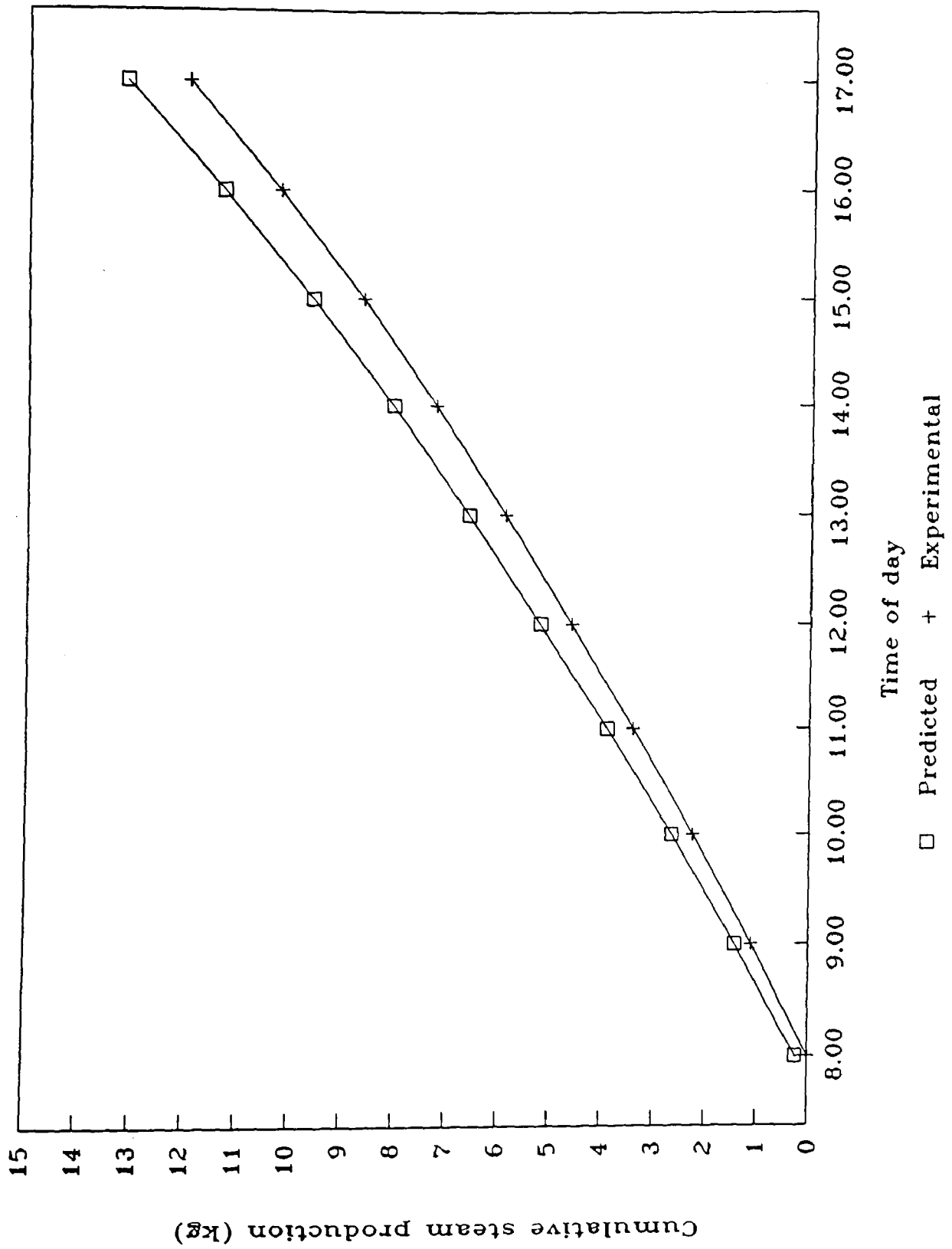

Fig. 5.9 System steam production against "PTCDES2" program predictions (September 2nd 1993)

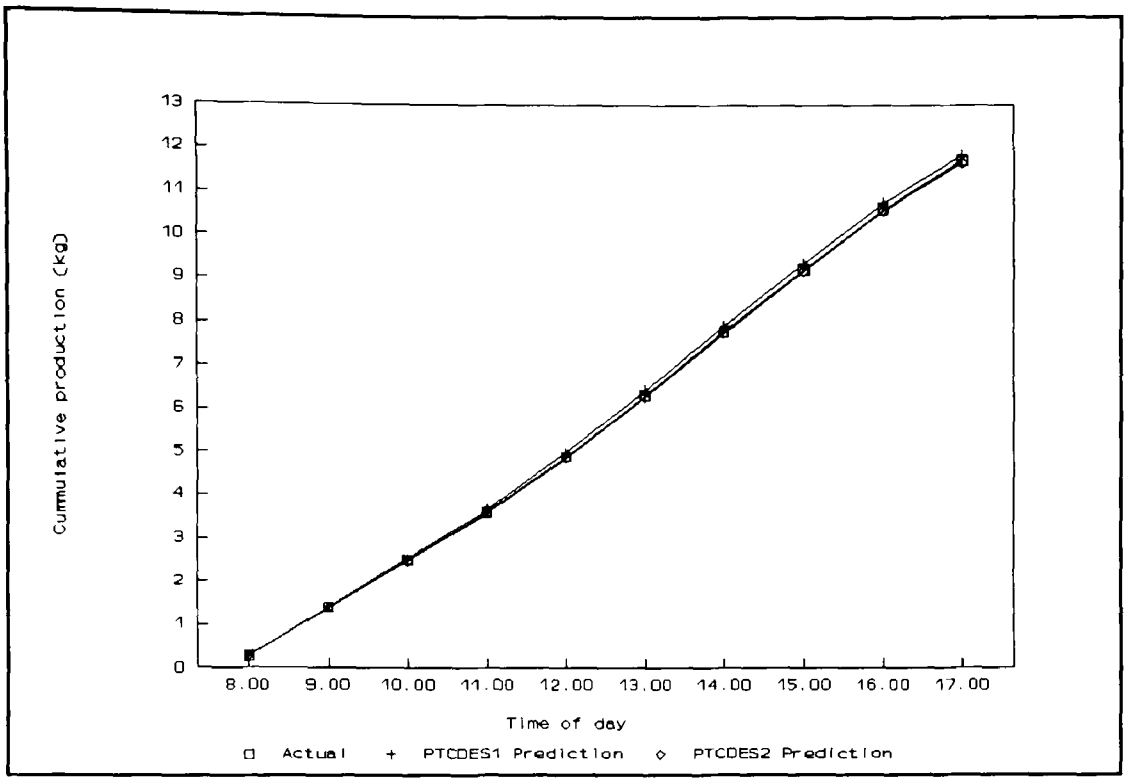

Fig. 5.10 Comparison between predicted and actual system performance (hot sunny day)

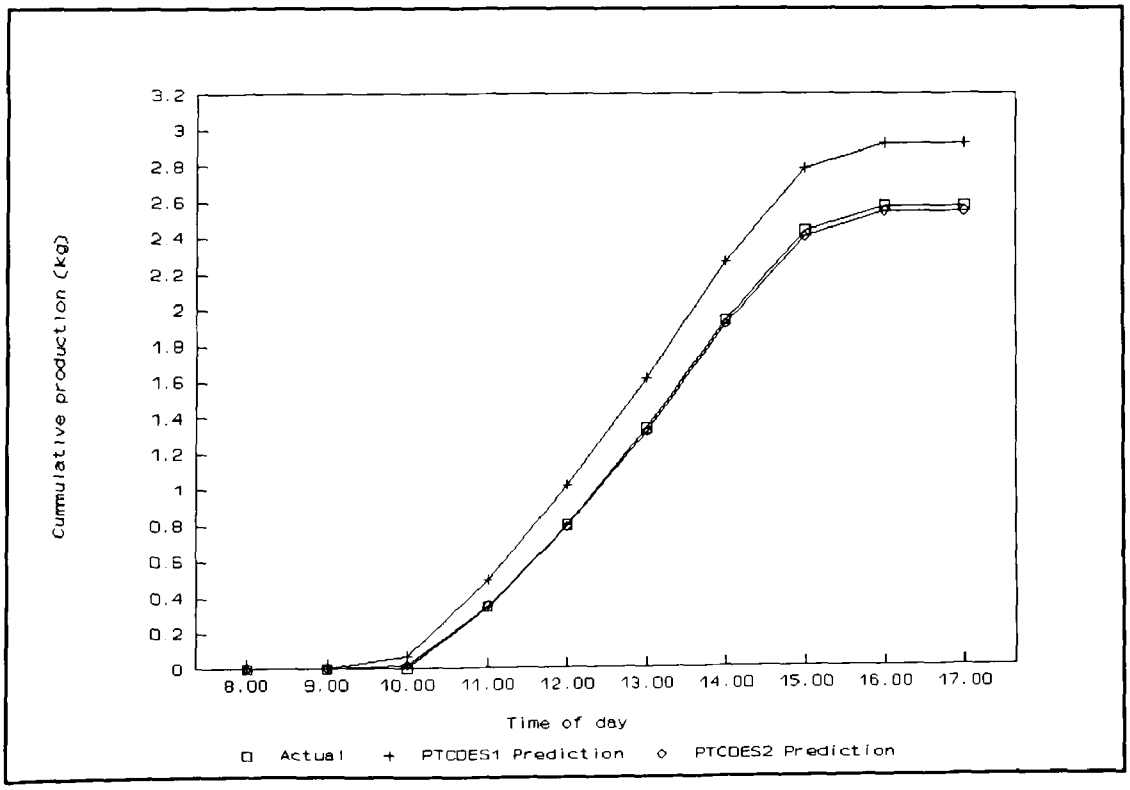

Fig. 5.11 Comparison between predicted and actual system performance (cold sunny day)

good predictions, especially "PTCDES2" which is accurate to within 1.2%.

From the above discussion it can be concluded that the accuracy of prediction would essentially depend on the data recorded in the reference year. This has been examined [Kalogirou *et al.*, 1993a] for a system modelling for hot water production and was found to agree within 7%. Therefore the modelled performance predictions of the system with program "PTCDES2" are considered as providing a good representation of long term system performance. For the 3.5m^2 model this is shown in Fig. 3.17.

ITEM	TOTAL SYSTEM PRODUCTION			PERCENTAGE DIFFERENCE WITH RESPECT TO ACTUAL	
	ACTUAL	PTCDES1 Prediction	PTCDES2 Prediction	PTCDES1	PTCDES2
Hot sunny day	11.72	11.86	11.68	+1.2	-0.3
Cold sunny day	2.57	2.92	2.54	+13.6	-1.2

Table 5.3 Cumulative summary between actual and predicted system performances

Blank page

CHAPTER 6

CHAPTER 6

SYSTEM DEVELOPMENT

This chapter deals with refinements which can be used to improve the overall system performance. It also deals with performance predictions for larger systems. The effect of operating the system under non-standard conditions is also examined.

6.1 SYSTEM REFINEMENT

From the test results shown in Fig. 5.8 it is evident that it would be desirable to reduce the system pre-heat energy requirement. This could be readily achieved by reducing the water capacity (48% of the pre-heat energy is used to provide sensible heat to the water) and also by optimising the flash vessel dimensions and construction in order to lower the system thermal capacity and losses. The following constraints on the optimisation should be noted, however:

- the mass of the circulating water contained in the pipes is fixed and cannot be changed.
- the system performance will reduce (in terms of steam production) if the thermal mass of the system is reduced too much. This is because the addition of make up water would then "dilute" the system temperature and possibly result in the performance and hence production of steam becoming unstable.

Another observation that can be drawn from the first tests is that the height of the flash vessel can be reduced. This is because the velocity of the steam is already small compared to the maximum allowed and also possible "contamination" of the steam with carried over water droplets is not serious as the water in the system is distilled so that there will be no effect on the overall system performance. Furthermore a reduced vessel height and hence a subsequent reduction in the system thermal capacity, will lead to a faster response of the system. Another possibility which should be considered as a system refinement is the use of the flash vessel as a storage vessel. This will have the advantage of starting the system in the morning with the water at a higher temperature but have the disadvantage of a greater water mass to heat up.

It is thus evident that the flash vessel dimensions and capacity need to be optimised. Two simulation programs called "FLASH" and "FLASH 1" were written for this purpose. The program "FLASH" flow chart is shown in Appendix 2. The programs are simplified version of the PTCDES family of programs. The first one uses a constant radiation input and ambient temperature throughout the day so that the system performance can be investigated theoretically independently of the weather conditions. The second allows input of hourly values of radiation and ambient air temperature and can be used for a detailed daily system analysis. This will be used exclusively for the system transient analysis. The programs take into account, in addition to the sensible heat and the thermal capacity of all the system components, all the heat losses from the system i.e. the flash vessel body, pipes and pump body.

For the heat loss from the flash vessel the following relation was used:

$$Q_{FS} = \frac{T - T_a}{\frac{\ln\frac{(t+D_i)}{D_i}}{2\,\pi\,k\,H} + \frac{\ln\frac{D_o}{(D_i+t)}}{2\,\pi\,k_i\,H} + \frac{1}{1.42\,\pi\,D_o\,H\,(\frac{DT}{L})^{0.25}}} \qquad (6.1)$$

where:

T water temperature [K]

k Flash vessel wall thermal conductivity [W/mK]

k_i Insulation thermal conductivity [W/mK]

T_a Ambient temperature [K]

H Flash vessel height [m]

D_i Internal flash vessel diameter [m]

D_o External flash vessel diameter including insulation [m]

t Flash vessel wall thickness [m]

The third term of the denominator of Eq. 6.1 estimates the free convection from the external flash vessel walls to environment, Holman [1989].

The flash vessel outer wall temperature is determined from:

$$T_w = T - \left[Q_{FS} \left(\frac{\ln \frac{(t+D_i)}{D_i}}{2 \pi k H} + \frac{\ln \frac{D_o}{(D_i+t)}}{2 \pi k_i H} \right) \right] \qquad (6.2)$$

The difference of wall temperature and ambient temperature is checked against DT value. If the difference is more than 1°C then DT is equated to $T_w - T_a$. This iteration process continues until DT - $(T_w - T_a)$ is less than 1°C.

For the heat loss from the pipes, the UA value approach, followed by many solar energy simulation programs like TRNSYS [Klein *et al.*, 1990] and F-Chart [Klein and Beckman, 1983], is used. The heat loss from the pipes is then:

$$Q_{pipes} = UA \ (T - T_a) \qquad (6.3)$$

The pump employed was of cylindrical form and positioned vertically. Therefore the heat loss from the pump body is calculated by the relations applied to vertical cylinders, i.e.:

$$Q_{pump} = 1.42 \ A_{pump} \ (T - T_a) \left(\frac{T - T_a}{H_p} \right)^{0.25} \qquad (6.4)$$

where:

H_p Pump height [m]

The losses during the over night cooling period were calculated assuming that the temperature of the water in the vessel at the beginning of this period as equal to the temperature T3 (flash vessel bottom). Thus the effect of using the flash vessel for thermal storage was investigated. After the night losses were calculated the initial flash vessel water temperature for the succeeding day was determined. The day time input energy is then determined by using the collector performance equation, with the appropriate thermal losses subtracted. The remaining energy is used either to pre-heat or, once the pre-heat cycle is complete, to produce steam. The programs can thus be used to model the behaviour of the system during pre-heat and predict the daily steam production of the system.

The input data to the program "FLASH" is shown in Table 6.1 whereas the dimensions of the different flash vessels considered in this simulation are shown in Table 6.2. The modelled performance of the system is shown in Fig. 6.1 where the daily production of steam is plotted against the flash vessel capacity and content. The vertical lines represent the different flash vessels simulated in this investigation.

As the energy input is the same for all cases, increased steam production means that less energy is used in the pre-heat cycle. It can be seen from Fig. 6.1 that the highest predicted steam production is for vessel #1 with a water content of 0.6 litres. Although a system with flash vessel #1 provides the maximum steam production its operation is not very stable as a possible drop of its water capacity would lower its performance

PARAMETER	VALUE
Solar radiation	500 W/m^2
Mass flow rate	0.042 kg/s
Flash vessel water content	0.6 kg
Aperture area	3.5 m^2
Collector efficiency	0.638
Ambient temperature	30 °C
Mass of circulated water	4 kg
Flash vessel outside diameter	94 mm
Flash vessel inside diameter	51 mm
Flash vessel wall thickness	1.2 mm
Flash vessel height	0.6 m
UA-value of the pipes	0.93 W/K
Pump body area	0.12 m^2
Insulation conductivity	0.035 W/mK
Flash vessel and pipes mass	10 kg
Pump mass	20 kg

Table 6.1 Program "FLASH" input data

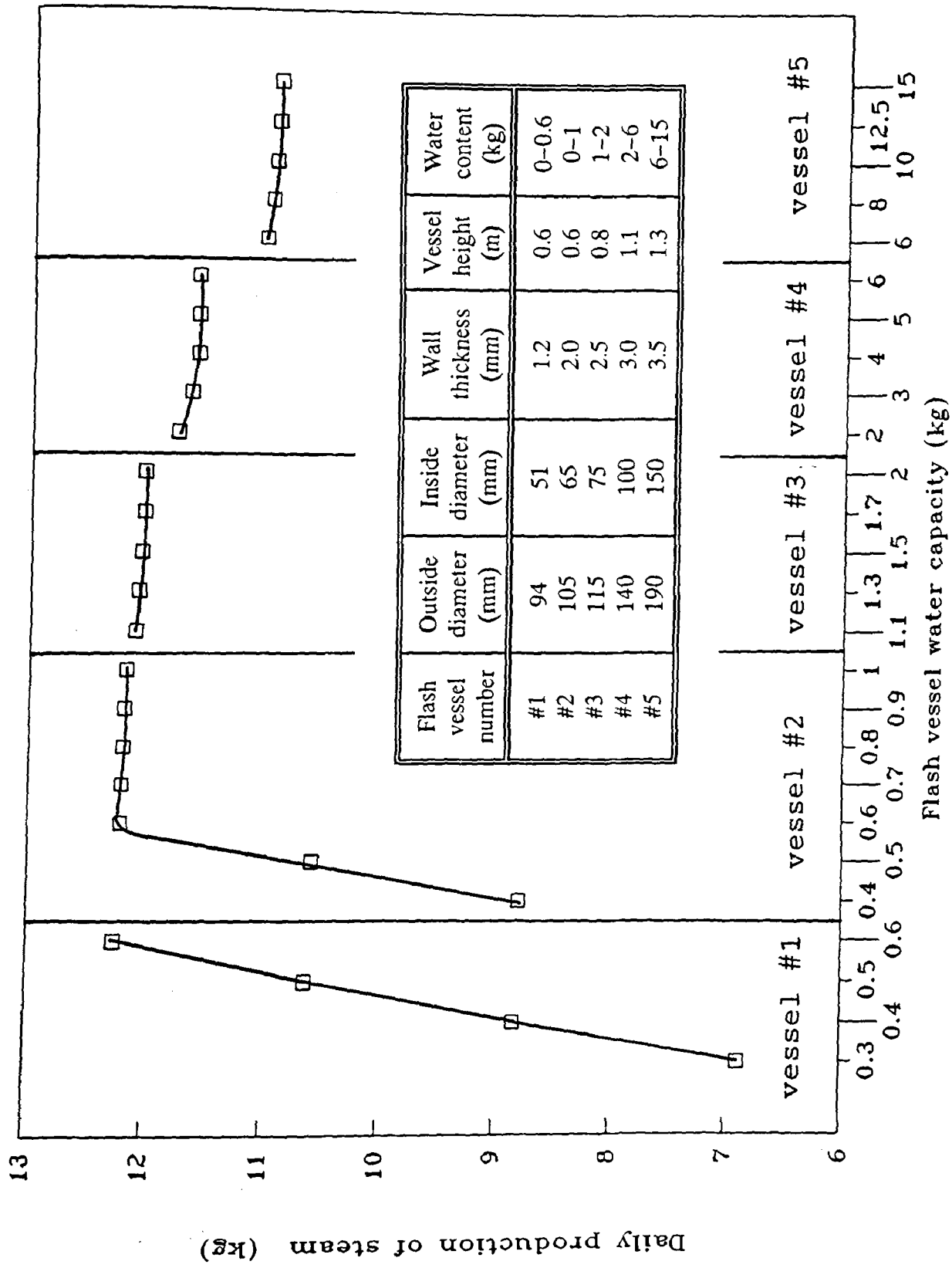

Flash vessel number	Outside diameter (mm)	Inside diameter (mm)	Wall thickness (mm)	Vessel height (m)	Water content (kg)
#1	94	51	1.2	0.6	0–0.6
#2	105	65	2.0	0.6	0–1
#3	115	75	2.5	0.8	1–2
#4	140	100	3.0	1.1	2–6
#5	190	150	3.5	1.3	6–15

Fig. 6.1 Predicted steam production for various size flash vessels

Flash vessel number	Outside diameter (mm)	Inside diameter (mm)	Wall thickness (mm)	Vessel height (m)	Water content (kg)
#1	94	51	1.2	0.6	0-0.6
#2	105	65	2.0	0.6	0-1
#3	115	75	2.5	0.8	1-2
#4	140	100	3.0	1.1	2-6
#5	190	150	3.5	1.3	6-15

Table 6.2 Flash vessel dimensions

drastically. A more sensible selection is flash vessel #2 with 0.7 litres capacity. This system presents only a 0.8% reduction in steam production when compared with the vessel #1 but is more stable. The system pre-heat energy will be evaluated for both vessels.

It should be stressed that because of complexity and interrelationship of the parameters, the analysis undertaken here cannot be generalised and should be applied to individual cases to determine the optimal design for a particular collector system.

6.1.1 Pre-heat Energy Evaluation of the Modified System

The actual pre-heat response of the system with the flash vessel #1 with 0.6 litres water content and flash vessel #2 with 0.7 litres water content is shown in Figures 6.2 and 6.3 respectively. 3.8 MJ and 4.3 MJ are now required to pre-heat the systems respectively in comparison to the 6.1 MJ required for the original vessel - a reduction of 38% and 30% respectively. Comparing the performance shown here against the initial system (Fig. 5.8) there is a significant difference. It should first be stated however, that the three tests took place under different weather conditions i.e. the initial test radiation level and ambient temperatures were 655 W/m^2 and 31°C. The corresponding values for the final tests were 570 W/m^2, 32°C and 690 W/m^2, 30.5°C. Despite this the plots of the T3 and T4 temperatures for the modified systems is in marked contrast for the plots shown in Fig. 5.8. The original design had a far greater thermal inertia which resulted

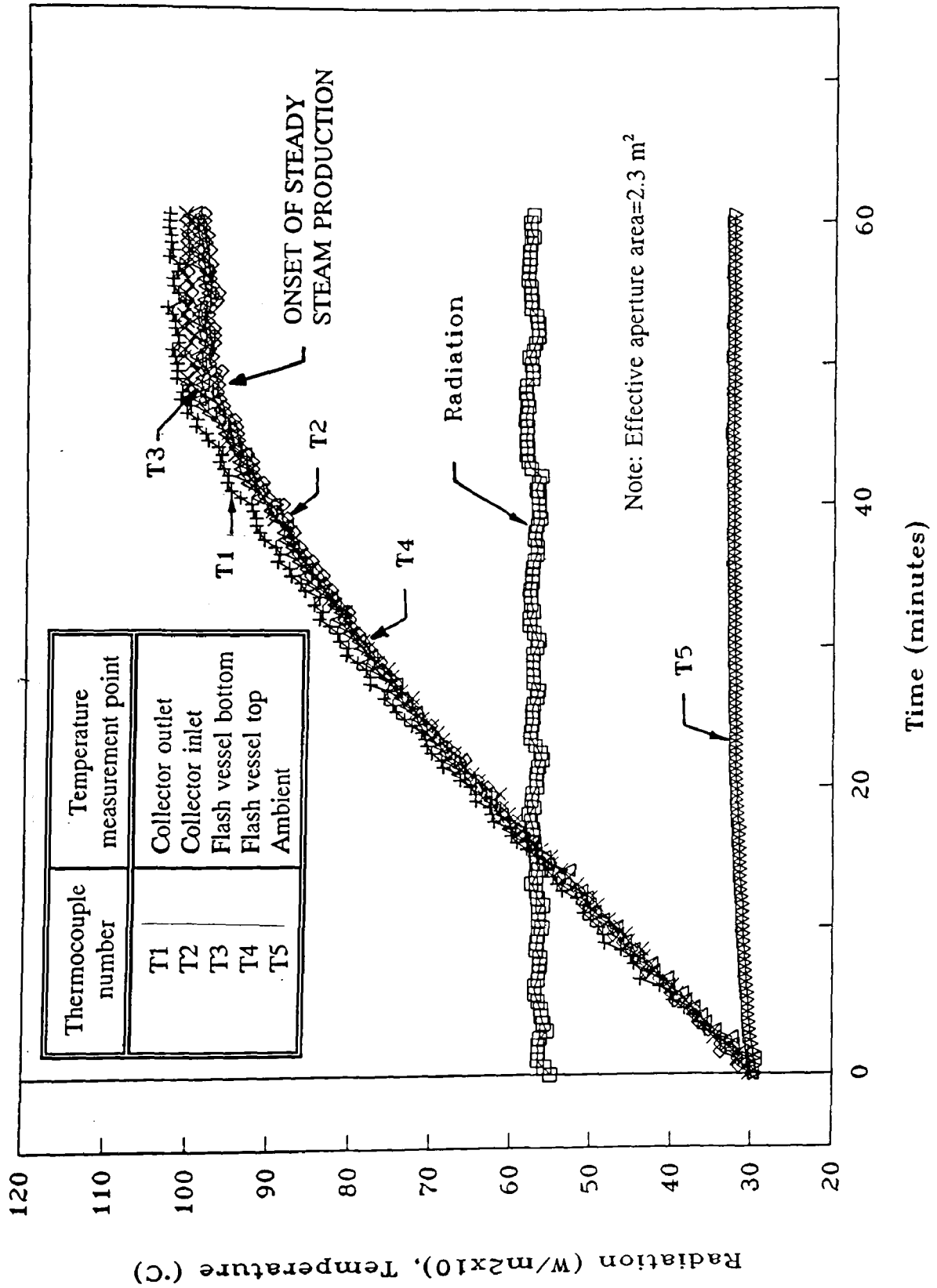

Fig. 6.2 System with flash vessel #1 – observed pre-heat cycle

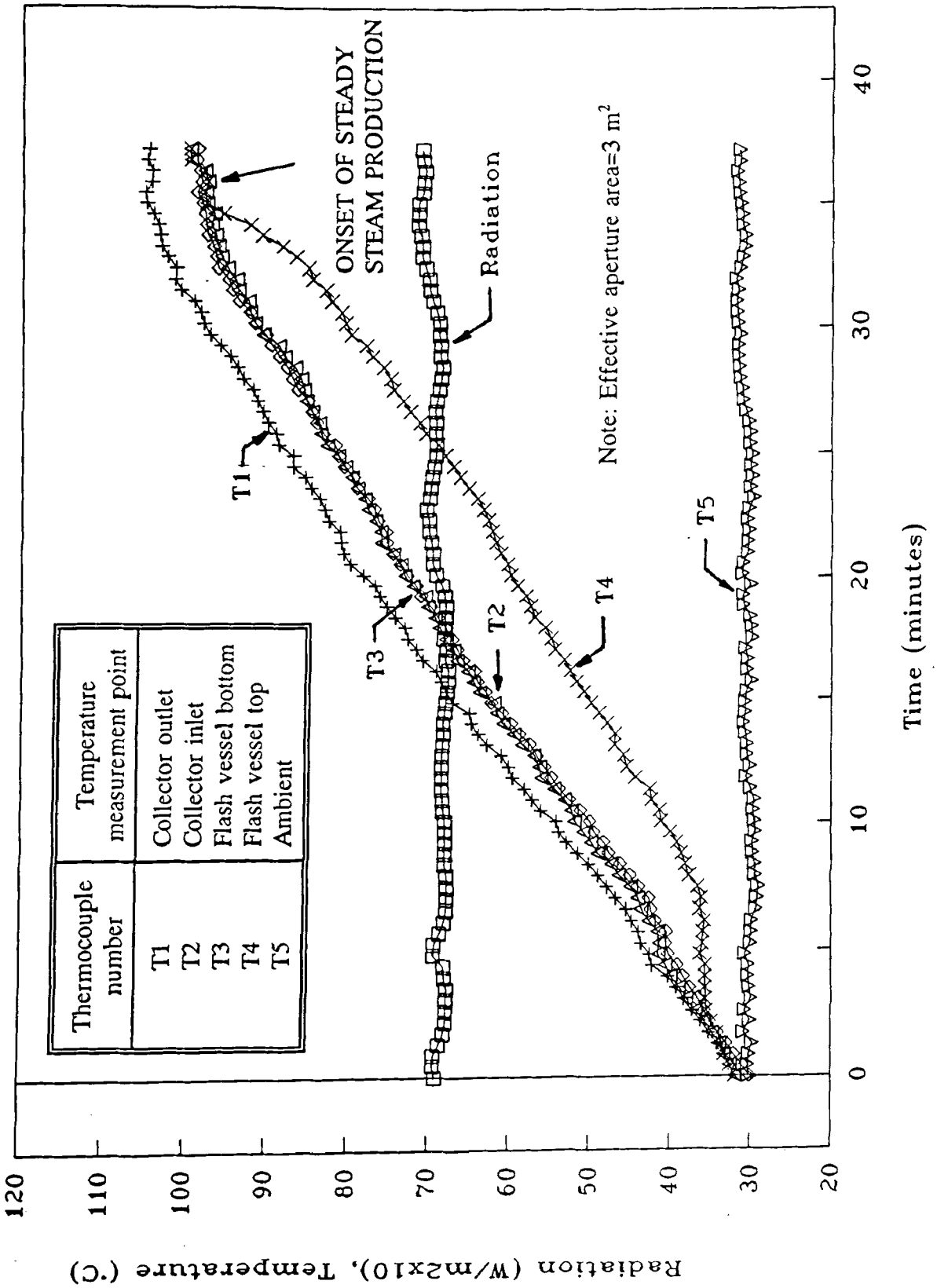

Fig. 6.3 System with flash vessel #2 – observed pre-heat cycle

in considerable temperature differences between the top and bottom of the flash vessel. A reduction in start-up energy is due to the reduced height, diameter and wall thickness of the new vessels. The onset of steady state steam production occurs when the whole system reaches a uniform temperature i.e. T3=T4 after a period of 46 minutes. For the modified system with flash vessel #1 installed the pre-heat time is 48 minutes and although this appears to be longer than that for the original design there is less energy input (radiation) so that there is faster response when the less favourable conditions are allowed for. The pre-heat time for the modified system with vessel #2 installed is 35 minutes.

From the above discussion it is evident that the final flash vessel to adopt is #2 with 0.7 litres water content. This is a stable system with a small pre-heat energy requirement. The new design (with flash vessel #2 installed) would yield an extra 0.21 kg of steam on a representative day. Moreover if the sunshine was intermittent then the system performance would be far better than that of the conventional design.

A plot of the temperature difference between T3 and T4 (flash vessel bottom and top) during the pre-heat cycle period for the three systems is shown in Fig. 6.4. The temperatures are the same at the beginning. As energy is added to the system the difference is increased. At almost half way through the pre-heat cycle the temperature difference reaches its maximum value and drops to zero again at the completion of the pre-heat cycle when the system reaches steady state. The maximum difference for the initial and the two modified systems is 28.6°C, 14.4°C and 1.9°C respectively and this quantifies the difference in the thermal inertia of the three systems.

6.1.2 Validation of the Optimisation Model

The model was validated by comparing the actual system response presented in Fig. 6.2 to the modelled response in Fig. 6.5. It can be seen that there is a good agreement and that differences in the pre-heat cycle completion time were about 6.5%.

To verify the accuracy of the modelling, the collector was fitted with flash vessels #1 and #3 and was tested with different water capacities. The daily steam production was

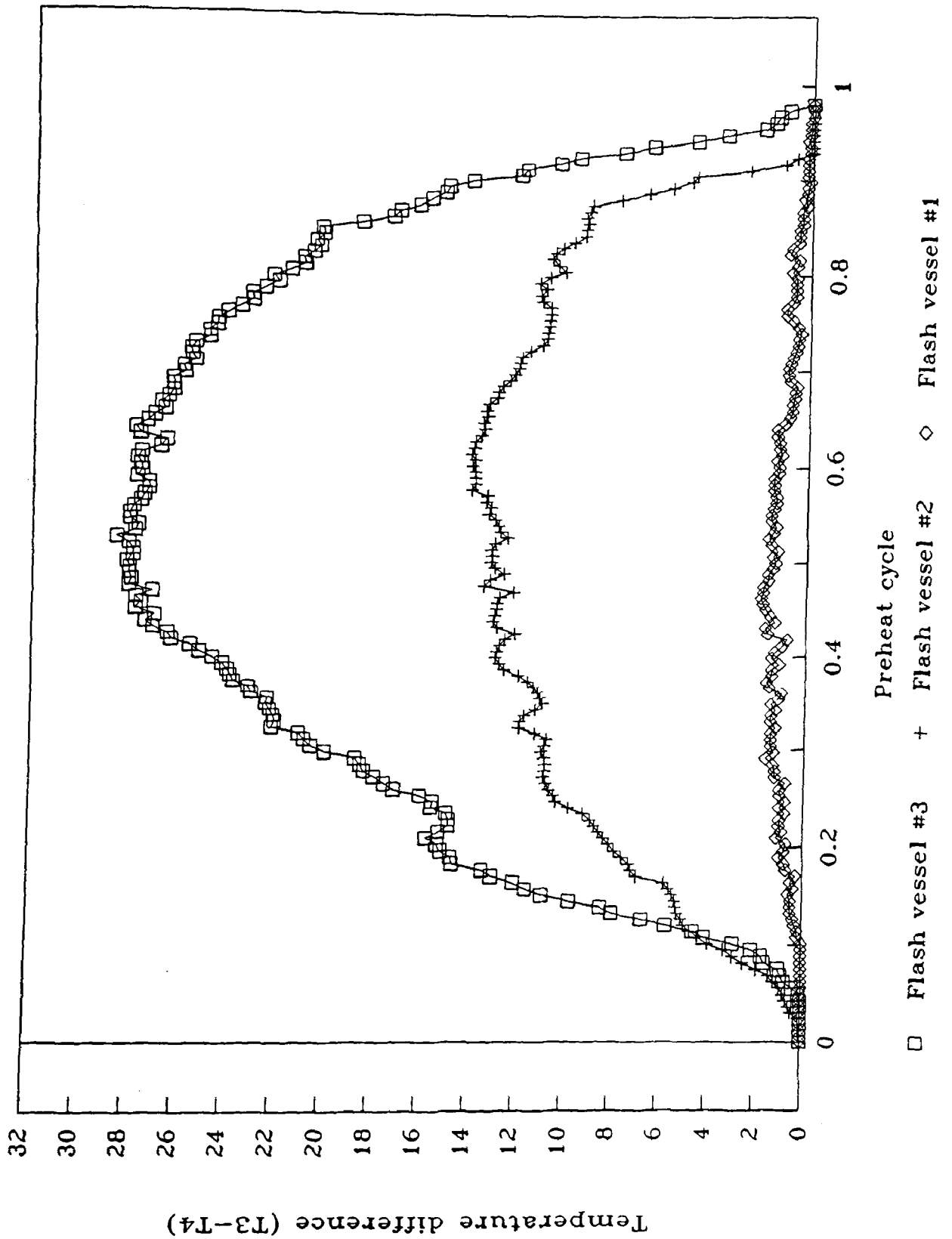

Fig. 6.4 Comparison of system thermal response for different flash vessels

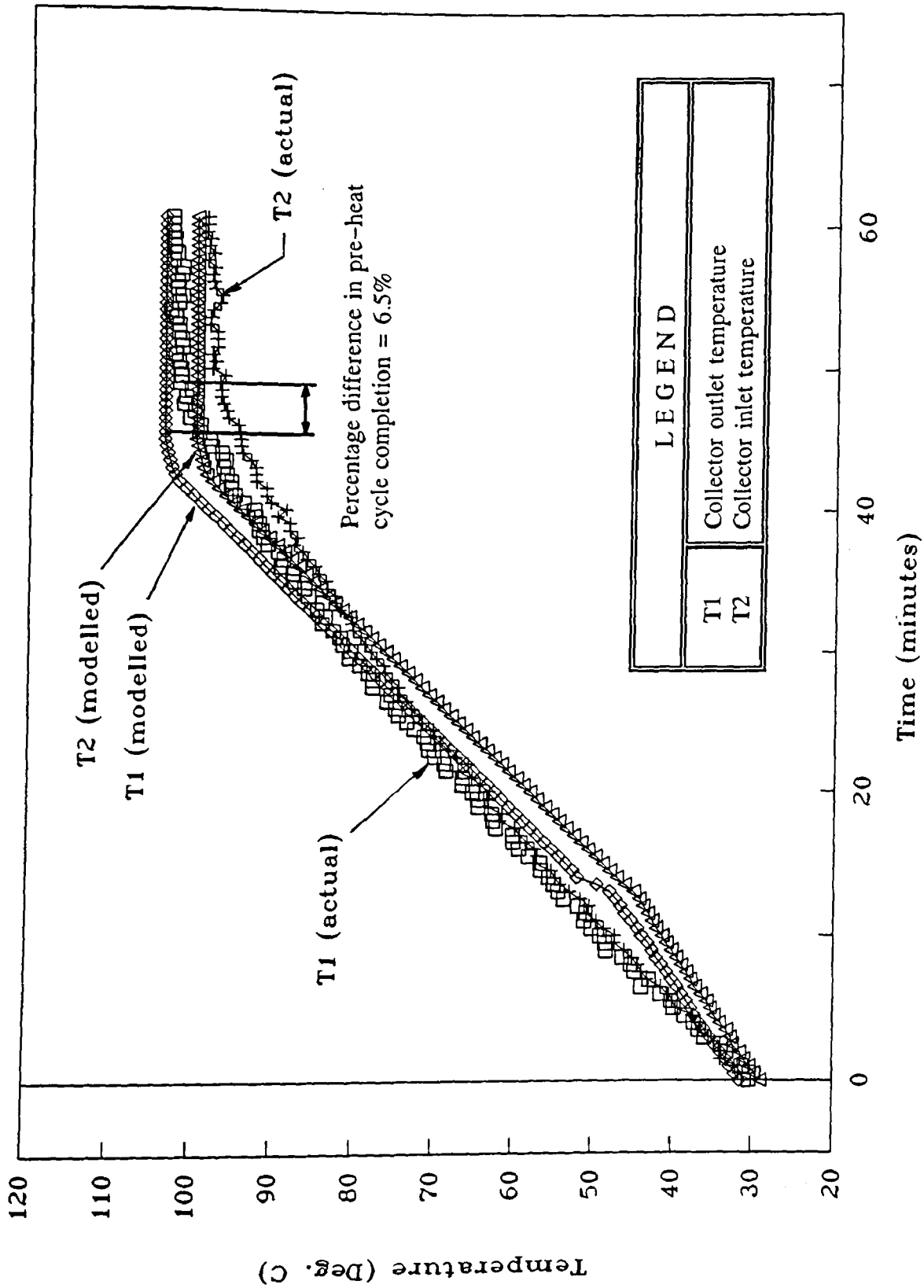

Fig. 6.5 Comparison of actual and predicted heat-up response

compared to the predicted performance. For this purpose "FLASH 1" was used which allows insertion of hourly values of solar radiation and ambient air temperature. The results are shown in Table 6.3 from where it can be seen that there is a good agreement between the actual and predicted results. The maximum difference (8%) is for flash vessel #1 with a water capacity of 0.3 litres. This can be attributed to the fact that the make-up water was manually added at different occasions as needed and not constantly as assumed by the program. This has a greater effect on the system with flash vessel #1 which is more sensitive to water capacity.

Flash vessel	Capacity (litres)	Actual steam production (kg)	Predicted steam production (kg)	Percentage difference between actual and predicted production
#1	0.3	8.38	7.76	8
	0.5	12.46	11.87	5
	0.6	13.87	13.47	3
#3	1.1	12.88	12.51	3
	1.5	12.58	12.34	2
	2.0	12.73	12.36	3

Table 6.3 Comparison between actual and predicted system performance for different flash vessels and capacities

In addition to the above testing procedure the performance of the system was also examined under transient conditions. This was achieved by shading the collector whilst keeping the system pump operating. The shading was removed after one hour. In this way the cooling and the heating of the system could be investigated.

In Fig. 6.6 the actual and the predicted collector inlet and outlet temperatures are plotted. In this case the collector inlet temperature is equivalent, to a good approximation, to the temperature T3 (flash vessel bottom). The agreement between the experimental and modelled plots is very good both with respect to time and temperature profiles and to the minimum water temperature reached at the end of the one hour period. It can be seen from Fig. 6.6 that initially the collector outlet temperature is greater than the inlet. This happens until the energy stored in the collector receiver is given up to the circulating fluid. After 2-3 minutes the situation is reversed and the collector inlet temperature is greater than the outlet temperature. This is because the

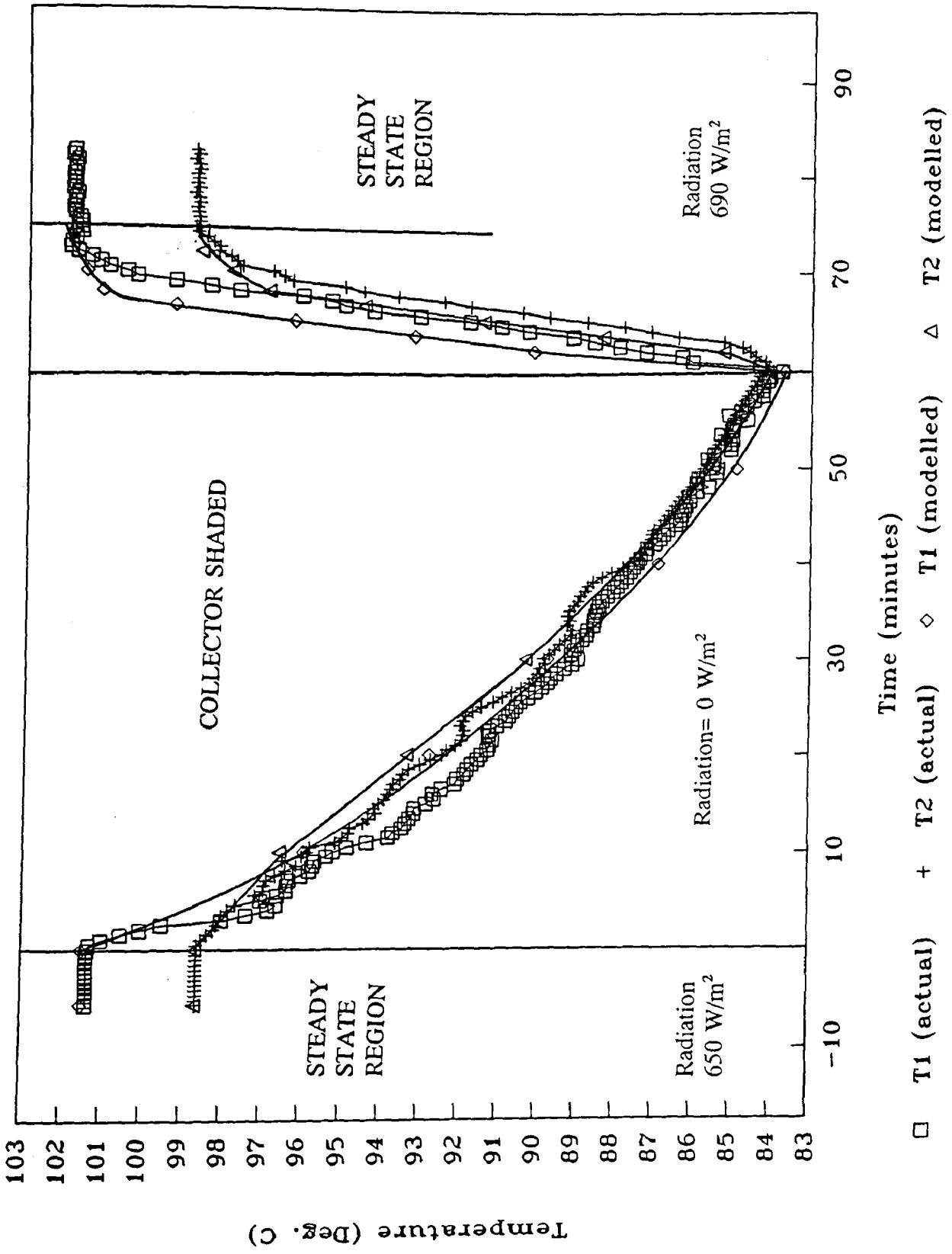

Fig. 6.6 Comparison of actual and predicted transient response

losses from the collector receiver are responsible for cooling down of the system. The receiver together with the pump are relatively poorly insulated parts of the system.

It can also be seen from Fig. 6.6 that only 13 minutes (1.6 MJ) are required for the system to recover and return to steady state condition after the shading is removed.

6.1.3 Theoretical System Energy Analysis

The results from the model simulation can to be used to produce theoretically the system Sankey diagram. Such an analysis for a day with constant radiation of 500 W/m^2 and all other parameters as shown in Table 6.1 is presented in Fig. 6.7. The analysis is performed for the 3.5 m^2 aperture area model with flash vessel #1 and 0.6 litres water capacity. The analysis shown graphically in Fig. 6.7, in the form of a Sankey diagram, indicates the magnitude of the various losses of the system.

From Fig. 6.7 it can be seen that only 48.9% of the solar energy falling on the collector is utilised for steam generation. A large percentage of the losses is due to collection losses, 41.5%, and the rest 6.9% is made up of thermal losses. Energy losses due to raising the water temperature from ambient to 100°C is 2.2% and for the rig is 0.5%.

A better representation of the thermal losses is shown in Fig. 6.8 where it can be seen that losses from the pipes amount to 52.6%, losses from the pump body amount to 37.5% and the rest 9.9% is due to flash vessel body losses.

6.2 LARGER SYSTEM PREDICTIONS

It has been shown that both modelling programs "FLASH" and "PTCDES2" provide good performance predictions. They will therefore now be used to predict the performance of larger systems. This performance will then be subject to an economic analysis in the next chapter to draw conclusions on the viability of some systems. The systems considered vary from a small domestic one to a large village size system, namely:

- Small domestic application

- Large domestic application
- Hotel application
- Village application

The name assigned to each application is indicative of the application area, considering the specific consumption shown in Table 1.3 of about 500 litres per day per consumer.

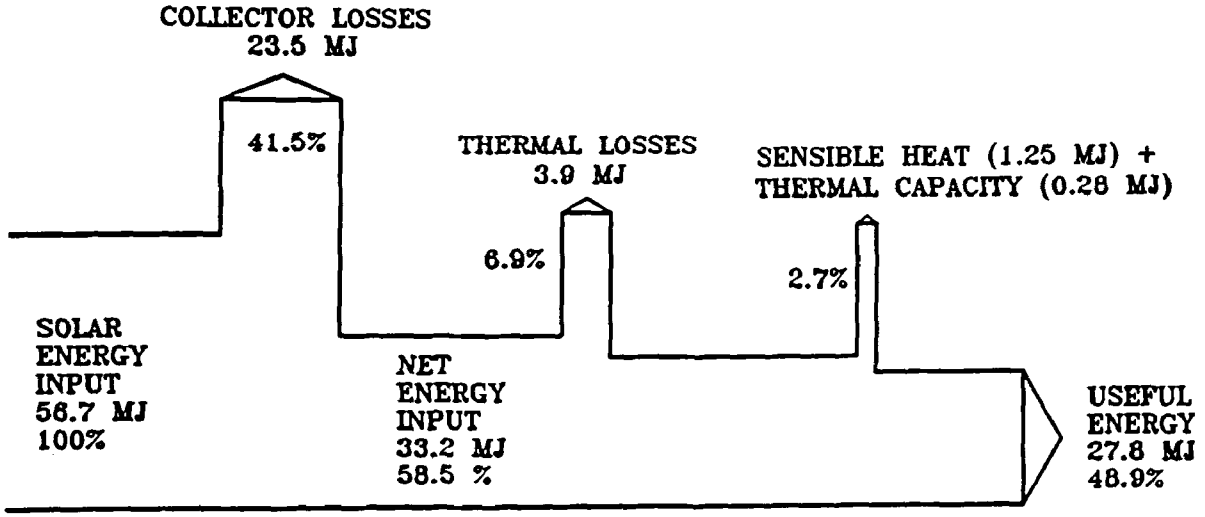

Fig. 6.7 System Sankey diagram

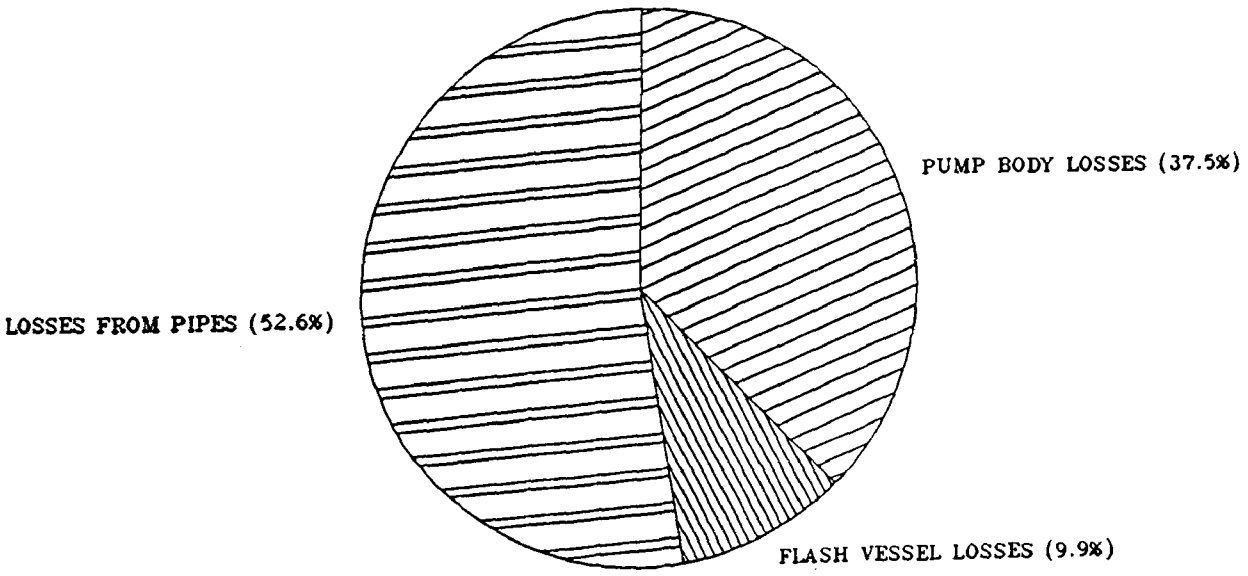

Fig. 6.8 Theoretical thermal losses from the system

6.2.1 Small Domestic Application

The system arrangement for this case is shown in Fig. 6.9. The collector area employed is 10 m^2 which can provide a maximum of approximately 480 litres of fresh water per day with a MEB evaporator performance ratio of 8. The collector width is kept constant to 1.46m so that the receiver pipe size is kept to 22mm (standard size).

Firstly the optimisation model is used to determine the optimum size of the flash vessel. The results are shown in Fig. 6.10 from which it can be seen that the optimum flash vessel size is #3 as given in Table 6.2 with 2 kg water content. By using the optimised flash vessel dimensions in the modelling program "PTCDES2" the system performance shown in Table 6.4 can be obtained.

Possible applications for this size of system besides the domestic application are for tourist bungalows, hairdressers and analytical labs where the ultra clean water produced by the system is required.

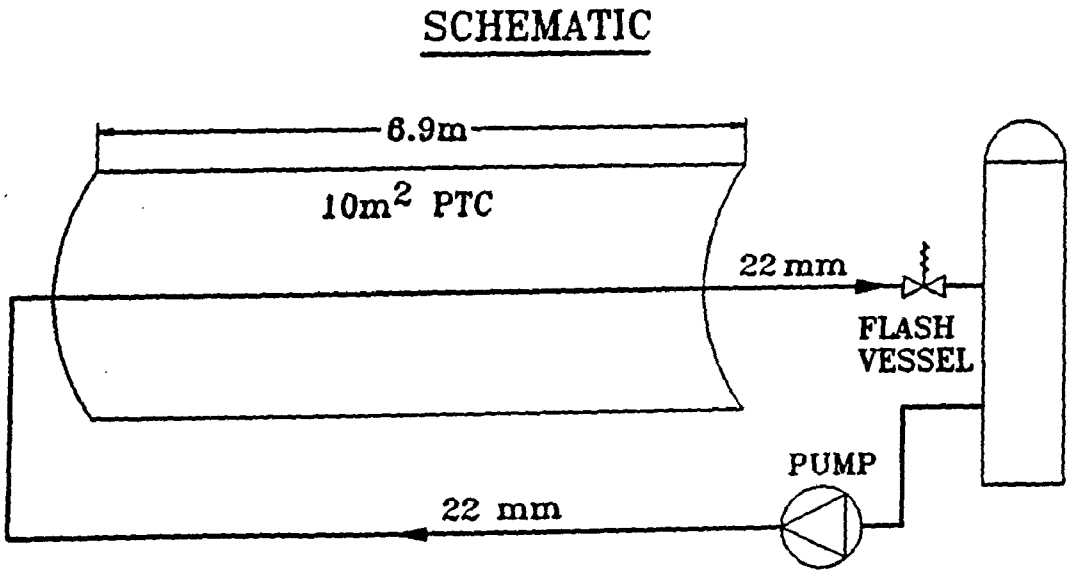

Fig. 6.9 Small domestic application schematic diagram

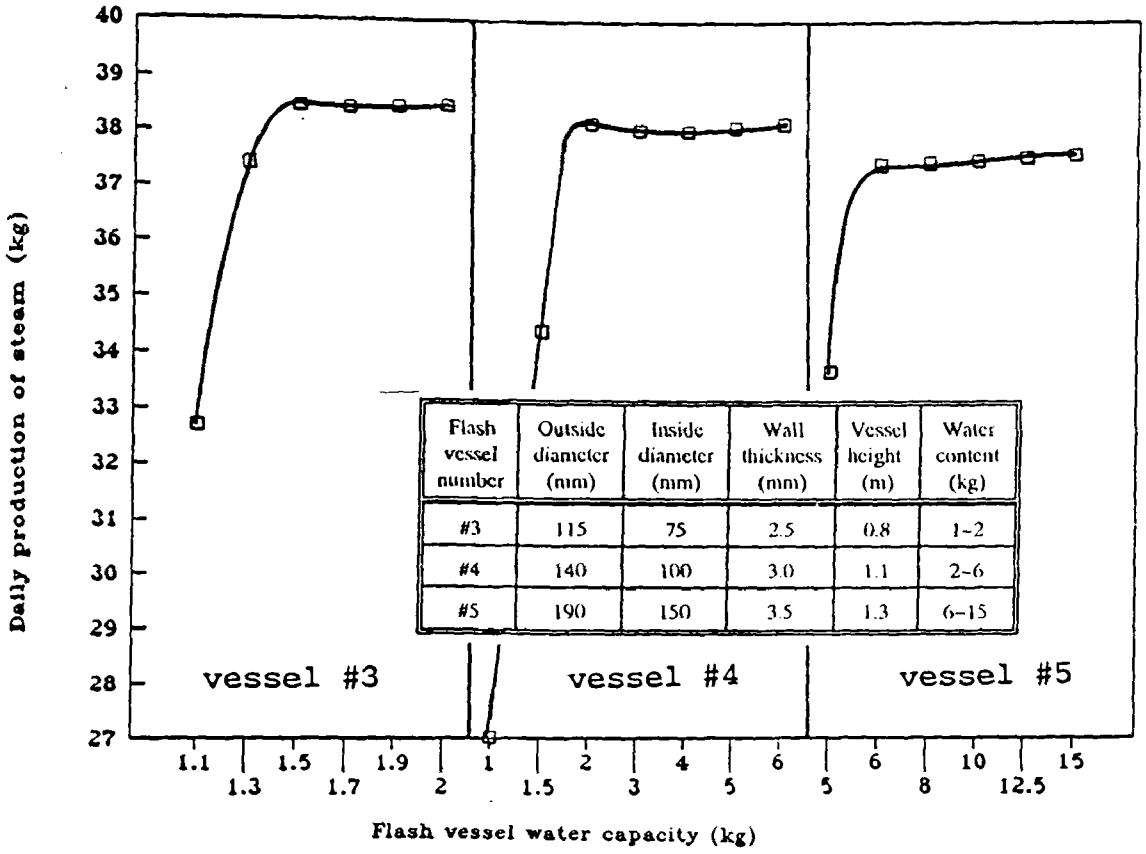

Flash vessel number	Outside diameter (mm)	Inside diameter (mm)	Wall thickness (mm)	Vessel height (m)	Water content (kg)
#3	115	75	2.5	0.8	1-2
#4	140	100	3.0	1.1	2-6
#5	190	150	3.5	1.3	6-15

Fig. 6.10 Flash vessel optimisation-small domestic application

MONTH	PRODUCTION (kg/m^2day)	MONTH	PRODUCTION (kg/m^2day)	MONTH	PRODUCTION (kg/m^2day)
JAN	0.387	MAY	4.086	SEP	4.439
FEB	0.702	JUN	6.014	OCT	2.422
MAR	2.198	JUL	6.467	NOV	1.033
APR	3.120	AUG	5.701	DEC	0.486
NOTE: Collector aperture area= 10 m^2					

Table 6.4 Predicted small domestic application performance

6.2.2 Large Domestic Application

The system arrangement for this case is shown in Fig. 6.11. The collector area employed is 60 m^2 which is considered as a standard collector area used in the two bigger

application cases considered here. The collector's receiver is split into 3 parts in order to reduce the flow rate and keep the pipe size to an optimum. The system can provide a maximum of approximately 3.5 m^3 of fresh water with a MEB evaporator performance ratio of 10. The results of the optimisation model show an increase in the system production proportional to the increase of the particular vessel capacity. Therefore only the maximum capacity production figure is presented here as shown in Table 6.5. The optimum solution in this case is for vessel #1 with dimensions as shown in Table 6.6 which lists standard vessel dimensions and price.

Vessel number	Vessel capacity (kg)	Total daily production of steam (kg)
#1	60	217.5
#2	160	217.2
#3	240	217.1
#4	400	216.2

Table 6.5 Flash vessel optimisation-large domestic application

Vessel number	Max. vessel capacity (kg)	Diameter (mm)	Height (m)	Cost (C£)
#1	60	450	0.80	150
#2	160	450	1.43	210
#3	240	550	1.45	270
#4	400	650	1.75	405
#5	630	750	1.92	485
#6	850	800	2.08	555
#7	1300	950	2.36	790
#8	1750	1100	2.41	935
#9	2200	1250	2.47	1070
#10	2650	1250	2.72	1220
#11	3600	1400	2.83	1495
#12	4500	1600	2.85	1755

Table 6.6 Standard vessel dimensions and prices (from manufacturers data)

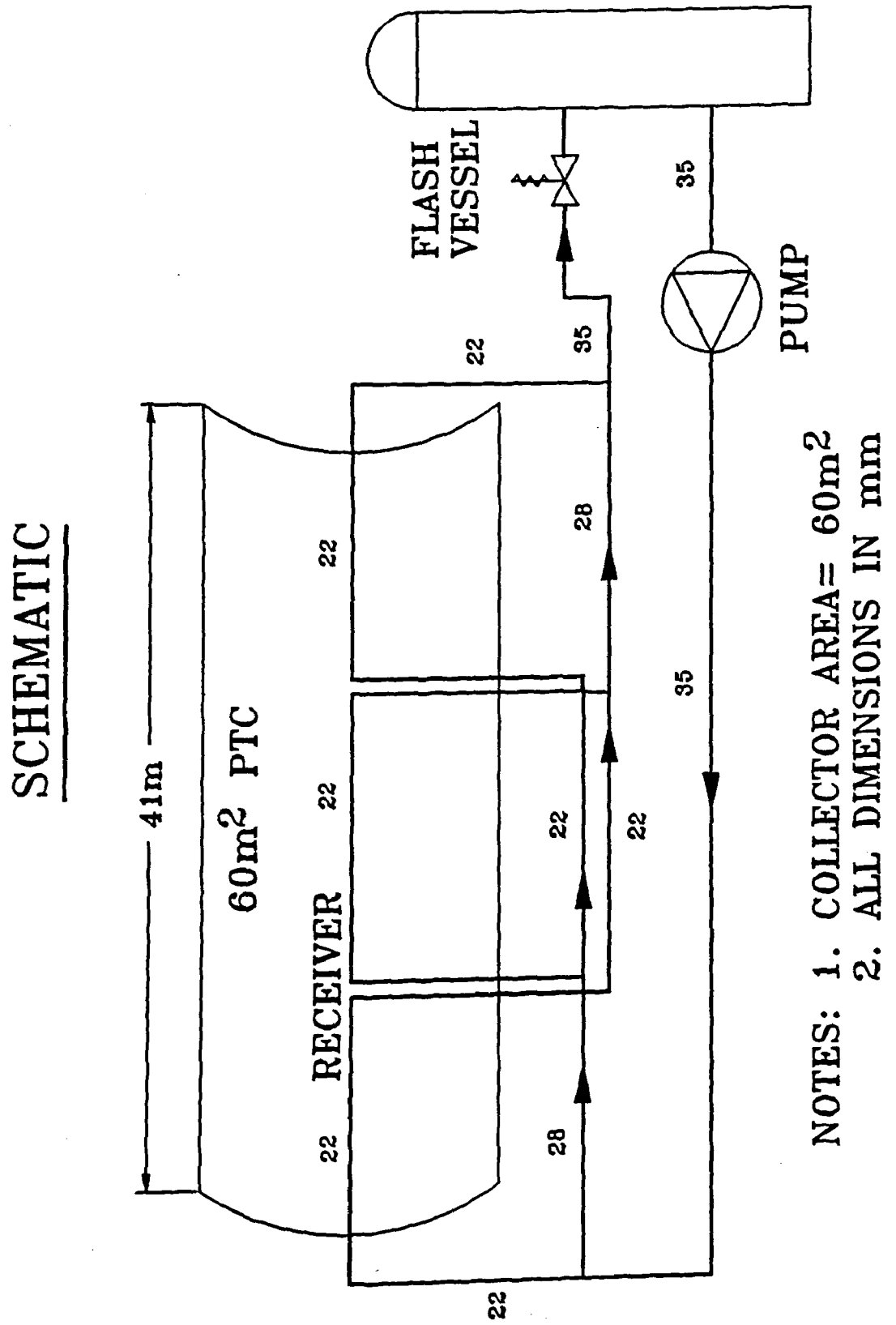

Fig. 6.11 Large domestic application schematic diagram

A flash vessel of smaller size may yield a better daily production but as vessel #1 is the smallest standard vessel available this was adopted. By using the optimum flash vessel dimensions in the modelling program "PTCDES2" the system performance shown in Table 6.7 can be obtained.

MONTH	PRODUCTION (kg/m^2day)	MONTH	PRODUCTION (kg/m^2day)	MONTH	PRODUCTION (kg/m^2day)
JAN	0.255	MAY	3.892	SEP	4.392
FEB	0.569	JUN	5.856	OCT	2.381
MAR	2.062	JUL	6.325	NOV	0.944
APR	2.980	AUG	5.616	DEC	0.388
NOTE: Collector aperture area= 60 m^2					

Table 6.7 Predicted large domestic application performance

Possible applications for this size of system are for luxury houses, groups of houses, blocks of 5–6 flats, and groups of tourist bungalows.

6.2.3 Hotel Application

The system arrangement for this case is shown in Fig. 6.12. The collector area employed is 540 m^2 which is made up of 9 collectors of 60 m^2 area each, as shown in Fig. 6.11. Bigger areas for an individual collector would give too great a collector length to fit onto the roof of a typical hotel. The system can provide a maximum of approximately 38 m^3 of fresh water with a MEB evaporator performance ratio of 12. Higher performance ratio is used here in comparison to the previous applications as is not considered as cost effective by the manufacturers to construct small units with high performance ratios.

The results of the optimisation model are shown in Table 6.8 where it can be seen that the maximum predicted production is given by flash vessels #5 and #6 with a capacity of 630 and 850 litres of water respectively. The flash vessel to be selected though is #2 with a capacity of 160 litres of water. The predicted production with this flash vessel installed is only 0.3% lower than the maximum but obviously this is a more economic

HOTEL APPLICATION SCHEMATIC

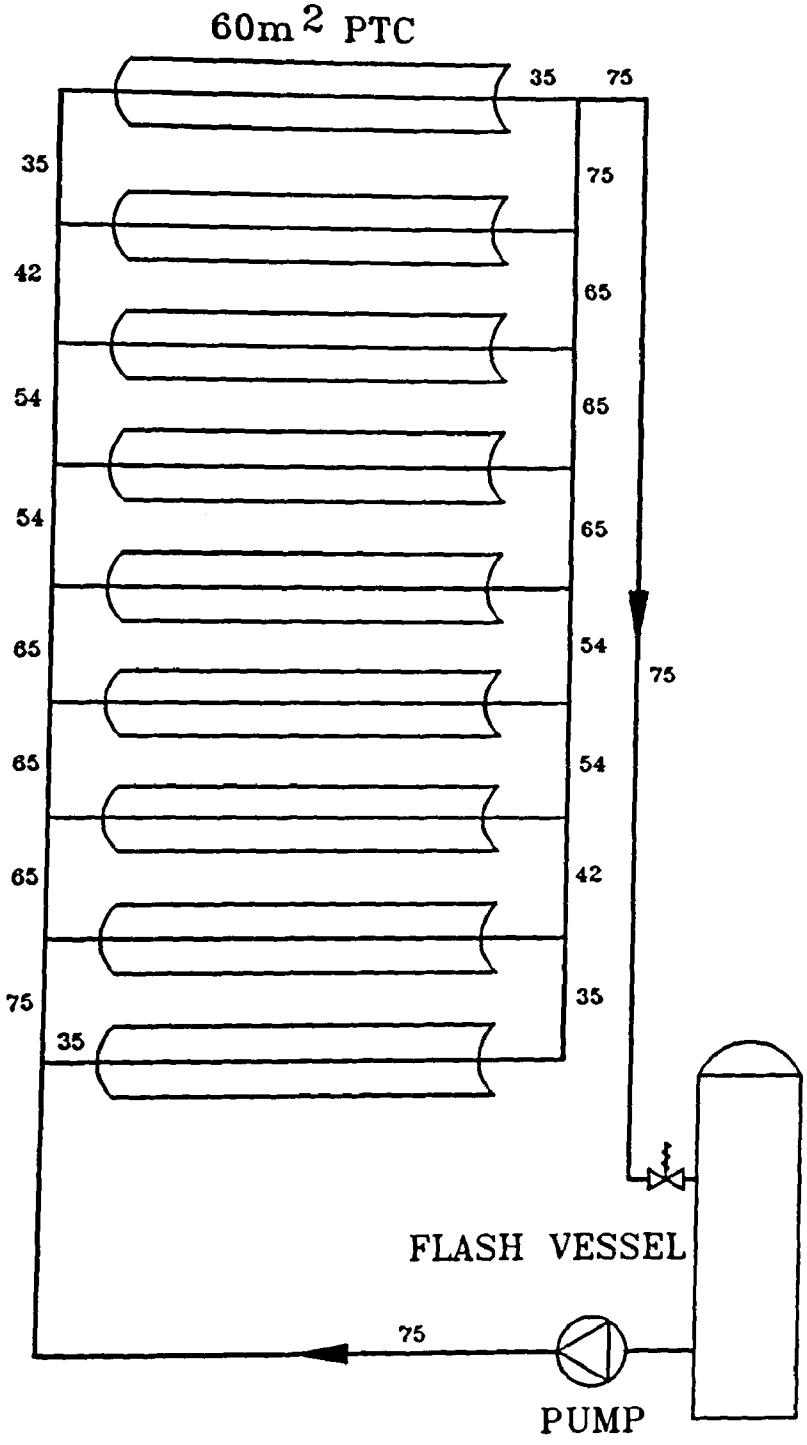

NOTES: 1. TOTAL COLLECTOR AREA= 540m^2
2. ALL DIMENSIONS IN mm

Fig. 6.12 Hotel application schematic diagram

Vessel number	Vessel capacity (kg)	Total daily production of steam (kg)
#1	60	933
#2	160	2037
#3	240	2041
#4	400	2042
#5	630	2043
#6	850	2043
#7	1300	2042

Table 6.8 Flash vessel optimisation - Hotel application

solution because of the lower capital cost. By using the selected flash vessel dimensions in the modelling program "PTCDES2" the system performance shown in Table 6.9 can be obtained.

In the economic analysis which follows in Chapter 7 this system will be evaluated in two respects:

(i) Use the system for desalination only throughout the year.

(ii) Use the system for hot water production and for desalination in different periods of the year.

MONTH	PRODUCTION (kg/m^2day)	MONTH	PRODUCTION (kg/m^2day)	MONTH	PRODUCTION (kg/m^2day)
JAN	0.384	MAY	4.091	SEP	4.552
FEB	0.721	JUN	6.036	OCT	2.539
MAR	2.241	JUL	6.503	NOV	1.095
APR	3.164	AUG	5.786	DEC	0.521
NOTE: Collector aperture area= 540 m^2					

Table 6.9 Predicted hotel application performance

6.2.4 Village Application

The system arrangement for this case is shown in Fig. 6.13. The collector area employed is 2160 m^2 which is made up of 4 modules each with the hotel's capacity. This system can provide a maximum of approximately 155 m^3 of fresh water with a MEB evaporator performance ratio of 12.

Vessel number	Vessel capacity (kg)	Total daily production of steam (kg)
#3	240	3685
#4	400	5780
#5	630	8081
#6	850	8219
#7	1300	8229
#8	1750	8231
#9	2200	8231
#10	2650	8231
#11	3600	8232
#12	4500	8231

Table 6.10 Flash vessel optimisation - Village application

The results of the optimisation model are shown in Table 6.10 where the maximum predicted production is given by the system using flash vessel #11 with a capacity of 3600 litres of water. The flash vessel to be employed though is #6 with a capacity of 850 litres of water. The predicted steam production with this flash vessel installed is only 0.16% lower than the maximum but is obviously a cheaper solution.

By using the selected flash vessel dimensions in the modelling program "PTCDES2" the system performance shown in Table 6.11 can be obtained.

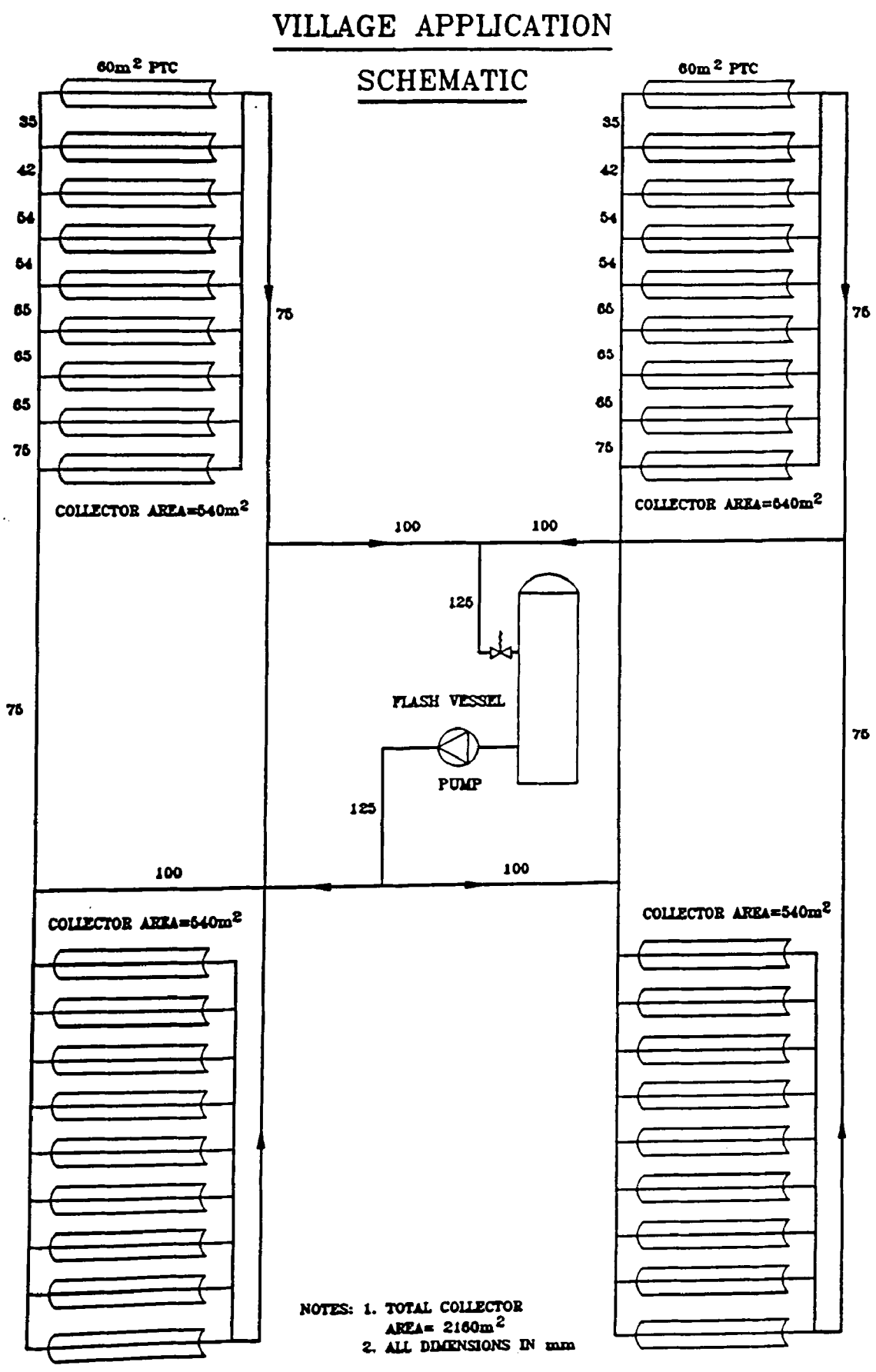

Fig. 6.13 Village application schematic diagram

MONTH	PRODUCTION (kg/m^2day)	MONTH	PRODUCTION (kg/m^2day)	MONTH	PRODUCTION (kg/m^2day)
JAN	0.432	MAY	4.136	SEP	4.593
FEB	0.772	JUN	6.083	OCT	2.576
MAR	2.289	JUL	6.546	NOV	1.128
APR	3.200	AUG	5.832	DEC	0.561
NOTE: Collector aperture area= 2160 m^2					

Table 6.11 Predicted village application performance

6.2.5 Comparison of the Systems

The modelling programs "FLASH" and "PTCDES2" were used for the design and selection of the systems considered for each application. Table 6.12 lists various parameters obtained by the programs for comparative purposes.

As it can be seen from Table 6.12 the flash vessel capacity per unit of collector area varies considerably (from 1 kg/m^2 to 0.2 kg/m^2). This is due to the selection of the 60 kg flash vessel for the large domestic application which was the smallest standard vessel available (see section 6.2.2). This variation confirms the statement made earlier for the complexity and interrelationship of the parameters and the use of the optimisation model for flash vessel selection for each particular collector system.

The maximum water production obtained by operating the system solely with solar energy is proportional to the collector area.

The morning starting temperature of the water in the flash vessel also varies considerably for the various systems. This depends mainly on the capacity of the flash vessel in each case. Despite of all the above, the variation in the specific annual production ($kg/m^2/yr$) is small.

ITEM	APPLICATIONS			
	Small domestic	Large domestic	Hotel	Village
Collector area (m^2)	10	60	540	2160
Flash vessel capacity (kg)	2	60	160	850
Flash vessel capacity per collector area (kg/m^2)	0.2	1	0.3	0.39
Performance Ratio (PR)	8	10	12	12
Maximum water production (m^3)	0.48	3.5	38	155
Morning starting temperature (°C)	33.4	89.5	94.2	95.9
Pre-heat energy (MJ)	5.7	11.9	48.3	135.0
Pre-heat energy per unit collector area (kJ/m^2)	570.0	198.3	89.4	62.5
Annual steam production (kg/m^2)	1111.7	1070.1	1129.0	1144.4

Table 6.12 Systems comparison

6.3 SYSTEM OPERATION FOR NON-STANDARD CONDITIONS

6.3.1 System Operation at Higher Collector Temperatures

A possible way for enhancing the system performance would be to operate at lower flow rates thus obtaining higher collector outlet temperatures. One problem though is that the collector performance indicators represented by the test slope and intercept of the collector performance curve are modified as the heat removal factor F_R is influenced by the flow rate. The result of this investigation is shown in Table 6.13 where it can be seen that the system performance is lowered proportionally to the decrease of mass flow rate. For the validation of the results shown in Table 6.13 one test was performed with 50% of the design flow rate. The actual steam production was 12.4 kg which against the predicted 12.14 kg indicates a reasonable difference of 2.1%. It must be stressed here that the upper limit of steam supply temperature is 120°C. Above this limit scaling problems in the evaporator become more apparent despite the use of scale inhibitor.

Flow rate (percentage with respect to design flow rate)	Maximum collector outlet temperature (K)	Predicted steam yearly production (kg/m^2)	Percentage difference with respect to 100% flow rate
100%	105	953	0%
50%	111	868	9%
10%	160	422	56%

Table 6.13 Effect of reduced flow rate on predicted system performance

6.3.2 System Operation at Sub-Atmospheric Pressure

By modifying the modelling program "PTCDES2" to predict system operation at sub-atmospheric pressure the system behaviour under this condition can be investigated. The modification was simulated for a range of pressures (i.e. 0.3, 0.5, 0.75 and 0.95 bar - absolute). The results from the modelling of the village size application with a flash vessel size equal to 2650 litres (#10) for a pressure of 0.3 Bar - absolute and a saturation temperature of about 69°C are shown in Table 6.14. From these results it can be concluded that there is a marked increase, of about 28%, in the system production. This is due to the following:

- The collector operates at a lower temperature and thus more efficiently.
- The specific enthalpy of evaporation is greater at this condition as compared to the atmospheric case.

The percentage increase in steam production for various sub-atmospheric pressures are shown graphically in Fig. 6.14. The number next to each data point on the graph represents the saturation temperature for the particular pressure. As it is shown in Fig. 6.14 the greater the vacuum the greater the steam production.

As no experimental verification was possible, these results can not be used confidently for system evaluation and the performances presented in section 6.2 are adopted.

MONTH	SYSTEM STEAM PRODUCTION (kg/m^{2}day)	
	VACUUM	ATMOSPHERIC
January	1.164	0.430
February	1.607	0.772
March	3.292	2.321
April	4.123	3.200
May	4.705	3.816
June	6.273	5.458
July	6.774	5.982
August	6.149	5.324
September	5.427	4.557
October	3.475	2.600
November	1.956	1.130
December	1.247	0.561
TOTAL	46.192	36.151

Table 6.14 Comparison of system performance under vacuum and atmospheric conditions

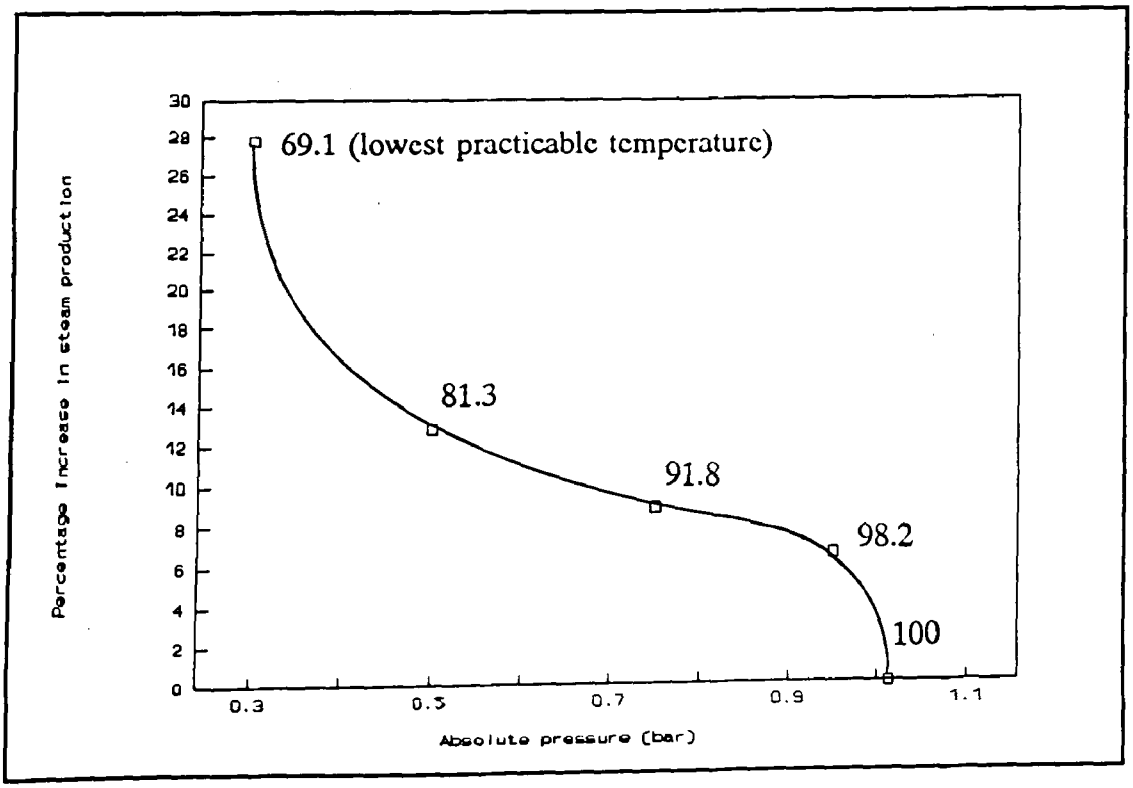

Fig. 6.14 Percentage increase in steam production for various vacuum pressures

Blank page

CHAPTER 7

CHAPTER 7

ECONOMIC ANALYSIS OF THE PROPOSED DESALINATION SYSTEMS

This chapter examines the economics of the parabolic trough collector desalination systems. The analysis considers four types of application, two domestic, a hotel and a village. The systems used for these applications can provide different amounts of fresh water depending upon the mode of usage. The maximum and minimum values are tabulated in Table 7.1 together with the possible area of use.

Application	Mean daily water production (m^3)		Area of use	
	Min.	Max.	Minimum	Maximum
Small domestic	0.25	1.3	Single family dwellings	Two family dwellings or a luxury house
Large domestic	1.8	9.8	Housing compounds, tourist bungalows	Same as in minimum case but bigger
Hotel	20	108	Small hotel or partly covering the requirements of a large hotel	Large hotel of about 200 rooms
Village	82	432	Village of 300 families	Village of 850 families

Table 7.1 Applications considered in economic analysis

The minimum water production is obtained by the system when operated solely with solar energy whereas the maximum refers to systems with full boiler back-up. The boiler back-up is used to supply the power required to run the desalination systems at periods of low solar radiation and overnight. The thermal efficiency of the boiler units in all cases is taken as 75%. The factors that influence the system economic viability are output and cost of the collector and desalination systems, the available solar radiation, the cost of alternative fuels and maintenance requirements.

7.1 METHOD OF ANALYSIS

The objective of the economic analysis is to determine the least cost method of covering the desalination demand, considering both solar and non-solar alternatives. The method employed for the economic analysis is called the life cycle savings analysis. The method takes into account the time value of money and allows detailed consideration of the complete range of costs.

Solar processes are generally characterised by high initial cost and low operating costs. Thus, the basic economic problem is one of comparing an initial known investment with estimated future operating costs.

The Life Cycle Cost (LCC) is the sum of all the costs associated with an energy delivery system over its lifetime in today's money by taking into account the time value of money. The Life Cycle Savings (LCS), for a solar plus auxiliary system, is defined as the difference between the LCC of a conventional fuel only system and the LCC of the solar plus auxiliary system. This is equivalent to the total present worth of the gains from the solar system compared to the fuel only system.

The economic analysis focuses on the determination of the water price that will give zero total LCS summed over the life of the system. The economic scenario used in the analysis is to pay 30% of the cost of the systems in advance and the remaining 70% in equal instalments over the life of the system. It is also estimated that the system is sold at the end of its life at 30% of the initial cost (i.e. the resale value).

The various applications are analysed by means of a spreadsheet, i.e. Lotus 1-2-3. The required inputs are the following:

1. The area dependent cost. Multiplying this cost by the collector area gives a cost related to the size of the system.
2. The area independent cost. This is the part of the collector system cost which is independent of the collector area together with the desalination system cost.
3. The period of economic analysis. This is equivalent to the life of the system and is taken as 20 years.

4. The annual market discount rate. This parameter is used to estimate the present worth of an expenditure and it can be obtained by multiplying the maximum interest rate i.e. 8% by the defence fund allowance (2%). This gives a value of 7.84%.
5. The system maintenance requirement is estimated initially at 2% of the initial system cost increased annually by 2% as the system ages [Water and Environment, 1993]. This includes the cost of descaling chemicals and cleaning of the evaporator and collector surfaces.
6. The pumping power of the system. This is required in order to calculate the pumping cost.
7. The price of electricity together with the annual increase in price.
8. First year fuel cost and fuel savings (accrued due to the use of the solar system for hot water production) together with the fuel cost annual increase. Diesel fuel in Cyprus is subsidised by the Government. In the analysis that follows non-subsidised fuel prices are also considered.
9. The system resale value. The percentage of the initial cost of the system that will be recovered at the end of its life taken as 30%.

A list of all the above parameters together with the values used, where applicable, are shown in Table 7.2.

In addition to the parameters given in Table 7.2 the amount of steam produced per m^2 of collector area in different months of the year is required. The performance values given in section 6.2 are used here.

The analysis is performed annually and the following costs are evaluated:

- Water cost
- Mortgage payment
- Maintenance cost
- Pumping cost
- Fuel savings, if a solar system producing in addition to desalinated water hot water
- Fuel cost, if any
- Tax savings
- System annual cost

A sample calculation sheet for the hotel case is shown in Appendix 4.

ITEM	VALUE	UNITS
Collector area	Depending on the case	m^2
Area dependent cost	Taken from Table 7.4	C£/m^2
Area independent cost	Taken from Tables 7.4 & 7.5	C£
Period of economic analysis	20	years
Market discount rate	7.84	%
Maintenance in year one	2	%
Annual increase in maintenance	2	%
Total pumping power	Taken from Table 7.5	kW
Price of electricity	0.04	C£/kWh
Annual increase in electricity price	2.9	%
First year fuel cost	Depending on the case	C£
First year fuel savings	Depending on the case	C£
Fuel cost annual increase	0.6	%
Resale value	30	%

Table 7.2 Economic parameters

In equation form the annual cost for either solar or non-solar systems to meet an energy need can be expressed as:

$$\begin{aligned} \text{System annual cost} &= \text{Mortgage payment} + \text{Maintenance cost} \\ &+ \text{Pumping cost} + \text{Fuel cost} \\ &- \text{Water cost} - \text{Fuel savings} - \text{Tax savings} \end{aligned} \qquad (7.1)$$

Finally the present worth (PW) of the system annual cost is expressed as:

$$PW = \frac{System\ Annual\ Cost}{(1+d)^N} \qquad (7.2)$$

where d = market discount rate

N = number of years

The water price per cubic meter is a variable in the calculation. In the analysis this price is varied until the LCS of the system gives a value close to zero. This can be considered as the price of water at which there is no loss or gain from the system. It can also be considered as the water price that the owner of the system could charge in order to sell the water without losing money–i.e. the market cost of water.

The mortgage payment is the annual sum of money required to cover the funds borrowed at the beginning to install the system. This includes interest and principal payment. The estimation of the annual mortgage payment can be found by dividing the amount borrowed by the Present Worth Factor (PWF). The PWF is estimated by using the inflation rate equal to zero (equal payments) and with the market discount rate equal to the mortgage interest rate (9%).

The income tax law in Cyprus determines that any expenses incurred for the production of a business income are tax exempt and the net profits are taxed at a fixed rate of 27%. Therefore costs such as maintenance, fuel, electricity, and money payed as interest are subtracted from the income for tax purposes. In addition there is a 20% investment allowance as an incentive to owners to build up new businesses and an annual 10% wear and tear allowance for ten years. Both allowances are calculated with respect to the total investment cost. The equation used for the tax savings estimation is:

$$\text{Tax savings} = 0.27\ [\ \text{maintenance cost} + \text{fuel cost} + \text{pumping cost} + \text{interest charges} + \text{wear and tear allowance}\ ] \quad (7.3)$$

At the end of the system's life the plant is considered to return 30% of its initial cost (resale value). Therefore there is a "balancing addition" cost that must be returned to the income tax because on this amount tax credit has already been claimed.

7.2 COST PARAMETERS

A cost breakdown for the 3.5m^2 parabolic trough solar collector for steam generation is tabulated in Table 7.3. The costs are related to the 3.5m^2 of collector area but they cannot be regarded as pro rata costs i.e. double the area would not double the cost. The

ITEM DESCRIPTION	COST (C£)
Parabola	55
Reflective material	50
Receiver	10
Framework	30
Labour cost	50
Sub-total	195
Design supervision overheads and profit @30%	59
Tracking mechanism	150
Piping, fittings and insulation	20
TOTAL	424
Pump	200
Flash vessel	15
Electrical installation	10
Installation labour cost	50
GRAND TOTAL	699

Table 7.3 Cost breakdown of the 3.5m^2 collector model

ITEM DESCRIPTION	COST (C£) (10m^2)	(60m^2)	(540m^2)	(2160m^2)
Parabola	160	960	nine	four
Reflective material	140	840	times	times the
Receiver	28	168	the costs	costs of
Framework	50	266	of 60m^2	540m^2
Labour cost	92	606		
Sub-total	470	2840	25560	102240
Design supervision overheads and profit	141	852	6390	20448
Tracking mechanism	150	350	3150	12600
Piping, fittings and insulation	20	300	2440	11100
Electrical installation	10	50	400	1500
TOTAL	791	4392	37940	147888
Area dependent cost (C£/m^2)	79.1	73.2	70.26	68.47
Pump	200	250	350	745
Flash vessel	30	150	270	555
Installation labour cost	100	500	3000	10000
GRAND TOTAL	1121	5292	41560	159188

Table 7.4 Parabolic trough collector system costs

labour cost used is taken from the local flat plate collector manufacturers and is estimated as a percentage of the materials cost. The cost of the pump as shown in Table 7.3 is exaggerated as it is equivalent to about 30% of the total cost. The value indicated is the actual cost of the pump which is oversized for the experimental model constructed but was the smallest available locally. To establish the cost for bigger collector areas Table 7.4 was constructed.

To finalise the analysis of cost parameters it is necessary to give the cost of the desalination equipment associated with each application. This is tabulated in Table 7.5 together with the performance ratio (PR) of each evaporator, the costs of other auxiliary equipment, and labour costs to install the plant and the piping from the sea to and from the evaporator. The desalination plant capacity is determined by the maximum steam capacity of the solar system.

ITEM	COLLECTOR AREA (m^2)			
	10	60	540	2160
DESALINATION EQUIPMENT DATA				
Maximum daily water production (m^3)	1.3	10	110	430
Performance ratio	8	10	12	12
Electrical power (kW)	0.2	0.9	8.7	36
DESALINATION SYSTEM COSTS (in C£)				
MEB evaporator	2280	16200	152000	585000
Piping	50	100	300	400
Pumps	100	250	400	800
Electrical installation	100	150	200	300
Labour cost to install plant and pipes	400	600	1000	1500
Boiler cost with auxiliaries	600	600	2280	5620
TOTAL	3530	17900	156180	593620

Table 7.5 Desalination system cost parameters
(from manufacturers data)

7.3 ANALYSIS OF PARTICULAR APPLICATIONS

The various applications are analysed by determining the unit cost of water produced in seven different types of operation mode. The different alternatives are shown in Table 7.6. During Winter the water demand is lower therefore there is an opportunity to operate the system at part load and this is considered in some scenarios.

The fuel cost and the fuel savings (where applicable) for the first year are given in all cases. From these figures the magnitude of the solar system contribution in each case can be seen. Diesel fuel in Cyprus is subsidised by the Government. The normal price of such fuel is double the today's price therefore in addition to the normal water price (calculated with the subsidised fuel price), the water price for the non-subsidised fuel cost is calculated in the analysis that follows.

OPERATION MODE	DESCRIPTION
#1	System operated with a conventional heat source.
#2	Same as mode #1 but system operated at 50% of nominal capacity during Winter.
#3	Solar only system with no back-up boiler.
#4	Full boiler back-up of solar system, with desalination plant working at full capacity all year round.
#5	Same as mode #4 but system operates at 50% of its nominal capacity throughout Winter.
#6	Desalination operates solely on fuel during nights and on solar during day time.
#7	Same as mode #6 but during Winter system operates at 50% of its nominal capacity when on boiler cycle.

Table 7.6 Types of operation considered in economic analysis

7.3.1 Small Domestic Application

The results of the economic analysis for the seven operation modes for this type of application are shown in Table 7.7. The water prices shown in Table 7.7 suggest that the system does not offer any economic benefit. It can be seen from the annual water production figures (Table 7.7), that the mean daily production of the system varies from

1.3 m^3/day (modes #1 and #4) to 0.25 m^3/day (mode #3). It can be shown that the life cycle savings (LCS) of the solar system compared with the fuel savings, incurred due to the use of the solar energy, is equal to -C£986 which proves the fact that the fuel only system (mode #1) results in lower water cost. The LCS is the money lost in building the system instead of buying the fuel. In Table 7.7 the LCS of the system operated under different modes, for a water price of C£1/m^3, a limit which is considered viable (see chapter 1), is tabulated. All the figures are negative because the normal water price in all modes is above the C£1/m^3 limit. These values represent the money lost by the owner if he decides to sell the water at C£1/m^3. As expected the water prices corresponding to the non-subsidised fuel cost are higher. It should be noted however that the water price between the systems operated on fuel only and on solar plus fuel (modes #1 and #4) are almost equal. The solar only system (mode #3) is insensitive to the fuel price as the system does not utilise any fuel. It can be shown that the life cycle savings (LCS) of the solar system compared with the fuel savings (at their non-subsidised price), incurred due to the use of the solar energy, is equal to -C£42 which proves the proximity of the water prices in mode #1 and #4 and modes #2 and #5.

Operation Mode	First year fuel cost (C£)	Mean daily water production (m^3/day)	LCS for C£1/m^3 water price (C£)	Water price (C£/m^3)	Water price for non-subsidised fuel cost (C£/m^3)
#1	468	1.33	-4604	1.97	2.99
#2	351	1.00	-4360	2.22	3.25
#3	0	0.25	-5110	6.70	6.70
#4	379	1.33	-5610	2.20	3.00
#5	262	1.00	-5367	2.50	3.26
#6	239	0.93	-5579	2.67	3.40
#7	179	0.76	-5350	2.96	3.65

Table 7.7 Results of the small domestic application economic analysis

For this application there are no tax incentives. This reflects on the water cost. The solar only system also gives a high water cost. This is due to the high relative cost of the desalination equipment. This means that it is not worth buying a desalination system and using it solely with solar energy which reflects that the system is inactive for half of the year (night time) and operated at its maximum capacity for only a few hours each day

for three months of the year during Summer.

7.3.2 Large Domestic Application

This application is analysed for two situations one "private type" without any significant tax savings and one "business type", like a small tourist establishment, which enjoys the full tax savings.

The results of the economic analysis for the "private type" system are shown in Table 7.8. Again the costs are high giving no real economic benefit. The lowest water price is given by the operation mode #1 which is C£1.45/m^3, whereas the full boiler back-up solar system (mode #4) is very near with C£1.49/m^3. It can be shown that the life cycle savings (LCS) of the solar system compared with the fuel savings, accrued due to the use of the solar energy, is equal to -C£1305. This reflects to the higher water prices given by the solar systems (modes #3-#7). The water prices given for the non-subsidised fuel cost suggest that the solar system is more viable than the fuel only system. This is also indicated by the LCS of the solar only system against the non-subsidised fuel savings which can be shown to be equal to C£4005.

Operation Mode	First year fuel cost (C£)	Mean daily water production (m^3/day)	LCS for C£1/m^3 water price (C£)	Water price (C£/m^3)	Water price for non-subsidised fuel cost (C£/m^3)
#1	2752	9.8	-15758	1.45	2.26
#2	2064	7.1	-16438	1.62	2.43
#3	0	1.8	-20611	4.23	4.23
#4	2242	9.8	-17084	1.49	2.15
#5	1554	7.1	-17764	1.67	2.28
#6	1404	6.8	-19124	1.78	2.38
#7	1053	5.6	-19006	1.95	2.50

Table 7.8 Results of the large domestic application economic analysis (no tax allowances)

A much better situation is seen in Table 7.9 which refers to the same system but with full tax allowances. Here a water price very near the C£1.00/m^3 limit is obtained. In

both cases the solar only systems are not viable.

It can be seen from the annual water production shown in both tables, that the mean daily water production of the system varies from 9.8 m^3/day (modes #1 and #4) to 1.8 m^3/day (mode #3).

Operation Mode	First year fuel cost (C£)	Mean daily water production (m^3/day)	LCS for C£1/m^3 water price (C£)	Water price (C£/m^3)	Water price for the non-subsidised fuel cost (C£/m^3)
#1	2752	9.8	-3110	1.09	1.68
#2	2064	7.1	-5977	1.23	1.82
#3	0	1.8	-14763	3.32	3.32
#4	2242	9.8	-4400	1.13	1.60
#5	1554	7.1	-7266	1.28	1.72
#6	1404	6.8	-8787	1.36	1.80
#7	1053	5.6	-9912	1.50	1.90

Table 7.9 Results of the large domestic application economic analysis (with tax allowance)

In both situations the system LCS for a water price of C£1/m^3 are negative as in all cases the normal water price is above the C£1/m^3 limit. It should be noted however that the magnitude of the LCS figure is a combination of the water price and the amount of water produced by the system in the various operation modes.

7.3.3 Hotel Application

This application is analysed for three types of system, the first one considers the system as a desalination system alone whereas the second and third are combinations of desalination and hot water production, for the Winter and Summer months.

7.3.3.1 Desalination only system

The results of the analysis for this type of application, for the system used solely for desalination year round, are shown in Table 7.10. Here the system provides real benefits

as the water price is C£0.89/m^3 for the system operated either with fuel only (mode #1) or on solar and fuel (mode #4). The fact that the water prices for these two modes are equal proves that for a higher fuel cost the solar systems would result in lower water prices compared to the fuel only systems. This is shown by the data in the final column tabulating the water prices for the non-subsidised fuel cost. It can be seen from the annual water production figures (Table 7.10), that the mean daily production of the system varies from 108 m^3/day (modes #1 and #4) to 20.4 m^3/day (mode #3). The system LCS for a water price of C£1/m^3 shown in Table 7.10 gives positive values for the modes where the normal water price is below the C£1/m^3 limit. This positive figure represent the amount of profit of the owner if he decides to sell the water at that price.

Operation Mode	First year fuel cost (C£)	Mean daily water production (m^3/day)	LCS for C£1/m^3 water price (C£)	Water price (C£/m^3)	Water price for non-subsidised fuel cost (C£/m^3)
#1	25245	108	40823	0.89	1.39
#2	18934	81	0	1.00	1.50
#3	0	20.4	-104500	2.43	2.43
#4	20425	108	40393	0.89	1.29
#5	14114	81	0	1.00	1.37
#6	12885	75.6	-18266	1.07	1.43
#7	9664	61.9	-36413	1.16	1.49

Table 7.10 Results of hotel application economic analysis

The water prices for the other operation modes (#5-#7) as outlined in Table 7.10 are again feasible as all of them give prices either equal or marginally greater than the C£1.00/m^3 limit. This means that even if the system is periodically inactive it will still be viable. Therefore, the author believes that the solar system may be used to power the desalination system and for hot water production either simultaneously or separately. Hot water is a commodity which is also required by a hotel. This analysis now follows.

7.3.3.2 Desalination and hot water

This case is analysed for two types of systems, firstly using the solar system producing hot water only, during the six Winter months and fresh water during the six Summer

months, secondly using part of the solar system to produce hot water during the Summer months only. The results for the first type of system are shown in Table 7.11 where the water price is higher than for the desalination only case. An alternative is to use the desalination system on fuel during the Winter months when the solar system is producing hot water. The results of the economic analysis for this alternative are also shown in Table 7.11. The results are very similar to the desalination only case but it should not be forgotten that the system is also covering the hotel's hot water demand.

Operation Mode	First year fuel savings (C£)	First year fuel cost (C£)	Mean daily water production (m^3/day)	Water price (C£/m^3)	LCS for C£1/m^3 water price (C£)	Water price for non-subsidised fuel cost (C£/m^3)
#4*	1070	8869	54	1.21	-40656	1.50
#6*	1070	5873	41.2	1.43	-63927	1.66
#4	1070	21492	108	0.89	43412	1.28
#6	1070	18495	95.2	0.94	20148	1.32
#7	1070	12184	68.2	1.09	-21889	1.42
Note: * Desalination system during Winter months is inactive						

Table 7.11 Results of hotel application economic analysis (desalination and hot water Winter)

As the desalination plant capacity is decided by the peak performance of the solar system a second mode of operation is to use part of the solar system to provide hot water during the Summer months only. In this way the desalination plant capacity is reduced as the collectors are supplying the excess energy for hot water production with a consequent reduction in the desalination plant cost. This analysis is shown in Table 7.12 where the water price is about the same as the desalination only case, but here the extra energy utilised for hot water production is replaced by the reduced water production. The mean daily water production in this case varies from 94 m^3/day (modes #1 and #4) to 17.8 m^3/day (mode #3).

From the above discussion it can be understood that the system is viable for a wide range of applications. What remains is for individual hotel managers to decide on the operation mode.

Operation Mode	First year fuel savings (C£)	First year fuel cost (C£)	Mean daily water production (m^3/day)	Water price (C£/m^3)	LCS for C£1/m^3 water price (C£)	Water price for non-subsidised fuel cost (C£/m^3)
#1	0	21963	94	0.91	31434	1.40
#2	0	16472	70.5	1.02	-4992	1.51
#3	641	0	17.8	2.45	-92600	2.45
#4	641	17784	94	0.90	32800	1.28
#5	641	12293	70.5	1.01	-3627	1.35
#6	641	11210	65.8	1.08	-18190	1.41
#7	641	8408	53.8	1.18	-33830	1.47

Table 7.12 Results of hotel application economic analysis (desalination and hot water Summer)

7.3.4 Village Application

The results of the economic analysis for this type of application is shown in Table 7.13. This system provides greater economic benefits than the hotel case although the cost of land for installing the solar system has not been considered. Therefore, the costs shown in Table 7.13, for the solar systems (modes #3 to #7), apply provided that the solar collectors are installed on Government land. Even in this case the use of solar energy alone to power the desalination system is not cost-effective due to the high percentage of inactive time. It can be seen from the annual water production figures (Table 7.13), that the mean daily production of the system varies from 432 m^3/day (modes #1 and #4) to 82.4 m^3/day (mode #3).

It should be noted here that the LCS of the system for C£1/m^3 water price gives figures with great differences. This is due to the combination of the water price and the large quantity of the water produced by the system.

Operation Mode	First year fuel cost (C£)	Mean daily water production (m^3/day)	LCS for C£1/m^3 water price (C£)	Water price (C£/m^3)	Water price for non-subsidised fuel cost (C£/m^3)
#1	101283	432.9	185712	0.88	1.37
#2	75962	324.6	18301	0.98	1.50
#3	0	82.4	-379690	2.28	2.28
#4	81851	432.9	196970	0.87	1.28
#5	56530	324.6	29560	0.97	1.35
#6	51697	303.7	-36923	1.03	1.40
#7	38772	248.4	-108675	1.12	1.46

Table 7.13 Results of village application economic analysis

7.4 SYSTEM COMPARISONS

The water price obtained in all operation modes for all the types of applications considered are shown in Fig. 7.1. In this figure the C£1/m^3 price limit is also drawn. In this way water prices falling below the limit can clearly be seen.

Comparison graphs for the mode #4 which is the full boiler back-up of the solar system are shown in Fig. 7.2. It can be seen from Fig. 7.2 that as the installation becomes bigger it produces more water whereas at the same time the unit water price is falling. The reduction of the life of the system to 5, 10 and 15 years imposes small differences in the water price which is shown graphically in Fig. 7.3.

7.5 SENSITIVITY ANALYSIS/CONCLUSIONS

An analysis was carried out to investigate the sensitivity of the economic model and the effect of the variation of the various parameters on the water price. The base figure is considered to be the full fuel back-up system for the hotel application which from Table 7.10 gives a value of C£0.89/m^3.

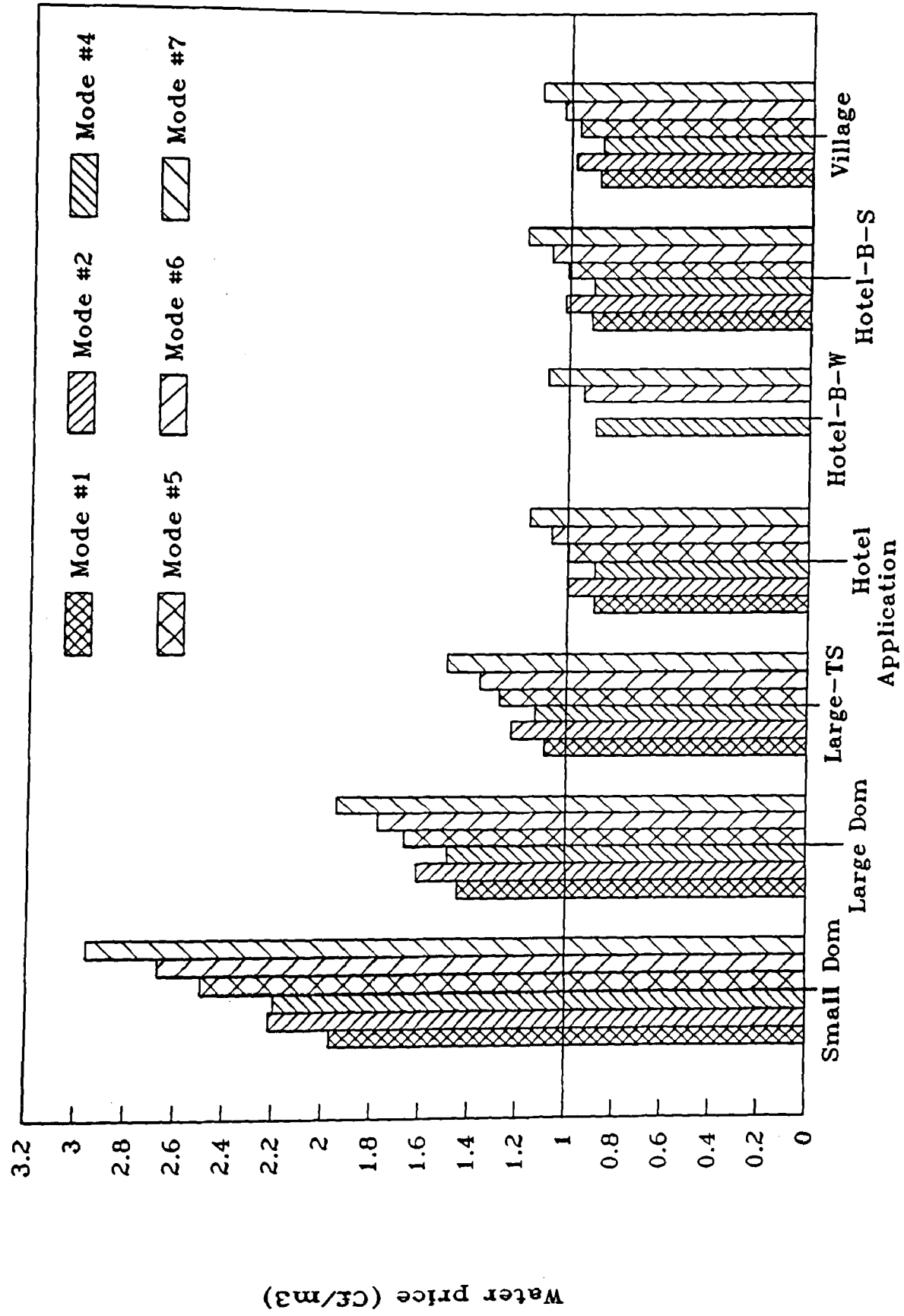

Fig. 7.1 Water price against operation mode for all applications considered

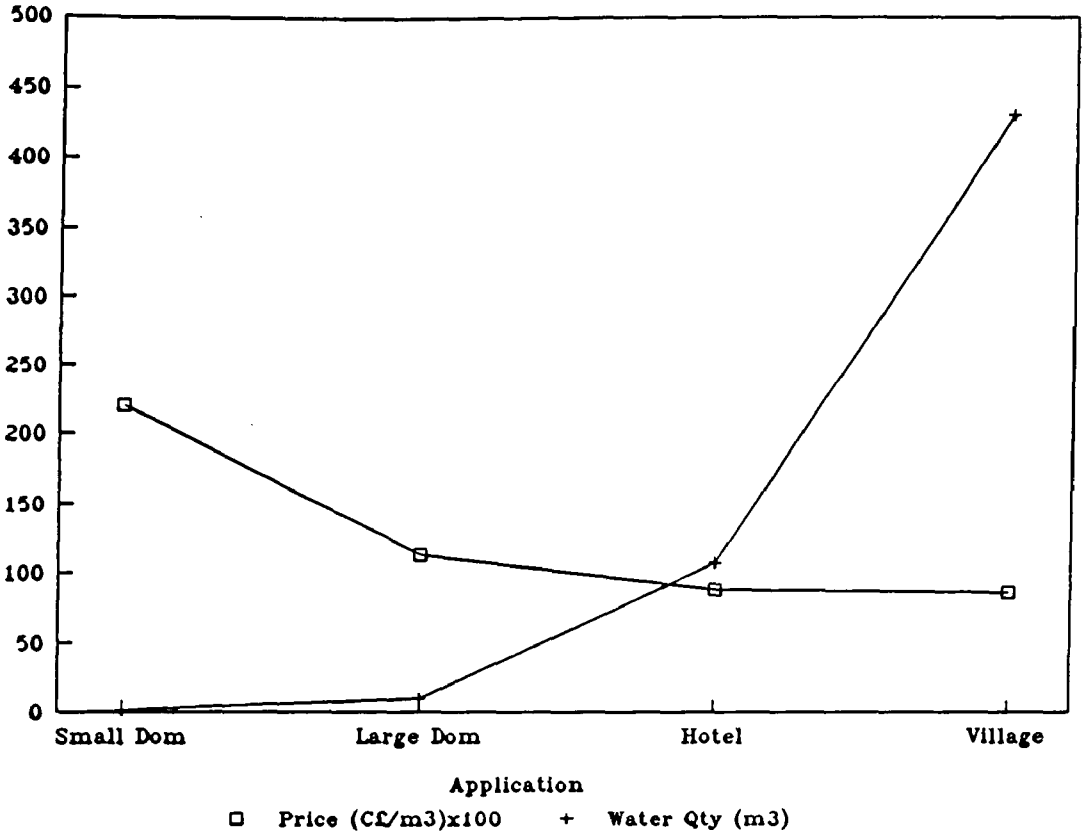

Fig. 7.2 Comparison of water quantity and water price for operation mode #4

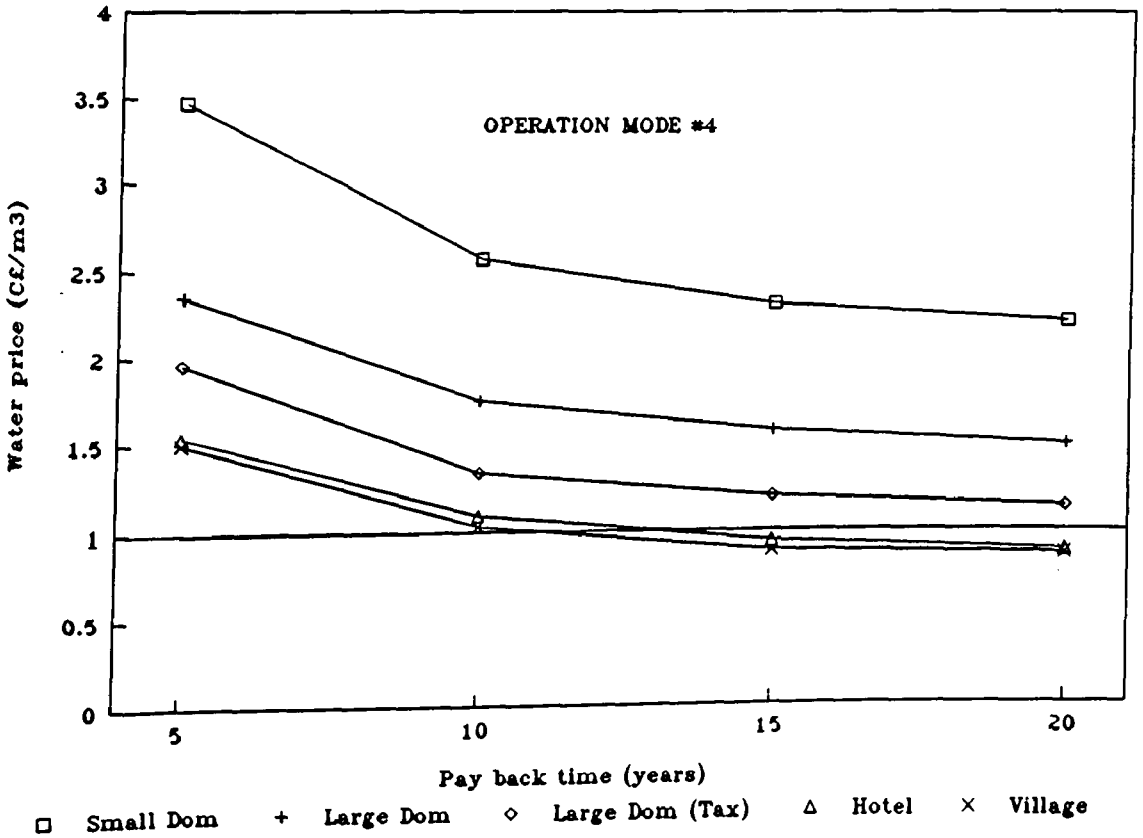

Fig. 7.3 Water price against pay-back time for operation mode #4

The effect of the area dependent and independent cost i.e. solar and desalination systems, is shown in Table 7.14. The difference in water price for 20% variation is about 8% which is a reasonable figure.

ITEM		PERCENTAGE DIFFERENCE			
		+20%	+10%	-10%	-20%
Area dependent cost	Price (C£/m^3)	0.91	0.90	0.88	0.87
	Difference	+2.2%	+1.1%	-1.1%	-2.2%
Area independent cost	Price (C£/m^3)	0.96	0.93	0.86	0.83
	Difference	+7.9%	+4.5%	-3.4%	-6.7%

Table 7.14 Effect of the desalination and solar cost on water price

The doubling of the rate of increase of electricity and fuel price gives 3.4% and 2.2% increase in water price respectively. The reduction of the initial payment to zero imposes a reduction of 1.1% on the water price whereas the elimination of any resale value leads to an increase of 3.4%. Finally, the modification of using the original analysis with only a 10 year mortgage recovery gives an increase of 1.9%.

From the above discussion it is clear that the water prices given in this section realistically reflect costs and their variation to possible change in the direct costs and method of payment is relatively insignificant.

Lately, in Cyprus there is a trend to liberate the bank rates. The Government declares that this is imposed by the European Union countries in view of Cyprus joining the Union. In such a case the market discount rate would be reduced to 6%. Such a change will reduce even further the water cost by 1.1%.

Further tax benefits are provided in sectors of the economy that the Government wants to promote, like the purchase of a robotic system. This benefit is the return of 100% wear and tear allowance at the end of the first year as if the equipment has a life of only one year. This is an extra incentive for enterprise owners to upgrade their businesses. As Cyprus is potentially facing a water shortage problem, the author believes that such

an incentive should be given to solar desalination as well. This will result in a reduction of the water price of 4.3%.

It can be concluded from the above analysis that solar desalination is viable for the two bigger installations (hotel and village) as shown above. It can also be concluded that the water cost is insensitive to the changes in the method of payment or to variations in direct costs. It is not worth operating the desalination system solely on solar energy due to the high cost of the desalination system and the high percentage of inactive time.

The author believes that even in cases where the fuel only systems results in lower or equal water price compared to a solar plus fuel system, the solar alternative should not be abandoned because as it was proved a possible increase in fuel price turns the system viability in favour of the solar system. The issues of global warming and climate change resulting from the increase in greenhouse gasses due to the burning of fuels should not be underestimated. According to a world-wide acceptable scenario of human activities, an increase in global average temperature by 0.3K per decade would occur [Houghton, 1992].

Although water prices above the ones charged by the various water boards in Cyprus have been obtained from the forgoing analysis, the author believes that the present system offers some benefits which should not be underestimated. In particular security of supply is very important to the hotel industry with Cyprus endeavouring to upgrade its tourist facilities. Most of the hotels in Cyprus have standby generators installed for security of electricity supply. Based on the same principle, the author believes that water supply should be treated the same way.

Blank page

CHAPTER 8

CHAPTER 8

THE FINAL SYSTEM

In this chapter detailed specifications of the system which has been developed are given followed by a list of conclusions gleaned from this research project and recommendations for future work.

8.1 SPECIFICATIONS

A solar system for steam generation has been developed. This includes a collector together with the tracking mechanism, the flash vessel and the high pressure circulating pump. The specifications of the system are tabulated in Table 8.1.

8.2 CONCLUSIONS

The following conclusions can be drawn from this research project:

1. Cyprus potentially faces a water shortage problem. An attempt was undertaken by the Government of Cyprus to solve the problem by building dams and associated reservoirs. This is a correct measure but by considering the fact that to date the maximum water quantity collected is just 74% of the overall dam capacity the erection of more dams is questionable.

2. The best desalination process suitable for solar energy is the multiple effect which offers low energy consumption, low equipment cost, simple sea-water treatment, and suitability for variable steam supply.

3. The mode of tracking suitable for multi-row collector installations is the E-W horizontal. This mode offers small aperture losses and therefore high optical performance. In addition small shadowing effects are encountered which is in favour of this mode in terms of land utilisation.

ITEM	VALUE/TYPE
Collector:	
Collector aperture area	$3.5m^2$
Collector aperture	1.46m
Aperture-to-length ratio	0.64
Rim angle	90°
Glass-to-receiver ratio	2.17
Receiver diameter	22mm
Concentration ratio	21.1
Collector intercept factor	0.94
Material area	$4.1m^2$
Parabola reflectance	0.85 (3M Scotchcal 5400)
Receiver absorptance	0.9 (Special paint)
Glass cover transmittance	0.9
Tracking mechanism:	
Tracking mechanism type	Electronic
Mode of tracking	E-W Horizontal
Collector performance:	
Test intercept	0.638
Test slope	$0.387\ W/m^2K$
Time constant (heating)	52s
Time constant (cooling)	48s
Collector acceptance angle	1°
System:	
Operating pressure	6 bar
Mass flow rate	2.52 kg/min
Flash vessel height	600mm
Flash vessel diameter	65mm

Table 8.1 System specifications

4. The steam-flash steam generation concept seems to be the best with respect to other steam generation systems due to the superiority of the water as a heat transfer fluid, the small capital cost of the system, the stability and guarantee of no fresh water contamination.

5. From the many arrangements of multiple effect boiling evaporators the multiple effect stack type is the most suitable for solar energy applications. This is due to its stable operation between virtually zero and 100% output even when sudden changes are made, and its ability to follow a varying steam supply without upset.

6. From the collector performance graph a test intercept of 0.638 and a test slope of 0.387 W/m^2K was obtained. Both values are well close to reported values as shown in Chapter 5. This proves that the design and model constructed are accurate.

7. The evaluation of the system performance gave results very close to the modelled performance especially with program "PTCDES2" which is in agreement to within 1.2%.

8. Preliminary tests on the model showed that the system heat-up response is critical to the achievement of good overall system performance and in particular to the start-up energy requirements. To achieve system optimisation a computer program was developed to model the system performance. From this analysis the optimum vessel size and capacity was selected. This reduces the system pre-heat energy requirement by 30% as compared to the initial design. The system simulation was compared to the actual response of the plant and gave agreement to within 6.5%. The modelled system response was also compared to the actual response under transient conditions. The agreement with respect to time and temperature profiles was very good.

9. From the economic analysis it can be concluded that the system is viable for the hotel and the village size cases and can give a water price below 0.89 $C£/m^3$. It is shown that the water cost is insensitive to the changes in the method of payment or to variations in direct costs. It was also shown that in Cyprus it is not cost effective to operate the desalination system solely on solar energy due to the combination of the high cost of the desalination system and the high percentage of inactive time.

8.3 RECOMMENDATIONS

The recommendations for future work on this subject are:

1. Build a system suited to the hotel capacity size and evaluate its performance. In this way the performance results of the actual system can be compared with the modelled system. The economic analysis can be performed again by using the actual system cost and the new water cost can be evaluated. Finally the practical problems such as descaling of the system can be assessed.

2. In addition to the above, the actual system can be set to operate under vacuum conditions in order to evaluate whether there is a significant increase of the system performance as predicted by the modelling program (see section 6.3.2).

Blank page

APPENDICES

APPENDIX 1

ENVIRONMENTAL CHARACTERISTICS

The operation of solar collectors and systems depends on the solar radiation input and the ambient air temperature. For this a typical year, called a Reference Year is defined as a year which sums up all the climatic information characterising a period equivalent to the mean life of the system. In this way the long term performance of a collector or a system can be calculated by determining its simulated performance over the reference year [Cena, 1985].

The available weather data for Cyprus covers only a relatively short period of time, much less than the life of the system (15–20 years). Two sources of information were available, the published data from Meteorology Services Department and data from the Institute of Agricultural Research Department of the Ministry of Agriculture and Natural Resources. Detail analysis of the radiation and temperature data from these two sources are given in [Kalogirou, 1991]. Since no other information is currently available these were used for the development of the Reference Year shown in Fig. A1.1 [Kalogirou, 1991].

For the evaluation of the performance of concentrating solar collectors the beam (or direct) component of global radiation is required. Therefore a Special Reference Year table has been constructed as shown in Fig. A1.2 which lists the beam radiation and the ambient air temperature.

TIME	JANUARY		FEBRUARY		MARCH		APRIL		MAY		JUNE		JULY		AUGUST		SEPTEMBER		OCTOBER		NOVEMBER		DECEMBER	
	RAD	TEMP	RAD	TEMP	RAD	TEMP	RAD	TEMP	RAD	TEMP	RAD	TEMP	RAD	TEMP	RAD	TEMP	RAD	TEMP	RAD	TEMP	RAD	TEMP	RAD	TEMP
1.00	0	7.1	0	7.9	0	10.1	0	12.6	0	16.9	0	20.7	0	23.3	0	23.1	0	20.8	0	17	0	11.3	0	8.8
2.00	0	7	0	7.6	0	9.7	0	12.3	0	16.6	0	20.4	0	23	0	22.7	0	20.4	0	16.6	0	11	0	8.6
3.00	0	6.8	0	7.3	0	9.4	0	12	0	16.2	0	20.1	0	22.6	0	22.3	0	20	0	16.3	0	10.7	0	8.4
4.00	0	6.6	0	7	0	9.1	0	11.8	0	15.9	0	19.7	0	22.3	0	21.8	0	19.6	0	16	0	10.7	0	8.3
5.00	0	6.4	0	6.9	0	9	0	11.5	0	15.7	0	19.6	0	22	0	21.4	0	19.2	0	15.8	0	10.4	0	8.2
6.00	0	6.4	0	6.8	0	8.7	12	11.8	36	16.9	58	21.3	39	23.1	13	21.8	1	19.1	0	15.6	0	10.3	0	8.2
7.00	5	6.4	8	7.1	30	9.3	108	14.2	174	19.6	219	23.9	197	25.9	135	24.5	77	21.2	27	16.8	3	10.4	0	8.2
8.00	45	7	90	8.3	150	11.1	279	16.8	354	21.9	413	26.3	401	28.6	334	27.4	261	24.6	159	19.9	70	12.2	40	8.9
9.00	160	9.4	240	10.9	310	13.5	466	18.9	540	24.1	598	28.3	594	30.5	528	29.5	451	27.1	332	22.9	200	15.4	140	11.3
10.00	280	11.5	360	12.8	470	15.5	620	20.3	693	25.7	746	29.9	747	32.2	691	31.5	600	29	478	24.9	340	17.7	260	13.3
11.00	340	12.9	470	14.1	580	16.7	729	21.3	779	27	835	31.1	846	33.6	794	33	707	30.4	573	26.1	440	19	350	14.6
12.00	390	13.5	520	14.8	650	17.6	729	22	796	27.7	868	31.9	893	34.7	846	34.2	749	31.5	613	27	460	20	380	15.2
13.00	400	13.9	510	15.1	630	18.2	712	22.1	722	27.7	829	32	874	35.1	814	34.6	715	31.9	583	27.3	440	20.3	370	15.6
14.00	340	14.1	440	15.3	560	18.8	635	22.3	637	27.8	731	32.4	808	35.4	735	34.9	611	32	515	27.5	360	20.4	320	15.7
15.00	260	13.7	330	14.8	480	18.3	530	21.5	545	26.7	633	31.1	679	34.4	610	33.7	474	30.8	396	26.3	260	19.6	220	15.1
16.00	140	13.1	210	14.3	340	17.4	399	20.5	429	25.9	542	30.4	539	33.4	479	32.6	346	29.5	230	24.9	130	18.6	110	14.4
17.00	40	11.9	80	13.2	160	16.5	239	19.3	307	24.5	376	29.5	364	31.9	300	31	185	28.3	89	23	30	17.1	20	13.1
18.00	4	10.7	10	11.9	50	15.3	93	17.6	147	22.7	203	27.2	179	30	114	28.9	40	25.8	7	21.5	1	15.7	0	12
19.00	0	9.7	0	10.8	10	14	9	16.3	25	20.9	50	25.1	33	27.8	9	26.9	0	24.4	0	20.4	0	14.7	0	11.2
20.00	0	8.9	0	10.1	0	13	0	15.4	0	19.8	0	23.6	0	26.1	0	25.7	0	23.5	0	19.6	0	13.7	0	10.5
21.00	0	8.4	0	9.5	0	12.3	0	14.6	0	19	0	22.8	0	25.2	0	24.9	0	22.8	0	18.9	0	13	0	10
22.00	0	8	0	9	0	11.7	0	14.1	0	18.4	0	22.1	0	24.3	0	24.4	0	22.3	0	18.3	0	12.4	0	9.6
23.00	0	7.6	0	8.5	0	11.1	0	13.6	0	17.9	0	21.6	0	24.1	0	23.9	0	21.8	0	17.7	0	11.9	0	9.3
24.00	0	7.3	0	8.2	0	10.6	0	13.2	0	17.5	0	21.2	0	23.8	0	23.5	0	21.3	0	17.2	0	11.5	0	9
TOTAL	2404	9.5	3268	10.5	4420	13.2	5560	16.5	6184	21.4	7101	25.5	7193	28.1	6402	27.4	5217	24.9	4002	20.7	2734	14.5	2210	11.1

RADIATION
AND
AVERAGE TEMPERATURE

UNITS: - Global Radiation [W/m^2]
- Ambient Air Temperature [°C]

Fig. A1.1 Reference year

TIME	JANUARY		FEBRUARY		MARCH		APRIL		MAY		JUNE		JULY		AUGUST		SEPTEMBER		OCTOBER		NOVEMBER		DECEMBER	
	RAD	TEMP	RAD	TEMP	RAD	TEMP	RAD	TEMP	RAD	TEMP	RAD	TEMP	RAD	TEMP	RAD	TEMP	RAD	TEMP	RAD	TEMP	RAD	TEMP	RAD	TEMP
1.00	0	7.1	0	7.9	0	10.1	0	12.6	0	16.9	0	20.7	0	23.3	0	23.1	0	20.8	0	17	0	11.3	0	8.8
2.00	0	7	0	7.6	0	9.7	0	12.3	0	16.6	0	20.4	0	23	0	22.7	0	20.4	0	16.8	0	11	0	8.6
3.00	0	6.8	0	7.3	0	9.4	0	12	0	16.2	0	20.1	0	22.6	0	22.3	0	20	0	16.3	0	10.7	0	8.4
4.00	0	6.6	0	7	0	9.1	0	11.8	0	15.9	0	19.7	0	22.3	0	21.8	0	19.6	0	16	0	10.7	0	8.3
5.00	0	6.4	0	6.9	0	9	0	11.5	0	15.7	0	19.6	0	22	0	21.4	0	19.2	0	15.8	0	10.4	0	8.2
6.00	0	6.4	0	6.8	0	8.7	2	11.8	12	16.9	37	21.3	22	23.1	4	21.8	0	19.1	0	15.6	0	10.3	0	8.2
7.00	0	6.4	2	7.1	8	9.3	38	14.2	81	19.6	141	23.9	135	25.9	82	24.5	44	21.2	12	16.8	0	10.4	0	8.2
8.00	7	7	19	8.3	69	11.1	146	16.8	206	21.9	300	26.3	310	28.6	244	27.4	196	24.5	103	19.9	28	12.2	13	8.9
9.00	73	9.4	94	10.9	186	13.6	295	18.9	354	24.1	472	28.3	489	30.5	415	29.5	370	27.1	244	22.9	112	15.4	106	11.3
10.00	161	11.5	174	12.8	303	15.5	420	20.3	493	25.7	607	29.9	630	32.2	567	31.5	506	29	365	24.9	223	17.7	217	13.3
11.00	209	12.9	254	14.1	382	16.7	508	21.3	558	27	684	31.1	729	33.6	664	33	604	30.4	447	26.1	305	19	292	14.5
12.00	241	13.5	327	14.8	419	17.6	492	22	556	27.7	708	31.9	765	34.7	705	34.2	637	31.6	478	27	317	20	300	15.2
13.00	246	13.9	307	15.1	389	18.2	463	22.1	477	27.7	666	32	735	35.1	668	34.6	597	31.9	453	27.3	308	20.3	285	15.6
14.00	212	14.1	243	15.3	339	18.8	402	22.3	406	27.8	577	32.4	664	35.4	586	34.9	486	32	392	27.5	243	20.4	225	15.7
15.00	136	13.7	162	14.8	277	18.3	311	21.5	324	26.7	454	31.1	519	34.4	453	33.7	357	30.8	284	26.3	167	19.6	153	15.1
16.00	56	13.1	96	14.3	182	17.4	186	20.6	215	25.9	328	30.4	348	33.4	313	32.6	235	29.5	141	24.9	67	18.6	64	14.4
17.00	7	11.9	27	13.2	72	16.5	79	19.3	127	24.5	193	29.5	196	31.9	163	31	105	28.3	40	23	7	17.1	7	13.1
18.00	0	10.7	0	11.9	10	15.3	17	17.6	49	22.7	98	27.2	86	30	49	28.9	14	25.8	3	21.5	0	15.7	0	12
19.00	0	9.7	0	10.8	0	14	1	16.3	7	20.9	25	25.1	12	27.8	2	26.9	0	24.4	0	20.4	0	14.7	0	11.2
20.00	0	8.9	0	10.1	0	13	0	15.4	0	19.8	0	23.6	0	26.1	0	25.7	0	23.5	0	19.6	0	13.7	0	10.6
21.00	0	8.4	0	9.6	0	12.3	0	14.6	0	19	0	22.8	0	25.2	0	24.9	0	22.8	0	18.9	0	13	0	10
22.00	0	8	0	9	0	11.7	0	14.1	0	18.4	0	22.1	0	24.3	0	24.4	0	22.3	0	18.3	0	12.4	0	9.6
23.00	0	7.6	0	8.5	0	11.1	0	13.6	0	17.9	0	21.6	0	24.1	0	23.9	0	21.8	0	17.7	0	11.9	0	9.3
24.00	0	7.3	0	8.2	0	10.6	0	13.2	0	17.5	0	21.2	0	23.8	0	23.5	0	21.3	0	17.2	0	11.5	0	9
TOTAL	1348	9.5	1705	10.5	2638	13.2	3360	16.5	3865	21.4	5290	25.5	5640	28.1	4915	27.4	4151	24.9	2962	20.7	1777	14.5	1662	11.1

RADIATION
AND
AVERAGE TEMPERATURE

UNITS: - Beam Radiation [W/m^2]
- Ambient Air Temperature [°C]

Fig. A1.2 Special reference year

APPENDIX 2

COMPUTER PROGRAM "SKDES"

A2.1 PROGRAM DESCRIPTION

The program is written in Quick Basic in a modular form compiled by the Quick Basic compiler. The program starts by typing "SKDES" followed by the Enter Key at the A> prompt. After a title page, the main menu appears (see Fig. A2.1). At this stage any module can be chosen by pressing the module number (1-8) or 9 to return to system.

For each module a number of inputs are required, and the form of output expected is explained. In all modules the user has the option to correct the data input before proceeding with the calculations. In most modules the user has the option of saving the output to a file. This data can be used later with another computer package (eg. Lotus 1-2-3) in order to produce graphs of the various parameters. In this case the following message appears on the screen:

Store DATA in a File (Y/N)?

If yes (Y or y) is typed the message "Enter Filename ?" appears. This must be of the following format:

FILENAME.EXT

SKDES PROGRAMME

**** MAIN MENU ****

1. PTC Incidence Angle Analysis (Days 90-210)
2. PTC Incidence Angle Analysis (Days 1-365)
3. PTC Local CR Estimation
4. PTC Intercept Factor Estimation
5. Weather Data Generator
6. PTCDES1 Desalination System Simulation
7. PTCDES2 Desalination System Simulation
8. Theoretical System Modelling
9. Return to SYSTEM

Enter Your Choice ¦ ¦

Fig. A2.1 SKDES program main menu

A filename can be any valid DOS name i.e. from one to eight characters in length. The optional filename extension can be three or less characters. Upper and lower case letters are allowed.

In the case of simulation module the input data can be read from a data file by typing yes (Y or y) as an answer to the question:

Use input DATA from a file ?

Then the following message appears:

Enter DATA filename ?

When a proper filename is used a list of the input variables required by the program is displayed together with the values assigned to each variable. If the filename is not found in the directory specified an error message appears with an option to list files. If no (N or n) is answered to the above question all the variables are presented on the screen with 0 (zero) values. At the end of the variable list there is a message to input the variable number the value of which is required to be changed or type 0 (zero) to proceed. When 0 (zero) is typed an option is provided to save the new list of variables in a file for later use.

At the end of all modules a message appears on the screen for the user to press any key in order to return to the main menu from which he can either choose another module or return to system. A diskette with all the programs is included at the end of the thesis.

A2.2 MODE OF TRACKING SELECTION PROGRAM

This program module is used to calculate the incidence radiation on inclined surfaces employing E–W tracking by considering optical effects only. This mode can be accessed by typing numbers 1 or 2 at the main menu. The calculation is done from day number 90 to 210 and from 1 to 365 respectively. The input data required are:

- Latitude [Deg]
- Tracking axis slope [Deg]
- Tracking axis azimuth [Deg]
- Maximum optical efficiency (at zero angle of incidence)
- Geometric factor

Tracking axis slope is the angle between the collector axis line and the projection of the axis into the horizontal plane. Tracking axis azimuth is the angle between the projection of the collector axis line onto the horizontal plane and local meridian (West positive, East negative).

The program outputs the solar radiation collected in kWh/m^2 every day of the period considered and the period's total at the end. The input data and the output of the program for the E-W horizontal mode for the period covering day number 90–210 (option 1) is shown in Fig. A2.2. The flow chart of the program is shown in Fig. A2.3 whereas the listing of the program is shown in Fig. A2.4.

A2.3 FLUX DISTRIBUTION ON A PTC RECEIVER PROGRAM

This program module can be accessed by typing number 3 at the main menu and is used for calculating the incident solar flux at various angles around the receiver of a PTC. The input data required are:

- Receiver radius [m]
- Angle of incidence [Deg]
- Collector focal length [m]
- Collector reflectance
- Total standard deviation of errors [rad]
- Step size of angle (β) [Deg]

The program outputs the local concentration ratio (LCR) at each step size of angle (β). The LCR is the multiplication factor of the input solar radiation. The input data and the output of the program for a step size of the angle β equal to 10° is shown in Fig. A2.5. The flow chart of the program is shown in Fig. A2.6 whereas the listing of the program is shown in Fig. A2.7.

INPUT DATA

LATITUDE = 35 Deg.
TRACKING AXIS SLOPE = 0
TRACKING AXIS AZIMUTH = 0
MAXIMUM OPTICAL EFFICIENCY = .66
GEOMETRIC FACTOR = .3045
1

OUTPUT DATA

DAY No	RADIATION(kWh/m^2)				
90.00	5.01	160.00	6.89	230.00	6.08
91.00	5.06	161.00	6.90	231.00	6.05
92.00	5.11	162.00	6.91	232.00	6.02
93.00	5.16	163.00	6.91	233.00	5.99
94.00	5.22	164.00	6.91	234.00	5.95
95.00	5.27	165.00	6.92	235.00	5.92
96.00	5.32	166.00	6.92	236.00	5.88
97.00	5.37	167.00	6.92	237.00	5.84
98.00	5.42	168.00	6.92	238.00	5.80
99.00	5.47	169.00	6.93	239.00	5.76
100.00	5.51	170.00	6.93	240.00	5.72
101.00	5.56	171.00	6.93	241.00	5.67
102.00	5.61	172.00	6.93	242.00	5.63
103.00	5.65	173.00	6.93	243.00	5.58
104.00	5.70	174.00	6.93	244.00	5.54
105.00	5.74	175.00	6.93	245.00	5.49
106.00	5.78	176.00	6.93	246.00	5.44
107.00	5.82	177.00	6.92	247.00	5.39
108.00	5.86	178.00	6.92	248.00	5.34
109.00	5.90	179.00	6.92	249.00	5.29
110.00	5.93	180.00	6.92	250.00	5.24
111.00	5.97	181.00	6.91	251.00	5.19
112.00	6.00	182.00	6.91	252.00	5.14
113.00	6.04	183.00	6.90	253.00	5.09
114.00	6.07	184.00	6.90	254.00	5.03
115.00	6.10	185.00	6.89	255.00	4.98
116.00	6.13	186.00	6.89	256.00	4.93
117.00	6.16	187.00	6.88	257.00	4.88
118.00	6.19	188.00	6.87	258.00	4.83
119.00	6.22	189.00	6.87	259.00	4.78
120.00	6.24	190.00	6.86	260.00	4.74
121.00	6.27	191.00	6.85	261.00	4.70
122.00	6.30	192.00	6.84	262.00	4.65
123.00	6.32	193.00	6.84	263.00	4.61
124.00	6.34	194.00	6.83	264.00	4.45
125.00	6.37	195.00	6.82	265.00	4.40
126.00	6.39	196.00	6.81	266.00	4.36
127.00	6.41	197.00	6.80	267.00	4.32
128.00	6.43	198.00	6.79	268.00	4.28
129.00	6.45	199.00	6.79	269.00	4.23
130.00	6.47	200.00	6.78	270.00	4.19
131.00	6.49	201.00	6.77	271.00	4.14
132.00	6.51	202.00	6.76	272.00	4.10
133.00	6.53	203.00	6.65	273.00	4.06
134.00	6.55	204.00	6.64	274.00	4.01
135.00	6.57	205.00	6.63	275.00	3.97
136.00	6.58	206.00	6.62	276.00	3.92
137.00	6.60	207.00	6.60	277.00	3.88
138.00	6.61	208.00	6.59	278.00	3.83
139.00	6.62	209.00	6.57	279.00	3.78
140.00	6.63	210.00	6.56	280.00	3.74
141.00	6.64	211.00	6.54	281.00	3.69
142.00	6.75	212.00	6.52	282.00	3.65
143.00	6.76	213.00	6.50	283.00	3.60
144.00	6.77	214.00	6.48	284.00	3.56
145.00	6.78	215.00	6.46	285.00	3.51
146.00	6.79	216.00	6.44	286.00	3.46
147.00	6.80	217.00	6.42	287.00	3.42
148.00	6.81	218.00	6.40	288.00	3.37
149.00	6.82	219.00	6.38	289.00	3.33
150.00	6.82	220.00	6.36	290.00	3.28
151.00	6.83	221.00	6.33	291.00	3.24
152.00	6.84	222.00	6.31	292.00	3.19
153.00	6.85	223.00	6.28	293.00	3.15
154.00	6.86	224.00	6.26	294.00	3.10
155.00	6.86	225.00	6.23	295.00	3.06
156.00	6.87	226.00	6.20	296.00	3.01
157.00	6.88	227.00	6.17	297.00	2.97
158.00	6.88	228.00	6.14	298.00	2.92
159.00	6.89	229.00	6.11	299.00	2.88
				300.00	2.84

PERIOD TOTAL = 1222.9 kWh/m2

Fig. A2.2 Input and output of the mode of tracking selection program

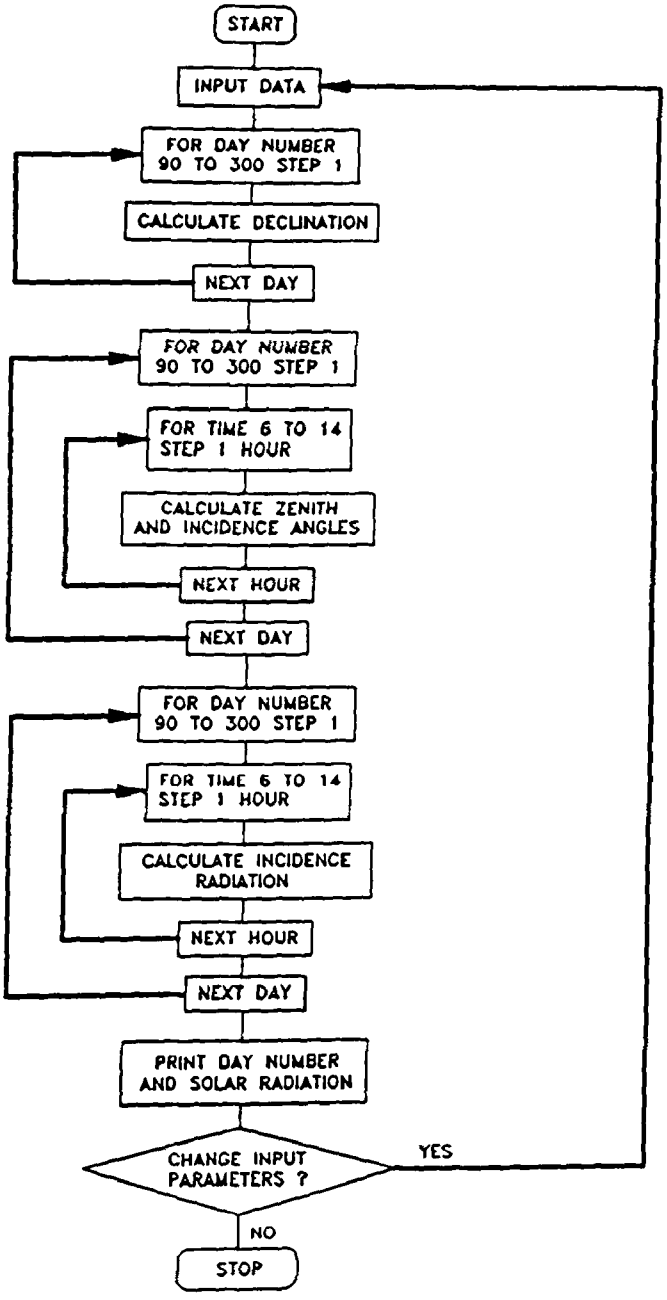

Fig. A2.3 Flow chart of the mode of tracking selection program

```
60 PRINT "  ***************************************************************"
70 PRINT "  Program for Calculating the Incident Radiation on Inclined Surfaces"
80 PRINT "                    Employing E-W Tracking"
90 PRINT "  ***************************************************************"
100 '
110 LOCATE 15,20:PRINT "** Press ANY key to Continue **";B$=INPUT$(1)
130 DIM DECL(210)
140 DIM ZEN(14,210)
150 DIM THETA(14,210)
160 DIM RAD(14,210)
170 DIM TOT(211)
180 CLS
190 A = 3.1416 / 180
200 INPUT "LATITUDE (Deg) ="; L
210 INPUT "TRACKING AXIS SLOPE (Deg) =";BT
220 INPUT "TRACKING AXIS AZIMUTH (Deg) =";GT
230 INPUT "MAXIMUM OPTICAL EFFICIENCY =";NM
240 INPUT "GEOMETRIC FACTOR =";GF
250 PRINT
260 INPUT "          *****> Pause at Every Page (Y/N)";S$
270 PRINT
280 INPUT "          *****> Store Data in a File (Y/N)";G$
290 IF (G$="Y") OR (G$="y") THEN GOTO 330
300 IF (G$="N") OR (G$="n") THEN GOTO 370
310 PRINT "  Wrong Response. Try Again"
320 GOTO 280
340 INPUT "          Enter Filename";XX$
350 FILE$=XX$
360 OPEN FILE$ FOR OUTPUT AS #1
370 PRINT
380 INPUT "          *****> Print Input/Output (Y/N)";Z$
390 IF Z$="y" OR Z$="Y" OR Z$="N" OR Z$="n" THEN GOTO 420
400 PRINT "  Wrong Response. Try Again"
410 GOTO 380
420 PRINT
430 PRINT TAB(10);"Press SPACE BAR to continue or <ESC> to correct data"
440 IF INKEY$<>"" THEN GOTO 440
450 SELECT$ = INKEY$
460 IF SELECT$ = "" THEN GOTO 450
470 IF SELECT$ = CHR$(27) THEN GOTO 180
480 IF SELECT$ = " " THEN GOTO 500
490 GOTO 440
500 CLS
510 LOCATE 10,20:PRINT "Calculating Declination ...."
520 FOR I = 0 TO 210
530 X = (360 / 365) * (284 + 90 + I) * A
540 DECL(I) = 23.45 * SIN(X)
550 NEXT I
560 LOCATE 12,20:PRINT "Calculating Zenith and Incidence Angles  ...."
570 FOR J = 0 TO 210
580 FOR I = 0 TO 14
590 H=(I+5-12)*15
600 HS1=TAN(DECL(J)*A)/TAN(L*A)
610 HS=1.570796-ATN(HS1/SQR(1-HS1*HS1))
620 HS=HS/A
630 IF ABS(H)<= HS THEN H1=1 ELSE H1=-1
640 IF L*(L-DECL(J))>=0 THEN H2=1 ELSE H2=-1
650 IF H>=0 THEN H3=1 ELSE H3=-1
660 Y = SIN(L * A) * SIN(DECL(J) * A) + COS(L * A) * COS(DECL(J) * A) * COS(H* A)
670 Y1 = ATN(Y / SQR(1 - Y * Y))
680 Y2=Y1/A
690 IF Y2<0 THEN GOTO 700 ELSE GOTO 710
700 Y=1
710 ZEN(I,J)=Y
720 IF Y2>=0 THEN GOTO 730 ELSE GOTO 900
730 Z=(SIN (H*A)*COS(DECL(J)*A))/COS(Y1)
740 ZS=ATN(Z/SQR(1-Z*Z))
750 ZS=H1*H2*ZS+((1-H1*H2)/2)*H3*3.1416
760 TH=Y*COS(BT*A)+SIN(1.570796-Y1)*SIN(BT*A)*COS(ZS-GT*A)
770 IF BT=0 THEN GOTO 780 ELSE GOTO 810
780 IF (ZS-GT*A)>=0 THEN G=GT*A+1.570796 ELSE G=GT*A-1.570796
790 B0=ATN(TAN(1.570796-Y1)*COS(G-ZS))
```

Fig. A2.4 Listing of the mode of tracking selection program

```
800 GOTO 860
810 G0=GT*A+ATN((COS(Y1)*SIN(ZS-GT*A))/(TH*SIN(BT*A)))
820 IF (G0-GT*A)*(ZS-GT*A)>=0 THEN G01=0 ELSE G01=1
830 IF (ZS-GT*A)>=0 THEN G02=1 ELSE G02=-1
840 G=G0+G01*G02*3.1416
850 B0=ATN(TAN(BT*A)/COS(G))
860 IF B0>=0 THEN B01=0 ELSE B01=1
870 B=B0+B01*3.1416
880 THETA(I,J)=Y*COS(B)+COS(Y1)*SIN(B)*COS(ZS-G)
890 GOTO 910
900 THETA(I,J)=0
910 NEXT I
920 NEXT J
930 LOCATE 14,20:PRINT "Calculating Incidence Radiation ...."
940 FOR J = 0 TO 210
950 FOR I = 0 TO 14
960 C = 1 / ZEN(I, J)
970 D = 1.255 * EXP(-.357 * (C ^ .678)) + .09471
980 XX=THETA(I,J)
990 IF XX=0 THEN GOTO 1060
1000 IF XX>=1 THEN GOTO 1020
1010 GOTO 1040
1020 RAD(I,J)=D*NM
1030 GOTO 1070
1040 TH=1.570796-ATN(XX/SQR(1-XX*XX))
1050 N=NM*(1-GF*TAN(TH))
1060 RAD(I,J)=D*N*THETA(I,J)
1070 NEXT I
1080 NEXT J
1090 FOR J = 0 TO 210
1100 Z=0
1110 FOR I = 0 TO 14
1120 Z = RAD(I, J) + Z
1130 NEXT I
1140 TOT(J)=Z
1150 NEXT J
1160 ZZ=0
1170 FOR I=0 TO 210
1180 ZZ=TOT(I)+ZZ
1190 NEXT I
1200 TOT(211)=ZZ
1210 CLS
1220 PRINT
1230 PRINT "  DAY No RADIATION(kWh/m2)"
1240 PRINT "  For a slope of ";BT;"Deg. and Tracking axis azimuth of";GT;"Deg."
1250 PRINT "*****************************************"
1260 IF Z$="y" OR Z$="Y" THEN GOTO 1270 ELSE GOTO 1400
1270 LPRINT "INPUT DATA"
1280 LPRINT "**********"
1290 LPRINT
1300 LPRINT "LATITUDE =";L;" Deg."
1310 LPRINT "TRACKING AXIS AZIMUTH =";GT
1320 LPRINT "MAXIMUM OPTICAL EFFICIENCY =";NM
1330 LPRINT "GEOMETRIC FACTOR =";GF
1340 LPRINT
1350 LPRINT "OUTPUT DATA"
1360 LPRINT "***********"
1370 LPRINT
1380 LPRINT "  DAY No RADIATION(kWh/m2)"
1390 LPRINT "  For a slope of ";BT;"Deg. and Tracking axis azimuth of";GT;"Deg."
1400 IF G$="y" OR G$="Y" THEN GOTO 1410 ELSE GOTO 1490
1410 PRINT #1,"LATITUDE =";L;" Deg."
1420 PRINT #1,"TRACKING AXIS SLOPE =";BT
1430 PRINT #1,"TRACKING AXIS AZIMUTH =";GT
1440 PRINT #1,"MAXIMUM OPTICAL EFFICIENCY =";NM
1450 PRINT #1,"GEOMETRIC FACTOR =";GF
1460 PRINT #1,
1470 PRINT #1,"  DAY No RADIATION(kWh/m2)"
1480 PRINT #1,"  For a slope of ";BT;"Deg. and Tracking axis azimuth of";GT;"Deg."
1490 FOR I = 0 TO 210
1500 IF S$="y" OR S$="Y" THEN GOTO 1510 ELSE GOTO 1530
1510 IF I=19 OR I=42 OR I=65 OR I=88 OR I=111 OR I=134 OR I=157 OR I=180 OR I=203 THEN GOTO 1520 ELSE GOTO 1530
1520 PRINT "**** Press ANY Key to Continue ****";B$=INPUT$(1)
```

Fig. A2.4 Listing of the mode of tracking selection program (cont.)

```
1530 PRINT USING "###.##        ";I + 90; TOT(I)
1540 IF Z$="y" OR Z$="Y" THEN GOTO 1550 ELSE GOTO 1560
1550 LPRINT USING "###.##        ";I + 90; TOT(I)
1560 IF G$="y" OR G$="Y" THEN GOTO 1570 ELSE GOTO 1580
1570 PRINT #1,USING "###.##        ";I + 90; TOT(I)
1580 NEXT I
1590 PRINT "PERIOD TOTAL =";TOT(211);" kWh/m2"
1600 IF G$="y" OR G$="Y" THEN GOTO 1610 ELSE GOTO 1620
1610 PRINT #1,"PERIOD TOTAL =";TOT(211);" kWh/m2"
1620 IF Z$="y" OR Z$="Y" THEN GOTO 1630 ELSE GOTO 1640
1630 LPRINT "PERIOD TOTAL =";TOT(211);" kWh/m2"
1640 CLOSE #1
1650 PRINT
1660 INPUT "      CHANGE INPUT PARAMETERS (Y/N)";AA$
1670 IF AA$="y" OR AA$="Y" THEN GOTO 180 ELSE GOTO 1680
1680 PRINT
1690 PRINT "** Press ANY key to Return to MAIN MENU **";B$=INPUT$(1):RUN"menu"
```

Fig. A2.4 Listing of the mode of tracking selection program (cont.)

INPUT DATA
****

RECEIVER RADIUS (m) = 0.011
ANGLE OF INCIDENCE (Deg.) = 0
COLLECTOR FOCAL LENGTH (m) = 0.365
COLLECTOR REFLECTANCE = 0.85
TOTAL STANDARD DEVIATION = 0.00864

RESULTS
****

B(Deg)	LCR
0.00	10.91
10.00	20.81
20.00	26.16
30.00	27.43
40.00	29.52
50.00	33.00
60.00	35.82
70.00	32.84
80.00	26.38
90.00	18.38
100.00	10.64
110.00	4.63
120.00	1.07
130.00	0.64
140.00	0.77
150.00	0.87
160.00	0.94
170.00	0.98
180.00	1.00

Fig. A2.5 Input and output of the flux distribution on a PTC receiver program

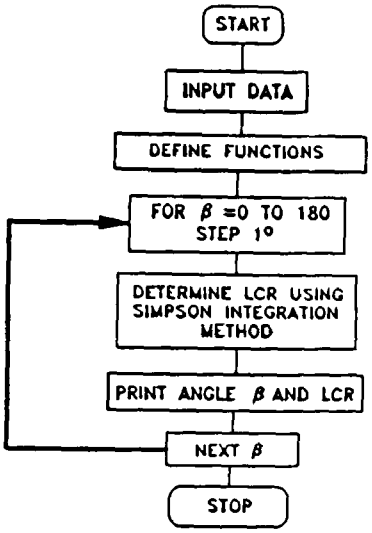

Fig. A2.6 Flow chart of the flux distribution on a PTC receiver program

```
10 '************************************
20 'PROGRAM WRITTEN BY SOTERIS KALOGIROU
30 '************************************
50 CLS
60 PRINT "  ***********************************************************************"
70 PRINT "          Program for Calculating the Distribution of Incident"
80 PRINT "          Solar Flux on a Parabolic Trough Collector Receiver"
90 PRINT "  ***********************************************************************"
100 '
110 LOCATE 15, 20: PRINT "** Press ANY key to Continue **"; B$ = INPUT$(1)
120 '
130 CLS
140 INPUT "RECEIVER RADIUS (m) ="; R
150 INPUT "ANGLE OF INCIDENCE (Deg) ="; TH
160 INPUT "COLLECTOR FOCAL LENGTH (m) ="; F
170 INPUT "COLLECTOR REFLECTANCE ="; RM
180 INPUT "TOTAL STANDARD DEVIATION OF ERRORS (rad) ="; SIG
190 INPUT "STEP SIZE FOR ANGLE B (Deg) ="; ST
200 PRINT
210 INPUT "          *****> Store Data in a File (Y/N)"; G$
220 IF (G$ = "Y") OR (G$ = "y") THEN GOTO 260
230 IF (G$ = "N") OR (G$ = "n") THEN GOTO 300
240 PRINT "  Wrong Response. Try Again"
250 GOTO 210
260 PRINT
270 INPUT "          Enter Filename"; XX$
280 FILE$ = XX$
290 OPEN FILE$ FOR OUTPUT AS #1
300 PRINT
310 INPUT "          *****> Print Input/Output (Y/N)"; Z$
320 IF Z$ = "y" OR Z$ = "Y" OR Z$ = "N" OR Z$ = "n" THEN GOTO 350
330 PRINT "  Wrong Response. Try Again"
340 GOTO 310
350 PRINT
360 PRINT TAB(10); "Press SPACE BAR to continue or <ESC> to correct data"
370 IF INKEY$ <> "" THEN GOTO 370
380 SELECT$ = INKEY$
390 IF SELECT$ = "" THEN GOTO 380
400 IF SELECT$ = CHR$(27) THEN GOTO 130
```

Fig. A2.7 Listing of the flux distribution on a PTC receiver program

```
410 IF SELECT$ = " " THEN GOTO 430
420 GOTO 370
430 CLS
440 PI = 3.1416: S = .009312
450 TH = TH * PI / 180
460 DEF FNUXY (PSI) = F / (COS(PSI / 2) * COS(PSI / 2))
470 DEF FNRXY (B, PSI) = SQR(R * R + FNUXY(PSI) * FNUXY(PSI) - 2 * FNUXY(PSI) * R * COS(B - PSI))
480 DEF FNDX (B, PSI) = (R * SIN(B - PSI)) / FNRXY(B, PSI)
490 DEF FNDXY (B, PSI) = ATN(FNDX(B, PSI) / SQR(1 - FNDX(B, PSI) * FNDX(B, PSI)))
500 DEF FNF0 (B, PSI) = ATN(TAN(TH) / COS(FNDXY(B, PSI)))
510 DEF FNTH0 (B, PSI) = COS(FNF0(B, PSI)) * (COS(FNDXY(B, PSI)) * COS(B - PSI) - SIN(FNDXY(B, PSI)) * SIN(B - PSI))
520 DEF FND (B, PSI) = COS(TH) * SIN(FNDXY(B, PSI))
530 DEF FND0 (B, PSI) = ATN(FND(B, PSI) / SQR(1 - FND(B, PSI) * FND(B, PSI)))
540 DEF FNF3 (B, PSI) = PSI / 2 - FNDXY(B, PSI)
550 DEF FNF1PSI (B, PSI) = FNUXY(PSI) * COS(FNF3(B, PSI)) / (FNRXY(B, PSI) * COS(PSI / 2) * COS(FNF0(B, PSI)))
560 DEF FNFPSI (B, PSI) = FNF1PSI(B, PSI) * COS(FNF0(B, PSI)) * COS(FNF0(B, PSI))
570 DEF FNX (B, PSI) = COS(S) / COS(FND0(B, PSI))
580 DEF FNX1 (B, PSI) = 1.570796 - ATN(XX / SQR(1 - XX * XX))
590 DEF FNX2 (B, PSI) = FNX1(B, PSI) / (SIG * 1.414214)
600 DEF FNX3 (B, PSI) = -4.636374E-03 + (1.1942 * FNX2(B, PSI)) - (.1653754 * FNX2(B, PSI) ^ 2) - (.3166263 * FNX2(B, PSI) ^ 3) +
(.1541824 * FNX2(B, PSI) ^ 4) - (2.071595E-02 * FNX2(B, PSI) ^ 5)
610 DEF FNY (B, PSI) = (RM / (SIG * 2.50663)) * FNFPSI(B, PSI) * EXP(-(FND0(B, PSI) * FND0(B, PSI)) / (2 * SIG * SIG)) * ERF *
FNTH0(B, PSI)
620 PRINT "   B(Deg)   LCR"
630 IF Z$ = "Y" OR Z$ = "y" THEN GOTO 640 ELSE GOTO 740
640 LPRINT "     INPUT DATA:"
650 LPRINT "     **********"
660 LPRINT "RECEIVER RADIUS (m) ="; R
670 LPRINT "ANGLE OF INCIDENCE (Deg) ="; TH
680 LPRINT "COLLECTOR FOCAL LENGTH (m) ="; F
690 LPRINT "COLLECTOR REFLECTANCE ="; RM
700 LPRINT "TOTAL STANDARD DEVIATION ="; SIG
710 LPRINT "     RESULTS:"
720 LPRINT "     ********"
730 LPRINT "   D(Deg)   LCR"
740 IF G$ = "y" OR G$ = "Y" THEN GOTO 750 ELSE GOTO 760
750 PRINT #1, "   B(Deg)   LCR"
760 FOR M = 0 TO 180 STEP ST
770 B = M * PI / 180
780 H = .017453
790 PSI = H
800 T1 = 0
810 K = 88
820 XX = FNX(B, PSI)
830 IF XX >= 1 THEN ERF = 0: GOTO 860
840 ERF = FNX3(B, PSI)
850 IF ERF > 1 THEN ERF = 1
860 D = FNUXY(PSI) * SIN(PSI - FNDXY(B, PSI))
870 IF D < R THEN T2 = 0 ELSE GOTO 890
880 GOTO 900
890 T2 = FNY(B, PSI)
900 FOR I = 2 TO K STEP 2
910 PSI = PSI + H
920 XX = FNX(B, PSI)
930 IF XX >= 1 THEN ERF = 0: GOTO 960
940 ERF = FNX3(B, PSI)
950 IF ERF > 1 THEN ERF = 1
960 D = FNUXY(PSI) * SIN(PSI - FNDXY(B, PSI))
970 IF D < R THEN GOTO 990 ELSE GOTO 980
980 T1 = T1 + FNY(B, PSI)
990 PSI = PSI + H
1000 XX = FNX(B, PSI)
1010 IF XX >= 1 THEN ERF = 0: GOTO 1040
1020 ERF = FNX3(B, PSI)
1030 IF ERF > 1 THEN ERF = 1
1040 D = FNUXY(PSI) * SIN(PSI - FNDXY(B, PSI))
1050 IF D < R THEN GOTO 1070 ELSE GOTO 1060
1060 T2 = T2 + FNY(B, PSI)
1070 NEXT I
1080 LCR = (FNY(B, 0) + (2 * T1) + (4 * T2) + FNY(B, 1.5708)) * .01164
1090 IF LCR < 1 AND LCR > 0 THEN GOTO 1100 ELSE GOTO 1110
1100 LCR = LCR + COS(TH) * COS(PI - B)
1110 IF LCR <= 0 THEN GOTO 1120 ELSE GOTO 1130
```

Fig. A2.7 Listing of the flux distribution on a PTC receiver program (cont.)

```
1120 LCR = COS(TH) * COS(PI - B)
1130 PRINT USING "  ###.##"; M; LCR
1140 IF Z$ = "Y" OR Z$ = "y" THEN GOTO 1150 ELSE GOTO 1160
1150 LPRINT USING "  ###.##"; M; LCR
1160 IF G$ = "Y" OR G$ = "y" THEN GOTO 1170 ELSE GOTO 1180
1170 PRINT #1, USING "  ###.##"; M; LCR
1180 NEXT M
1190 CLOSE #1
1200 PRINT
1210 PRINT "** Press ANY key to Return to MAIN MENU **"; A$ = INPUT$(1): RUN "menu"
```

Fig. A2.7 Listing of the flux distribution on a PTC receiver program (cont.)

A2.4 INTERCEPT FACTOR CALCULATION PROGRAM

This program module can be accessed by typing number 4 at the main menu and is used to calculate the intercept factor of a PTC. The input data required are:

- Collector rim angle [Deg]
- Receiver diameter [mm]
- Collector concentration ratio
- Random error distribution (σ) [rad]
- Tracking errors (β) [rad]
- Receiver mislocation and reflector profile errors (dr) [mm]

The program outputs the intercept factor by converting the above errors into "universal error parameters". The flow chart of the program is shown in Fig. A2.8 whereas the listing of the program is shown in Fig. A2.9.

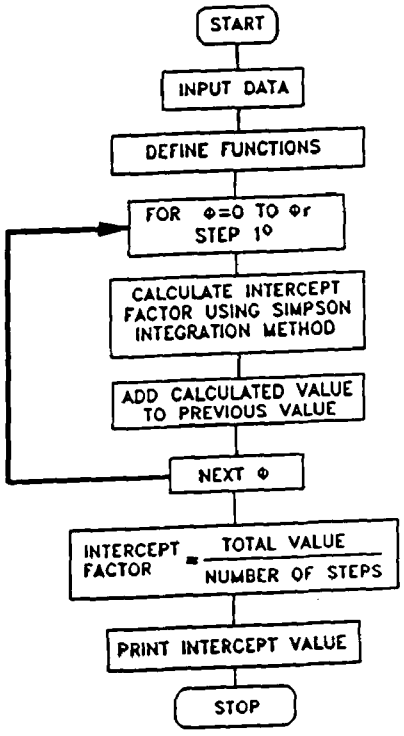

Fig. A2.8 Flow chart of the intercept factor calculation program

```
60 PRINT "  ***********************************************************************"
70 PRINT "            Program for calculating the Intercept Factor of a"
80 PRINT "                    Parabolic Trough Collector"
90 PRINT "  ***********************************************************************"
100 '
110 LOCATE 15, 20: PRINT "** Press ANY key to Continue **"; B$ = INPUT$(1)
120 '
130 CLS
140 INPUT "COLLECTOR RIM ANGLE (Deg) ="; PHR
150 INPUT "RECEIVER DIAMETER (mm) ="; DR
160 INPUT "COLLECTOR CONCENTRATION RATIO ="; CR
170 INPUT "RANDOM ERROR DISTRIBUTION 'Sigma' (rad) ="; SIGMA1
180 INPUT "TRACKING ERRORS 'Beta' (rad) ="; B1
190 INPUT "RECEIVER MISLOCATION & REFLECTOR PROFILE ERRORS 'd' (mm) ="; D1
200 SIGMA=SIGMA1*CR
210 B=B1*CR
220 D=D1/DR
230 PRINT
240 INPUT "          *****> Store Data in a File (Y/N)"; G$
250 IF (G$ = "Y") OR (G$ = "y") THEN GOTO 290
260 IF (G$ = "N") OR (G$ = "n") THEN GOTO 330
270 PRINT "   Wrong Response. Try Again"
280 GOTO 240
290 PRINT
300 INPUT "          Enter Filename"; XX$
310 FILE$ = XX$
320 OPEN FILE$ FOR OUTPUT AS #1
330 PRINT
340 INPUT "          *****> Print Input/Output (Y/N)"; Z$
350 IF Z$ = "y" OR Z$ = "Y" OR Z$ = "N" OR Z$ = "n" THEN GOTO 380
360 PRINT "   Wrong Response. Try Again"
370 GOTO 340
380 PRINT
390 PRINT TAB(10); "Press SPACE BAR to continue or <ESC> to correct data"
400 IF INKEY$ <> "" THEN GOTO 400
410 SELECT$ = INKEY$
420 IF SELECT$ = "" THEN GOTO 410
430 IF SELECT$ = CHR$(27) THEN GOTO 130
440 IF SELECT$ = " " THEN GOTO 460
450 GOTO 400
460 CLS
470 LOCATE 12,25:PRINT "*****  Calculating  *****"
480 Z2=0
490 PI=3.1416
500 PHR=PHR*PI/180
510 H=.0174533
520 DEF FNY(X)=(Y1-Y3)/(1+COS(X))*((1+COS(PHR))/(2*SIN(PHR)))
530 A2=4.442883*SIGMA*(1+COS(PHR))
540 FOR J=0 TO PHR STEP H
550 A1=(SIN(PHR)*(1+COS(J))*(1-2*D*SIN(J))-PI*B*(1+COS(PHR)))/A2
560 A3=(SIN(PHR)*(1+COS(J))*(1+2*D*SIN(J))+PI*B*(1+COS(PHR)))/A2
570 IF A1>2.9 THEN A1=2.9
580 IF A3>2.9 THEN A3=2.9
590 Y1=-4.636374E-03+1.1942*A1-(.1653754*A1^2)-(.3166263*A1^3)+(.1541824*A1^4)-(2.071595E-02*A1^5)
600 Y3=+4.636374E-03-1.1942*A3+(.1653754*A3^2)+(.3166263*A3^3)-(.1541824*A3^4)+(2.071595E-02*A3^5)
610 T1=0
620 X=H
630 T2=FNY(X)
640 FOR I=2 TO 88 STEP 2
650 X=X+H
660 T1=T1+FNY(X)
670 X=X+H
680 T2=T2+FNY(X)
690 NEXT I
700 Z1=(FNY(0)+(2*T1)+(4*T2)+FNY(PHR))*(H/3)
710 Z2=Z2+Z1
720 NEXT J
730 Z2=Z2/91
740 CLS
750 PRINT "For Sigma =";SIGMA1;" (rad) Beta =";B1;" (rad) and for d =";D1;" (mm)"
760 PRINT "Gamma =";Z2
770 IF Z$="y" OR Z$="Y" THEN GOTO 780 ELSE GOTO 820
780 LPRINT "Sigma =";SIGMA1
```

Fig. A2.9 Listing of the intercept factor calculation program

```
790 LPRINT "Beta =";B1
800 LPRINT "d =";D1
810 LPRINT "Intercept factor =";Z2
820 IF G$="y" OR G$="Y" THEN GOTO 830 ELSE GOTO 880
830 PRINT #1,"Sigma =";SIGMA1
840 PRINT #1,"Beta =";B1
850 PRINT #1,"d =";D1
860 PRINT #1,"Intercept factor =";Z2
870 CLOSE #1
880 PRINT
890 PRINT "** Press ANY key to Return to MAIN MENU **";A$=INPUT$(1):RUN"menu"
```

Fig. A2.9 Listing of the intercept factor calculation program (cont.)

A2.5 WEATHER DATA FILE GENERATOR

This program module can be accessed by typing number 5 at the main menu and is used to generate the data file required by the simulation programs. The input data required are the temperature in degrees centigrade and the solar radiation in W/m^2 on a horizontal surface for a typical day of each month. At the beginning of the program the user has to input the hourly steps per month required and the weather data filename for which the rules shown in section A2.1 must be followed. The user has also the option to correct the data at the end of each month. When the inputs of all months are finished the file is saved. The listing of the program is shown in Fig. A2.10.

A2.6 SIMULATION PROGRAMS

These programs can be accessed by typing numbers 6 or 7 at the main menu and are used to simulate PTC steam generation systems. The difference of the two programs is that in the second one the collector efficiency is calculated by considering the local concentration ratios on the collector receiver. The input data required are:

- Aperture area [m^2]
- Aperture width [m]
- Maximum optical efficiency
- Geometric factor A_f
- Mass flow rate [kg/s]
- Flash vessel volume [kg]
- Slope of n Vs $\Delta T/I$ graph [W/m^2K]
- Flash vessel outside diameter (including insulation) [mm]
- Flash vessel inside diameter [mm]

- Flash vessel height [m]
- Flash vessel wall thickness [mm]
- Insulation conductivity [W/mK]
- Pipes UA-value [W/K]
- Pump area [m^2]
- Mass of circulated water [kg]
- LCR values (if required)

The time step of the program is one second. The sequence of the various calculations can be seen in the program flow chart, which for the program "PTCDES1", is shown in chapter 3, Fig. 3.16. The output of the program "PTCDES2" is also shown in chapter 3, Fig. 3.17. The listing of the program "PTCDES1" is shown in Fig. A2.11.

```
70 '* Weather Data File Generator *
90 '****************************
100 '
110 CLS
120 DIM T(12,12),R(12,12)
130 DIM A$(12)
140 FOR I=1 TO 12
150 READ A$(I)
160 NEXT I
170 LOCATE 12,20:INPUT "INPUT Hourly steps per month";N
180 LOCATE 14,20:INPUT "Enter Weather Data Filename";B$
190 FILE$=B$
200 OPEN FILE$ FOR OUTPUT AS #1
210 CLS
220 FOR MONTH=1 TO 12
230 CLS
240 LOCATE 2,5:PRINT SPC(79):LOCATE 2,5:PRINT "Weather Data for the Month of ";A$(MONTH)
250 FOR NUM=1 TO N
260 LOCATE NUM+3,5:PRINT SPC(79):LOCATE NUM+3,5:PRINT "Data Point ";NUM;: INPUT "TEMP(DEG.C), RAD(W/M2)
",T(MONTH,NUM),R(MONTH,NUM)
270 NEXT NUM
280 FOR I=1 TO N
290 LOCATE I+3,5:PRINT SPC(79):LOCATE I+3,5:PRINT "Data Point ";I,T(MONTH,I),R(MONTH,I)
300 NEXT I
310 LOCATE 18,20:PRINT SPC(79):LOCATE 18,20:INPUT "Parameter # to Change or 0 for none";X
320 IF X>N THEN GOTO 310
330 IF X=0 THEN GOTO 380
340 LOCATE 18,20:PRINT SPC(79):LOCATE 22,10:PRINT "Point ";X;"Enter Data Temp, Rad ";:INPUT X1,X2
350 T(MONTH,X)=X1:R(MONTH,X)=X2
360 LOCATE X+3-17*DISP,1:PRINT SPC(79);:LOCATE CSRLIN,5:PRINT "Data Point ";X,T(MONTH,X),R(MONTH,X)
370 GOTO 310
380 NEXT MONTH
390 CLS
400 LOCATE 14,20:PRINT "Saving Data ....."
410 FOR J=1 TO 12
420 FOR I=1 TO N
430 PRINT #1,T(J,I),R(J,I)
440 NEXT I,J
450 CLOSE #1
460 CLS:LOCATE 14,20:PRINT "Data successfully saved"
470 LOCATE 16,20:PRINT "Strike any Key to Return to MAIN MENU":C$=INPUT$(1):RUN "menu"
480 DATA
JANUARY,FEBRUARY,MARCH,APRIL,MAY,JUNE,JULY,AUGUST,SEPTEMBER,OCTOBER,NOVEMBER,DECEMBER
```

Fig. A2.10 Listing of the weather data generator program

```
10 '*******************************
20 'Program Written By S. Kalogirou
30 '*******************************
40 '
50 '*************************
60 '*                       *
70 '*     Program PTCDES1   *
80 '*                       *
90 '*************************
100 '
110 CLS
120 DIM T(141)
130 DIM R(141)
140 LOCATE 16,20:PRINT "NOTE: For the city of Nicosia Enter 'Nic'"
150 LOCATE 14,22:INPUT "Enter Weather Data Filename ";WEATHER$
160 FILE$=WEATHER$
170 OPEN FILE$ FOR INPUT AS #1
180 FOR J=1 TO 141
190 INPUT #1,T(J),R(J)
200 NEXT J
210 CLOSE #1
230 ON ERROR GOTO 290
240 LOCATE 14,20:INPUT "Use INPUT Data from File";XA$
250 IF XA$="y" OR XA$="Y" THEN GOTO 260 ELSE GOTO 390
260 LOCATE 16,20:INPUT "Enter Data Filename";DAT$
270 FILE$=DAT$
280 OPEN FILE$ FOR INPUT AS #2
290 IF ERR=53 THEN GOTO 300 ELSE GOTO 370
300 CLS:LOCATE 14,20:INPUT "FILE NOT FOUND. DO YOU WANT TO LIST FILES (Y/N)";XXXA$
310 IF XXXA$ ="Y" OR XXXA$="y" THEN GOTO 320 ELSE GOTO 350
320 LOCATE 16,20:INPUT "Enter Drive Letter";AAX$
330 FILES AAX$:
340 PRINT "Strike any KEY to Continue";INPUT$(1):GOTO 350
350 CLS:RESUME 240
360 ON ERROR GOTO 0
370 INPUT #2,AA,WA,NX,AF,M,MF,SLOPE,D0,DI,L,THI,KI,UA,AP,MC
380 CLOSE #2
390 CLS
400 LOCATE 2,20:PRINT "1. APERTURE AREA=              ";AA;"m²"
410 LOCATE 3,20:PRINT "2. APERTURE WIDTH=             ";WA;"m"
420 LOCATE 4,20:PRINT "3. MAXIMUM OPTICAL EFFICIENCY =  ";NX
430 LOCATE 5,20:PRINT "4. GEOMETRIC FACTOR Af =       ";AF
440 LOCATE 6,20:PRINT "5. MASS FLOW RATE =            ";M;"Kg/s"
450 LOCATE 7,20:PRINT "6. FLASH VESSEL VOLUME =       ";MF;"Kg"
460 LOCATE 8,20:PRINT "7. SLOPE OF DT/I GRAPH =       ";SLOPE
470 LOCATE 9,20:PRINT "8. FLASH VESSEL OUTSIDE DIAMETER=";D0;"mm"
480 LOCATE 10,20:PRINT "9. FLASH VESSEL INSIDE DIAMETER =";DI;"mm"
490 LOCATE 11,20:PRINT "10. FLASH VESSEL HEIGHT =      ";L;"m"
500 LOCATE 12,20:PRINT "11. FLASH VESSEL WALL THICKNESS = ";THI;"mm"
510 LOCATE 13,20:PRINT "12. INSULATION CONDUCTIVITY =  ";KI;"W/m°C"
520 LOCATE 14,20:PRINT "13. PIPES UA - VALUE =         ";UA;"W/°C"
530 LOCATE 15,20:PRINT "14. PUMP AREA =                ";AP;"m2"
540 LOCATE 16,20:PRINT "15. MASS OF CIRCULATED WATER =  ";MC;"kg"
550 LOCATE 18,20:INPUT "INPUT the Number of Parameter OR 0 to Continue";XXX
560 IF XXX=1 THEN LOCATE 20,20:INPUT "1.APERTURE AREA=";AA
570 IF XXX=2 THEN LOCATE 20,20:INPUT "2.APERTURE WIDTH=";WA
580 IF XXX=3 THEN LOCATE 20,20:INPUT "3.MAXIMUM OPTICAL EFFICIENCY=";NX
590 IF XXX=4 THEN LOCATE 20,20:INPUT "4.GEOMETRIC FACTOR Af=";AF
600 IF XXX=5 THEN LOCATE 20,20:INPUT "5.MASS FLOW RATE=";M
610 IF XXX=6 THEN LOCATE 20,20:INPUT "6.FLASH VESSEL VOLUME=";MF
620 IF XXX=7 THEN LOCATE 20,20:INPUT "7.SLOPE OF DT/I GRAPH=";SLOPE
630 IF XXX=8 THEN LOCATE 20,20:INPUT "8.FLASH VESSEL OUTSIDE DIAMETER=";D0
640 IF XXX=9 THEN LOCATE 20,20:INPUT "9.FLASH VESSEL INSIDE DIAMETER=";DI
650 IF XXX=10 THEN LOCATE 20,20:INPUT "10.FLASH VESSEL HEIGHT=";L
660 IF XXX=11 THEN LOCATE 20,20:INPUT "11.FLASH VESSEL WALL THICKNESS=";THI
670 IF XXX=12 THEN LOCATE 20,20:INPUT "12.INSULATION CONDUCTIVITY=";KI
680 IF XXX=13 THEN LOCATE 20,20:INPUT "13.PIPES UA - VALUES=";UA
690 IF XXX=14 THEN LOCATE 20,20:INPUT "14.PUMP AREA=";AP
700 IF XXX=15 THEN LOCATE 20,20:INPUT "15.MASS OF CIRCULATED WATER=";MC
710 IF XXX=0 THEN GOTO 730
720 GOTO 390
730 LOCATE 21,20:INPUT "SAVE INPUT DATA TO A FILE (Y/N)";DAT1$
740 IF DAT1$="y" OR DAT1$="Y" THEN GOTO 750 ELSE GOTO 810
```

Fig. A2.11 Listing of PTCDES1 program

```
750 LOCATE 23,20:INPUT "ENTER INPUT  DATA FILENAME";DAT2$
760 FILE$=DAT2$
770 OPEN FILE$ FOR OUTPUT AS #3
780 PRINT #3,AA,WA,NX,AF,M,MF,SLOPE,D0,DI,L,THI,KI,UA,AP,MC
790 CLOSE #3
800 GOTO 810
810 CLS
820 PRINT
830 INPUT "        ****>STORE OUTPUT DATA IN A FILE (Y/N)";G$
840 IF (G$="Y") OR (G$="y") THEN GOTO 880
850 IF (G$="N") OR (G$="n") THEN GOTO 920
860 PRINT "WRONG RESPONSE. TRY AGAIN"
870 GOTO 830
880 PRINT
890 INPUT "        ENTER FILENAME";XX$
900 FILE$ = XX$
910 OPEN FILE$ FOR OUTPUT AS #1
920 PRINT
930 INPUT "        PAUSE AT EVERY PAGE (Y/N)";S$
940 PRINT
950 INPUT "        PRINT INPUT / OUTPUT (Y/N)";Z$
960 IF Z$="Y" OR Z$="y" OR Z$="N" OR Z$="n" THEN GOTO 990
970 PRINT "        ****> WRONG RESPONSE. TRY AGAIN"
980 GOTO 950
990 CLS
1000 IF Z$="Y" OR Z$="y" THEN GOTO 1010 ELSE GOTO 1210
1010 LPRINT "INPUT DATA"
1020 LPRINT "=========="
1030 LPRINT "APERTURE AREA";AA;"m2"
1040 LPRINT "APERTURE WIDTH";WA;"m"
1050 LPRINT "MAXIMUM OPTICAL EFFICIENCY=";NX
1060 LPRINT "GEOMETRIC FACTOR=";AF
1070 LPRINT "MASS FLOW RATE=";M;"Kg/s"
1080 LPRINT "FLASH VESSEL VOLUME=";MF;"Kg"
1090 LPRINT "SLOPE OF DT/I GRAPH=";SLOPE
1100 LPRINT "FLASH VESSEL OUTSIDE DIAMETER=";D0;"mm"
1110 LPRINT "FLASH VESSEL INSIDE DIAMETER=";DI;"mm"
1120 LPRINT "FLASH VESSEL HEIGHT=";L;"m"
1130 LPRINT "FLASH VESSEL WALL THICKNESS=";THI;"mm"
1140 LPRINT "INSULATION CONDUCTIVITY=";KI;"W/m°C"
1150 LPRINT "PIPES UA - VALUES=";UA;"W/°C"
1160 LPRINT "PUMP AREA=";AP;"m2"
1170 LPRINT "MASS OF CIRCULATED WATER=";MC;"kg"
1180 LPRINT
1190 LPRINT "SIMULATION RESULTS"
1200 LPRINT "=================="
1220 PI=3.1416
1230 FOR J=1 TO 141
1240 IF J>0 AND J<=10 THEN TIME=J
1250 IF J>=11 AND J<=20 THEN TIME=J-10
1260 IF J>=21 AND J<=32 THEN TIME=J-20
1270 IF J>=33 AND J<=44 THEN TIME=J-32
1280 IF J>=45 AND J<=58 THEN TIME=J-44
1290 IF J>=59 AND J<=72 THEN TIME=J-58
1300 IF J>=73 AND J<=86 THEN TIME=J-72
1310 IF J>=87 AND J<=98 THEN TIME=J-86
1320 IF J>=99 AND J<=110 THEN TIME=J-98
1330 IF J>=111 AND J<=121 THEN TIME=J-110
1340 IF J>=122 AND J<=131 THEN TIME=J-121
1350 IF J>=132 THEN TIME=J-131
1360 LST=(TIME+TM)*60
1370 IF J=1 THEN GOSUB 2510
1380 IF J=11 THEN GOSUB 2550
1390 IF J=21 THEN GOSUB 2590
1400 IF J=33 THEN GOSUB 2630
1410 IF J=45 THEN GOSUB 2670
1420 IF J=59 THEN GOSUB 2710
1430 IF J=73 THEN GOSUB 2750
1440 IF J=87 THEN GOSUB 2790
1450 IF J=99 THEN GOSUB 2830
1460 IF J=111 THEN GOSUB 2870
1470 IF J=122 THEN GOSUB 2910
1480 IF J=132 THEN GOSUB 2950
```

Fig. A2.11 Listing of PTCDES1 program (cont.)

```
1490 B=(360/364)*(N0-81)
1500 ET=9.87*SIN(2*B*PI/180)-7.53*COS(B*PI/180)-1.5*SIN(B*PI/180)
1510 AST=(LST+ET+13.32)/60
1520 H=(AST-12)*15
1530 D=23.45*SIN((360/365)*(284+N0)*(PI/180))
1540 PH=SIN(35*PI/180)*SIN(D*PI/180)+COS(35*PI/180)*COS(D*PI/180)*COS(H*PI/180)
1550 TH=SQR(PH*PH+COS(D*PI/180)*COS(D*PI/180)*SIN(H*PI/180)*SIN(H*PI/180))
1560 TH1=1.570796-ATN(TH/SQR(1-TH*TH))
1570 IF PH<.1 THEN GOTO 1590
1580 R(J)=R(J)*TH/PH
1590 NO=NX*(1-AF*ABS(TAN(TH1)))*TH
1600 IF J=1 OR J=11 OR J=21 OR J=33 OR J=45 OR J=59 OR J=73 OR J=87 OR J=99 OR J=111 OR J=122 OR J=132 THEN GOTO 1610
ELSE GOTO 1870
1610 CLS
1620 TI=100:DT=2:TA=T(J):TB=TA-.5
1630 FOR I=1 TO 12
1640 QN=(TI-TB)*3600/((LOG((THI+DI)/DI)/(2*PI*385*L))+(LOG(D0/(DI+THI))/(2*PI*KI*L))+(1/(1.42*PI*(D0/1000)*L*(DT/L)^.25)))
1650 TW=TI-QN/3600*((LOG((THI+DI)/DI)/(2*PI*385*L))+(LOG(D0/(DI+THI))/(2*PI*KI*L)))
1660 IF ((TW-TB)-DT)>=1 THEN GOTO 1670 ELSE GOTO 1690
1670 DT=TW-TB
1680 GOTO 1640
1690 TI=TI-(QN/(MF*4190))
1700 IF TI<TB THEN TI=TB
1710 NEXT I
1720 IF TI<TA THEN TI=TA
1730 TF=TI
1740 PRINT "MONTH =";C$
1750 PRINT "  TIME    COLLECTOR  HOURLY  CUMULATIVE  USEFUL  ENERGY"
1760 PRINT "          EFFICIENCY PRODUCTION PRODUCTION  ENERGY  LOSS"
1770 IF Z$="Y" OR Z$="y" THEN GOTO 1790 ELSE GOTO 1820
1780 LPRINT
1790 LPRINT "MONTH =";C$
1800 LPRINT "  TIME    COLLECTOR  HOURLY  CUMULATIVE  USEFUL  ENERGY"
1810 LPRINT "          EFFICIENCY PRODUCTION PRODUCTION  ENERGY  LOSS"
1820 IF G$="Y" OR G$="y" THEN GOTO 1830 ELSE GOTO 1870
1830 PRINT #1,
1840 PRINT #1,"MONTH =";C$
1850 PRINT #1,"  TIME    COLLECTOR  HOURLY  CUMULATIVE  USEFUL  ENERGY"
1860 PRINT #1,"          EFFICIENCY PRODUCTION PRODUCTION  ENERGY  LOSS"
1870 TA=T(J)
1880 DIS2=0:N=NO:N1=0:DT=10:E8=0:E7=0
1890 FOR I=1 TO 3600
1900 E2=(TI-TA)/((LOG((THI+DI)/DI)/(2*PI*385*L))+(LOG(D0/(DI+THI))/(2*PI*KI*L))+(1/(1.42*PI*(D0/1000)*L*(DT/L)^.25)))
1910 TW=TI-E2*((LOG((THI+DI)/DI)/(2*PI*385*L))+(LOG(D0/(DI+THI))/(2*PI*KI*L)))
1920 IF ((TW-TA)-DT)>=1 THEN GOTO 1930 ELSE GOTO 1950
1930 DT=TW-TA
1940 GOTO 1900
1950 E3=UA*(TI-TA)
1960 E4=1.42*(((TI-TA)/.3)^.25)*AP*(TI-TA)
1970 ELOSS=E2+E3+E4
1980 E7=E7+ELOSS
1990 E1=R(J)*AA*N
2000 E=E1-(ELOSS)
2010 T0=TI+E/(M*4190)
2020 TF=(T0*M+TI*(MF+MC-M))/(MF+MC)
2030 IF TF>100 THEN TF=100
2040 N3=NO-((TI-TA)/R(J))*SLOPE
2050 IF N3<0 THEN N3=0
2060 IF ABS(N3-N)>.01 THEN GOTO 2070 ELSE GOTO 2090
2070 N=N3
2080 GOTO 1990
2090 N1=N1+N
2100 E8=E8+E
2110 IF T0<100 THEN GOTO 2160 ELSE GOTO 2120
2120 HFG=(4.368619+4.071468*T0+7.571396E-04*T0^2)-419.04
2130 DIS=(HFG/2257)*M
2140 TF=((MF-DIS)*TF+(TA+10)*DIS)/MF
2150 DIS2=DIS2+DIS
2160 TI=TF
2170 NEXT I
2180 DIST2=DIST2+DIS2
2190 N2=N1/3600
2200 QU=E8/3600
```

Fig. A2.11 Listing of PTCDES1 program (cont.)

```
2202 IF QU<0 THEN QU=0
2210 QU2=QU2+QU
2220 DIST=DIST2/AA
2230 PRINT USING "######.##   ";TIME+TM;N2;DIS2;DIST2;QU;E7/3600
2240 IF Z$="Y" OR Z$="y" THEN GOTO 2250 ELSE GOTO 2260
2250 LPRINT USING "######.##   ";TIME+TM;N2;DIS2;DIST2;QU;E7/3600
2260 IF G$="Y" OR G$="y" THEN GOTO 2270 ELSE GOTO 2280
2270 PRINT #1,USING "######.##   ";TIME+TM;N2;DIS2;DIST2;QU;E7/3600
2280 IF J=10 OR J=20 OR J=32 OR J=44 OR J=58 OR J=72 OR J=86 OR J=98 OR J=110 OR J=121 OR J=131 OR J=141 THEN GOTO 2290
ELSE GOTO 2460
2290 IF S$="Y" OR S$="y" THEN GOTO 2300 ELSE GOTO 2360
2300 PRINT
2310 PRINT "Month average production =";DIST;" kg/m2-day"
2320 PRINT
2330 PRINT "Month Total USEFUL ENERGY =";QU2;"Wh"
2340 PRINT
2350 PRINT "Strike ANY key to continue":A$=INPUT$(1)
2360 IF Z$="Y" OR Z$="y" THEN GOTO 2370 ELSE GOTO 2420
2370 LPRINT
2380 LPRINT "Month average production =";DIST;" kg/m2-day"
2390 LPRINT
2400 LPRINT "Month Total USEFUL ENERGY =";QU2;"Wh"
2410 LPRINT
2420 IF G$="Y" OR G$="y" THEN GOTO 2430 ELSE GOTO 2460
2430 PRINT #1,
2440 PRINT #1,"Month average production =";DIST;" kg/m2-day"
2450 PRINT #1,"Month Total USEFUL ENERGY =";QU2;"Wh"
2460 NEXT J
2470 CLOSE #1
2480 PRINT
2490 PRINT "** Press ANY Key to Return to MAIN MENU **":B$=INPUT$(1):RUN"MENU"
2500 STOP
2510 C$="JANUARY"
2520 N0=17:TM=7
2530 DIST2=0:QU2=0
2540 RETURN
2550 C$="FEBRUARY"
2560 N0=47:TM=7
2570 DIST2=0:QU2=0
2580 RETURN
2590 C$="MARCH"
2600 N0=75:TM=6
2610 DIST2=0:QU2=0
2620 RETURN
2630 C$="APRIL"
2640 N0=105:TM=6
2650 DIST2=0:QU2=0
2660 RETURN
2670 C$="MAY"
2680 N0=135:TM=5
2690 DIST2=0:QU2=0
2700 RETURN
2710 C$="JUNE"
2720 N0=162:TM=5
2730 DIST2=0:QU2=0
2740 RETURN
2750 C$="JULY"
2760 N0=198:TM=5
2770 DIST2=0:QU2=0
2780 RETURN
2790 C$="AUGUST"
2800 N0=228:TM=6
2810 DIST2=0:QU2=0
2820 RETURN
2830 C$="SEPTEMBER"
2840 N0=258:TM=6
2850 DIST2=0:QU2=0
2860 RETURN
2870 C$="OCTOBER"
2880 N0=288:TM=6
2890 DIST2=0:QU2=0
2900 RETURN
2910 C$="NOVEMBER"
2920 N0=318:TM=7
2930 DIST2=0:QU2=0
2940 RETURN
2950 C$="DECEMBER"
2960 N0=344:TM=7
2970 DIST2=0:QU2=0
2980 RETURN
```

Fig. A2.11 Listing of PTCDES1 program (cont.)

A2.7 SYSTEM OPTIMISATION PROGRAMS

Two program modules are written, called "FLASH" and "FLASH 1". They are used for theoretical system modelling to optimise the flash vessel dimensions and capacity. The programs can be accessed by typing number 8 at the main menu. A sub-menu appears from which the particular program can be accessed. The difference between the two programs is that for the first one a single constant value of solar radiation and ambient air temperature are used whereas in the second, hourly values are allowed. The optimisation is done by evaluating the daily steam production of the system. The output of the program for various sizes and capacities can be compared to select the system which produce the maximum quantity of steam. The program "FLASH" also gives the energy losses from the various parts of the system, therefore a theoretical energy analysis can be performed. Program "FLASH 1" outputs the time, thermal efficiency, collector outlet and inlet temperatures, useful energy and energy loss. These data are printed every minute when the system is under transient condition or every ten minutes under steady state conditions. At the end of each hour, the hourly and cumulative steam production are printed instead of the temperatures.

The program "FLASH" flow chart is shown in Fig. A2.12 from which it can be seen that after the night losses are considered the initial flash vessel water temperature is determined. This is followed by the determination of the input energy from which the thermal losses are subtracted. The remaining energy is used either as a pre-heat or, after the pre-heat cycle is completed, to produce steam. The time step used in the programs is one second. The programs can be used to model the behaviour of the system during pre-heat and to determine the daily steam production of the system. The input data required are shown in Table 6.1 in chapter 6. A sample output of the program "FLASH" for the input data presented in Table 6.1 is shown in Fig. A2.13. The listing of the program is shown in Fig. A2.14.

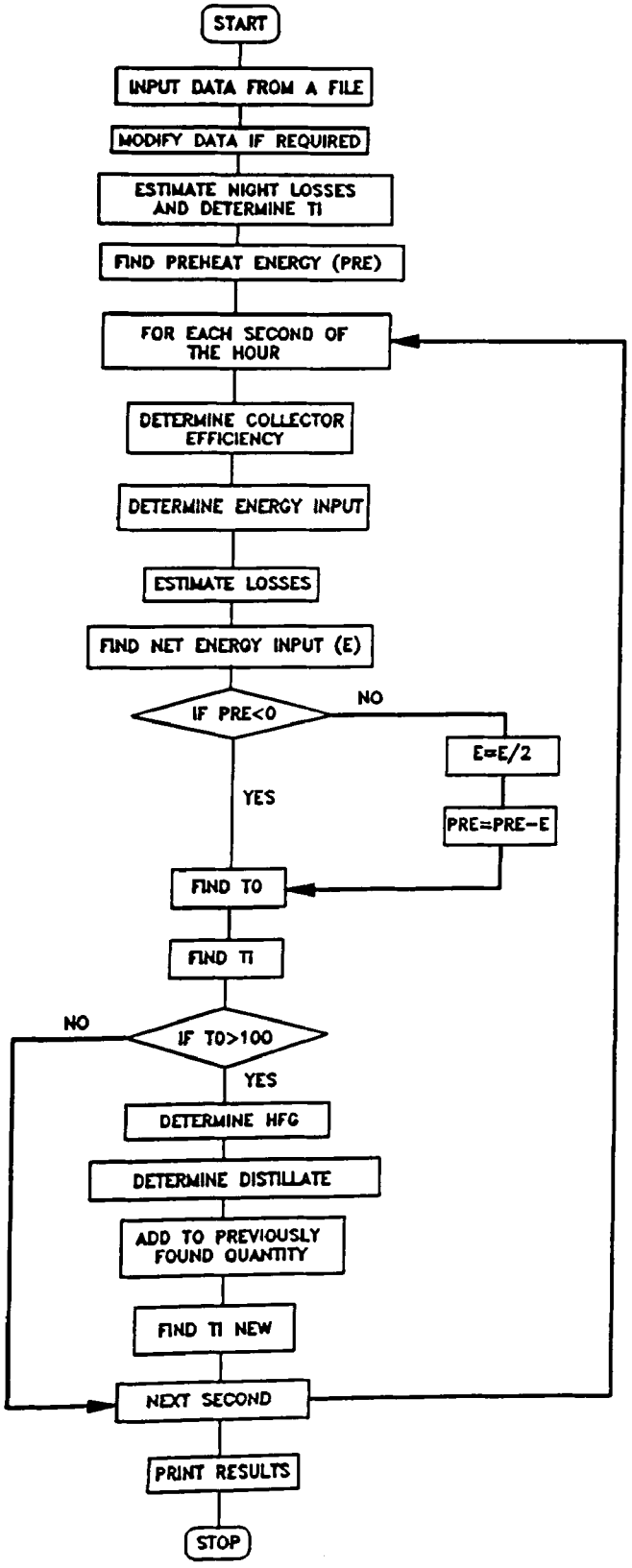

Fig. A2.12 Program FLASH flow chart

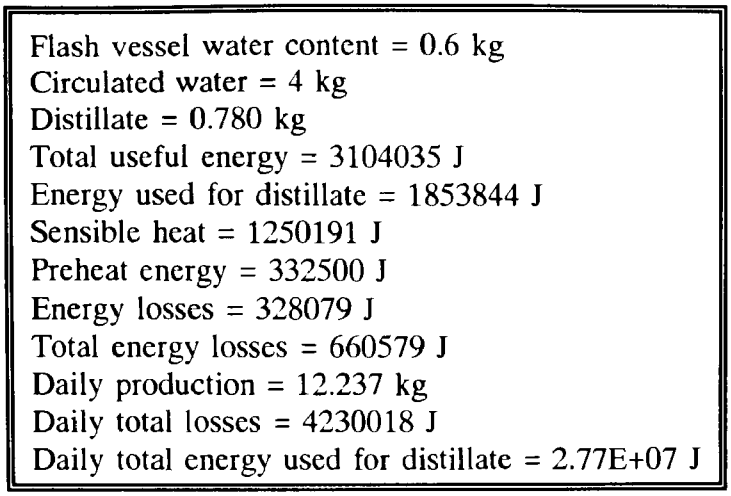

Fig. A2.13 Program FLASH sample output

```
10 CLS
20 CLEAR
30 PI=3.1416
40 COLOR 14,1,1
50 ON ERROR GOTO 110
60 LOCATE 14,20:INPUT "Use INPUT Data from File";XA$
70 IF XA$="y" OR XA$="Y" THEN GOTO 80 ELSE GOTO 210
80 LOCATE 16,20:INPUT "Enter Data Filename";DAT$
90 FILE$=DAT$
100 OPEN FILE$ FOR INPUT AS #2
110 IF ERR=53 THEN GOTO 120 ELSE GOTO 190
120 CLS:LOCATE 14,20:INPUT "FILE NOT FOUND. DO YOU WANT TO LIST FILES (Y/N)";XXXA$
130 IF XXXA$ ="Y" OR XXXA$="y" THEN GOTO 140 ELSE GOTO 170
140 LOCATE 16,20:INPUT "Enter Drive Letter";AAX$
150 FILES AAX$:
160 PRINT "Strike any KEY to Continue";INPUT$(1):GOTO 170
170 CLS:RESUME 60
180 ON ERROR GOTO 0
190 INPUT #2,RAD,M,MF,AA,N,TA,MC,D0,DI,TH,L,UA,AP,KI,MP,MPUMP
200 CLOSE #2
210 CLS
220 LOCATE 2,20:PRINT "1. Solar Radiation =          ";RAD;"W/m2"
230 LOCATE 3,20:PRINT "2. Mass Flow Rate =           ";M;"Kg/s"
240 LOCATE 4,20:PRINT "3. Flash Vessel Water Content = ";MF;"kg"
250 LOCATE 5,20:PRINT "4. Aperture Area =            ";AA;"m2"
260 LOCATE 6,20:PRINT "5. Collector Efficiency =     ";N
270 LOCATE 7,20:PRINT "6. Ambient Temperature =      ";TA;"°C"
280 LOCATE 8,20:PRINT "7. Circulated Water =         ";MC;"kg"
290 LOCATE 9,20:PRINT "8. Flash Vessel Outside Dia. = ";D0;"mm"
300 LOCATE 10,20:PRINT "9. Flash Vessel Inside Dia. = ";DI;"mm"
310 LOCATE 11,20:PRINT "10. Flash Vessel Wall Thickness =";TH;"mm"
320 LOCATE 12,20:PRINT "11. Flash Vessel Height =    ";L;"m"
330 LOCATE 13,20:PRINT "12. Pipes UA Value =         ";UA;"W/°C"
340 LOCATE 14,20:PRINT "13. Pump Body Area =         ";AP;"m2"
350 LOCATE 15,20:PRINT "14. Insulation Conductivity = ";KI;"W/m°C"
360 LOCATE 16,20:PRINT "15. F.V. and Pump Mass =     ";MP;"kg"
370 LOCATE 17,20:PRINT "16. Pump Mass =              ";MPUMP;"kg"
380 LOCATE 19,15:INPUT "***>INPUT the Number of Parameter OR 0 to Continue";XXX
390 IF XXX=1 THEN LOCATE 22,20:INPUT "Para #1.=";RAD
400 IF XXX=2 THEN LOCATE 22,20:INPUT "Para #2.=";M
410 IF XXX=3 THEN LOCATE 22,20:INPUT "Para #3.=";MF
420 IF XXX=4 THEN LOCATE 22,20:INPUT "Para #4.=";AA
430 IF XXX=5 THEN LOCATE 22,20:INPUT "Para #5.=";N
440 IF XXX=6 THEN LOCATE 22,20:INPUT "Para #6.=";TA
450 IF XXX=7 THEN LOCATE 22,20:INPUT "Para #7.=";MC
460 IF XXX=8 THEN LOCATE 22,20:INPUT "Para #8.=";D0
470 IF XXX=9 THEN LOCATE 22,20:INPUT "Para #9.=";DI
```

Fig. A2.14 Program FLASH listing

```
480 IF XXX=10 THEN LOCATE 22,20:INPUT "Para #10.=";TH
490 IF XXX=11 THEN LOCATE 22,20:INPUT "Para #11.=";L
500 IF XXX=12 THEN LOCATE 22,20:INPUT "Para #12.=";UA
510 IF XXX=13 THEN LOCATE 22,20:INPUT "Para #13.=";AP
520 IF XXX=14 THEN LOCATE 22,20:INPUT "Para #14.=";KI
530 IF XXX=15 THEN LOCATE 22,20:INPUT "Para #15.=";MP
540 IF XXX=16 THEN LOCATE 22,20:INPUT "Para #16.=";MPUMP
550 IF XXX=0 THEN GOTO 570
560 GOTO 210
570 LOCATE 21,20:INPUT "SAVE INPUT DATA TO A FILE (Y/N)";DAT1$
580 IF DAT1$="y" OR DAT1$="Y" THEN GOTO 590 ELSE GOTO 650
590 LOCATE 23,20:INPUT "ENTER INPUT  DATA FILENAME";DAT2$
600 FILE$=DAT2$
610 OPEN FILE$ FOR OUTPUT AS #3
620 PRINT #3,RAD,M,MF,AA,N,TA,MC,D0,DI,TH,L,UA,AP,KI,MP,MPUMP
630 CLOSE #3
640 GOTO 650
650 CLS
660 LOCATE 14,20:INPUT "Consider NIGHT Losses (Y/N)";N$
670 IF N$="y" OR N$="Y" THEN GOTO 680 ELSE GOTO 780
680 TI=100:DT=2:TB=TA-15
690 FOR I=1 TO 12
700 QN=(TI-TB)*3600/((LOG((TH+DI)/DI)/(2*PI*385*L))+(LOG(D0/(DI+TH))/(2*PI*KI*L))+(1/(1.42*PI*(D0/1000)*L*(DT/L)^.25)))
710 TW=TI-QN/3600*((LOG((TH+DI)/DI)/(2*PI*385*L))+(LOG(D0/(DI+TH))/(2*PI*KI*L)))
720 IF ((TW-TB)-DT)>=1 THEN GOTO 730 ELSE GOTO 750
730 DT=TW-TB
740 GOTO 700
750 TI=TI-(QN/(MF*4190))
760 IF TI<TB THEN TI=TB
770 NEXT I
780 IF TI<TA THEN TI=TA
790 CLS
800 PRINT "Starting Temperature =";TI;" °C"
810 LOCATE 13,30: PRINT "Calculating ...."
820 DT=2
830 PRE=MP*385*(100-TI)+MPUMP*45*(100-TA)
840 E6=PRE
850 DIST=0:TF=TI:EF=0:ELOSS=0
860 IF N$="n" OR N$="N" THEN TI=TA
870 FOR I=1 TO 3600
880 IF TI<TA THEN TI=TA
881 N1=N-(.387*(TI-TA)/RAD)
890 E1=RAD*AA*N1
900 E2=(TI-TA)/((LOG((TH+DI)/DI)/(2*PI*385*L))+(LOG(D0/(DI+TH))/(2*PI*KI*L))+(1/(1.42*PI*(D0/1000)*L*(DT/L)^.25)))
910 TW=TI-E2*((LOG((TH+DI)/DI)/(2*PI*385*L))+(LOG(D0/(DI+TH))/(2*PI*KI*L)))
920 IF ((TW-TA)-DT)>=1 THEN GOTO 930 ELSE GOTO 950
930 DT=TW-TA
940 GOTO 900
950 E3=UA*(TI-TA)
960 E4=1.42*(((TI-TA)/.3)^.25)*AP*(TI-TA)
970 ELOSS=E2+E3+E4
980 ET=ET+ELOSS
990 E5=E1-(ELOSS)
1000 IF PRE>0 THEN GOTO 1010 ELSE GOTO 1050
1010 PRE2=E5/2
1020 PRE=PRE-PRE2
1030 E=PRE2
1040 GOTO 1060
1050 E=E5
1060 EF=EF+E
1070 T0=TI+E/(M*4190)
1080 IF T0>100 THEN GOTO 1090 ELSE GOTO 1120
1090 IF H$="Y" THEN GOTO 1120
1100 E7=EF
1110 H$="Y"
1120 TI=(T0*M+TF*(MF+MC-M))/(MF+MC)
1130 IF TI>100 THEN TI=100
1140 TF=TI
1150 IF T0<100 THEN GOTO 1220 ELSE GOTO 1160
1160 HFG=(4.368619+4.071468*T0+7.571396E-04*T0^2)-419.04
1170 IF HFG*M*1000>E THEN HFG=E/(M*1000)
1180 DIS=(HFG/2257)*M
1190 TF=((MF-DIS)*TF+TA*DIS)/MF
```

Fig. A2.14 Program FLASH listing (cont.)

```
1200 TI=TF
1210 DIST=DIST+DIS
1220 IF I=360 THEN J=10
1230 IF I=720 THEN J=20
1240 IF I=1080 THEN J=30
1250 IF I=1440 THEN J=40
1260 IF I=1800 THEN J=50
1270 IF I=2160 THEN J=60
1280 IF I=2520 THEN J=70
1290 IF I=2880 THEN J=80
1300 IF I=3240 THEN J=90
1310 LOCATE 25,30:COLOR 4,7:PRINT J;"% Completed"
1320 COLOR 14,1,1
1330 NEXT I
1340 CLS
1350 PRINT"Distillate =";DIST;"kg"
1360 SOUND 250,5
1370 PRINT
1380 PRINT "Total Useful Energy =";EF;"J"
1390 PRINT
1400 PRINT "Energy Used for Distillate =";EF-E7;"J"
1410 PRINT
1420 PRINT "Sensible Heat =";E7;"J"
1430 PRINT
1440 PRINT "Preheat Energy =";E6;"J"
1450 PRINT
1460 PRINT "Energy Losses =";ET;"J"
1470 PRINT
1480 PRINT "Total Energy Losses =";ET+E6;"J"
1490 PRINT
1500 PRINT "Daily Production = ";DIS*28800+DIST;"kg"
1510 PRINT
1520 PRINT "Daily Total Losses =";ELOSS*28800+ET+E6;"J"
1530 PRINT
1540 PRINT "Daily Total Energy used for Distillate =";E*28800+EF-E7;"J"
1550 PRINT
1560 INPUT "***>> PRINT RESULTS (Y/N)";C$
1570 IF C$="Y" OR C$="y" THEN GOTO 1580 ELSE GOTO 1720
1580 LPRINT "Flash Vessel Water Content =";MF;"kg"
1590 LPRINT "Circulated Water =";MC;"kg"
1600 LPRINT"Distillate =";DIST;"kg"
1610 LPRINT "Total Useful Energy =";EF;"J"
1620 LPRINT "Energy Used for Distillate =";EF-E7;"J"
1630 LPRINT "Sensible Heat =";E7;"J"
1640 LPRINT "Preheat Energy =";E6;"J"
1650 LPRINT "Energy Losses =";ET;"J"
1660 LPRINT "Total Energy Losses =";ET+E6;"J"
1670 LPRINT "Daily Production = ";DIS*28800+DIST;"kg"
1680 LPRINT "Daily Total Losses =";ELOSS*28800+ET+E6;"J"
1690 LPRINT "Daily Total Energy used for Distillate =";E*28800+EF-E7;"J"
1700 LPRINT
1710 LPRINT
1720 PRINT
1730 INPUT "Repeat Again (Y/N)";A$
1740 IF A$="Y" OR A$="y" THEN GOTO 1750 ELSE GOTO 1760
1750 J=0:GOTO 10
1760 PRINT "** Press ANY key to Return to MAIN MENU **":B$=INPUT$(1):RUN"menu"
1770 STOP
```

Fig. A2.14 Program FLASH listing (cont.)

APPENDIX 3

DATA ACQUISITION SYSTEM PROGRAM

This appendix list program "DAS" used with DAS-8 board and EXP-16 multiplexer.

```
5 CLS
6 CLEAR, 49152!
10 INPUT "Save Data in a File (Y/N)";X$
20 IF X$="y" OR X$="Y" THEN 30 ELSE 60
30 INPUT "Enter Data Filename";XX$
40 FILE$=XX$
46 MD%=1
50 OPEN FILE$ FOR OUTPUT AS #1
60 INPUT "INPUT number of data  sequences to linearise";X3
70 CLS
150 SCREEN 0,0,0: KEY OFF : CLS : WIDTH 80
155 GOSUB 2000:CLS
160 'This program performs scanning and measurement of K type thermocouples
170 'connected to one EXP-16. The program can be expanded to handle multiple
180 'EXP-16's.
190 'Steps are:-
200 '       1 - Initialize DAS-8 and load thermocouple look up tables
210 '       2 - Dimension other arrays and provide set up information
220 '       3 - Measure temperature of connector block from CJC channel
230 '           (CJC = cold junction compensation)
240 '       4 - Measure output voltages of thermocouples on EXP-16
250 '       5 - Convert, correct and linearize thermocouple outputs to degrees
260 '       6 - Display output
320 '
330 '---- STEP 1: Contract BASIC workspace, load DAS8.BIN and initialize -----
340 '
385 LOCATE 25,1:COLOR 0,7:PRINT"-PLEASE WAIT-";:COLOR 7,0:PRINT"  Loading DAS-8 I/O address and thermocouple lookup table
data":LOCATE 1,1
390 DEF SEG = 0
400 SG = 256 * PEEK(&H511) + PEEK(&H510)
410 SG = SG + 49152!/16
420 DEF SEG = SG
430 BLOAD "DAS8.BIN", 0
440 OPEN "DAS8.ADR" FOR INPUT AS #2
450 INPUT #2, BASADR%    'initialize & declare CALL parameters
460 CLOSE #2
470 DAS8 = 0
480 FLAG% = 0
490 MD% = 0              'Mode 0 = initialization
500 CALL DAS8 (MD%, BASADR%, FLAG%)
510 IF FLAG% <>0 THEN PRINT"INSTALLATION ERROR"
520 '
530 'Load thermocouple linearizing look up data
540 GOSUB 50000
542 'Get gain setting of EXP-16
545 CLS:INPUT "EXP-16 Gain setting (100,200,1000 etc.): ",AV
547 CLS
550 '---- STEP 2: Initialize an integer array D%(15) to receive data ------
560 DIM D%(15)  '16 elements, one for each EXP-16 channel
570 'Also initialize a corresponding real array to receive temperature data
580 DIM T(X3,6)
581 DIM RAD(X3)
582 DIM TT(5)
591 FOR J=1 TO X3
600 '----- STEP 3: Get cold junction compensation temperature ------------
610 'Output of CJC channel is scaled at 24.4mV/deg.C. This corresponds to
620 '0.1 deg.C./bit. Dividing output in bits by 10 yields degrees C.
630 '
640 'Lock DAS-8 to channel #7 (CJC channel selected) using mode 1
650 MD%=1 : LT%(0)=7 : LT%(1) = 7
660 CALL DAS8 (MD%, LT%(0), FLAG%)
670 IF FLAG% <> 0 THEN PRINT "ERROR IN SETTING CJC CHANNEL" : END
680 'Next get CJC data from this channel using Mode 4
```

Fig. A3.1 Listing of program DAS

```
690 MD% = 4 : CJ% = 0
700 CALL DAS8 (MD%, CJ%, FLAG%)
710 'Change output in bits to real temperature
720 CJC = CJ%/10
730 '
740 '----- STEP 4: Get the thermocouple data ----------
750 CH% = 0
760 GOSUB 1000
790 ' CH% - specifies DAS-8 channel that EXP-16 is connected to (0-7).
800 ' D%(15) - integer data array to receive data from channels.
810 '
820 '----- STEP 5: Convert data to volts and linearize ----------
830 'AV = Gain setting on Dipswitch of EXP-16 (change to suit).
840 FOR I = 1 TO 5
850 V = (D%(I)*5)/(AV*2048)
860 GOSUB 51000 'perform look-up linearization
870 T(J,I)=TC
880 NEXT I
881 V=D%(0)*5/(AV*2048)
882 RAD(J)=V/1.127E-05
883 NEXT J
890 '
900 '----- STEP 6: Linearise & Display temperature data ----------
902 FOR J=1 TO 5
903 XX=0
904 FOR I=1 TO X3
906 XX=XX+T(I,J)
908 NEXT I
910 TT(J)=XX/X3
911 NEXT J
913 XX=0
914 FOR I=1 TO X3
916 XX=XX+RAD(I)
918 NEXT I
920 R=XX/X3
921 PRINT TIME$
922 PRINT " Rad Temp#1 Temp#2 Temp#3 Temp#4 Temp#5 CJC"
924 PRINT " W/m2 °C °C °C °C °C"
926 PRINT USING "####.## ";R;TT(1);TT(2);TT(3);TT(4);TT(5);CJC
931 IF X$="y" OR X$="Y" THEN 932 ELSE 934
932 PRINT #1,TIME$
933 PRINT #1,USING "####.## ";R;TT(1);TT(2);TT(3);TT(4);TT(5);CJC
934 GOTO 591
1000 '---- Subroutine to convert EXP-16 channels to number of bits --------
1010 'First lock DAS-8 on the one channel that EXP-16 is connected to.
1020 LT%(0) = CH% : LT%(1) = CH% : MD% = 1
1030 CALL DAS8 (MD%, LT%(0), FLAG%)
1040 IF FLAG% <> 0 THEN PRINT "ERROR IN SETTING CHANNEL" : END
1050 'Next select each EXP-16 channel in turn and convert it.
1060 'Digital outputs OP1-4 drive the EXP-16 sub-multiplexer address, so use
1070 'mode 14 to set up the sub-multiplexer channel.
1080 FOR SUB% = 0 TO 5 'note use of integer index SUB%
1090 MD% = 14
1100 CALL DAS8 (MD%, SUB%, FLAG%) 'address set
1110 IF FLAG% <> 0 THEN PRINT "ERROR IN EXP-16 CHANNEL NUMBER" : END
1120 'Now that channel is selected, perform A/D conversion using mode 4.
1130 'Transfer data to corresponding array element D%(SUB%)
1140 MD% = 4 'do 1 A/D conversion
1150 CALL DAS8 (MD%, D%(SUB%), FLAG%)
1160 IF FLAG% <> 0 THEN PRINT "ERROR IN PERFORMING A/D CONVERSION"
1170 'Now repeat sequence for all other EXP-16 channels
1180 NEXT SUB%
1200 RETURN
1210 '
2000 '---- Subroutine to describe operation and connections (pre-amble) -----
2010 CLS
2020 PRINT" This program demonstrates the operation of K thermocouples"
2030 PRINT"with the EXP-16/DAS-8 combination. It performs the following:-"
2040 PRINT
2050 PRINT" 1. Acquires the data"
2060 PRINT" 2. Linearizes and performs cold junction compensation"
2070 PRINT" 3. Displays data"
2080 PRINT" 4. Repeats display until <Ctrl-Break> is pressed"
```

Fig. A3.1 Listing of program DAS (cont.)

```
2090 PRINT
2190 PRINT:COLOR 0,7:PRINT" - Press any key to continue - ";:COLOR 7,0
2200 IF INKEY$="" GOTO 2200
2210 RETURN
50000 '-------- Table lookup data for K type thermocouple ----------
50010 'Run this subroutine only in the initialization section of your program
50020 'Number of points, voltage step interval (mV), starting voltage (mV)
50030 DATA  309 ,  .2 , -6.6
50040 READ NK, SIK, SVK
50050 'Temperature at -6.6mv, -6.4mV, -6.2mV etc.
50060 DATA -353.5,-249.3,-224.0,-207.6,-194.3,-182.8,-172.3,-162.8,-153.8,-145.4
50070 DATA -137.3,-129.6,-122.3,-115.2,-108.3,-101.6, -95.1, -88.7, -82.5, -76.4
50080 DATA  -70.4, -64.6, -58.8, -53.1, -47.5, -42.0, -36.6, -31.2, -25.9, -20.6
50090 DATA  -15.4, -10.2,  -5.1,  -0.0,   5.0,  10.1,  15.1,  20.0,  25.0,  29.9
50100 DATA   34.8,  39.7,  44.6,  49.5,  54.3,  59.1,  64.0,  68.8,  73.6,  78.4
50110 DATA   83.2,  88.0,  92.9,  97.7, 102.5, 107.4, 112.2, 117.1, 122.0, 126.9
50120 DATA  131.8, 136.7, 141.7, 146.6, 151.6, 156.5, 161.5, 166.5, 171.5, 176.5
50130 DATA  181.6, 186.6, 191.6, 196.6, 201.6, 206.6, 211.6, 216.6, 221.5, 226.5
50140 DATA  231.5, 236.4, 241.4, 246.3, 251.2, 256.1, 261.0, 265.9, 270.8, 275.6
50150 DATA  280.5, 285.3, 290.2, 295.0, 299.8, 304.6, 309.4, 314.3, 319.1, 323.9
50160 DATA  328.7, 333.4, 338.2, 343.0, 347.8, 352.6, 357.3, 362.1, 366.9, 371.6
50170 DATA  376.4, 381.1, 385.9, 390.6, 395.4, 400.1, 404.8, 409.6, 414.3, 419.0
50180 DATA  423.8, 428.5, 433.2, 437.9, 442.6, 447.3, 452.0, 456.8, 461.5, 466.2
50190 DATA  470.9, 475.6, 480.3, 485.0, 489.7, 494.4, 499.1, 503.8, 508.5, 513.1
50200 DATA  517.8, 522.5, 527.2, 531.9, 536.6, 541.3, 546.0, 550.7, 555.4, 560.0
50210 DATA  564.7, 569.4, 574.1, 578.8, 583.5, 588.2, 592.9, 597.6, 602.3, 607.0
50220 DATA  611.7, 616.4, 621.2, 625.9, 630.6, 635.3, 640.0, 644.8, 649.5, 654.2
50230 DATA  658.9, 663.7, 668.4, 673.2, 677.9, 682.7, 687.4, 692.2, 696.9, 701.7
50240 DATA  706.5, 711.3, 716.1, 720.8, 725.6, 730.4, 735.2, 740.0, 744.8, 749.7
50250 DATA  754.5, 759.3, 764.1, 769.0, 773.8, 778.7, 783.5, 788.4, 793.3, 798.1
50260 DATA  803.0, 807.9, 812.8, 817.7, 822.6, 827.5, 832.4, 837.3, 842.2, 847.2
50270 DATA  852.1, 857.1, 862.0, 867.0, 872.0, 876.9, 881.9, 886.9, 891.9, 896.9
50280 DATA  901.9, 906.9, 911.9, 916.9, 922.0, 927.0, 932.0, 937.1, 942.2, 947.2
50290 DATA  952.3, 957.4, 962.5, 967.6, 972.7, 977.8, 982.9, 988.0, 993.1, 998.2
50300 DATA 1003.4,1008.5,1013.7,1018.8,1024.0,1029.2,1034.4,1039.6,1044.8,1050.0
50310 DATA 1055.2,1060.4,1065.6,1070.8,1076.1,1081.3,1086.6,1091.9,1097.2,1102.4
50320 DATA 1107.7,1113.0,1118.3,1123.7,1129.0,1134.3,1139.7,1145.0,1150.4,1155.8
50330 DATA 1161.2,1166.6,1172.0,1177.4,1182.9,1188.3,1193.8,1199.2,1204.7,1210.2
50340 DATA 1215.7,1221.2,1226.8,1232.3,1237.9,1243.5,1249.1,1254.7,1260.3,1265.9
50350 DATA 1271.6,1277.3,1282.9,1288.6,1294.3,1300.1,1305.8,1311.5,1317.3,1323.1
50360 DATA 1328.9,1334.7,1340.5,1346.4,1352.2,1358.1,1363.9,1369.8,1375.7
50370 DIM TK(NK-1)
50380 FOR I = 0 TO NK-1:READ TK(I):NEXT I
50390 RETURN
50400 '
51000 '-------- Interpolation routine to find K thermocouple temperature -----
51010 'Entry variables:-
51020 '    CJC = cold junction compensator temperature in deg. C.
51030 '      V = thermocouple voltage in volts
51040 'Exit variables:-
51050 '     TC = temperature in degrees Centigrade
51060 '     TF = temperature in degrees Fahrenheit
51080 'Perform CJC compensation for K type
51090 VK = 1000*V + 1! + (CJC-25)*.0405     'VK in mV
51100 '
51110 'Find look up element
51120 EK = INT((VK-SVK)/SIK)
51130 IF EK<0 THEN TC=TK(0):GOTO 51170 'Out of bounds, round to lower limit
51140 IF EK>NK-2 THEN TC=TK(NK-1):GOTO 51170 'Out of bounds,round to upper limit
51150 'Do interpolation
51160 TC = TK(EK) + (TK(EK+1) - TK(EK))*(VK-EK*SIK-SVK)/SIK   'Centigrade
51170 TF = TC*9/5 + 32   'Fahrenheit
51180 RETURN
```

Fig. A3.1 Listing of program DAS (cont.)

APPENDIX 4

SAMPLE ECONOMIC ANALYSIS

A sample economic analysis for the hotel application (desalination only) operating with mode #4 is described in this appendix.

As it is already stated in Chapter 7 the economic analysis was performed with a spreadsheet program (i.e. Lotus 1-2-3). Spreadsheets consists of a number of cells which can contain either labels, numbers or formulae. Printouts of the various parts of the spreadsheet used in the economic analysis are shown in the figures included in this appendix.

Table A4.1 gives a list of the input parameters. The mortgage payment and the electric power requirements in kWh shown at the bottom of the figure are calculated values. The former is calculated by dividing the total system cost with the PWF for inflation rate equal to zero (equal instalments), interest rate equal to 9% and 20 years mortgage payment time. The latter is calculated by multiplying the operation hours of the desalination and solar systems by the kW rating of the plant.

The main calculation sheet is shown in Table A4.2. The calculation is carried out annually in different rows of the spreadsheet as shown in Table A4.2 for which the various costs are calculated. The relations described in Chapter 7 are used here. The various costs are added in the column labelled life cycle savings and the present worth (PW) of these savings is calculated in the next column. At the bottom of the table the present worth of the life cycle savings is added.

A secondary table is required for the calculation of some of the costs required in the main calculation sheet shown in Table A4.2. These are the annual interest charges on remaining capital and the wear and tear allowance as shown in Table A4.3.

Spreadsheets have the ability to recalculate the table when one of the input values is

changed. The input value changed in this case is the water price (included in the list of input parameters, Table A4.1) which is changed until such a figure is used that turns the sum of the life cycle savings equal to zero.

ECONOMIC PARAMETERS		
COLLECTOR AREA	540	m^2
COST PER UNIT AREA	70.26	C£/m^2
AREA INDEPENDENT COST	159800	C£
PRICE OF ELECTRICITY	0.04	C£/kWh
ANNUAL INCREASE OF ELECTRICITY PRICE	2.9	%
PERIOD OF ECONOMIC ANALYSIS	20	YEARS
ANNUAL MARKET DISCOUNT RATE	7.84	%
MAINTENANCE IN YEAR 1 (2% of total system cost)	3954.8	C£
ANNUAL INCREASE IN MAINTENANCE	2	%
PUMPING POWER REQUIREMENTS (DESALIN.)	8.7	kW
OPERATION HOURS (DESALINATION)	8640	
PUMPING POWER REQUIREMENTS (SOLAR)	2	kW
OPERATION HOURS (SOLAR)	4230	
FIRST YEAR FUEL COST	20425	C£
FIRST YEAR FUEL SAVINGS	0	C£
FUEL PRICE ANNUAL INCREASE	0.6	%
INITIAL PAYMENT	30	%
WATER PRICE (VARIABLE)	0.89	C£/m^3
WATER PRODUCED BY THE SYSTEM (ANNUAL)	38880	m^3
ANNUAL MORTGAGE PAYMENT	15163.3	C£
ELECTRICITY (ANNUAL)	83628	kWh

Table A4.1 List of input parameters

YEAR	WATER COST	MORTAGE PAYMENT	MAINTENANCE COST	PUMPING COST	TOTAL M&P COST	TAX SAVINGS	FUEL COST	FUEL SAVINGS	SYSTEM ANNUAL COST	P.W. OF SYSTEM COST
0						10678.0			-48644.1	-48644.1
1	34797.6	15163.3	3954.8	3345.1	7299.9	16188.3	20425.0	0	8097.6	7508.9
2	34797.6	15163.3	4033.9	3442.1	7476.0	16203.2	20547.6	0	7813.9	6719.0
3	34797.6	15163.3	4114.6	3542.0	7656.5	16213.5	20670.8	0	7520.5	5996.6
4	34797.6	15163.3	4196.9	3644.7	7841.5	16218.9	20794.9	0	7216.7	5336.1
5	34797.6	15163.3	4280.8	3750.4	8031.2	16218.6	20919.6	0	6902.1	4732.4
6	34797.6	15163.3	4366.4	3859.1	8225.6	16212.2	21045.1	0	6575.8	4180.9
7	34797.6	15163.3	4453.8	3971.0	8424.8	16198.9	21171.4	0	6237.0	3677.2
8	34797.6	15163.3	4542.8	4086.2	8629.0	16178.1	21298.4	0	5884.9	3217.4
9	34797.6	15163.3	4633.7	4204.7	8838.4	16148.9	21426.2	0	5518.6	2797.7
10	34797.6	15163.3	4726.4	4326.6	9053.0	16110.6	21554.8	0	5137.1	2415.0
11	34797.6	15163.3	4820.9	4452.1	9273.0	10723.1	21684.1	0	-599.7	-261.4
12	34797.6	15163.3	4917.3	4581.2	9498.5	10663.5	21814.2	0	-1015.0	-410.3
13	34797.6	15163.3	5015.7	4714.1	9729.7	10591.6	21945.1	0	-1449.0	-543.2
14	34797.6	15163.3	5116.0	4850.8	9966.7	10506.2	22076.8	0	-1903.1	-661.5
15	34797.6	15163.3	5218.3	4991.5	10209.7	10406.0	22209.2	0	-2378.7	-766.7
16	34797.6	15163.3	5322.7	5136.2	10458.9	10289.5	22342.5	0	-2877.5	-860.1
17	34797.6	15163.3	5429.1	5285.2	10714.3	10155.2	22476.6	0	-3401.3	-942.7
18	34797.6	15163.3	5537.7	5438.4	10976.1	10001.3	22611.4	0	-3952.0	-1015.7
19	34797.6	15163.3	5648.4	5596.1	11244.6	9825.8	22747.1	0	-4531.5	-1080.0
20	34797.6	15163.3	5761.4	5758.4	11519.8	9626.9	22883.6	0	-5142.2	-1136.5
20						-16017.0			43305.1	9570.7

Note: All values in C£ Total: 0.0

System annual cost = Mortgage payment + maintenance cost + pumping cost + fuel cost − water cost − fuel savings − tax savings

Table A4.2 Economic analysis sample calculation sheet (hotel case operation mode #4)

YEAR	WEAR & TEAR ALLOWANCE	MORTGAGE PAYMENT	INTEREST PAYED	REMAINING PRINCIPAL
0				138418.2
1	19774	15163.3	12457.6	135712.6
2	19774	15163.3	12214.1	132763.4
3	19774	15163.3	11948.7	129548.8
4	19774	15163.3	11659.4	126044.9
5	19774	15163.3	11344.0	122225.6
6	19774	15163.3	11000.3	118062.6
7	19774	15163.3	10625.6	113524.9
8	19774	15163.3	10217.2	108578.9
9	19774	15163.3	9772.1	103187.7
10	19774	15163.3	9286.9	97311.3
11	0	15163.3	8758.1	90906.0
12	0	15163.3	8181.5	83924.2
13	0	15163.3	7553.2	76314.1
14	0	15163.3	6868.3	68019.1
15	0	15163.3	6121.7	58977.5
16	0	15163.3	5307.9	49122.1
17	0	15163.3	4421.0	38379.8
18	0	15163.3	3454.2	26670.7
19	0	15163.3	2400.4	13907.7
20	0	15163.3	1251.7	0
20	0			0

Table A4.3 Secondary table for calculation of various costs

APPENDIX 5

LIST OF PUBLICATIONS

1. Kalogirou, S. 1991. *Solar Energy Utilisation Using Parabolic Trough Collectors in Cyprus*, MPhil Thesis, The Polytechnic of Wales.

2. Kalogirou, S. and Lloyd, S. 1992a. Construction Details and Performance Characteristics of a Parabolic Trough Collector System, *Proceedings of the Applications of Solar and Renewable Energy Congress*, Cairo, Egypt, no. 40, pp. 437–446.

3. Kalogirou, S. and Lloyd, S. 1992b. Use of Solar Parabolic Trough Collectors for Hot Water Production in Cyprus – A Feasibility Study, *Renewable Energy Journal*, vol. 2, no. 2, pp. 117–124.

4. Kalogirou, S., Lloyd, S. and Ward, J. 1992c. A Tracking Mechanism for Medium to High Concentration Ratio Parabolic Trough Collectors, *Proceedings of the Second World Renewable Energy Congress*, Reading U.K., vol. 2, pp. 1086–1091.

5. Kalogirou, S., Lloyd, S. and Ward, J. 1993a. Modelling of a Parabolic Trough Collector System for Hot Water Production, *Proceedings of ISES World Congress*, Budapest, Hungary, vol. 5, pp. 145–150.

6. Kalogirou, S., Lloyd, S. and Ward, J. 1993b. Solar Desalination: The Solution to Cyprus Water Shortage Problem, *Proceedings of the Environmental Engineering Congress*, Leceister U.K., vol. 1.

7. Kalogirou, S., Eleftheriou, P., Lloyd, S. and Ward, J. 1994a. Design and Performance Characteristics of a Parabolic–Trough Solar–Collector System, *Applied Energy Journal*, vol. 47, pp. 341–354.

8. Kalogirou, S., Eleftheriou, P., Lloyd, S. and Ward, J. 1994b. Low Cost High Accuracy Parabolic Troughs – Construction and Evaluation, *Proceedings of the Third World Renewable Energy Congress*, Reading U.K., part I, pp. 384–386.

9. Kalogirou, S., Lloyd, S. and Ward, J. 1994c. Sea Water Desalination: An Alternative to Water Imports in Cyprus, *Proceedings of the Third World Renewable Energy Congress*, Reading U.K., part III, pp. 1068–1071.

10. Kalogirou, S., Eleftheriou, P., Lloyd, S. and Ward, J. 1995. Optimisation of the Initial Response of a Solar Steam Generation Plant, *Proceedings of the 1995 ASME/JSME/JSES International Solar Energy Conference*, Lahaina, Maui, Hawaii. Proceedings publication pending.

REFERENCES

Akinsete, V.A. and Duru, C.U. 1979. A Cheap Method of Improving the Performance of Roof Type Solar Stills, *Solar Energy*, vol. 23, pp. 271–272.

ASHRAE Standard 93–1986. *Methods of Testing to Determine the Thermal Performance of Solar Collectors*, ANSI/ASHRAE 93–1986.

Braun, J.E. and Mitchell, J.C. 1983. Solar Geometry for Fixed and Tracking Surfaces, *Solar Energy*, vol. 31, pp. 439–444.

Cena, V. 1985. *Solar Energy Availability*, Sogesta.

Daniels, F. 1974. *Direct Use of the Sun's Energy*, ch. 10, New Haven and London, Yale University Press, sixth edition.

Deffenbaugh, D.M., Green, S.T. and Svedeman, S.J. 1986. The Effect of Dust Accumulation on Line–Focus Parabolic Trough Solar Collector Performance, *Solar Energy*, vol. 36, pp. 139–146.

Duffie, J.A. and Beckman, W.A. 1980. *Solar Engineering of Thermal Processes*, John Willey & Sons.

Economic Report 1991. *Ministry of Finance, Department of Statistics and Research.*

Eibling, J.A., Talbert, S.G. and Lof, G.O.G. 1971. Solar Stills for Community Use – Digest of Technology, *Solar Energy*, vol. 13, pp. 263–276.

Eggers–Lura, A. 1979. *Solar Energy in Developing Countries*, pp. 35–40, Pergamon Press.

Grutcher, J. 1983. Desalination: A PV Oasis, *Photovoltaics International*, pp.24–26, June/July.

Guven, H.M. and Bannerot, R.B. 1985. Derivation of Universal Error Parameters for Comprehensive Optical Analysis of Parabolic Troughs, *Proceedings of the ASME–ISES Solar Energy Conference*, Knoxville, USA, pp. 168–174.

Guven, H.M. and Bannerot, R.B. 1986. Determination of Error Tolerances for the Optical Design of Parabolic Troughs for Developing Countries, *Solar Energy*, vol. 36, pp. 535–550.

Holman, J.P. 1989. *Heat Transfer*, McGraw–Hill Book Company.

Houghton, J. 1992. Climate Change: The Current State of Scientific Knowledge, *Proceedings of the Second World Renewable Energy Congress*, Reading U.K., vol. 1, pp. 1–23.

Hurtado, P. and Kast, M. 1984. *Experimental Study of Direct In-Situ Generation of Steam in a Line Focus Solar Collector*, SERI.

Jetter, S.M. 1987. Analytical Determination of the Optical Performance of Practical Parabolic Trough Collectors from Design Data, *Solar Energy*, vol. 39, pp. 11-21.

Kalogirou, S. 1991. *Solar Energy Utilisation Using Parabolic Trough Collectors in Cyprus*, MPhil Thesis, The Polytechnic of Wales.

Kalogirou, S. and Lloyd, S. 1992a. Construction Details and Performance Characteristics of a Parabolic Trough Collector System, *Proceedings of the Applications of Solar and Renewable Energy Congress*, Cairo, Egypt, no. 40, pp. 437-446.

Kalogirou, S. and Lloyd, S. 1992b. Use of Solar Parabolic Trough Collectors for Hot Water Production in Cyprus - A Feasibility Study, *Renewable Energy Journal*, vol. 2, no. 2, pp. 117-124.

Kalogirou, S., Lloyd, S. and Ward, J. 1992c. A Tracking Mechanism for Medium to High Concentration Ratio Parabolic Trough Collectors, *Proceedings of the Second World Renewable Energy Congress*, Reading U.K., vol. 2, pp. 1086-1091.

Kalogirou, S., Lloyd, S. and Ward, J. 1993a. Modelling of a Parabolic Trough Collector System for Hot Water Production, *Proceedings of ISES World Congress*, Budapest, Hungary, vol. 5, pp. 145-150.

Kalogirou, S., Lloyd, S. and Ward, J. 1993b. Solar Desalination: The Solution to Cyprus Water Shortage Problem, *Proceedings of the Environmental Engineering Congress*, Leceister U.K., vol. 1.

Kalogirou, S., Eleftheriou, P., Lloyd, S. and Ward, J. 1994a. Design and Performance Characteristics of a Parabolic-Trough Solar-Collector System, *Applied Energy Journal*, vol. 47, pp. 341-354.

Kalogirou, S., Eleftheriou, P., Lloyd, S. and Ward, J. 1994b. Low Cost High Accuracy Parabolic Troughs - Construction and Evaluation, *Proceedings of the Third World Renewable Energy Congress*, Reading U.K., part I, pp. 384-386.

Klein, S.A. *et al.* 1990. TRNSYS, A Transient Simulation Program, Solar Energy Laboratory, University of Wisconsin, Madison, WI.

Klein, S.A. and Beckman, W.A. 1983. F-CHART, F-Chart Software, Middleton, Wisconsin.

Kreider, J.F. and Kreith, F. 1981. *Solar Energy Handbook*, ch.18, McGraw-Hill Book Company.

Lobo, P.C. and Araujo, S.R. 1978. A Simple Multi-Effect Basin Type Solar Still, *SUN, Proceedings of the International Solar Energy Society* - New Delhi, India, vol. 3, pp. 2026-2030, Pergamon.

Luft, W. 1982. Five Solar-Energy Desalination Systems, *International Journal of Solar Energy*, vol. 1, pp. 21-32.

Lytras, C.St. 1991. *Water Development Department-Annual Report 1991.*

Malik, M.A.S., Tiwari, G.N., Kumar, A. and Sodha, M.S. 1985. *Solar Distillation*, Pergamon Press.

Marinos, D., Assimacopoulos, D. and Provatas, F. 1991. The Experience of Local Authorities with Water Desalination in the Islands of Southern Europe, *Proceedings of the New Technologies for the Use of Renewable Energy Sources in Water Desalination*, Athens, Greece, section V, pp. 48-56.

Meinel, A.B. and Meinel, M.P. 1976. *Applied Solar Energy - An Introduction*, Addison-Wesley Publishing Company.

Meteorological Service 1991. Ministry of Agriculture and Natural Resources, *Some Studies of the Amounts of Precipitation on Cyprus.*

Morris, R.M. and Hanbury, W.T. 1991. Renewable Energy and Desalination - A Review, *Proceedings of the New Technologies for the Use of Renewable Energy Sources in Water Desalination*, Athens, Greece, section I, pp. 30-50.

Moustafa, S.M.A., Jarrar, D.I. and Mansy, H.I. 1985. Performance of a Self-Regulating Solar Multistage Flush Desalination System, *Solar Energy*, vol. 35, pp. 333-340.

Murphy, L.M. and Keneth, E. 1982. *Steam Generation in Line-Focus Solar Collectors: A Comparative Assessment of Thermal Performance, Operating Stability, and Cost Issues*. SERI/TR-1311.

Mustacchi, C. and Cena, V. 1978. Solar Water Distillation, *Technology for Solar Energy Utilisation*, pp. 119-124, United Nations.

Mustacchi, C. and Cena, V. 1981. *Solar Desalination - Design, Performances, Economics*, Sogesta.

Peterson, P.J. and Keneth, E. 1982. *Flow Instability During Direct Steam Generation in a Line-Focus Solar Collector System*, SERI/TR-1354.

Porteous, A. 1975. *Saline Water Distillation Processes*, Longman.

Prapas, D.E., Norton, B., Molidonis, E. and Probert, S.D. 1988. Response Function for Solar-Energy Collectors, *Solar Energy*, vol. 40, pp. 371-383.

Rabl, A. and Bendt, P. 1982. Effect of Circumsolar Radiation on Performance of Focussing Collectors, *ASME Journal of Solar Energy Engineering*, vol. 104, pp. 237-250.

Rajvanshi, A.K. 1981. Effects of Various Dyes on Solar Distillation, *Solar Energy*, vol. 27, pp. 51-65.

Sodha, M.S., Kumar, A., Tiwari, G.N. and Tyagi, R.C. 1981. Simple Multiple Wick Solar Still: Analysis and Performance, *Solar Energy*, vol. 26, pp. 127–131.

Sodha, M.S., Mathur, S.S. and Malik, M.A.S. 1984. *Reviews of Renewable Energy Resources*, vol. 2, Wiley Eastern Limited.

Spiegler, K.S. and Laird, A.D.K. (Editors) 1980a. *Principles of Desalination*, second edition, Part A, Academic Press.

Spiegler, K.S. and Laird, A.D.K. (Editors) 1980b. *Principles of Desalination*, second edition, Part B, Academic Press.

Surface Sea–Water Temperature (coastal) 1988. *Ministry of Agriculture and Natural Resources Meteorological Service – Department of Fisheries.*

Tabor, H. 1990. Solar Energy Technologies for the Alleviation of Fresh–Water Shortages in the Mediterranean Basin, Euro–Med Solar, *Proceedings of the Meditarranean Business Seminar on Solar Energy Technologies*, Nicosia, Cyprus, pp. 152–158.

Tata, A. 1980. *Solar Assisted Desalination Pilot Plant*, Snia Techint SpA.

Thomas, A., Rao, R., Balasubramanian, V., Sankarasubramanian, G. and Guven, H.M. 1986. Measurement of Flux Distribution Around the Receiver of a Parabolic Trough Concentrator, *Proceedings of the ASME Solar Energy Conference*, Anaheim, California, pp. 20–24.

Tleimat, B.W. 1978. Solar Distillation: The State of the Art, *Technology for Solar Energy Utilisation*, pp. 113–118, United Nations.

Water and Environment 1993. *Caribbean Co–Generation*, no. 5, pp. 14–23.

WHO 1984. *Guidelines for Drinking – Water Quality*, World Health Organisation.

Zarza, E., Ajona, J.I., Leon, J., Genthner, K. and Gregorzewski, A. 1991a. Solar Thermal Desalination Project at the Plataforma Solar De Almeria, *Proceedings of the Biennial Congress of the International Solar Energy Society*, Denver, Colorado, USA, vol. 1, part II, pp. 2270–2275.

Zarza, E., Ajona, J.I., Leon, J., Genthner, K. Gregorzewski, A., Alefeld, G., Kahn, R., Haberle, A., Gunzbourg, J., Scharfe, J. and Cord'homme, C. 1991b. Solar Thermal Desalination Project at the Plataforma Solar De Almeria, *Proceedings of the New Technologies for the Use of Renewable Energy Sources in Water Desalination*, Athens, Greece, section III, pp. 62–81.

BIBLIOGRAPHY

Duffie, J.A. and Beckman, W.A. 1980. *Solar Engineering of Thermal Processes*, John Willey & Sons.

Hans-Gunter Heitmann (Editor). 1990. *Saline Water Processing*, VCH Publishers, New York.

Kreider, J.F. and Kreith, F. 1981. *Solar Energy Handbook*, McGraw-Hill Book Company.

Malik, M.A.S., Tiwari, G.N., Kumar, A. and Sodha, M.S. 1985. *Solar Distillation*, Pergamon Press.

Meinel, A.B. and Meinel, M.P. 1976. *Applied Solar Energy - An Introduction*, Addison-Wesley Publishing Company.

Mustacchi, C. and Cena, V. 1981. *Solar Desalination - Design, Performances, Economics*, Sogesta.

Porteous, A. 1975. *Saline Water Distillation Processes*, Longman.

Sodha, M.S., Mathur, S.S. and Malik, M.A.S. 1984. *Reviews of Renewable Energy Resources*, volumes 1 and 2, Wiley Eastern Limited.

Solar Energy Journal. The Journal of Solar Energy Science and Technology, Pergamon Press.

Spiegler, K.S. and Laird, A.D.K. (Editors) 1980. *Principles of Desalination*, second edition, Parts A and B, Academic Press.